DOCTOR OF PHILOSOPHY

Transcriptomic studies of the early stages of potato infection by Phytophthora infestans

Kandel, Kabindra Prasad

Award date:
2014

Transcriptomic studies of the early stages of potato infection by *Phytophthora infestans*

Kabindra Prasad Kandel

Doctor of Philosophy

College of Life Sciences

The University of Dundee

and

Cell and Molecular Sciences

The James Hutton Institute

June 2014

Declaration

The results presented here are of investigations conducted by myself. Work other than my own is clearly identified with references to relevant researchers and/or their publications. I hereby declare that the work presented here is my own and has not been submitted in any form for any degree at this or any other university.

Kabindra P. Kandel

We certify that Kabindra Prasad Kandel has fulfilled the relevant ordinance and the regulations of the University Court and is qualified to submit this thesis for the degree of Doctor of Philosophy.

Dr. Steve Whisson

Dr. Petra Boevink

Cell and Molecular Sciences

The James Hutton Institute

Professor Paul Birch

College of Life Sciences

University of Dundee

Table of contents

List of abbreviations

AF	apoplastic fluid
ANOVA	analysis of variance
Avr	avirulence (protein/gene)
CBEL	cellulose-binding elicitor lectin
cDNA	complimentary deoxyribonucleic acid
CHPs	conserved hypothetical proteins
CIP	International Potato Centre
CMPG1	cysteine methionine proline glycine protein 1
CRN	crinkler
cv.	cultivar
DAMP	damage associated molecular pattern
dpi	days post-inoculation
EHX	extrahaustorial matrix
EPI	extracellular protease inhibitors
EST	expressed sequence tag
ETI	effector-triggered immunity
ETS	effector-triggered susceptibility
FAO	Food and Health Organisation
GC	germinating cysts
GFP	green fluorescent protein
GIP	glucanase inhibitors
GM	genetically modified
Hmp1	haustorial membrane protein 1
HPs	hypothetical proteins
hpi	hours post-inoculation
HR	hypersensitive response
INF	infestin
IPM	intregrated pest management
LI	leaf infection
LIM	zinc-binding domain present in Lin-11, Isl-1, Mec-3
LRR-RK	leucine rich repeat- receptor kinase
MAMP	microbe-associated molecular pattern
MAPK	mitogen activated protein kinase
mRFP	monomeric red fluorescent protein
Myc	mycelium
NBS-LRR/ NB-LRR	nucleotide- binding leucine rich repeat
NCBI	National Centre for Biotechnology Information
NLP	Nep1-like protein
ni	non-infection
NLS	nuclear localisation signal
NPP	necrosis-inducing *Phytophthora* protein
PAMP	pathogen-associated molecular pattern

PB	pea broth
Pep13	13-amino-acid peptide fragment of transglutaminase
PR	pathogenesis-related
PRR	pattern recognition receptor
PTI	pattern-triggered immunity
PTS	pattern-triggered susceptibility
QRT-PCR	quantitative reverse transcription polymerase chain reaction
R	disease resistance
RIN	RNA integrity number
RNA	ribonucleic acid
ROS	reactive oxygen species
RxLR	arginine, any amino acid, leucine, arginine
SP	signal peptide
SP2	spectrum II
Spo	sporangia
SW	sterile distilled water
tdTomato	tandem dimer tomato
TFs	transcription factors
TI	tuber infection
TPs	transmembrane proteins
T3SS	type III secretion system
Zo	zoospores

List of figures

List of tables

List of annexes in additional compact disc

Annex 3a	Predicted 18,024 *P. infestans* transcripts
Annex 3b	15,264 transcripts detected either in one or both of the two *in vitro* (sporangia and germinating cysts) stages, or any of the *in planta* (12, 24, 36, 48, and 60 hpi) infection stages
Annex 3c	5,975 transcripts detected in any and/or all of the *in planta* infection and non-infection (ni) stages
Annex 3d	1,707 transcripts detected as differentially expressed in the *in planta* infection stages
Annex 3e	Volcano plot analysis of differentially expressed transcripts during *in planta* infection
Annex 3f	137 transcripts co-expressed with *Cdc14 in planta*
Annex 3f	186 genes was co-expressed with *Hmp1 in planta*
Annex 3f	400 transcripts co-expressed with the necrotrophy marker gene *NPP1 in planta*
Annex 3g	17 infection- specific transcripts
Annex 5a	15,513 transcripts detected either in *P. infestans* zoospores, or zoospore inoculated apoplastic fluid, pea broth, or sterile distilled water sampled at 24 and 48 hpi
Annex 5b	13,819 transcripts detected as differentially expressed in zoospores, or zoospore inoculated apoplastic fluid, pea broth, or sterile distilled water sampled at 24 and 48 hpi
Annex 5b	813 transcripts co-expressed with *Cdc14* in zoospores, or zoospore inoculated apoplastic fluid, pea broth, or sterile distilled water sampled at 24 and 48 hpi
Annex 5b	288 transcripts co-expressed with *Hmp1* in zoospores, or zoospore inoculated apoplastic fluid, pea broth, or sterile distilled water sampled at 24 and 48 hpi
Annex 5b	416 transcripts co-expressed with *Avr3a* in zoospores, or zoospore inoculated apoplastic fluid, pea broth, or sterile distilled water sampled at 24 and 48 hpi
Annex 5c	Flag value analysis of differentially expressed transcripts in zoospores, or zoospore inoculated apoplastic fluid, pea broth, or sterile distilled water sampled at 24 and 48 hpi
Annex 5d	Volcano plot analysis of differentially expressed transcripts in zoospores, or zoospore inoculated apoplastic fluid, pea broth, or sterile distilled water sampled at 24 and 48 hpi

List of appendices in additional compact disc

Acknowledgements

This journey originally started more than 11 years ago with my arrival in Japan as a student at the Tokyo University of Agriculture. My professors there were inspirational and I developed a strong interest in plant science, specifically in meristem culture. After completing my Undergraduate and Masters degrees in this specialism I was keen to continue my development and learn about molecular plant sciences, broadening my knowledge of this area. Professor Natsuaki spoke to me about the University of Dundee and the Scottish Crop Research Institute (now James Hutton Institute), recommending them highly. I was so lucky as I had the opportunity to meet with Professor Paul Birch, Dr Steve Whisson, and Dr Petra Boevink who would later become my supervisory team after applying to Dundee. There are so many people (professors, family members, friends, colleagues and peers) who have helped, contributed and supported me through this journey and I cannot begin to explain how their ideas, support, inspiration, encouragement, and enthusiasm for plant sciences helped me to arrive where I am today. I am most grateful to all of them.

For this PhD thesis I'd like to particularly acknowledge my supportive and ever patient supervisory team: Prof Paul Birch (University of Dundee), Dr Steve Whisson (James Hutton Institute) and Dr Petra Boevink (James Hutton Institute). Your feedback, comments and advice over the duration of my PhD has been invaluable. I'm also extremely grateful for the input from others including Anna Avrova, David Cooke, Dionne Turnbull, Eleanor Gilroy, Eva Randall, Gaetan Thilliez, Hazel McLellan, Ingo Hein, Jenny Morris, Julie Squires, Kath Wright, Laurence Ducreux, Leighton Pritchard, Miles Armstrong, Peter Cock, Pete Hedley, Ralph Wilson, Ramesh Vetukuri, Sarah Robertson, Sonia Gomez, and Stefan Engelhardt.

I also greatly appreciate the valuable contribution to my viva by Prof Pieter van West and Dr Edgar Huitema. Thank you!

Another important acknowledgment is overdue to my family. This PhD thesis would not have been possible without the continued emotional support and love from you. Your encouragement enabled me to pursue my studies literally around the world! Thank you for standing by me throughout this (long) process. Your unwavering support has kept me motivated both during the times I felt I was moving backwards as well as when I could see the finish line!

And finally, the support of my friends who came to visit me from Japan as well as those I made along the way in Scotland has been truly great!

Thank you to all who made this thesis possible,

Kabindra Prasad Kandel

Publication arising from this work

Zheng, X., McLellan, H., Fraiture, M., Liu, X., Boevink, P. C., Gilroy, E. M., Chen, Y., Kandel, K., Sessa, G., Birch, P. R. J., and Brunner, F. (2014). Functionally Redundant RXLR Effectors from Phytophthora infestans Act at Different Steps to Suppress Early flg22-Triggered Immunity. *PLoS pathogens*. 10 (4): e1004057.

Abstract

The late blight pathogen, *Phytophthora infestans,* is the most destructive pathogen of its solanaceous hosts potato and tomato. It is a threat to global food security and it is therefore important to understand the cellular and molecular dynamics underlying colonisation of its host plants. This greater understanding will inform strategies to improve host plant resistance. In addition to studying the cell biology of the interaction, it is important to understand the temporal changes in gene expression and regulation during host-pathogen interactions at the earliest infection time points. Previously published transcriptomic studies of *P. infestans* used two days post infection (dpi) as the earliest sampling time point. Expression of a marker gene (*Hmp1*) for biotrophy and a selection of effector coding genes has been reported as early as 12 hours post inoculation (hpi), suggesting that infection was initiated before then. Transcriptomic studies of *P. infestans* have focussed mostly on leaf tissue, and there is still a lack of research on the transcriptome of *P. infestans* grown in alternative plant tissues such as tubers, or in host cell-free apoplastic fluid. This thesis explores transcriptomic studies of the early, biotrophic stages of potato infection by *Phytophthora infestans,* which is critical for understanding which genes are involved at what stages of infection development.

By using the latest sensitive microarray technology to study the *P. infestans* transcriptome in an infection time course that remained biotrophic for its duration, a list of 1,707 transcripts of *P. infestans* were discovered to be differentially expressed. This list included 114 transcripts for RxLR effectors, out of which 26 were detected from 12 hours post infection, including: *Avr2, Avr3a, Avrblb1 (ipi01), Avrblb2*, and the recently characterised *RD2*. Also of interest was that transcripts encoding a PAMP (CBEL) detected at 12 hours, were suppressed in the pathogen by 24 hours. Transcripts encoding 55 RxLR effectors were co-expressed (with >95 % correlation coefficient) with the

biotrophy marker gene *Hmp1*, suggesting that these effectors are important throughout the biotrophic stages of infection. QRT-PCR and cell biology data supported the expression of the biotrophy marker gene *Hmp1* as early as 12 hours after infection and this was further supported by the co-expression of avirulence genes such as *Avr2* and *Avr3a*. A set of 17 transcripts, including six cytoplasmic effectors (RxLR effectors), as well as a transcript encoding an apoplastic effector (glucanase inhibitor), was found to be infection-specific, supporting the hypothesis that these genes might have roles in establishing biotrophy.

By examining pathogen behaviour in tuber tissue, clear cell biology evidence of functional haustoria was found. Gene expression analysis of a selection of leaf infection-related genes suggested that effectors are used to promote infection also in host tuber tissue. However, some cytoplasmic RXLR effector proteins such as PITG_05146 and PITG_15128, which were up-regulated during biotrophic infection of leaf tissue, were not detected during tuber infection, indicating potential differences in pathogenic requirements.

A microarray experiment was conducted on *in vitro* stages of zoospores, and mycelium grown in apoplastic fluid of *N. benthamiana*, nutrient rich pea broth, and sterile water. This revealed 13,819 transcripts that were differentially expressed between any two conditions. This list included transcripts encoding 322 RxLR effectors, of which avirulence effectors such as *Avr2*, *Avr3a*, and *RD2* were highly up-regulated during hyphal growth in apoplastic fluid compared to other *in vitro* stages. This provides evidence that the apoplast contains chemical signals that induce expression of infection-related genes in *P. infestans*. Curiously, the leaf infection-specific genes identified in Chapter 3 were not expressed when *P. infestans* was grown in apoplastic fluid, revealing

that additional stimuli are required for induction of all necessary pathogen genes during infection.

Future research, building upon the findings from this project, should be focused on the following areas: 1) Explore whether haustoria are produced only in order to deliver effectors or if there are other purposes as well, such as nutrient uptake; 2) The continued exploration of differences between genes co-expressed with *Hmp1* during leaf infection, tuber infection, and in apoplastic fluid to further dissect the transcriptional regulation of these genes; 3) Identify whether *Hmp1*-co-expressed genes of unknown function may play a role in haustorium formation; 4) Investigate, using molecular transformation and cell biology, whether secreted proteins co-expressed with *Hmp1* are secreted from haustoria; 5) Investigate the role(s) of infection-specific genes in establishing disease. 6) Transcriptomic studies of *P. infestans* biotrophic infection of tuber tissue to determine the differences in pathogenic adaptation in this tissue type, compared to leaf infection.

Chapter 1. Literature review

1.1 General introduction

In general, natural and managed plant ecosystems, including crops, are damaged due to the action of various pathogens such as bacteria, viruses, fungi, nematodes, and oomycetes. All of these pathogens have an impact on food security due to poor crop yields as well as damaging natural vegetation. This thesis focuses on one particularly devastating oomycete plant pathogen, *Phytophthora infestans*. This pathogen causes late blight disease of potato, the most serious disease of this globally important crop. It also causes severe crop losses in tomato, another major crop plant.

1.2 Morphological characteristics and life cycle of oomycetes

Oomycetes are effectively unicellular organisms. They have morphological similarities to fungi, since their life cycle includes fungal-like stages such as spores, appressoria, and filamentous hyphae. However, phylogenetic studies have revealed that they belong to the stramenopiles, which are not related to fungi (Figure 1.1). Oomycetes are diploid for most of their life cycle whereas most true fungi are haploid or dikaryotic. The oomycete cell wall is made up of cellulose and β1-3-glucans. Compared with fungi they have a low level of chitin in their cell wall (Erwin and Ribeiro, 1996). A distinct reproduction cycle also distinguishes oomycetes from true fungi. Sexual reproduction includes characteristics unique to oomycetes, including different male and female gametangia (antheridia and oogonia, respectively), the use of secondary metabolites to regulate sexual compatibility and differentiation, and gametangial meiosis during the diploid vegetative stage (Judelson, 2009). By comparison, fungi typically use proteinaceous mating hormones during reproduction (Judelson, 2009).

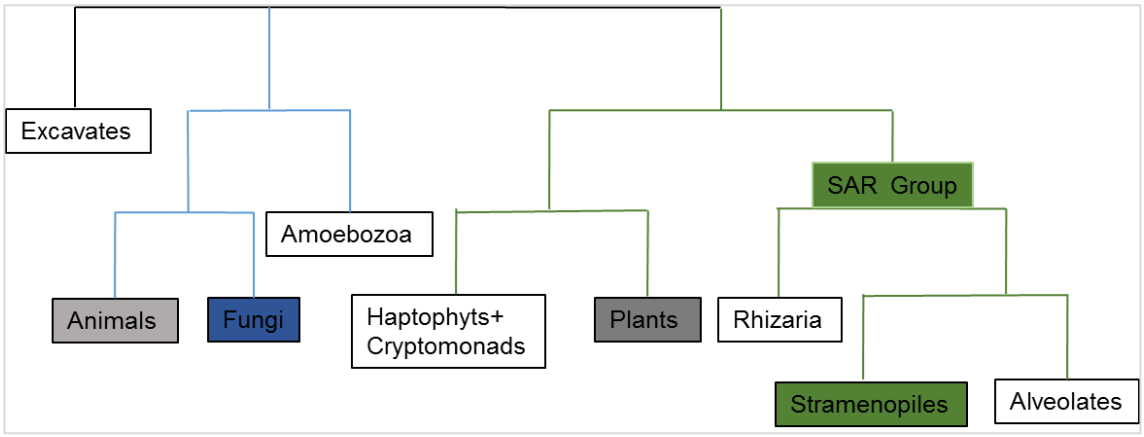

Figure 1.1 This figure is adapted from Burki *et al*. (2008). The Bayesian unrooted phylogenetic tree (CAT model in PHYLOBAYES) from the multigene dataset assembly (65 species, 135 genes) shows the different relationship between fungi and oomycetes. Fungi are more closely branched with the animal kingdom, whereas oomycetes, which belong to the stramenopiles, are more closely branched with the plant kingdom.

Oomycete reproduction can either be sexual or asexual (Figure 1.2). The sexual life cycle of oomycetes can be categorized into homothallic (sexual reproduction in single culture) or heterothallic (distinct sexual compatibility types). Homothallic species are capable of producing oospores during vegetative growth in culture plates or during infection in host tissues by a self-fertility mechanism. Some examples of homothallic oomycetes are *Hyaloperonospora arabidopsidis*, *Phytophthora sojae,* and *Pythium ultimum*. Distinct sexual compatibility types in *Phytophthora* are known as A1 and A2 mating types, which are needed for sexual reproduction to produce oospores. Sexual reproduction in oomycetes is hormone-dependent. A1 and A2 mating types secrete α1 and α2 hormones, respectively, to induce oospores in each different type (Qi *et al*., 2005). In heterothallic species, opposite mating types form antheridia and oogonia. Some examples of heterothallic oomycetes are *P. infestans, P. palmivora, P. ramorum,* and *Bremia lactucae*. In most cases, sexual development begins with the formation of male and female gametangia, antheridia and oogonia, respectively. Antheridia are confined by a septum and secrete adhesive materials which facilitate pairing (Judelson, 2009), leading to organ-swelling. Simultaneously, meiosis occurs within both male and female gametangia. A

fertilization tube develops in between the antheridium and oogonium that transmits a single, haploid nucleus to the female gametangia. Most of the peronosporales family produce a single oospore within each oosphere.

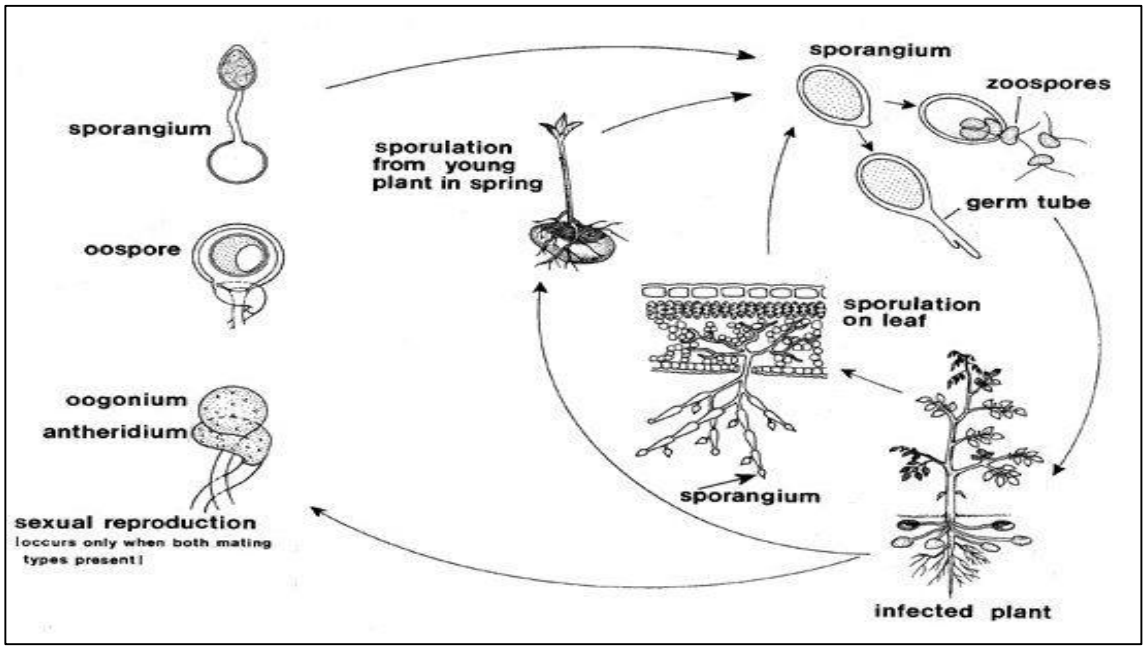

Figure 1.2 This figure is adapted from Schumann and D'Arcy (2000). Life cycle of *P. infestans* showing the sexual reproduction cycle on the left, and asexual reproduction cycle on the right, during plant infection.

There are two main phases in asexual reproduction in oomycetes. During the sporangiogenesis phase, multinucleate, lemon-shaped sporangia are formed. Subsequently during zoosporogenesis, the multinucleate cytoplasm of the sporangium cleaves to form uninucleate, motile, biflagellate, ovoid-shaped, zoospores which are released from sporangia. Multinucleate sporangia may germinate directly to hyphae, or cleave to produce zoospores, depending on the pathogen species and environmental conditions (Judelson, 2009). Both asexual sporangia and zoospores play important roles in initiating host infection.

1.3 Phylogenetic position of oomycetes

Oomycetes are not fungi, and belong to the stramenopiles super group (Birch and Whisson 2001; Burki *et al*., 2007). Also called heterokonts (kingdom Chromista), they are most closely related to brown algae and diatoms (Baldauf *et al*., 2000; Cavalier-Smith and Chao, 2006; Thines & Kamoun, 2010; Beakes *et al*., 2012). Sequencing of conserved genes from different organisms has helped to set the phylogenetic placement of oomycetes. Evidence from expressed sequence tag (EST) data from Burki *et al.* (2007) and Baldauf (2008) suggest the existence of the super-group SAR (stramenopiles, alveolates, rhizaria) forming the largest and most diverse division within eukaryotes. Stramenopiles are characterised by flagella consisting of rows of stiff and tripartite hairs, which enable swimming in water by dragging the cell forward. Cavalier-Smith and Chao (2006) suggested the evolutionary phylogenetic relationships of oomycetes and their relatives are within the super-kingdom chromalveolata. The kingdoms alveolata and chromista belong to this super-kingdom. Within the alveolata there are three groups; dinoflagellates, apicomplexans, and ciliates. Kingdom chromista contains the heterokonta (stramenopila), comprising five phyla: bigyra (labyrinthulids thraustochytrids, becoicids and opalinids), ochrophyta (ochrophytes), pseudofungi (hypochitrids, pirsonia, developayella, and oomycetes), haptophyta, and cryptophyta. According to Cavalier-Smith and Chao (2006), there are eight different groups within ancestral photosynthetic heterokonts: apicomplexan and ciliates in alveolata; labyrinthulids, thraustochytrids, becoicids and opalinids in bigyra; hypochitrids, pirsonia, developayella, and oomycetes in pseudofungi. In oomycetes, the plastid has been lost to become non-photosynethetic organisms (Figure 1.3). Baldauf (2008) described that stramenopila can either be photosynthetic, such as algae, diatoms, or xanthophytes, or non-photosynthetic, such as oomycetes, bicosoecids, or opalinids. The non-photosynthetic oomycetes are

holophyletic (Cavalier-Smith and Chao, 2006) and are one of the large groups of protists (including apicomplexans such as malaria parasites), having apical complex structures involved in penetrating host cells during infection.

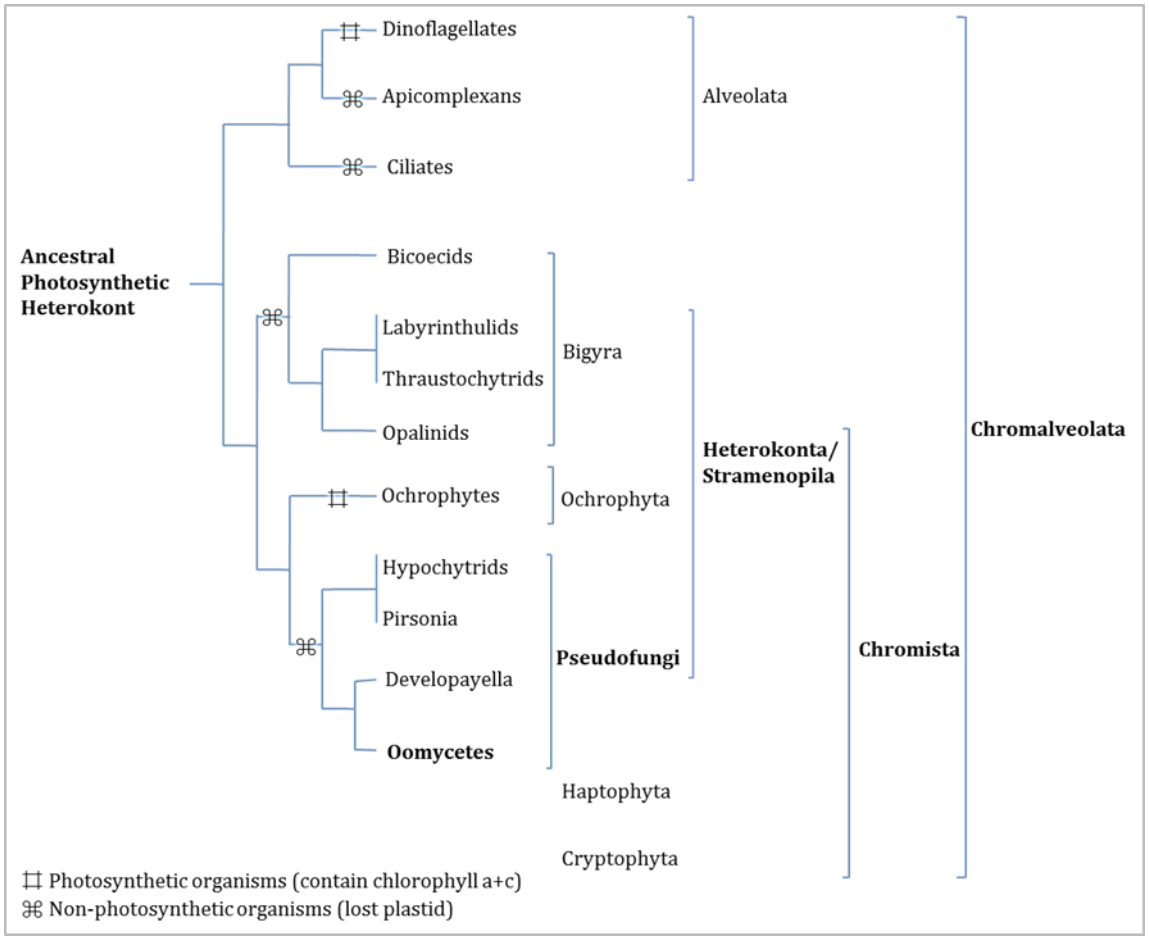

Figure 1.3 This figure is adapted from Beakes and Sekimoto (2009), as a summary of the ancestral photosynthetic heterokont in the super-kingdom Chromalveolata, described in Cavalier-Smith and Chao (2006). The figure summaries eight lineages including oomycetes, which have lost their plastid during phylogenetic evolution within the super-kingdom Chromalveolata. Two lineages, dinoflagellates and ochrophytes, are still photosynthetic.

1.4 Diversity of oomycetes

There are over 800 characterised diverse species of oomycetes (Govers, 2009). Some of the best known are the potato late blight pathogen, *P. infestans*; the soybean pathogen *P. sojae*; the 'sudden oak death' pathogen, *P. ramorum*; the obligate biotrophic pathogen of model plant *Arabidopsis thaliana*, *H. arabidopsidis*; the root rot pathogen of legumes,

Aphanomyces euteiches; turf-grass blight caused by *Pythium ultimum*; the fresh water fish pathogen, *Saprolegnia parasitica*; and pythiosis in mammals (including human) caused by *Pythium insidiosum* (Vanittanakom *et al*., 2004; Beakes and Sekimoto, 2009). Among these diverse genera of oomycetes, *Phytophthora* is one genus that has maintained interest within the research community due to the devastating impact of member species as plant pathogens. However, several other oomycetes such as *Bremia lactucae* (Hulbert *et al*., 1988), *Plasmopara viticola* (Dai *et al*., 1995), and *Peronospora tabacina* (Ye *et al*., 1989) are equally virulent to their plant hosts. Until recently more than 80 *Phytophthora* species were characterized (Kamoun, 2003; Hein *et al.*, 2009). Since then another 37 species have been defined, totalling 117 *Phytophthora* species (del Castillo-Munera *et al*., 2013). Additional species of *Phytophthora* continue to be described (Martin *et al*., 2013; 2014).

1.5 Oomycete genomes

ESTs are short sub-sequences of complimentary DNA (cDNA), synthesized from messenger RNA, and provide a sampling of the active gene content of an organism. EST datasets of different oomycetes such as *P. infestans* (Kamoun *et al*., 1999), *P. sojae* (Qutob *et al*., 2000), *S. parasitica* (Torto-Alalibo *et al*., 2005), *H. arabidopsidis* (Casimiro *et al*., 2006), *A. euteiches* (Gaulin *et al*., 2008), *P. ultimum* (Cheung *et al*., 2008), and *P. capsici* (Lamour *et al*., 2012) have been generated from different developmental stages of these pathogens. These datasets were developed to achieve valuable information of genes that are expressed at different lifecycle stages and during infection (Kamoun *et al*., 1999). *P. infestans* is the best characterized oomycete by ESTs. According to the *Phytophthora* GeneBank database (http://www.ncbi.nlm.nih.gov/nucest/?term= phytophthora) at the National Centre for Biotechnology Information (NCBI), *P. infestans* has the largest number of EST entries at 111,106, followed by *P. capsici* with 56,495, and

P. sojae with 28,467, as the next best characterized oomycetes. Large insert DNA libraries, which are beneficial for genetic analysis, have also been established for some oomycete species (Randall and Judelson, 1999). Several studies have used bacterial artificial chromosome or cosmid libraries, in conjunction with genetic linkage maps, to identify, clone and analyse oomycete genes (e.g. Randall and Judelson 1999; Whisson *et al*., 2001; Rehmany *et al*., 2003; Whisson *et al*., 2004).

The genome size of *P. infestans* is 240 megabases (Mb), which is considerably larger than other oomycetes, and the most complex oomycete genome sequenced (Haas *et al*., 2009). The sister taxa to *P. infestans*, such as *P. phaseoli*, *P. ipomeae* and *P. mirabilis* also have similar sized genomes (Raffaele *et al*., 2010). The next largest sequenced genomes are *H. arabidopsidis* (100 Mb; Baxter *et al*., 2010), *P. sojae* (95 Mb; Levesque *et al*., 2010), *P. ramorum* (65 Mb; Tyler *et al*., 2006), *P. capsici* (64 Mb; Lamour *et al*., 2012), *Saprolegnia parasitica* (63 Mb; Jiang *et al*., 2013), *Albugo candida* (45 Mb; Links *et al*., 2011), *Py. ultimum* (42.8 Mb; Levesque *et al*., 2010) and *Albugo laibachii* (up to 37 Mb; Kemen *et al*., 2011). Although *P. infestans* has the largest genome size, interestingly it shares similar gene content, after the exclusion of transposable elements and other repeats, with *P. capsici, P. sojae and P. ramorum* (Lamour *et al*., 2012). However, there is a higher proportion of non-repetitive genes in *P. capsici* compared to other well-characterized *Phytophthora* species (Tyler *et al*., 2006; Haas *et al*., 2009; both cited in Lamour *et al*., 2012).

1.6 Genomic comparisons between oomycetes and fungi

Due to the morphological similarities of oomycetes with fungi, interest has been drawn to gene comparisons between these groups. For example, according to expressed gene contents of oomycete and fungal pathogens, both have common conserved pectate lyases

(Randall *et al*., 2005). Pectate lyase-like genes have several functions and are found in different organisms. In plants pectate lyase-like genes are expressed in different tissues such as germinating seeds, pollen cells, and ripening fruit, and are functionally active in cell wall degradation and fruit ripening (Marin-Rodriguez, *et al.,* 2002). Walton (1994) defined pectate lyases as a cell wall degrading component of fungal pathogens, which may be necessary for pathogenicity. The analysis of pectate lyase genes in oomycetes was recently reported for *P. capsici*. Pectate lyase Pcpel1 in *P. capsici* is strongly expressed during host interactions, suggestive of involvement in host infection dynamics, especially in host cell wall degradation (Fu *et al*., 2013). Other than pectate lyases, there are several other genes, such as alkaline non-lysosomal ceramidase, homogentisate 1,2-dioxygenase, molybdenum cofactor biosynthesis protein, metal tolerance protein, serine protease, gephyrin, lysophospholipase, and COP9 signalosome complex subunit 6, that exhibit sequence similarities characteristic of a common evolutionary origin in oomycetes and fungi (Richards *et al*., 2006; 2011; Soanes *et al*., 2008).

1.7 Background of *Phytophthora infestans* and its relationship with *Solanaceae*

The etymology of *Phytophthora* is ‘plant destroyer’ (Erwin and Ribiero, 1996; Birch and Whisson, 2001). The scientific study of this aggressive and destructive pathogen began in 1876, when de Bary named *Phytophthora* as a separate genus. The best-studied oomycete species is *P. infestans*, the causal agent of late blight in potato and tomato. This pathogen infects solanaceous species such as potato and tomato (Fry and Goodwin, 1997a) and can destroy entire plants within a week (Birch and Whisson, 2001; Figure 1.4e). Disease symptoms on infected potato leaves start as a water–soaked lesion which gradually blackens. Purple–black or brown–black lesions typically start at the leaf tip and spread across the entire leaf, and eventually to the stem. Masses of sporangia develop on

the underside of the leaf (Figure 1.4a). Infected tuber symptoms occur later in the season and appear as slightly brown or purple blotches on the skin (Figure 1.4b). According to Chowdappa *et al*. (2013), the symptoms of tomato blight are similar to potato blight, as infection in tomato leaves shows the typical water–soaked brown lesions on the leaves (Figure 1.4c) and stems. Usually, *P. infestans* infects green fruit but there is also some evidence of the pathogen infecting ripe fruit (Figure 1.4d). The surface of the infected fruit looks necrotic, leathery and has white sporulation.

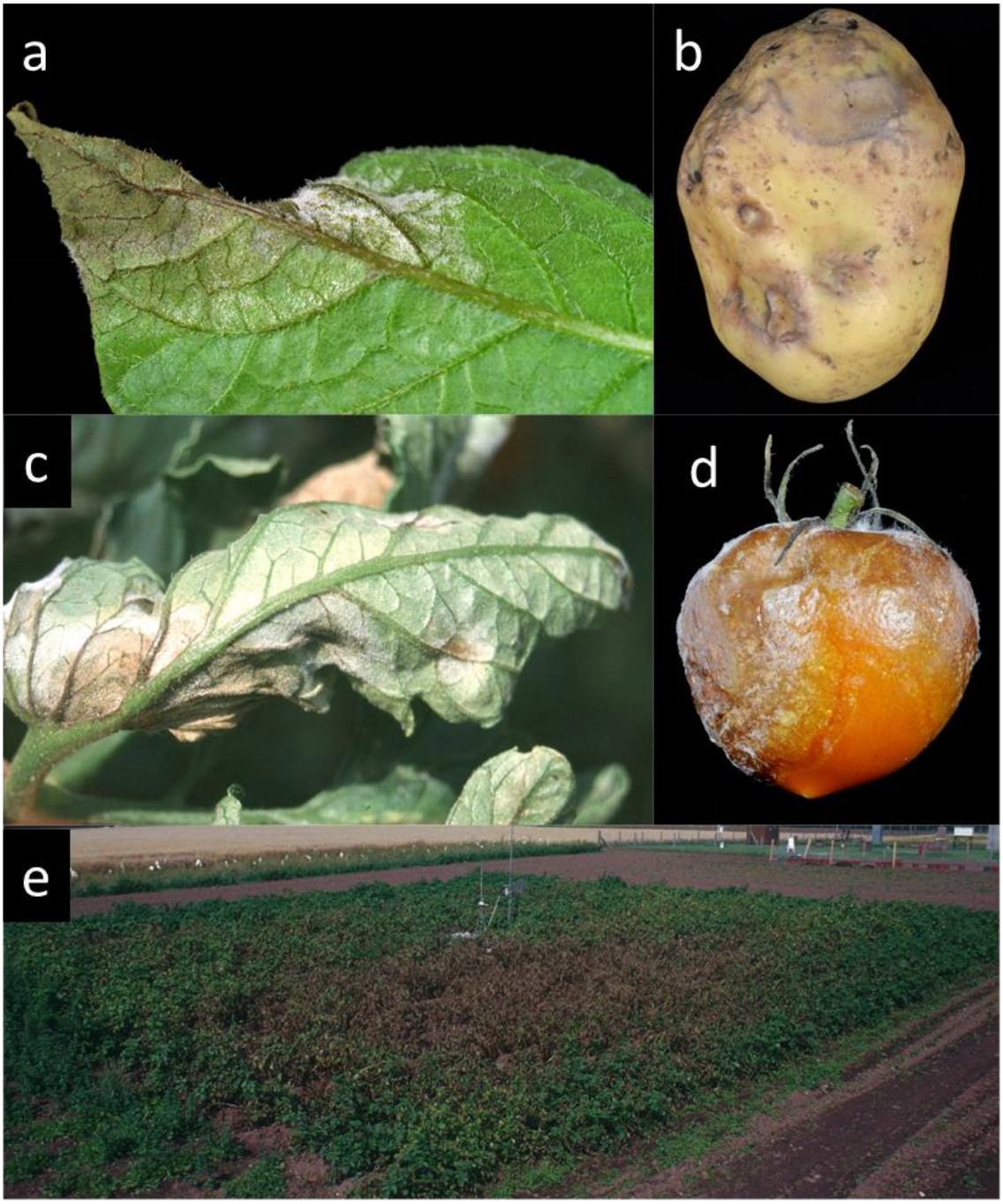

Figure 1.4 These figures (sourced from David Cooke, James Hutton Institute) show *P. infestans* disease symptoms in *Solanaceae* such as potato (a and b) and tomato (c and d). Potato field (e) showing disease epidemic within a week from the start of the initial infection.

The late blight pathogen *Phytophthora infestans* (de Bary, 1876) is an economically important pathogen. There are several epidemics of plant diseases which have impacted on human health, food and nutrition, and also the environment. One of the most disastrous epidemics was the Irish potato famine during the 1840s, resulting in the death of approximately one million people from starvation, as well as the immigration of two million of the Irish population to Great Britain and North America (Bartoletti, 2001) due to the disastrous potato crop losses. Even today potato late blight remains a problem, especially during wet summers. In these conditions, farmers have little choice but to apply more control chemicals to crops and/or plant new resistant potato varieties such as Sarpo Axona or Sarpo Mira. Metalaxyl/Mefenoxam is an early oomycete-specific control chemical and has been used as an effective chemical agent to control disease caused by a wide range of oomycetes. Resistance of some of the *P. infestans* population to Metalaxyl was reported early after its initial use (Davidse *et al*., 1981). Since then this trait has been used as a phenotypic marker to differentiate pathogen populations (Fry *et al*., 2009). Despite the large amounts of chemical control agents applied to potato and tomato crops, naturally occurring *P. infestans* strains resistant to other oomycete control chemicals have not been reported in the literature.

1.8 Population diversity of *Phytophthora infestans*

Initially, phenotypic markers such as mating type (A1 and A2), virulence spectrum, and Metalaxyl sensitivity determined the diversity of *P. infestans*. Phenotypic markers such as mating type are considered as robust markers, although this is controversial as other variable factors can lead to the unintentional production of gametangia, which could result in a change of mating type (Groves and Ristaino, 2000). Eleven specific *R* genes, originating from *Solanum demissum*, were used to define virulence characteristics of

pathogen populations (Fry, 2008). The combination of specific *R* genes overcome by isolates of *P. infestans* provided an overview of pathogen population diversity.

In recent years, research innovations in molecular technologies have led to development of genotyping methods which are more precise for identifying population diversity. Molecular markers have been used for genotyping *P. infestans* populations such as allozymes, mitochondrial haplotypes, simple sequence repeats (SSRs or microsatellites), restriction fragment length polymorphisms (RFLPs), and amplified fragment length polymorhisms (AFLPs) (Cooke and Lees, 2004).

The origin of *P. infestans* is considered to be the Toluca Valley, located in Central Mexico (Grunwald and Flier, 2005), where both A1 and A2 mating types were discovered before the 1970s. However, there is also an opinion that *P. infestans* originated in South America (Gomez-Alpizar *et al*., 2007). With the exception of central Mexico, the *P. infestans* populations were only A1 mating type. The migration of the A2 mating type of *P. infestans* to Europe is thought to have occurred in 1976 (Hohl and Iselin, 1984). Current populations of *P. infestans* in central Mexico, believed to be the origin of this pathogen, have a 1:1 ratio between A1 and A2 mating types, whereas northern Mexico is still dominated by clonal lineages (Goodwin *et al.*, 1992). Until 1980, only the A1 mating type was found in all tested *P. infestans* isolates in Europe. Since 1981, A2 mating types were reported outside Mexico, subsequently influencing the diversity of the global population (Fry *et al*., 2009). According to Nattrass and Ryan (1951), *P. infestans* was first reported in Africa in 1941. Although initially only the A1 mating type of *P. infestans* was identified in 1958 in South Africa (Smooth *et al.*, 1958), in Northern Africa both A1 and A2 mating types were reported in the late 1990s (Shaat, 2002). The *P. infestans* populations in South America are differently distributed. Southern parts of South America such as Argentina,

and southern Brazil were dominated by A2 mating types and the northern parts such as Peru and Colombia were dominated by A1 mating types until the late 1990s (Forbes *et al*., 1998). So far the pathogen population circumstances in South America remain unchanged (Fry *et al*., 2009). Current *P. infestans* populations in Asia are diverse. Although in many Asian countries the existence of the old clonal US-1 lineage has been reported as the dominant population until the 1980s (Goodwin *et al*., 1994), new and diverse populations have replaced the old lineage since then (Fry *et al*., 1993). According to Ghimire *et al*. (2003), 11 isolates amongst 280 tested from South-Asia (Nepal) had diverse multi-locus genotypes, based on RG57 fingerprinting (DNA RFLP probe) analysis. Similarly, the United States and Canada were dominated by the US-1 *P. infestans* lineage until the first report of the A2 mating type in the USA (Deahl *et al*., 1991). Both mating types, A1 and A2, are now common in the USA and Canada (Fry *et al*., 2009).

1.9 Disease impact

Solanaceous species such as potatoes and tomatoes are important global crops. According to the FAO data (2012), potato was ranked as the third commodity in terms of global production (more than 324 million metric tonnes) (Birch *et al*., 2012), whilst ranked 12th according to its value (more than 50.27 billion USD). At present, more than 800 million people, out of the global population of nearly seven billion, are suffering from chronic hunger and malnutrition (Can and Notes, 2011). Major crops such as potatoes and tomatoes have an important food security role. On the other hand, farmers are having difficulties in maintaining a high level of productivity owing to the destructive pathogen *P. infestans*. For example, because *P. infestans* is highly pathogenic and can spread rapidly, it can annihilate an entire crop within a few weeks unless it is controlled well in

advance. According to the International Potato Centre (CIP), the potato crop loss costs in developing countries and former Eastern Bloc countries totals €10 billion per year (CIP, 2010; Haverkort *et al*., 2009) possibly due to inadequate approaches to integrated pest management (IPM) and available resources. The impact is much lower within developed countries but is still significant; the cost of control and damage by late blight in Europe is estimated at €1 billion annually (CIP, 2010; Haverkort *et al*., 2009). Managing the impact of *P. infestans* is costly on a number of levels such as the economic costs linked with the resulting low yields, the costs of chemical inputs (van Damme *et al*., 2009), as well as health and environmental concerns (CIP, 2010).

Non-genetically modified (GM) breeding programs have been unsuccessful in providing a long-term solution using resistant cultivars (Fry, 2008) leading to an excessive reliance upon chemical usage. However, due to the perceived negative environmental impact of chemical control, and that the pathogen population is able to rapidly overcome genetically resistant cultivars and some fungicides, for example Metalaxyl, *P. infestans* is difficult to manage (Gisi and Cohen, 1996). Potato resistance breeding strategies have been developed but these will require several years to produce resistant cultivars (Fry, 2008). Haverkort *et al*. (2008) discussed the impact of this pathogen in terms of the triple P concept and principles (Profit, Planet, People) suggesting that increasing potato resistance would lead to increased yields, make production more environmentally friendly by reducing chemical usage, and would improve global food security. *P. infestans* has played a negative role in affecting global food security and poverty reduction since the Irish potato famine to the present day, and will continue to threaten food security into the future until a robust strategy for managing its impact has been successfully developed. However, a relatively new strategy is emerging with the cloning of broad-spectrum resistance genes, such as *RB* (*Rpi-blb1*) and *Rpi-blb2* (van der Vossen *et al*., 2003; 2005), from the wild

potato *Solanum bulbocastanum* (Song *et al*., 2003), which potentially could lead to breeding programmes offering late blight resistant potato varieties.

1.10 Cell biology of *P. infestans* infection

For as many different pathogens that exist, there potentially exists a wide diversity of approaches and systems for causing disease. However, all of them are selected to colonize the host by using the specific attributes which enable them to evade host defenses, replicate, and finally to leave the infected host in order to spread the disease further (Alberts *et al*., 2008).

Pathogens such as oomycetes can be classified by their lifestyle into three basic categories: biotrophic, hemibiotrophic, and necrotrophic. Biotrophic pathogens, such as *H. arabidopsidis* and *B. lactucae*, require living hosts in order to survive. Hemibiotrophic pathogens start by colonizing tissues without killing the cells. *P. infestans* is a good example of a hemibiotrophic oomycete that interacts with its host in a biotrophic relationship during early infection and switches to necrotrophic growth for the completion of its life cycle (van Damme *et al*., 2009). Necrotrophic pathogens such as *Py. ultimum* colonise and kill plant cells by releasing toxins and lytic enzymes which break down the tissue for their utilization (van Kan, 2006).

Sporangia of *P. infestans* cleave and release zoospores under damp conditions below 12°C, which then rapidly encyst and produce germ tubes (Birch and Whisson, 2001). Sporangia of *P. infestans* germinate directly at higher temperatures (Sunseri *et al*., 2002). Zoospores encyst and germinate when any physical or nutrient uptake obstructions are encountered (Coffey and Gees, 1991). An appressorium forms at the tip of the germ tube, enabling penetration of the host cell surface to establish further infection. Appressoria are

formed within two hours of zoospore encystment and germination. The appressorium produces an infection peg that penetrates the host cells (Figure 1.5). Gees and Hohl (1988) state that most spores penetrate host tissue via stomata, although infection also occurs through direct penetration of epidermal cells. After host penetration, an infection vesicle is formed in the first infected cell which then develops into secondary hyphae which spread into surrounding plant tissue. Inside host tissue, hyphae spread intercellularly throughout the growing lesion, regularly producing haustoria to establish a biotrophic interaction. *P. infestans* can form biotrophic interactions in infected plant tissue through formation of primary infection vesicles and haustoria that are formed within host cells and are encased by the host cell plasma membrane. Depending on the pathogen species, for example *P. infestans*, after 3-5 days sporangiophores emerge through stomata to the outside of the leaf (Birch and Whisson, 2001; Avrova *et al*., 2008).

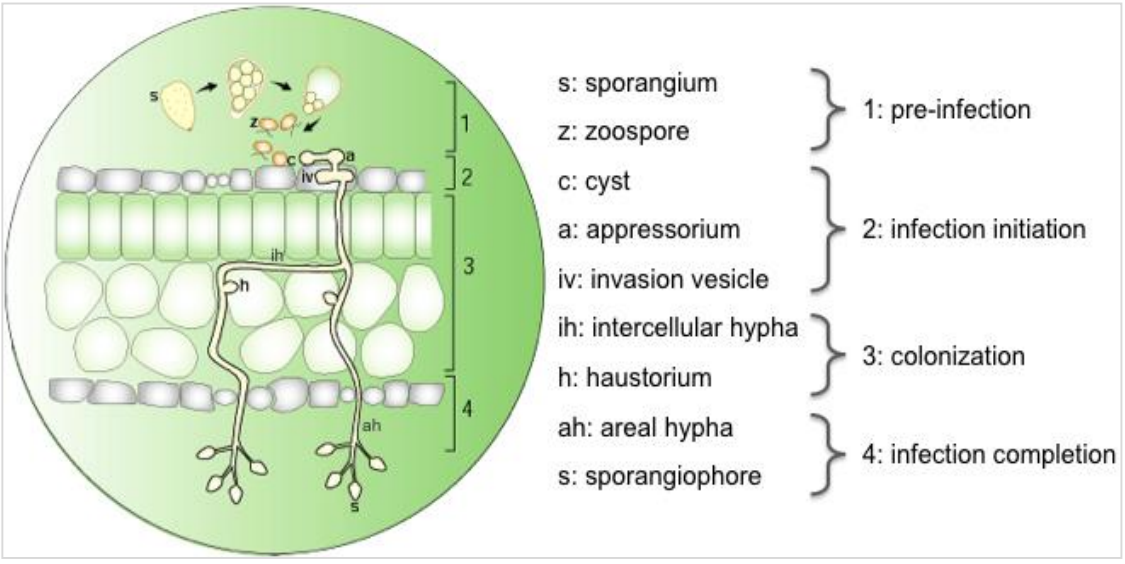

Figure 1.5 This figure is adapted from Paul Birch (University of Dundee). The figure explains the asexual infection lifecycle of hemibiotrophic *P. infestans*. In the presence of water and cool temperature, the cytoplasm of the sporangium on the leaf surface cleaves and produces biflagellate, motile zoospores that encyst and stick to the leaf cuticle. The appressorium, along with the infection peg penetrates the plant cell, developing an infection vesicle. Colonization occurs, forming intercellular hyphae along with haustoria in contacted host cells. Completion of the infection lifecycle occurs when the hyphae emerge out of the stomata, forming aerial sporangiophores.

1.11 Plant - pathogen interactions as an inter-molecular battle

Many authors (Ingle *et al*., 2006; Thines and Kamoun, 2010; Cournoyer and Dinesh-Kumar, 2011; van Damme *et al*., 2012) write about plant pathogen interactions using military terminology to describe and frame the interplay between plants and pathogens, which is similar to a war being played out at the molecular level. Both plants and pathogens have evolved defensive and offensive strategies to protect and conquer, respectively.

1.12 Plant immunity and disease resistance

Disease is a relatively rare phenomenon in any living organism, including plants. Plants alter their responses to multiple aggressors by activating defense signalling according to the nature of the pathogen. It is necessary to investigate and uncover the key mechanisms by which plants respond to their attackers (Pieterse and Dicke, 2007) in order to identify the molecules required by plants to protect themselves against potential microbial pathogens. Plants do not have mobile, adaptive defender cells and have to rely upon their innate immune system which can be classified into two branches. These include pattern recognition receptors (PRRs), which initiate the first line of defense, and specific resistance proteins which characterize the second line of defense (Cournoyer and Dinesh-Kumar, 2011; Jones and Dangl, 2006). Disease resistance can be classified into two different classes: as host-specific, or non-host specific. According to Ingle *et al*. (2006), non-host plant species can resist infection from many pathogen species due to pre-formed barriers such as antimicrobial compounds, a thick waxy cuticle, or are unsuitable as a source of nutrients. However, assuming that non-host resistance does not rely mostly on pre-formed barriers, other active perception and response mechanisms are used by plants to prevent infection.

PRRs at the plant cell surface are able to recognize foreign molecules that have conserved features, allowing the plants to distinguish them as non-self or modified-self. According to Segonzac and Zipfel (2011), plant PRR proteins are modular proteins that have an extracellular domain comprising leucine rich repeats (LRR) or chitin binding LysM domains in plants. These transmembrane PRRs respond to slowly evolving microbial- or pathogen-associated molecular patterns (MAMPs/PAMPs) that are characteristic of broad groups of microbes (Jones and Dangl, 2006; Boller and Felix, 2009). Non-self-molecules are PAMPs/MAMPs, while modified-self molecules include damage-associated molecular patterns (DAMPs). Upon recognition of these molecules by PRRs, the plant innate immune system responds to initiate defense responses, resulting in immunity to a non-pathogen. This is termed PAMP-triggered immunity (PTI) (Jones and Dangl, 2006). Interestingly, PRRs in both plant and animal cells consist of LRR domain proteins, which enable recognition of foreign molecules at the cell surface in both kingdoms (Postel and Kemmerling, 2009). PTI requires a range of defence responses such as activation of mitogen-activated protein kinases (MAPKs), production of reactive oxygen species (ROS), callose deposition, transcriptional reprogramming, and biosynthesis of hormones and secondary metabolites (Belkhadir *et al*., 2012).

The prevailing model of molecular plant-microbe interactions is the zig-zag model (Jones and Dangl, 2006; Hein *et al*., 2009) (Figure 1.6) which is believed to work in four phases. In the first phase, PTI that halts further colonization by potential pathogens. For example, the cell surface PRRs of the LRR-RK group in plants, such as FLS2 and EF-Tu, are activated in response to bacterial flagellin and elongation factor Tu, respectively, which triggers immune responses against microbes displaying these foreign molecules (Belkhadir *et al*., 2012).

The second phase is evolution and deployment of effectors to interfere with PTI, resulting in effector triggered susceptibility (ETS). In the third phase, plants evolve resistance (R) proteins to recognize specific effectors deployed by the pathogen, resulting in effector triggered immunity (ETI). This is often termed host-specific resistance, where genotypes of the plant host are susceptible to pathogens, but specific host genotypes recognize specific pathogen effectors to initiate resistance responses. Recognized effectors are termed avirulence (Avr) proteins. ETI often includes the hypersensitive response (HR), a form of programmed cell death (PCD) which restricts further pathogen growth by biotrophic or hemibiotrophic pathogens. In the fourth phase, the pathogen evolves to avoid ETI either by shedding or diversifying the effector genes recognized by the plant proteins, or by evolving new effectors that suppress ETI.

Pathogen-induced HR is often associated with activation of salicylic acid (SA)-regulated defense mechanisms in both local and distal parts of the plants, leading to systemic acquired resistance (SAR). Arabidopsis plants resist infection by pathogens including the bacterial pathogen *Pseudomonas syringae*, the eukaryotic oomycete *Hyaloperonospora arabidopsidis* (syn. *Peronospora parasistica*) and the obligate biotrophic fungal pathogen *Erysiphe orontii* via a combination of SAR, ETI (race-specific) and PTI (basal resistance) (Ausubel *et al*., 1995; Cao *et al*., 1997; Dewdney *et al*., 2000; Glazebrook, 2005; Reuber *et al*., 1998). Race specific resistance (ETI) in plants, characterized by the interactions between (typically) dominant resistance (*R*) genes and corresponding avirulence (*Avr*) genes, is explained in part by the gene-for-gene hypothesis (Flor, 1971).

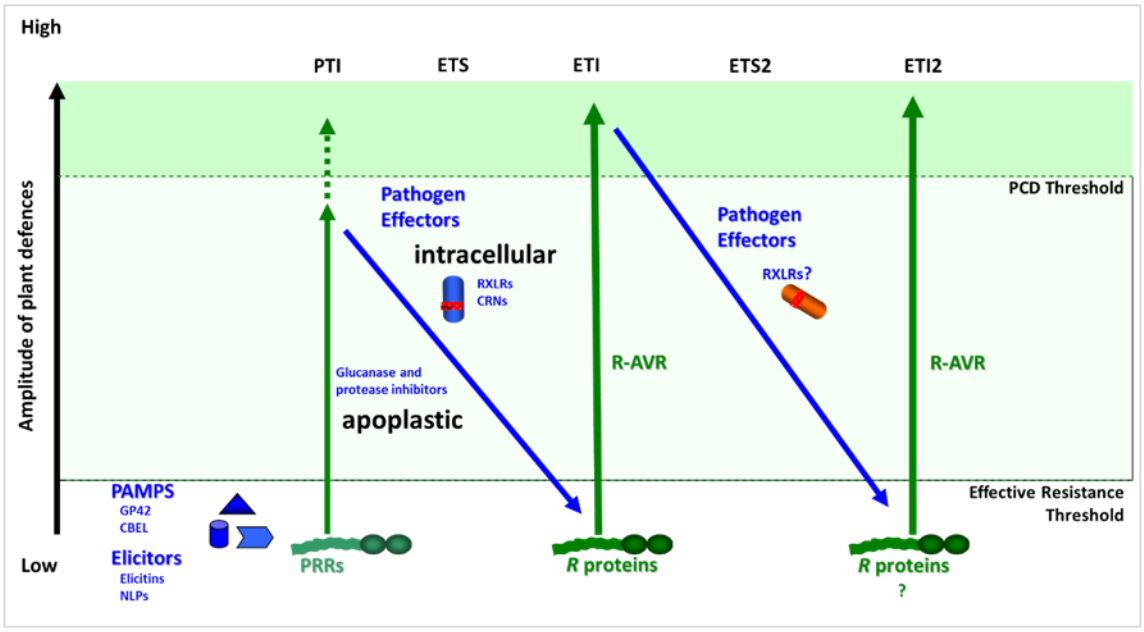

Figure 1.6 This figure is adapted from Hein *et al*. (2009) and explains the oomycete-plant interactions in the zig-zag-zig model. PAMPs and other elicitors from oomycetes trigger responses in the plant, leading to PTI. Effectors suppress these responses (ETS). Plant resistance proteins evolve to recognise effectors (ETI), leading to HR. The strength of plant response to pathogen attack is shown on the y axis, which shows the threshold of response beyond which PCD is initiated, and the threshold at which defence responses control pathogen growth.

PRRs are typically surface localized receptors, whereas R proteins are localised largely inside plant cells, responding to the pathogen effectors during infection. R proteins may also be surface receptor-like proteins, such as the Cf resistance proteins from tomato, conferring resistance to the fungal pathogen *Cladosporium fulvum*. However, the major class of R protein are intracellular and contain nucleotide binding site and leucine rich repeat domains (NB-LRRs). R proteins need to be located at the site where the effectors are or where the effectors are targeting, such as the NB-LRR protein in *A. thaliana* called RRS1-R that has been observed in the nucleus when triggered by the cognate PopP2 effector from *Ralstonia solanacearum* (bacterial wilt) (Deslandes *et al*., 2003). In addition, R proteins have to be located where they can initiate signals, triggering the plant's defense mechanisms (Cournoyer and Dinesh-Kumar, 2011). Recently it has been shown that different NB-LRRs may have different localizations, and also that sequences of some NB-LRRs do not predict their localizations (Elmore *et al*., 2011; Bernoux *et al*.,

2011; Jupe *et al*., 2012). It might be possible that NB-LRRs are able to travel throughout cell compartments either continuously or when triggered (Cournoyer and Dinesh-Kumar, 2011). Analyses of oomycete pathogen *Avr* genes with host *R* genes show that many genes conferring resistance to these pathogens have been discovered (Table 1.1). Analysis of these resistance genes shows that they belong to the NB-LRR class of resistance genes located in the plant cytoplasm, which implicates the translocation of oomycete Avr proteins into the host cell cytoplasm (Gururani *et al.,* 2012).

Table 1.1 This table is adapted from Gururani *et al*. (2012), which gives examples of four different species of oomycetes and their avirulence (*Avr*) genes interacting with corresponding resistance (*R*) genes from their hosts. Effectors that are recognized by the hosts are categorized as *Avr* genes, and host resistances that recognize effector proteins are referred as *R* genes.

Pathogen	**Host**	***Avr* gene**	***R* gene**	**Reference**
P. infestans	*S. tuberosum*	*Avr1*	*R1*	Ballvora *et al*., 2002
		Avr2	*R2*	Lokossou *et al*., 2009; Thomas *et al*., 1997
		Avr3a	*R3a*	Armstrong *et al*., 2005
	S. bulbocastanum	*Ipi-O1*	*Rpi-blb1*	Champouret *et al*., 2009
		Avr-blb1	*Rpi-blb1*	Vleeshouwers *et al*., 2008
P. sojae	*G. max*	*Avr1a, Avr3a Avr3c,*	*Rps1a, Rps3a, Rps3c*	Dong *et al*., 2009; Mao *et al*., 1996; Qutob *et al*., 2009
B. lactucae	*L. sativa*	*Avr3*	*Dm3*	Meyers *et al*., 1998; Michelmore *et al*., 2008
H. arabidopsidis	*A. thaliana*	*ATR1*	*RPP1-Nd/WsB,*	Rehmany *et al*., 2005
		AvrB, AvrRPP1A,	*RPP1,*	Botella *et al*., 1998
		ATR13	*RPP13-Nd*	Allen *et al*., 2004; Bittner-Eddy *et al*., 2000
		AvrRPP1B, AvrRPP1C, AvrRPP2	*RPP2,*	Parker *et al*., 1996
		AvrRPP4, AvrRPP5, AvrRPP8	*RPP4, RPP5, RPP8*	van der Biezen *et al*., 2002; Parker *et al*., 1997; McDowell *et al*., 1998

Due to the continuing threat to food security posed by plant diseases caused by fungi and oomycetes, it has become essential to develop new strategies for developing resistant varieties of valuable crops. Breeding strategies that have focused on using *R* genes are now thought to be less durable, compared with adopting a strategy that entails the use of mutated susceptibility (*S*) genes (Cooke *et al*., 2012; Andrivon *et al*., 2013). However, in

a plant breeding programme, identifying the *S* genes is difficult as they are genetically recessive. The hypothesis behind the use of mutated *S* genes in a breeding strategy is to destroy the probable connection between pathogen effectors and their virulence targets. Effector proteins are thought to interact directly with the target proteins, and therefore the target proteins are implicated in resistance/susceptibility in plants. By mutation of the susceptibility genes that are targeted by the effector genes, such that the effectors cannot interact, can lead to inhibition of disease development (Gawehns *et al*., 2013). However, some *S* genes that are involved in susceptibility are also important for plant growth and development. For example, *S* gene *Xa13* in rice is necessary for pollen development (Chu *et al*., 2006). Mutation analyses of these *S* genes with dual functions is a challenge in this strategy for resistance development.

One of the most widely studies *S* genes is the *mlo* gene in a variety of hosts, which provides resistance to fungal pathogen *Oidium neolycopersici* targeting *SlMlo1* in *S. lycopersicum* (Bai *et al*., 2008), bacterial pathogen *Pseudomonas syringae* targeting *MLO2* in *A. thaliana* (Lewis *et al*., 2012), and oomycete pathogen *H. arabidopsidis* targeting the pepper (*Capsicum annuum*) *MLO* gene *CaMLO2* when expressed in *A. thaliana* (Kim and Hwang, 2012). In these cases it is obvious these pathogens target MLO that serves as a negative regulator in disease resistance. However, there are other fungal, bacterial, and oomycete effector targets such as *MPK4* (Wang *et al*., 2009), *RIN4* (Mackey *et al*., 2002), and *CMPG1* (Bos *et al*., 2010; Gilroy *et al*., 2011) respectively, that could provide enhanced resistance to each pathogen if mutated to avoid binding to effectors. The more effector targets that are discovered, the more candidate *S* genes will be available for breeding to reduce susceptibility**,** to provide durable immunity in plants (Gawehns *et al*., 2013). Alternatively, it may be possible to identify non-host resistance genes that will confer broad spectrum resistance to multiple pathogens. For example, the

A. thaliana PSS1 gene has been shown to be a novel non-host resistance gene against a hemi-biotrophic oomycete pathogen, *P. sojae,* and a necrotrophic fungal pathogen, *Fusarium virguliforme* (Sumit *et al*., 2012).

1.13 PAMPs and elicitor molecules from *Phytophthora*

PAMPs and MAMPs are typically conserved molecules presented by diverse sets of pathogens. These evolutionary conserved molecules are functionally important and may be essential in contributing to disease development in plants. Commonly researched PAMPs and/or MAMPs in plant immunity studies encompass a 22 amino acid peptide from flagellin (flg22), an 18 amino acid peptide from elongation factor Tu (elf18) in bacteria, chitin in the cell walls of fungi (Belkhadir *et al*., 2012), and β-1,3-glucans in the cell wall of oomycetes (Aronson *et al*., 1967; Billon-Grand *et al*., 1997). Several other PAMPs associated with conserved molecules are well characterized in *Phytophthora* pathogens (Hein *et al*., 2009).

Phytophthora secretes a diverse array of PAMPs, elicitors, and effector proteins in order to colonise host plants. Three well characterized proteinaceous PAMPs are known from *Phytophthora*: Pep13, CBEL, and the elicitin infestin 1 (INF1).

Pep-13 is a PAMP which is highly conserved in several *Phytophthora* species such as *P. infestans*, *P. capsici*, *P. sojae,* and *P. parasitica*. It is characterized as a surface-exposed, 13 amino acid oligopeptide fragment of a calcium-dependent cell wall transglutaminase (TGase), which was initially detected in *P. sojae*. Pep-13 activates PTI in diverse host plants such as parsley and potato (Brunner *et al*., 2002; Halim *et al*., 2004). Brunner *et al*. (2002) showed that Pep-13 treated potato cells accumulated defence-related transcripts encoding lipoxygenase, 4-coumarate-CoA ligase, and PR protein 1. Halim *et al*. (2004)

reports that Pep-13 triggers defence responses by generating ROS in potato plants, and also triggering SA and JA -dependant defence responses.

The cellulose binding elicitor lectin (CBEL) is another PAMP from *Phytophthora* (Gaulin *et al*., 2002) which elicits plant defence. This glycoprotein was initially characterized from *P. parasitica* and its involvement in *Phytophthora* cell wall deposition and adhesion to cellulose substrates was reported (Gaulin *et al*., 2002). A later study (Gaulin *et al*., 2006) revealed that CBEL contains two cellulose-binding domains (CBDs) in Carbohydrate Binding Module1 (CBM1), which are responsible for inducing defence responses in plants. One of the CBM1 proteins is embedded in the hyphal cell wall of *P. infestans* (Jones and Ospina-Giraldo, 2011). Besides plant hosts, the purification of CBEL in methylotrophic yeast *Pichia pastoris*, followed by treatment of plants with purified protein, has also confirmed that this protein is a powerful elicitor of immune responses (Larroque *et al*., 2011).

Infestin 1 (INF1) is the major secreted sterol carrier elicitin protein from *P. infestans*, which is involved in scavenging sterols from the environment (*Phytophthora* spp. are sterol auxotrophs) and triggers PTI in different species of solanaceous plants (Boissy *et al*., 1999; Huitema *et al*., 2005). Gene expression analysis shows that *INF1* is highly expressed in mycelium grown in different culture media, but expression in sporangiophores, zoospores, cysts, and germinating cysts was not observed. INF1 does not seem to enhance or mediate disease response in plants during *P. infestans* infection (Kamoun *et al*., 1997). However, the *brassinosteroid insensitive 1-associated receptor kinase 1* (*BAK1*) gene in plant hosts, which contributes to intracellular signal transduction, seems to respond to PAMPs, supporting that the absence of BAK1 reduces the INF1 mediated response in *N. benthamiana* (Heese *et al*., 2007). Recent research (Chaparro-

Garcia *et al*., 2011) also found that an LRR-RLK protein related to BAK1, called SERK3 (somatic embryogenesis receptor kinase 3), which when silenced in *N. benthamiana* enhanced disease susceptibility to *P. infestans*. NbSERK3 significantly contributed to regulation of immune responses triggered by the *P. infestans* PAMP, INF1.

1.14 Secreted effector proteins

Phytopathogenic bacteria can inject type III effector proteins (T3Es) direct into the plant cell cytoplasm via the type-III secretion system (T3SS) to suppress host defence (Block *et al*., 2008). Nonetheless, plant resistance proteins are able to recognize T3Es and cause ETI. In this process, R proteins are matched with the T3Es, leading to HR (Hueck, 1998).

All pathogenic oomycetes, including *Phytophthora,* manipulate their hosts by secreting an arsenal of effector proteins which target plant molecules and alter host plant processes. The predominant localization of the effector genes to dynamic regions of the genome probably contributes to rapid evolutionary changes resulting in evasion of plant resistance, and accounts for the considerable expansion in numbers of effector genes (Haas *et al*., 2009; Thines and Kamoun, 2010).

1.14.1 Apoplastic effectors

The intercellular space of plant tissue is called the apoplast. Most microbial pathogens, when trying to access plant cells, have to make their way through the plant apoplast. The plant immune system produces defense molecules to create a biochemical barrier within the apoplast, making it difficult for the pathogen to spread within the plant tissue. When a pathogen does enter the apoplast, it is recognized by the plant immune system, activating PTI, which launches defense responses comprising strengthened cell walls and releasing a range of antimicrobial proteins and other compounds. Plant pathogens secrete

different classes of effectors into the apoplast and cytoplasm of plants so that they can suppress host defense mechanisms and facilitate successful infection (Jones and Dangl, 2006; Chisholm *et al*., 2006). The extra haustorial matrix (EHM) can also be considered as part of the plant apoplast. The effectors that are secreted into the plant apoplast or EHM are called apoplastic effectors. According to Stassen and Van den Ackervecken (2011), during interaction with the host, oomycete pathogens secrete at least three types of apoplastic effectors which interfere with host defence processes and promote pathogen colonization: host enzyme inhibitors, RGD (Arginine-Glycine-Aspartic acid) containing proteins, and toxins. Kamoun (2006) has listed the identification of several oomycete apoplastic effectors based on biochemical purification as well as bioinformatic predictions, including glucanase inhibitors GP1 and GP2, serine protease inhibitors EPI1 and EPI10, cysteine protease inhibitors EPIC1 and EPIC2, and small cysteine-rich proteins (PcF, PcF-like SCR74, SCR91, Ppat12, Ppat14, Ppat23, Ppat24). In addition, a class of secreted proteins of unknown function, the Nep1-like (NLP) family (PaNie, NPP1, PsojNIP, PiNPP1) are also secreted into the apoplast, where they can cause host cell cytotoxocity. The model is that apoplastic effectors such as glucanase and protease inhibitors are secreted into the plant extracellular space where they interact with their plant targets and inhibit enzymatic activities of plant PR proteins. There are several apoplastic effectors that have been identified (Table 1.2) in different fungal and oomycete plant pathogens (Doehlemann and Hemetsberger, 2013).

Table 1.2 This table is adapted from Doehlemann and Hemetsberger, 2013. Apoplastic effectors from various filamentous pathogens and their functions are listed.

Organism	Effector	Life style	Phenotype/task	Known target	Citation
Cladosporium fulvum	*Avr2*	Biotroph	Cysteine protease inhibition	*PIP1, RCR3*	Rooney *et al*., (2005); van Esse *et al*. (2008)
C. fulvum	*Ecp6*	Biotroph	Reduced virulence/ chitin sequestration	Chitin	Bolton *et al*. (2008); de Jonge *et al*. (2010)
C. fulvum	*Ecp7*	Biotroph	Reduced virulence	Unknown	Bolton *et al*. (2008)
Colletotrichum higginsianum	*ChEC3*	Hemibiotroph	Unknown	Unknown	Kleemann *et al*. (2012)
Colletotrichum orbiculare	*NIS1*	Hemibiotroph	Unknown	Unknown	Yoshino *et al*. (2012)
Fusarium oxysporum f. sp. lycopersici	*Six1*	Hemibiotroph	Required for full virulence	Unknown	Rep *et al*. (2004)
F. oxysporum f. sp. lycopersici	*Avr1 (Six4)*	Hemibiotroph	Suppression of I-2 and I-3 resistance	Unknown	Houterman *et al*. (2007)
Fusarium verticillioides	Fumosin *B1*	Hemibiotroph	Glucanase inhibition	β–1,3–Glucans	Sanchez-Rangel *et al*. (2012)
Phytophthora. infestans	*EPI1*	Hemibiotroph	Serine protease inhibition	Serine proteases	Tian *et al*. (2004)
P. infestans	*EPI10*	Hemibiotroph	Serine protease inhibition	Serine proteases	Tian *et al*. (2005)
P. infestans	*EPIC1*	Hemibiotroph	Cysteine protease inhibition	*PIP1, RCR3*	Tian *et al*. (2007); Song *et al*. (2009)
P. infestans	*EPIC2B*	Hemibiotroph	Cysteine protease inhibition	*PIP1, RCR4*	Tian *et al*. (2007); Song *et al*. (2009)
Phytophthora sojae	*GIP1*	Hemibiotroph	Glucanase inhibition	β–1,3–Glucans	Rose *et al*. (2002)
Leptosphaeria maculans	*AvrLm4-7*	Hemibiotroph	Unknown	Unknown	Parlange *et al*. (2009)
Mycosphaerella graminicola	*Mg1LysM, Mg3LysM*	Hemibiotroph	Chitin sequestration & shielding	Chitin	Marshall *et al*. (2011)
Melampsora lini	*AvrP(123)*	Biotroph	Contains serine protease inhibitor motif	Unknown	Catanzariti *et al*. (2006)
Magnaporth oryzae	*Slp1*	Hemibiotroph	Chitin sequestration	Chitin	Mentlak *et al*. (2012)
Rhynchosporium secalis	*Nip1*	Hemibiotroph	Unknown	Unknown	Rohe *et al*. (1995)
Ustilago maydis	*Pep1*	Biotroph	Biotroph peroxidase inhibition	*POX12*	Doehlemann *et al*. (2009); Hemetsberger *et al*. (2012)
U. maydis	*Pit2*	Biotroph	Cysteine protease inhibition	*CP2, CP1A/B, XCP2* proteases	Doehlemann *et al*. (2011); Mueller *et al*. (2013)
Verticilium dahliae	*Ave1*	Hemibiotroph	Contributes to virulence	*Ve1* receptor	de Jonge *et al*. (2012)

Extracellular protease inhibitor EPI1 of *P. infestans* interacts with PR protein P69B of tomato. EPI1 is part of a family of proteins in *P. infestans* with kazal-like extracellular serine protease inhibitor activity that inhibits subtilisin-like serine protease P69B in tomato to enhance disease susceptibility (Tian *et al*., 2004). Although there might be various levels of interaction occurring during a successful infection, the evidence suggests that the P69B protein in tomato might be a necessary target for *P. infestans* infection.

More protease inhibitor families have been found that overcome the action of plant proteases during infection. Tian *et al*. (2007) described EPIC1, EPIC2, EPIC3, and EPIC4 in *P. infestans* that form a family of cystatin-like protease inhibitors that inhibit the action of plant cysteine proteases. Among these protease inhibitors, EPIC1 and EPIC2 are unique to *P. infestans*, compared to *P. sojae* and *P. ramorum*, and are up-regulated during tomato infection. During interaction, EPIC2B binds and inhibits the action of tomato PR protein PIP1 (*Phytophthora* Inhibited Protein 1).

Besides protease inhibitors, there are several other apoplastic inhibitors which are well characterized in oomycete pathogens. The production of endo-β-1, 3-glucanases by plants is essential for defense by degrading β-1, 3/1, 6-glucans in pathogen cell walls or for the release of elicitors such as oligosaccharides (Rose *et al*., 2002). GIPs in *P. sojae* are secreted to block the endoglucanase function in soybean. Rose *et al*. (2002) identified two soybean endoglucanases, EGaseA that has high-affinity binding with GIP1, and EGaseB where no link to GIPs is indicated. However, GIPs are believed to be used by pathogens for the suppression of plant defenses (Rose *et al*., 2002).

There are many *Phytophthora* proteins that are related to causing cell death in plants. According to Fellbrich *et al*. (2002), necrosis-inducing *Phytophthora* protein 1 (NPP1) has homologs in oomycetes, fungi, and bacteria. This protein from *P. parasitica* plays an important role in inducing cell-death in parsley. Small cysteine rich proteins such as *scr74* (Liu *et al*., 2005), and *scr91* (Bos *et al*., 2003), are two types of PcF-like genes found in *P. infestans*, and may be toxic to the host, as the PCF protein from *P. cactorum* triggers responses in plants that are similar to disease symptoms (Orsomando *et al*., 2001).

1.14.2 Cytoplasmic effectors

Besides apoplastic effectors, there are also cytoplasmic effectors which are secreted by the pathogen for plant colonization. The difference is that cytoplasmic effectors are delivered or translocated inside the plant cell cytoplasm where they may be associated with different subcellular compartments (Kamoun, 2006; Whisson *et al*., 2007). In oomycetes, cytoplasmic effectors include all the race-specific Avr proteins that have the conserved amino (N) terminal motif Arginine-any amino acid-Leucine-Arginine (RxLR). This peptide sequence is similar to a signal required for the delivery of proteins from malaria parasites to their host cell cytoplasm (Birch *et al*., 2006; Kamoun, 2006). The RxLR motif is frequently followed by a less conserved motif Glutamic acid-Glutamic acid-Arginine (EER) (Birch *et al*., 2006). Together the motifs mediate delivery of these effectors inside host plant cells (Whisson *et al*., 2007). An additional class of oomycete effectors, called Crinkle and Necrosis proteins (Crinklers; CRN) possess a conserved LFLAK domain (Haas *et al*., 2009), which is proposed to direct translocation into host cells (Schornack *et al*., 2010). From genome sequence analysis, the predicted RxLR genes in *P. infestans* genome total 563 genes, compared to *P. sojae* (335 genes) and *P. ramorum* (309 genes). The predicted crinkler effectors are very diverse, with 196 genes detected in *P. infestans,* compared to 100 genes in *P. sojae,* and 19 genes *in P. ramorum*. The modular crinkler proteins have a highly conserved N-terminal domain and 60% of them possess a predicted signal peptide (Haas *et al*., 2009).

Support for the hypothesis that oomycetes deliver RxLR effector proteins into plant cells was initially based upon the detection of *AVR3a* by cognate *R3a* protein within the plant cytoplasm. R3a is a predicted cytoplasmic protein which only detected Avr3a when paired within the plant cytoplasm (Armstrong *et al*., 2005). Further support for effector

translocation came from the identification of the virulence target of Avr3a as CMPG1, a plant cytoplasmic ubiquitin E3 ligase (Bos *et al*., 2010). Furthermore, recognition of *P. infestans* effector protein Avr3a in the endosomal compartment by plant resistance protein R3a (Engelhardt *et al*., 2012), the association of BSL1 with *P. infestans* Avr2 and host R2 (Saunders *et al*., 2012) provide more evidence on the effector localisation into the host cell. Similarly, the recognition of *H. arabidopsidis* effectors in the host cell cytoplasm provides further evidence of translocation of oomycete effectors inside plant cells (Caillaud *et al*., 2012).

Unlike bacterial pathogens, which secrete effectors via the T3SS directly into the plant cell cytoplasm (Hueck, 1998; Cornelis, 2006; Coburn *et al*., 2007; Abramovitch *et al*., 2006; Segonzac and Zipfel, 2011) oomycete plant pathogens secrete their effectors through haustoria (Whisson *et al*., 2007; van Poppel *et al*., 2008; Gilroy *et al*., 2011), from where they are translocated into host cells. The haustorium is a biotrophic pathogen structure, thought to be necessary in effector translocation mechanisms. There is strong evidence that avirulence proteins AvrL567 from the fungal pathogen *Melampsora lini* (*M. lini*) are induced during infection and are highly expressed in haustoria (Dodds *et al*., 2004). Apart from oomycete pathogens, several known effectors from fungi such as AvrL567 (Dodds *et al*., 2004), and Uf-RTP1 (Kemen *et al*., 2005) from the Faba-bean rust pathogen (*Uromyces fabae*) are also secreted and delivered through haustoria (Birch *et al*., 2006).

1.15 Transcription factors and regulation of gene expression

Although bacteria (prokaryotic) and oomycetes (eukaryotic) share many similar principles of gene regulation, gene regulation in oomycetes and fungi is comparatively more complex as these eukaryotic organisms have longer stretches of DNA between co-

regulated genes and have many more proteins involved in gene regulation. RNA polymerases are needed by all genes to initiate transcription. Eukaryotic cells have three types of RNA polymerases in their nuclei: *RNA polymerase I*, *RNA polymerase II*, and *RNA polymerase III*. Genes encoding transfer RNA, ribosomal RNA, and several other small RNAs are transcribed by RNA polymerases I and III, whereas RNAs encoding proteins are transcribed by RNA polymerase II. General transcription factors (GTFs) are needed in transcription initiation by RNA polymerase II, where all single transcription factors have their independent role in promoters (Alberts *et al*., 2008). Many transcription factors are categorized according to their function, as they are the part of regulatory networks that bind to the promotor regions of target genes in order to regulate transcription (Ye *et al*., 2013). For example, the TATA box (double helix of DNA sequence composed of T and A) which is located 25 nucleotides upstream from the transcription start site, is recognized by TBP (TATA-binding protein) in TFIID (transcription factor for polymerase II D) (Alberts *et al*., 2008).

The role of transcription factors is as variable as the profiles of gene expression during infection and metabolism. Transcription factors such as WRKY in plants respond to abiotic and biotic stresses (Chen *et al*., 2012) and play vital roles in plant immunity (Pandey and Somssich, 2009). The *WRKY1* gene induced by a fungus-derived elicitor was regulated by WRKY transcription factors during early defence responses and found to accumulate in and around the infection site (Eulgem *et al*., 1999). Similarly, NAC transcription factors in plants are also equally important in responding to abiotic stresses (Nakashima *et al*., 2012) as well as oomycete pathogens (McLellan *et al*., 2013).

Although there has been recent research on oomycete transcription factors (Ye *et al*., 2013; Xiang and Judelson, 2014), in general, the role of transcription factors in regulating

oomycete gene expression during infection is poorly understood. *P. infestans* and other oomycetes have highly dynamic transcriptomes (Judelson *et al*., 2008), and coordination of groups of genes at specific stages will require the action of many stage-specific transcription factors. Oomycete genomes, including *P. infestans,* encode hundreds of candidate transcription factors (Seidl *et al*., 2012). However, these have not been explored to any great extent, especially during infection where a biotrophic interaction is occurring and effectors are tightly regulated (Whisson *et al*., 2007; Wang *et al*., 2011). The class of basic leucine zipper (bZIP) transcription factors in oomycetes undergo major transcriptional changes during zoospore formation, germinating cysts, and host infection (Ye *et al*., 2013). Xiang and Judelson (2010; 2014) have described the role of Myb transcription factors in growth and development in *P. infestans*. However, the specific function of this class of transcription factors in oomycetes is still not clear. According to Zhang *et al*. (2012), Myb transcription factors in *P. sojae* are required for zoospore development.

1.16 Transcriptome studies of oomycetes

In every eukaryotic pathogen, such as *P. infestans*, genes are regulated so that they are expressed at the right time and at the correct levels to maintain the cell or promote growth and proliferation. To gain information about gene functions relating to cell differentiation occurring during morphological or metabolic changes, which are caused by biotic and abiotic signals, knowledge and understanding of gene expression is required (Birch and Avrova, 2009). Oomycetes, including *P. infestans,* go through different life cycle stages as mentioned in the section "Morphological characteristics and life cycle of oomycetes". During different infection phases the pathogen passes through various developmental stages, providing clusters of molecular events. Molecular events during different sexual

and/or asexual stages of the lifecycle of oomycete pathogens were previously recorded in the form of ESTs (Randall *et al*., 2005; Torto-Alalibo *et al*, 2005, 2007; Le Berre *et al*., 2008; Gaulin *et al*., 2008), providing a platform for investigating oomycete biology.

In recent years, several reports were published on oomycete gene expression. Judelson *et al*. (2008) used an Affymetrix GeneChip microarray to find differentially expressed genes in different *in vitro* life stages of *P. infestans*. The first transcriptome profile of an obligate biotrophic oomycete, cucurbit pathogen *Pseudoperonospora cubensis* (*Ps. cubensis*) used mRNA-Seq analysis to reveal 2,383 differentially expressed transcripts, including 271 RxLR-type effectors, in sporangia and during cucumber infection (Savory *et al*., 2012). Similarly, transcriptome sequencing analysis of the lettuce downy mildew pathogen *B. lactucae* conducted by Stassen *et al*. (2012) found 16,372 protein coding sequences, including 1,023 encoding secreted proteins. Another RNA-Seq analysis was performed to reveal the global transcriptome of the lima bean pathogen *P. phaseoli* (Kunjeti *et al*., 2012). Out of 10,427 *P. phaseoli* genes, 318 were homologous to *P. infestans* genes, including INF1, INF4, and RxLR effectors such as PITG_04074. Similarly, EST analysis of the oomycete sunflower pathogen *Plasmopara halstedii* revealed five RxLR effectors (As-sadi *et al*., 2011). Transcriptomic studies of 19,027 predicted genes (Tyler *et al*., 2006) have provided a platform for digital gene-expression analysis of the soybean pathogen *P. sojae* (Ye *et al*., 2011). Gene expression results showed 396 RxLR effectors highly up-regulated in germinating cysts (GC) compared to early infection time points from 1.5 hours to 2 days. NimbleGen based microarray analysis of the *P. infestans* transcriptome has facilitated broader insights into the large repertoire of conserved and secreted proteins involved *in vitro* and in the interaction with the host. A diverse set of genes encoding PAMPs, RxLRs, CRNs, NLPs, SCR proteins, as well as metabolic enzymes, were up-regulated during infection (Haas *et al*., 2009). However, the first

sampled time point of infection in that study was at 48 hours post inoculation, and may have missed many genes that are specifically expressed early in the establishment of infection.

1.17 Research scope of this thesis

Although there are many other oomycete species which can infect different hosts such as algae, nematodes, crustaceans, aquatic animals, mammals, and various microorganisms, the focus of the research in this thesis will be based on the notorious pathogen *Phytophthora infestans*. There are many questions regarding *P. infestans* infection biology that remain to be addressed. Gaps in the knowledge for this pathogen include transcriptome studies of early biotrophy in *P. infestans*, identifying the 'core set' of effectors expressed by different *P. infestans* isolates; the potential roles of effectors in *P. infestans* infection of potato tuber tissues; and *P. infestans* transcriptome responses to growth in plant apoplast extracts. Topics arising in these areas are addressed as detailed below:

While there have been whole transcriptome studies of *P. infestans* during plant infection, none have focused on the earliest stages of infection, when the outcome of the infection is determined by PTI, ETS and ETI. The major hypothesis to be addressed here is that the pathogen molecules such as PAMPs, elicitors, and effectors, known to be necessary for the pathogen to colonise its host, should be differentially expressed from the earliest stages of infection. Here, potato leaves were inoculated with a fluorescently tagged *P. infestans*. RNAs from a time course of infection (12-60 hours post-inoculation) were hybridized to an Agilent-1-color microarray representing all *P. infestans* genes. The cell biology study of leaf infection was followed by confocal microscopy. Microarray results were analyzed using GeneSpring software and the expression of selected genes validated

by QRT-PCR. To determine a 'core set' of effectors in different isolates of *P. infestans*, effector expression determined here was compared to previous published studies that used different isolates (Haas *et al*., 2009; Cooke *et al*., 2012).

Tuber infection is little considered in models of *P. infestans* pathogenicity, but it is known that *P. infestans* can complete its infection cycle in potato tuber tissue. The hypotheses to be tested in this section of research are that *P. infestans* also expresses effectors during tuber infection, and that there are differences in pathogen gene expression in leaf and tuber tissue. Here, tuber infection was examined using fluorescently tagged *P. infestans* and followed by confocal microscopy. Prioritized PAMPs, RxLR effectors and other stage-specific genes were analyzed using QRT-PCR and compared to their expression during leaf infection. This revealed if there were differences in gene expression during tuber infection, compared to leaf infection.

P. infestans growth in leaf tissue is primarily in the apoplast, with only the small haustoria intimately contacting host cells. It is therefore essential to understand pathogen behavior in host apoplast. Several *P. infestans* effectors, such as glucanase and protease inhibitors, are known to be secreted into the host apoplast. The hypothesis to be tested in this section of research is that there are soluble signals present in the host plant apoplast that are perceived by *P. infestans* to up-regulate the expression of infection-related genes. Here, apoplastic fluid was extracted from host plant leaves and used as a growth substrate for *P. infestans*. A microarray experiment was conducted using 24 and 48 hours growth samples, and results analyzed using GeneSpring software. Expressed genes were compared with the leaf infection time course, and with *in vitro* growth in rich medium and starvation conditions. *P. infestans* growth was followed by light microscopy.

Chapter 2. Materials and methods

2.1 Maintenance of *P. infestans* cultures

P. infestans transformant 88069tdTomato10 (transgenic *P. infestans* isolate 88069 constitutively expressing the tandem dimer Tomato [tdTomato] fluorescent protein), and 88069-2c5mRFP11 (Avrova *et al*., 2008) expressing cytoplasmic GFP and Hmp1-mRFP were selected from the culture collection at the James Hutton Institute. Wild-type isolate 88069 was initially isolated from tomato in the Netherlands in 1988 (Kamoun *et al*., 1998). Transformation to produce the 88069tdTomato10 strain was done at the James Hutton Institute before this PhD project (S. Grouffaud, S.C. Whisson, P.R.J. Birch, unpublished). Cultures were grown on rye agar medium (Caten and Jinks, 1968; Judelson and Roberts, 2002) supplemented with 10 µg/ml of G418 (geneticin) antibiotic, at 18° C in darkness. Rye agar media was prepared by the media kitchen at the James Hutton Institute.

2.2 Plant growth conditions

Solanaceous plants *S. tuberosum* (cv. Bintje) and *N. benthamiana*, which are susceptible to *P. infestans*, were grown in the plant growth room and glasshouse respectively. The plant growth room was artificially illuminated and was set for a 16/8 hours light/dark photoperiod at 22°C. *N. benthamiana* plants were grown in a controlled environment glasshouse at 22 °C, with natural daylight supplemented with artificial lighting in the winter months. Growth of potato cv. Bintje was initiated from tubers stored at 4 °C, and grown in sterilized potting compost. Plants were checked twice a week to assure favourable growth conditions and absence of pests or disease.

2.3 Passage of *P. infestans* in potato micro plants

S. tuberosum cv. Pentland Ace (P. Ace) was used for passage of *P. infestans* to maintain pathogenicity. This cultivar carries the *R3a* gene for resistance to *P. infestans.* All isolates used in this thesis are able to overcome *R3a,* and so this cultivar was used for pathogen passaging. At first *in vitro* grown P. Ace micro plants were collected from the plant tissue culture unit at the James Hutton Institute, and then cultures were sub-cultured and maintained under 16/8 hours light/dark photoperiod conditions at 22° C until used. P. Ace was cultured in nutrient rich MS (Murashige and Skoog, 1962) medium.

A mixture of sporangia and mycelium of *P. infestans* 88069tdTomato10, grown on rye agar as described, were collected by flooding 14 day agar plate cultures with sterile distilled water at room temperature, and rubbing with a sterile spreader. The sporangia/mycelia suspension was decanted, centrifuged at 1118 × g, the supernatant discarded, and 10µl of the remaining suspension was inoculated onto *in vitro* grown (P. Ace) leaves in sterile conditions and incubated overnight in the dark. After six days, mycelium from the infected leaves was re-isolated on rye agar supplemented with 10 µg/ml geneticin and incubated in the dark at 18°C.

2.4 *P. infestans* 88069tdT10 inoculation on potato and sampling (infection time course)

2.4.1 Inoculum preparation

P. infestans 88069tdT10 was grown in 60 Petri dishes (90 mm diameter) of rye agar medium supplemented with geneticin antibiotic and checked for contamination by bright-field microscopy after 13 days growth. Each plate was flooded with 10 ml of ice-cold sterilised distilled water (SDW) under sterile conditions in the laminar flow hood. Flooded plates were separated into three batches to provide three separate biological

replicates and were incubated in the refrigerator at 4°C for three to four hours to let the sporangial cytoplasm cleave and release zoospores. Swimming zoospores were carefully decanted from plates into 50 ml centrifuge tubes at the ratio of four plates into one centrifuge tube. Gentle centrifugation at 1118 × g (relative centrifugal force; RCF) for 10 minutes was carried out to concentrate the suspension. Supernatants were gently decanted, leaving approximately 200 µl in each tube and pellets were re-suspended in 2 ml sterile distilled water. Re-suspended zoospores were collected in three separate tubes, with each tube representing a biological replicate (one tube representing one batch of source plate cultures, from above). 10 µl of the zoospore suspension was diluted 1:10 in sterile distilled water and counted on a haemocytometer (Modified Fuchs Rosenthal Counting Chamber - depth 0.2 mm; Weber Scientific International, Teddington, UK) under a bright-field microscope.

The zoospore dilution was thoroughly mixed by pipette and loaded onto both sides of the haemocytometer. The total number of motile zoospores on the four corner-quadrants with 16 squares were counted according to the protocol provided by Experimental Biosciences (http://www.ruf.rice.edu/~bioslabs/methods/ microscopy/cellcounting.html) and divided by four to calculate the average number of zoospores in one quadrant. This number was then multiplied by 10,000 to calculate the final concentration of the zoospores per ml in the stock suspension. Zoospore concentrations ranged from 3.4-6.8 × 10^5. The spore concentration for the inoculum was adjusted by dilution in sterile distilled water to yield the final concentration of 100,000 zoospores per ml.

2.4.2 Preparation of plant leaves for inoculation with *P. infestans*

Detached leaves from potato cv. Bintje were used for time course experiments. Three pots of plants grown for four to five weeks (before flowering) were selected and leaves from

these plants were detached using sterile scissors. Detached leaves from each of the different plants were placed in different plastic boxes and transferred to the laboratory bench. Damp (SDW) paper towels were spread inside clear plastic boxes to provide humid conditions. Detached leaves from each plant were arranged in rows inside the boxes on the damp paper towel, with each row representing a different plant. Leaves were placed abaxial side upward. A separate box was prepared for the mock inoculation for negative control samples.

2.4.3 Preparation of potato tubers for inoculation with *P. infestans*

Tubers from potato cv. Bintje were obtained from the James Hutton Institute, and organic potato tubers were bought from TESCO supermarket. Tubers were washed with SDW to remove any soil, and sprayed with 70% ethanol. The ethanol was immediately wiped from the tuber skin and six potato tubers were sliced using a sterile kitchen knife. The potato slices were approximately 5 mm thick. Separate high humidity plastic boxes were prepared as described above and slices were placed on the damp paper towel inside the boxes. A separate box was prepared for the mock inoculation for negative control samples.

2.4.4 Inoculation of leaf and tuber tissues

Zoospores (10 µl; 10^5 zoospores per ml) were drop inoculated onto the abaxial side of the detached leaves, and cut surfaces of sliced tubers at 20:00 hours GMT. Four sites on each detached leaf and tuber slice were inoculated. Water (mock) inoculation was also carried out for negative controls. Once inoculation was completed, boxes were gently wrapped with plastic cling-film, covered with black plastic, and incubated overnight at 19°C. The following morning, the black plastic covers were removed, and disease incubation

continued under 16/8 hours light/dark conditions. This experiment was repeated twice to complete three biological replications.

2.5 Digital imaging of infected leaves and tubers

Inoculated and non-inoculated leaves and tuber samples were removed from the high humidity plastic boxes and placed on black cotton for taking digital images. A 7.1 megapixel Canon ixus 75 digital camera with 3X zoom was used for digital image capture. Photos were taken before sampling for RNA extraction at each of the time points at 12 hourly intervals from 12hpi to 60hpi, and seven days post inoculation (dpi) (samples from 7dpi were not collected for RNA extraction) to observe macroscopic disease development.

2.6 Sampling of infected and mock inoculated samples for RNA extraction

Inoculated and mock-inoculated leaf and tuber tissues were collected during time course sampling. The first sampling at 12 hours post inoculation (hpi) was done at 08:00 in the morning and the following 12 hour intervals: 24hpi, 36hpi, 48hpi, 60hpi and 72hpi. Both leaf and tuber samples were cut using a 13 mm diameter cork borer with the inoculation droplet at the centre. Leaf samples were immediately transferred to 2 ml micro-centrifuge tubes and snap-frozen in liquid nitrogen prior to storage at -70 °C. Each centrifuge tube contained three leaf discs from three different leaves which were from three different plants to provide technical and biological replications. Similarly, tuber samples were stored in 5 ml bijou tubes. Three tuber discs from three different slices from three different tubers were collected in one bijou tube and immediately snap-forzen in liquid nitrogen prior to storage at -70°C. Non-infected leaves and tuber slices were also sampled as described for infected tissues.

2.7 Sampling of *P. infestans in vitro* lifecycle stages for RNA extraction

Four different stages of *P. infestans* were prepared *in vitro* for RNA extraction: sporangia, motile zoospores, germinating cysts, and cultured non-sporulating mycelium.

2.7.1 Sampling of sporangia for RNA extraction

P. infestans 88069tdT10 was grown on 20 plates of rye agar medium for 13 days in darkness at 19 °C. Cultures were flooded with 10 ml of room temperature SDW and sporangia rubbed off with a sterile glass spreader. The sporangial suspension was poured onto another plate and the process repeated for a total of five plates. The concentrated suspension was filtered through 60 µm nylon mesh (Millipore) in a sterile filter unit (Nalgene reusable plastic filter unit). This process was repeated until all 20 plates were harvested. The sporangia filtered through the mesh were pelleted by centrifugation in 50 ml centrifuge tubes at 1610 × g. The supernatant was discarded and pelleted sporangia were re-suspended in 200 µl of SDW per tube. The sporangial suspension was distributed as 100 µl aliquots in 1.5 ml micro-centrifuge tubes and frozen in liquid nitrogen prior to storage at -70 °C. This experiment was repeated twice to provide three biological replicates.

2.7.2 Sampling zoospores for RNA extraction

Twenty plates of *P. infestans* 88069tdT10 were used to prepare zoospores. Zoospores were prepared as described for plant inoculation. Gentle centrifugation at 1118 × g was carried out and supernatants were gently decanted, leaving approximately 100 µl in each tube. Pellets were re-suspended and transferred to 1.5 ml micro-centrifuge tubes. Five samples were prepared and frozen using liquid nitrogen prior to storage at -70 °C. This experiment was repeated twice to provide three biological replicates.

2.7.3 Sampling germinating cysts for RNA extraction

Zoospores were prepared as described in the preceding section. Re-suspended zoospores were transferred to one 50 ml centrifuge tube and induced to encyst using mechanical agitation on a vortex mixer for two minutes. Encysted zoospores were then incubated at 4 °C in a refrigerator overnight to allow cyst germination. The following morning, germinating cysts were observed under the microscope, to confirm that germination had occurred. The suspension was divided in 100 µl aliquots in 1.5 ml micro-centrifuge tubes, and frozen in liquid nitrogen prior to storage at -70°C. The experiment was repeated twice to provide biological replication.

2.7.4 Sampling vegetative mycelia for RNA extraction

Sporangia were collected from 20 rye agar plate cultures of *P. infestans* 88069tdT10 as described. The concentrated sporangial suspension was distributed as 100 µl aliquots in 300 ml bottles containing 250 ml sterile pea broth media (Whisson *et al*., 2005) and incubated at room temperature (19°C) for 60 hours. The mycelia were then filtered through 100 µm nylon mesh, washed with 5 ml SDW and immediately transferred to a 1.5 ml micro-centrifuge tube and frozen in liquid nitrogen prior to storage at -70°C. The process was repeated for five bottles. This experiment was repeated twice to provide biological replicates.

2.8 Live cell imaging - Confocal microscopy

A Leica TSC-SP2 AOBS confocal microscope was used to image pathogen infection progression in host tissues. *P. infestans* 88069tdT10 inoculated potato leaves and tubers from 12 hpi to 60 hpi were used for confocal microscopy. The pieces of leaf containing inoculation sites of each leaf were fixed to glass slides using adhesive tape to steady the

tissue while imaging, and mounted on the confocal microscope. Imaging of red fluorescent protein (tdTomato) was conducted using a lime laser that allowed a laser line of 561 nm excitation, and 570 to 610 nm emission (Shaner *et al*., 2004, 2008). Auto-fluorescence from chlorophyll was imaged with 488 nm excitation and 650 to 680 nm emission. GFP and mRFP imaging conditions were as described in Whisson *et al*. (2007) and Avrova *et al*. (2008). SDW was used for the water dipping lenses. Tuber tissues were sliced thinly before mounting on the slides and were covered with cover slips after adding a few drops of SDW directly onto the tuber slice. While imaging tuber infection with water dipping lenses, water was dropped on the cover glass to connect with it. tdTomato, mRFP, and GFP imaging were conducted on the tuber infection. HCX APO L U-V-I 40X0.8 and HCX APO L U-V-I 20X0.5 water dipping lenses were used in all imaging.

2.9 Apoplastic fluid isolation

Leaves of six week old glasshouse-grown *N. benthamiana* plants were collected (approximately four leaves per plant). A plastic vacuum chamber was three-quarter filled with ice-cold, sterile water and 20 leaves were submerged in water. A Millipore vacuum/ pressure pump with the maximum vacuum of 635 mm Hg was used to infiltrate the water into the apoplastic spaces of the leaves. The vacuum was applied for two minutes and then the infiltrated leaves were removed from the water. Excess water was removed by gentle blotting of the leaf surfaces with tissue paper. Six leaves were gently wrapped in muslin cloth, without damaging the leaves, and inserted into 20 ml syringes with the petiole facing downwards. The syringes were inserted into 50 ml centrifuge tubes and a gentle centrifugation at 280 × g was applied for 10 minutes to collect apoplastic fluid. Extracted apoplastic fluid was sterilised using a 0.2 µm syringe filter to avoid any bacterial contamination. Sterile apoplastic fluid was stored at -20°C until required.

2.10 *P. infestans* inoculation of apoplastic fluid (*N. benthamiana*), pea-broth and SDW, and sampling for RNA isolation

Zoospores of *P. infestans* 88069tdT10 were prepared as described and 50 µl of zoospores (10^5 zoospores per ml) were inoculated into 15 ml tubes containing either 5 ml of sterile apoplastic fluid from *N. benthamiana*, 5 ml of sterile pea-broth medium, or 5 ml of sterile distilled water. The lids of the tubes were closed and further sealed with Nescofilm, and the cultures were incubated in darkness at 19°C. Inoculations were completed as three biologically replicated samples for all three conditions (apoplastic fluid, pea broth, SDW). Two time points (24 hpi and 48 hpi) for each of the three different conditions were sampled for RNA isolation, by centrifuging the 15 ml tubes at 2205 × g for 10 minutes and decanting the supernatant, leaving approximately 100 µl to re-suspend the pellet. The re-suspended hyphae samples (100 µl) were then transferred into 1.5 ml micro centrifuge tubes, snap frozen in liquid nitrogen, and stored at -70°C.

2.11 Total RNA isolation

2.11.1 Leaf samples

Total RNA from frozen inoculated and mock inoculated leaf samples from all replicates was isolated using the RNeasy Plant Mini Kit and protocol provided by the manufacturer (Qiagen Inc., Valencia, CA, USA). Extraction buffer RLT (containing guanidinium thiocyanate) supplied with the kit was used in the extraction. Approximately 100 mg of frozen leaf tissue was ground to a fine powder in liquid nitrogen using sterile pestles and mortars. Total RNA was eluted using 50 µl RNase free water provided by the manufacturer. Immediate after the elution, the quantity and quality of the total RNA from each sample was assessed on a Nanodrop ND-1000 Spectrophotometer (Thermo Fisher Scientific Inc., Waltham, MA, USA) following the manufacturer's protocol to measure

full-spectrum ultraviolet and visible light (UV-Vis) absorbance of the RNA. Integrity of the RNA was assessed by 1% agarose gel electrophoresis of a 2 µl sample, staining with SYBR safe gel stain (Invitrogen), and image capture on a UV transilluminator.

2.11.2 *In vitro P. infestans* stages

Approximately 100 µl of frozen samples from all conditions (apoplastic fluid, pea-broth, and SDW inoculations; *in vitro* samples of sporangia, zoospores, germinating cysts, and cultured hyphae [60hpi]) were ground to a fine powder separately in liquid nitrogen using sterile pestles and mortars. Total RNA was extracted as described for infected leaf samples, except that total RNA was eluted in 35µl of RNase free water. Quantity, quality, and integrity of total RNA was assessed as described.

2.11.3 Tuber samples

Before RNA isolation, tuber discs collected in 5 ml bijous for RNA extraction were lyophilised using an Edwards freeze dryer (Edwards High Vacuum Pump, Crawley, Sussex, England) according to the online protocol provided by the manufacturer (http://www.edwardsvacuum.com/Support/Reference.aspx). RNA of high starch containing tuber tissues was extracted using the Tris Hydrochloride (Tris HCl) - sodium dodecyl sulfate (SDS) method (Stushnoff *et al*., 2010; Li and Trick, 2005). Prior to RNA extraction, RNA extraction buffer was prepared from the stock solution (Table 2.1). Approximately 600 mg of freeze-dried tuber tissue was used for RNA extraction for each sample. 7 ml of 50% (v/v) pH equilibrated liquid phenol was added to 7 ml of extraction buffer containing 50 mM Tris-HCl (pH 8.0), 50 mM LiCl, 5 mM EDTA (pH 7.0), 0.5% SDS, and 10 ml SDW and heated in a water bath (80°C) for 15 minutes. Concurrently, 16 ml of 4 M LiCl per sample was prepared and stored in a -20°C freezer. Lyophilised tuber discs were ground to a fine powder in liquid nitrogen using sterile pestles and mortars.

For each sample, 14 ml of hot phenol/extraction buffer was added to the mortar and ground further. The suspension was poured into a 50 ml phenol and chloroform-resistant centrifuge tube and mixed again using a vortex mixer. 10ml of SDW was added to it and it was mixed again. 15ml of chloroform: isoamyl alcohol (24:1) was then added and mixed for 2 minutes. The mixture was then centrifuged at 4°C at 14000 × g for 20 minutes and 16 ml of the aqueous layer was transferred into a 50 ml centrifuge tube containing an equal volume (16 ml) of 4 M LiCl. The mixture was incubated overnight at -80°C. The following morning, the mixture was centrifuged at 4°C at 14000 × g for 40 minutes and the supernatant was discarded. The pellet was re-suspended in a mixture of 5 ml of SDW and one-tenth volume (500 µl) of 3 M sodium acetate (NaOAc; pH 5.2) and three volumes (15 ml) of 100% ethanol were added to it. This mixture was incubated for 1 hour at -80°C, and centrifuged as described above for 40 minutes. The supernatant was discarded, the pellet was washed with 10 ml of ice-cold 70% (v/v) ethanol and centrifuged again. The ethanol was removed and the RNA pellet was air-dried before re-suspension in 500 µl of RNase free water. The quality, quantity, and integrity of the total RNA was assessed as described.

Table 2.1 Reagents for RNA extraction buffer used for freeze-dried tuber RNA extraction.

Reagents	Per sample (ml)- 7ml	Quantity prepared each time (ml)- 25ml
Tris-HCl (1M, pH 8.0)	0.7	2.5
LiCl (4M)	0.168	0.6
EDTA (0.5M) pH 7.0	0.14	0.5
SDS 20 % (w/v)	0.35	1.25
SDW	5.642	20.15

2.12 DNase treatment

DNase treatments for all extracted RNA samples from leaves, tubers, and *in vitro* samples; sporangia, zoospores, germinating cysts, and mycelia (20 µl of RNA per sample)

were carried out in order to remove any possible genomic DNA contamination in the samples. All RNA samples were diluted to 250 ng/µl before DNase treatment. The TURBO DNA-*free*™ Kit and protocol provided by the manufacturer (Applied Biosystems) was used.

2.13 Quality control of the extracted RNA (Bioanalyzer analysis)

Quality control of the extracted RNA was assessed using an Agilent Bioanalyser. All samples to be used for microarray experiments were assessed in this manner: mock inoculated leaves, infection time course (12hpi, 24hpi, 36hpi, 48hpi, and 60hpi), apoplastic fluid inoculations (24hpi and 48hpi), pea broth inoculations (24hpi and 48hpi), SDW inoculations (24hpi and 48hpi), and *in vitro* samples (sporangia, zoospores, and germinating cysts). For each sample, RNA was diluted to 100 ng/µl and 5 µl of this dilution was assessed on the Bioanalyser. The Agilent 2100 Bioanalyzer Expert Kit was used, following the protocol provided in the manufacturer's user guide (Agilent Technologies, Inc., Santa Clara, CA, USA).

2.14 Microarray hybridization and data analysis

Each Agilent GeneChip array comprised 18,256 probe sequences from the predicted transcriptome of *P. infestans* (Haas *et al*., 2009) and were designed using eArray software (Agilent Technologies, Inc., Santa Clara, CA, USA). Arrays were designed by the Genome Analysis Facility at the James Hutton Institute, and ordered from Agilent. Each microarray slide contained eight *P. infestans* microarrays (8 × 60K format slides). All RNA labelling, microarray array hybridizations, and primary data acquisition were performed by the Genome Analysis Facility at the James Hutton Institute. Briefly, 100 ng of total RNA for all control, *in planta* and *in vitro* samples were single colour labelled, and the microarray hybridization was performed following the Agilent One Colour Low

Input Quick Amp Labelling Kit, version 6.5, using the manufacturer's protocol (Agilent Technologies, Inc., Santa Clara, CA, USA). Total RNA samples were labelled with one-colour (cy3) spike mix, purified cRNAs were quantified using a NanoDrop spectrophotometer, hybridized overnight for 17 hours at 65°C in the buffers provided by the manufacturer, and washed with pre-warmed wash buffer overnight at 37°C.

Extracted *P. infestans* datasets were quality filtered according to the flag values that are present or marginal in two-thirds of the replicates and quantile-normalized using Genomic Suite software (Partek Inc., St Louis, MO, USA). Data analysis was conducted using Genespring software (version 7.3) provided by Agilent (Agilent Technologies, Inc., Santa Clara, CA, USA). A set of 57 genes were selected as reference genes for data normalization. These genes were selected from previously reported microarray data of *in vitro* growth life stages (Judelson *et al.*, 2008) and were selected due to their constitutive expression in all *in vitro* growth stages of the *P. infestans* life cycle such as sporangia, zoospores, germinating cysts, and cultured hyphae. The reference numbers of all 57 housekeeping genes used are listed in table 2.2 below.

Table 2.2 Control genes used in microarray data normalization. These genes were selected according to their constitutive expression in various *in vitro* life stages of *P. infestans* published in Judelson *et al*. (2008).

Description	**Primary accession**
3-hydroxyisobutyrate dehydrogenase, putative	PITG_17998
cytochrome oxidase biogenesis (Oxa1) family	PITG_13344
DEAD/DEAH box RNA helicase, putative	PITG_02856
folylpolyglutamate synthase, putative	PITG_01065
folylpolyglutamate synthase, putative	PITG_16937
geranylgeranyl transferase, putative	PITG_19200
H/ACA ribonucleoprotein complex subunit 3	PITG_18717
HSF-type DNA-binding protein, putative	PITG_03306
HSF-type DNA-binding protein, putative	PITG_05353
mannosyl-oligosaccharide alpha-1,2-mannosidase, putative	PITG_07365
mediator of RNA polymerase II transcription subunit, putative	PITG_14623
methylenetetrahydrofolate reductase, putative	PITG_05377
methyltransferase	PITG_05300
molybdenum cofactor sulfurase, putative	PITG_04515
notchless family protein	PITG_04722
nucleolar complex protein 3	PITG_12225
phosphoserine phosphatase	PITG_00166
polycomb protein EZH2, putative	PITG_13838
pre-mRNA-splicing factor ISY1	PITG_19064
ribosomal protein S6 kinase, putative	PITG_07055
transmembrane protein, putative	PITG_07279
ubiquitin family protein, putative	PITG_03160
conserved hypothetical protein	PITG_00025
conserved hypothetical protein	PITG_00456
conserved hypothetical protein	PITG_00723
conserved hypothetical protein	PITG_00995
conserved hypothetical protein	PITG_01119
conserved hypothetical protein	PITG_01740
conserved hypothetical protein	PITG_02193
conserved hypothetical protein	PITG_02244
conserved hypothetical protein	PITG_02790
conserved hypothetical protein	PITG_03932
conserved hypothetical protein	PITG_04699
conserved hypothetical protein	PITG_05128
conserved hypothetical protein	PITG_08084
conserved hypothetical protein	PITG_08183
conserved hypothetical protein	PITG_08307
conserved hypothetical protein	PITG_08673
conserved hypothetical protein	PITG_09522

Table 2.2 **(continued)**

Description	Primary accession
conserved hypothetical protein	PITG_09583
conserved hypothetical protein	PITG_09818
conserved hypothetical protein	PITG_11691
conserved hypothetical protein	PITG_12576
conserved hypothetical protein	PITG_13185
conserved hypothetical protein	PITG_14816
conserved hypothetical protein	PITG_15595
conserved hypothetical protein	PITG_16388
conserved hypothetical protein	PITG_19055
conserved hypothetical protein	PITG_19237
conserved hypothetical protein	PITG_20312
conserved hypothetical protein	PITG_20631
conserved hypothetical protein	PITG_21219
conserved hypothetical protein	PITG_21627
hypothetical protein	PITG_00235
hypothetical protein	PITG_02323
hypothetical protein	PITG_15137
hypothetical protein	PITG_19804

Normalized data were analysed using one-way ANOVA (analysis of variance with the principle of Benjamini and Hochberg multiple testing correction, $P \leq 0.005$) to discover genes for which expression changed significantly during the experiment.

To determine sets of genes that are differentially distributed among different conditions in an experiment, venn-diagrams (Bioinformatics: jquery.venny; http://bioinfo.genotoul.fr/index.php?id=116) were used. Genes that were co-expressed with previously published stage specific marker genes (sporulation, biotrophy, and necrotrophy markers) were grouped according to the minimum Pearson correlation of at least 95% from the ANOVA list.

2.15 General bioinformatics and data analysis

SignalP (version 4; http://www.cbs.dtu.dk/services/SignalP/) with the cut-off score of less than 0.5 was applied, adopting hidden Markov model (HMM) and neural network model

(NN), for identifying candidate secreted proteins (Petersen *et al*., 2011; Dyrløv *et al*., 2004). TMHMM (version 2; http://www.cbs.dtu.dk/services/TMHMM/) was used to identify predicted transmembrane helices in proteins (Krogh *et al*., 2001). These transmembrane proteins were separated out from the secreted protein set and previously identified effector proteins such as RxLRs and CRNs were added in order to confirm the existence of secreted effector proteins.

2.16 cDNA synthesis

First strand cDNA was synthesized from 20 µl of DNase-treated total RNA (250 ng/µl) using SuperScript^{TM} II Reverse Transcriptase and Oligo dT priming, following the protocol provided by the manufacturer (Invitrogen Corp., Carlsbad, CA, USA).

2.1 Microarray validation: quantitative real-time reverse transcribed polymerase chain reaction (QRT-PCR).

A set of *P. infestans* genes were selected from the microarray experiment according to their expression profile and/or the type of protein they encode. DNA sequences for selected genes (table 2.3) were retrieved from the *Phytophthora* genome sequence database (http://www.broadinstitute.org/annotation/genome/phytophthora_infestans/MultiHome.html). Primer sequences (forward and reverse) for quantitative real-time reverse transcribed polymerase chain reaction (QRT-PCR) (see table 11.1) were designed using Primer3 software (Primer3web, version 4.0; http://primer3.ut.ee/).

Table 2.3 List of QRT-PCR primers for microarray validation and gene expression analysis.

Primary accession	Description	Oligo name	Primer sequence
PITG_00058	EpiC4	qRT_00058_F	ACCAACTACCGCTTCCACAT
		qRT_00058_R	AAAATCTGCACCACGAAGCC
PITG_00513	TF-Myb	qRT_00513_F	CCACGCACAAAAATATCAGG
		qRT_00513_R	CGTCAATACGATGCTCAGGA
PITG_00366	RxLR	qRT_00366_F	GACTGAACACGCTGCTTCTC
		qRT_00366_R	GAATAGGTCAGCTGCTCCGT
PITG_00623	4-aminobutyrate aminotransferase	PITG_00623F	GTGTCCTTCGTGCCATATCC
		PITG_00623R	CTGCTTCAATGCGGTGTCTA
PITG_02860	RxLR	qRT_02860_F	ACTTGCTTTCCTCCTGCTTG
		qRT_02860_R	ATTAGACCAGGCGACACCAC
PITG_03616	CHP	qRT_03616_F	AACTACCCAACTGTCGCTACA
		qRT_03616_R	GCTGTTGGCGTATGAGTCG
PITG_03637	CBEL	qRT_03637_F	GCTATCTGAAGAGCGGAACC
		qRT_03637_R	CCGTCAAGATACCCGAGACT
PITG_03978	TF-TFIID	For_TF-03978_qRT	CAGTGCTTCGTCGTCGTTAT
		Rev_TF-03978_qRT	GTAAGAGGCTCTCGCCAAAC
PITG_04097	RxLR	For_04097_qRT	CTGGAAAGCCATAGCCCATA
		Rev_04097_qRT	CGTCTATCTCCGGCTTCTTG
PITG_04145	RxLR	For_04145_qRT	GCCGTCTTAGCTCGCTGTAG
		Rev_04145_qRT	AGCTGAGAGTCATCGGCATT
PITG_04272	glycoside hydrolase	For_04272_qRT	CAGTGGACCAGGACATGAAG
		Rev_04272_qRT	CTGCGTGTACTCCGTAGCAT
PITG_04339	RxLR	qRT_04339_F	AGGGCGTGTACTGGGAATAC
		qRT_04339_R	CGGGCAGGGGTTTATTTGAC
PITG_05000	MtN3-like	qRT_05000_F	GCATTCTTCCAGTGGTGATG
		qRT_05000_R	CGCAGAGAAGGTGACTGTTG
PITG_05146	RxLR	For_05146_qRT	ACCCAGCACGAGAAGAGATT
		Rev_05146_qRT	CGAACAGATTCAGCAGCACT
PITG_05225	4-aminobutyrate aminotransferase	PITG_05225F	TCGAGAACGACAGCTTGCTA
		PITG_05225R	CCTTGACCACGCACATTAGA
PITG_05339	transglutaminase M81-like	For_05339_qRT	CTGGATCGTCGAGTCTGGTA
		Rev_05339_qRT	TGTCTACAAGCCCTGTGCTC
PITG_05387	ABC transporter	qRT_05387_F	TACACGACGTACAGCGGTCT
		qRT_05387_R	CAGCCATAGCCATGAACAAA
PITG_05440	Epi6	qRT_05440_F	AGCAGAACATCGTGGAGGAA
		qRT_05440_R	TTACACGACAGGCAGGATGT
PITG_05989	TF-Myb	For_TF-05989_qRT	AATGACAATGCCACCTCAAA
		Rev_TF-05989_qRT	GCCTTCACCTCATCACTCAG
PITG_06087	RxLR	For_06087- qRT	ACGATGAACAACAACCAGGA
		Rev_06087- qRT	GCACGATAATTGATCCTCCA
PITG_06201	TF-TATA-box DNA binding	For_TF-06201_qRT	GGAGCTGTTCCCAGGACTTA
		Rev_TF-06201_qRT	CGGAAGACTCACACCCAGTA

Table 2.3 **(continued)**

Primary accession	Description	Oligo name	Primer sequence
PITG_06432	RxLR	qRT_06432_F	CGTTAGCCCTGTTGTGTACG
		qRT_06432_R	GACAGTCCTTGGAACCTTGG
PITG_06748	TF-Myb	For_TF-06748_qRT	ATCACTACGACAACCCACGA
		Rev_TF-06748_qRT	CTTGTGGCACTCGAAGATGA
PITG_07059	TF-MADS-box	For_TF-07059_qRT	CTCTCAGGTCACCACATGCT
		Rev_TF-07059_qRT	GTTGTTGGAGACGGGAGAAT
PITG_07134	ABC transporter	qRT_07134_F	CGAGCTACCAGGGACTCAAC
		qRT_07134_R	CTCCTCCGACGTAATGGGTA
PITG_07283	threonine dehydratase catabolic	qRT_07283_F	AGATGGAAAAGGTCGTGGTG
		qRT_07283_R	CTTGTCGTCGATCAGAGCAG
PITG_07345	transmembrane protein	QRT_07345_F	CTAGTGGCAACCCAAGACCT
		QRT_07345_R	CACGTCCGTTAATGATCTCG
PITG_07387	Avr4	qRT_07387_F	ACAGCTCCTTAGGTGGGTTG
		qRT_07387_R	GGCGAGCAGCAACAGTATTA
PITG_08912	pectinesterase	qRT_08912_F	ACACCAACGCTTCCATGAAC
		qRT_08912_R	CGTCACCAAGCTCACTGTTC
PITG_09088	POT	For_09088_qRT	TTCAATCAAGCCCACAAGAG
		Rev_09088_qRT	TACAGAACCGTCCCGAGAA
PITG_09160	RxLR	qRT_09160_F	CGAAGGTGACAACGAAGAGA
		qRT_09160_R	TCGTCTTGAATACTTGGTCCAG
PITG_09279	bZIP transcription factor	For_TF-09279_qRT	AGGAGGTAAGCCCCTCAAAT
		Rev_TF-09279_qRT	TGCGTGAATGGAAAAGTGTT
PITG_09280	bZIP transcription factor	For_TF-09280_qRT	GAAGACAAAGACGACGGTGA
		Rev_TF-09280_qRT	GGTTCTTCTCGTTCCAAAGC
PITG_09503	RxLR	qRT_09503_F	GCGTCTCACTGTCGTGCTAC
		qRT_09503_R	ACTGGTGGGAGAACCTTGAC
PITG_09526	TF-BTF3-like	For_TF-09526_qRT	GCATCATTTTTGCCTGGTC
		Rev_TF-09526_qRT	TGATTGCGTCAGCCATATTT
PITG_09585	RxLR	For_09585_qRT	TACACGACCGAGTGTTTGGT
		Rev_09585_qRT	GAGGATCTGGGCGTAGAGAG
PITG_09680	CHP	For_09680_qRT	GCATCATCACACTTGGAACC
		Rev_09680_qRT	GATGGCGGAGAGAAGAAGAC
PITG_09716	NPP1	qRT_09716_F	TGACATTAGCAGCGGTCTCA
		qRT_09716_R	CAGCCCACTTGTCCTTGAAC
PITG_09757	RxLR	For_09757_qRT	TGACGACAGCACAGAGTTCA
		Rev_09757_qRT	GCAAATATGGCGTCTGAGAA
PITG_10396	RxLR	qRT_10396_F	TCGACAAAACCTGAATCCAA
		qRT_10396_R	CGGGACAGCCTTGATAGACT
PITG_10654	RxLR	qRT_10654_F	GAAGTCCGTCATTGCCAAGG
		qRT_10654_R	GCTCTTCAAGACCAACCAGC
PITG_10767	CHP	qRT_10767_F	TCCGAGACCTTCCTACAACC
		qRT_10767_R	GACAAAGAGGCAATCAAGCA

Table 2.3 **(continued)**

Primary accession	Description	Oligo name	Primer sequence
PITG_11239	nuclear LIM factor interactor	qRT_11239_F	GCCACATCTTTGGGAGTGTT
		qRT_11239_R	TGCCTTTTGCTGATCTTCCT
PITG_11940	chitin-binding	qRT_11940_F	GTCAAGCCCAGTACCGACTC
		qRT_11940_R	GTGGCGAAGTTGCTGAAGTA
PITG_12120	NPL4-like	For_NLP4- 12120_qRT	ACCAGTGCGTTGAGATGTTC
		Rev_NLP4- 12120_qRT	TATGCTCGTTCTCCATCAGC
PITG_12551	INF1	For_INF1-12551_qRT	TAGTGGCCTGGTACTCAACG
		Rev_INF1-12551_qRT	ATAGCGACGCACACGTAGAC
PITG_12824	glutamate carboxypeptidase	qRT_12824_F	ACGCTAGTGTTCCACACACG
		qRT_12824_R	GTGAAGTGGGTACGACAGCA
PITG_13063	purine-cytosine permease	qRT_13063_F	GCTTCGTATGGACATTGGTG
		qRT_13063_R	ACATCCAGTAGCCGATGACA
PITG_13157	SNE1	qRT_13157_F	CGGTGATGACAAGTCGAAGC
		qRT_13157_R	CCCTGCTTCTGGTTCTGAGA
PITG_13507	RxLR	qRT_13507_F	GTGACACCAAACGAAGACGA
		qRT_13507_R	ACGCCTCGAAAGTCTGTTGT
PITG_13567	endo-1,3(4)-beta-glucanase	For_1-3,βGlu-13567_qRT	CATCAAAGAGCTGGACAGGA
		Rev_1-3,βGlu-13567_qRT	AAGAAAGGGTCGTCTGTGCT
PITG_13638	GIP1	For_13638_qRT	AGAGTGTTGGCGTTGAAGTG
		Rev_13638_qRT	CCAGCACAGACAGACGAGTT
PITG_13661	transmembrane protein	qRT_13661_F	GACCACTGCCATTGTCTTGA
		qRT_13661_R	GTAGCCGTTGTCGTCAGTCA
PITG_13959	RxLR	For_13959_qRT	ACGTGGATGTTCACTCCTCA
		Rev_13959_qRT	TTCGACCTTGTCATCCGTTA
PITG_14400	TF-Myb-like	For_TF-14400_qRT	TCGACGTGACCAGAAGAAAC
		Rev_TF-14400_qRT	TGCCGACTGTGTAGGGATTA
PITG_14596	TF-IIB	For_TF-14596_qRT	TTACGATGATTGGCGAGAAG
		Rev_TF-14596_qRT	ACCACACCCTCGAAAAGC
PITG_14623	mediator of RNA polymerase II transcription	For_TF-14623_qRT	GTCCAGAAGATCCAGCCATT
		Rev_TF-14623_qRT	GCAACTTTTTGTCGCTTGG
PITG_14645	PcF SCR74-like	For_SCR74-14645_qRT	TGCGTCGGAAATATAATCCA
		Rev_SCR74-14645_qRT	CGAACAATCCGAGCTGTATG
PITG_14984	RxLR	qRT_14984_F	GTGGCAACTCTCCTTGTTCC
		qRT_14984_R	GACTTAGCTCTTCGGGTGGA
PITG_14788	RxLR	qRT_14788_F	CCTCCACGCTGTCAATTTGG
		qRT_14788_R	GCGGCCCTCAGATTCAATTC
PITG_15123	RxLR	qRT_15123_F	CAACTTGGGGTCCTGGATCT
		qRT_15123_R	TCCATCCCATTCGTGAGCTT
PITG_15128	RxLR	For_15128_qRT	GACGTTTCTCAGTGGCAAGA
		Rev_15128_qRT	CCTGGGGTCGTTAAAGATGT
PITG_15606	RRP41-like	For_15606_qRT	AACTGCGAGTTCACACAAGC
		Rev_15606_qRT	TGACAGCCAGCGACATCT

Table 2.3 **(continued)**

Primary accession	Description	Oligo name	Primer sequence
PITG_15679	RxLR	For_15679_qRT	CCACGAAGAACATGGACAAG
		Rev_15679_qRT	CCGACAGACTCAGCTTTTCA
PITG_16866	NPP1-like	qRT_16866_F	ATCCTTCAGCTCTTCGCATC
		qRT_16866_R	TGGGGCTTGAACTTGATACC
PITG_17552	TF-Myb-like	For_TF-17552_qRT	TCAGCCTTCTCAAACCAATG
		Rev_TF-17552_qRT	GACCATAACCCTCGCTCAAT
PITG_17567	TF-Myb-like	For_TF-17567_qRT	GTGCTCACATTTTGCGAGTT
		Rev_TF-17567_qRT	GCTCACCATGACTTTGTTGC
PITG_18215	RxLR	For_18215_qRT	ATGCGAGCCTACTTTGTCCT
		Rev_18215_qRT	CAACACGAAGAGAGCGAGTC
PITG_18428	cleavage induced	qRT_18428_F	GAAGCATCCTGATCCAACCT
		qRT_18428_R	TCGGAGTCAATGTTGTCGTT
PITG_21410	INF4	For_21410_qRT	TATCCGAAGCCTCATTCTCC
		Rev_21410_qRT	ATCATCGAGTAGCCCGAATC
PITG_22375	RxLR	qRT_22375_F	TCGACAAAACCTGAATCCAA
		qRT_22375_R	CGGGACAGCCTTGATAGACT
PITG_22675	RxLR	qRT_22675_F	CGGCAAACCCTTCCAAAGAC
		qRT_22675_R	CGGGCCATTCAAGAAAACCA
PITG_22760	CHP	For_22760_qRT	AACTGTTGCTGCTATGTCTGC
		Rev_22760_qRT	CCACCACAAGAACCTCCAT
PITG_22916	NPP1-like	qRT_22916_F	AAGGAAAAGGCTGCTGTCAA
		qRT_22916_R	ATCCGTCCTCGATGTAAAGC
PITG_23077	SCR91	qRT_23077_F	GGTATGCCGTGACGAAGGTA
		qRT_23077_R	CCGCACTTATTGATGCAGCA
PITG_23094	NPP1-like	For_23094_qRT	TTGCTCTAAGCTGCTTGGTC
		Rev_23094_qRT	GAGAACCTCAGGGAATGGAA
tdTomato	tdTomato	tdTomato_QRT1_for	GACACCAAGCTGGACATCAC
		tdTomato_QRT1_Rev	CCATGCCGTACAGGAACA

When using Primer3, the primer melting temperature was set from a minimum of 58°C to a maximum of 60°C, and product size ranges were set between 50 and 150 bp. Candidate nucleotide primer sequences were analysed for primer secondary structure using NetPrimer software (http://www.premierbiosoft.com/netprimer) to identify hairpins, self-dimers, cross-dimers, and palindromes in primer pairs, to minimise the formation of primer dimers. All selected primer pairs were used as query sequences for BLASTn search against NCBI Genbank (http://blast.ncbi.nlm.nih.gov) to confirm that the primer sequences were unique to *P. infestans* and would not cross-react with potato sequences. Primers which were already in existence in the laboratory (Table 2.4) were also used.

Table 2.4 Additional QRT-PCR primers; these primers were already in the primer collection in the *P. infestans* laboratory at the James Hutton Institute.

Oligo name/ Specificity	Primary accession	Primer direction	Primer sequence	Reference
SSHac2C5/ Hmp1	PITG_00375	Forward	GCCAGCGGTCAAGGTAAAGA	Avrova *et al*., 2008
		Reverse	GCCTGCTAACGGCAACGT	
E7.6199.C1/ RxLR	PITG_03192	Forward	CCTGCTCGTCGTCAGTGTGA	Whisson *et al*., 2007
		Reverse	TCGAAATTCCGGTTATTCATGA	
rpvb_12884.y1.abd/ RxLR	PITG_04314	Forward	GGTTGCCCTATCTACGAGCAAA	Whisson *et al*., 2007
		Reverse	GGGACCTGACGATGCTGTTTT	
rpch_15494.y1.abd/ RXLR	PITG_04388	Forward	CGATCATTCGACGCCCATAT	Whisson *et al*., 2007
		Reverse	CGGTCGGAAGCCCTCTCT	
qNud/ RxLR	PITG_06308	Forward	TCTCCGACCCAACAAGCATT	Vetukuri *et al*., 2012
		Reverse	TGGCCCCTCTGTCTTCACCT	
E7.8373.C1/ RxLR	PITG_06478	Forward	CCTTCTTCGCTTGGGCTTCT	Whisson *et al*., 2007
		Reverse	TGAGCAATCAGCTTCGACTTGT	
Qrt7987Elli/ RxLR (Avr2)	PITG_08943	Forward	ACCCTGAAGAAGCTCAATCC	Breen, 2012
		Reverse	CTTTTCCGTGACCTCTTTAGC	
PV004C8.XT7/ RxLR	PITG_13628	Forward	GCCTCCGACCAGAATTCGA	Whisson *et al.*, 2007
		Reverse	TTGACTTTTATGGTAGCGTGATGAGT	
Avr3av/ RxLR (Avr3a)	PITG_14371	Forward	CGCCATAAACTTTGCAACCA	Whisson *et al*., 2007
		Reverse	TGCCGGCTGAATCGTGTAT	
E7.589.C2/ RxLR	PITG_14833	Forward	GACTCGTCTCCGACGCTCAT	Whisson *et al*., 2007
		Reverse	CGACACTGACGTCTTATCCTTGTT	
ActA/ Actin	PITG_15117	Forward	CATCAAGGAGAAGCTGACGTACA	Grenville-Briggs *et al*., 2008
		Reverse	GACGACTCGGCGGCAG	
E7.6301.C1/ RxLR	PITG_15287	Forward	TGGCGAGGAGAGGGTCAAT	Whisson *et al*., 2007
		Reverse	GATAGGCCAAGCGCATCAGT	
qRTPCR_16663b/ RxLR (Avr1)	PITG_16663	Forward	GAGCAAGATCGACGAGTTCA	Vetukuri *et al*., 2012
		Reverse	CCTCAGGTGATCCTCCACTT	
Avr3b/ RxLR (Avr3b)	PITG_18215	Forward	CATCAGAACTGGGACGCTCT	Vetukuri *et al*., 2012
		Reverse	GGAGTACGCTCTCAGCCATC	
CDC14qRT/ Spore	PITG_18578	Forward	TGCACTTTTAACTTGACTATTCTTGA	Bos *et al*., 2009
		Reverse	AGATCAAACGTCTTAGTGGAGATG	
CV970797/ RxLR (Avrblb2)	PITG_20303	Forward	CGTCGCAGCATTCCCAAT	Whisson *et al*., 2007
		Reverse	GCCACAGTGTCAGGAGATGTCTT	
IpiO1/ RxLR (Avrblb1)	PITG_21388	Forward	TGCGTTCGCTC CTGTTGA	Whisson *et al*., 2007
		Reverse	CGGTGTTGAGATTGGATGAAAC	

Primer pairs were ordered, lyophilised, from Sigma-Aldrich and dissolved in RNase- free sterile water to give a stock concentration of 100 µM. Primer concentrations were optimized using genomic DNA of *P. infestans*, and cDNA from an infection time course of *P. infestans* using several dilutions (50 nM, 100 nM, 300 nM, and 900 nM) from the

primer stocks. To detect and quantify the PCR product through the generation of fluorescent signal, SYBR® Green master mix (Applied Biosystems, Foster City, CA, USA) was used. Primer optimization was conducted using duplicate 12 µl reactions, which included 2 µl of template genomic DNA (39 ng/µl) or cDNA (1:5 dilution of first strand synthesis). A Bio-Rad thermocycler (DNA Engine®, Peltier Thermal Cycler, Chromo4, Real Time PCR Detector, USA) was used for running QRT-PCR. The operating manual for the Bio-Rad thermocycler was followed (http://arboretum.harvard.edu/wp-content/uploads/ptc200_manual.pdf). Similarly, QRT-PCR experiments for gene expression analysis was conducted using duplicate 12µl total volume of QRT-PCR reaction including SYBR green (6µl), optimised QRT-PCR primers (forward and reverse: 1µl each), diluted cDNA (1:5 dilution of 250ng/µl stock; 2µl), and HPLC H_2O (2µl). A duplicate of NTC (no template cDNA control) for each primer was used in order to verify the quality of primers. Thermal cycling parameters for primer optimization and gene expression quantification were: 95 °C for 15 minutes, followed by 40 cycles of 95 °C for 15 seconds, 59 °C for 30 seconds, and 72 °C for 30 seconds. To confirm the absence of non-specific amplification, a melting curve was generated using real-time PCR software, Opticon Monitor (version 3.1) provided by Bio-Rad Laboratories, Inc. Data from QRT-PCR were analysed by relative quantification 'delta delta Ct' method (Livak and Schmittgen, 2001). The Ct value from the QRT-PCR was normalised with *P. infestans* actinA (PITG_15117; Gene ID: 9476003) in relation to sporangia. Sporangia were assigned the expression value of 1 and the expression in other stages was shown relative to the expression in sporangia.

Chapter 3. Transcriptional change in *P. infestans* during leaf infection

3.1 Introduction

There is a dynamic exchange of signals between plant and pathogen during infection, leading to large scale transcriptome and proteome changes in both organisms. One way to understand the molecular interplay during infection is to assess the change in mRNA levels for selected genes, or for the transcriptome as a whole.

It is important to determine the molecular aspects of host infection by the hemi-biotrophic pathogen *P. infestans* in order to understand its pathogenicity and disease development. It is also important to identify similarities between previously published data sets for different genotypes of the same species, so that core pathogenicity components can be identified. There are several transcriptomic studies (Tripathy *et al*., 2012; Lévesque, *et al*., 2010; Haas *et al*., 2009; Tyler *et al*., 2006; Cooke *et al*., 2012), which have provided fundamental knowledge of the expression of genes encoding secreted proteins in oomycetes. This is critical for understanding the plant-pathogen interaction under study (cross ref to zig-zag-zig model: Chapter-1, Figure 1.6, sub-heading 1.11). In the genome analysis report of the aggressive and invasive lineage 13_A2 (Blue_13) by Cooke *et al*. (2012) it was shown that the population of *P. infestans* undergoes major changes. This could be due, in part, to pathogen strategies that evolve to overcome disease resistance during the pathogen-host arms race. If the detectable transcriptome of one strain of *P. infestans* is different from another, then these differences may be associated with the degree to which these genotypes overcome host immunity. In this chapter, microarray analysis was used to investigate dynamic changes in the transcriptome of a well-studied isolate of *P. infestans* (88069), to better understand the ways in which it both triggers and

suppresses the potato immune system. For this, infection of the susceptible cultivar Bintje was studied across a range of time-points after pathogen inoculation.

Previous microarray studies have only been sensitive enough to detect differential gene expression from two days post-inoculation (Haas *et al*., 2009; Cooke *et al*., 2012), and yet QRT-PCR studies have revealed that transcriptional changes occur earlier than this (Liu *et al*., 2005; Whisson *et al*., 2007; Avrova *et al*., 2008), and indeed cell biological analyses indicate that haustoria are detected within 24 hours-post-inoculation (Avrova *et al*., 2007). The use of the more sensitive Agilent microarray system here was to enable a detailed study of the *P. infestans* transcriptome within the first 1-2 dpi of potato infection, and test the hypothesis that the expression of effectors, PAMPs, and other infection-related genes are differentially expressed from the earliest stages of infection.

3.2 Results

Overview

Initially, the cell biology and the molecular interactions between the hemi-biotrophic pathogen *P. infestans* 88069 and potato were examined during the early stages of infection. A microarray experiment was conducted over an infection time course of 12, 24, 36, 48 and 60 hpi. This experiment also included two *in vitro* samples (sporangia and germinating cysts) and a mock inoculation (leaf inoculation carried out by sterile distilled water). The progression of infection was observed using a fluorescently tagged strain of *P. infestans* and confocal microscopy.

From the microarray, genes were grouped according to the level and pattern of their expression, and included stage-specific marker genes encoding PAMP proteins, avirulence proteins, RxLR effectors, NLP (necrosis-inducing like protein) proteins, and other genes which are involved in infection and differentially expressed during infection.

Transcripts that were only present during infection were also identified. Transcript accumulation of a selection of genes from all groupings were validated using quantitative real-time RT-PCR (QRT-PCR).

3.2.1 Macroscopic symptoms on potato leaves

Phenotypic changes during disease progression were recorded using digital photography (Figure 3.1a to f). The inoculation (droplet) on the leaf surface was slowly absorbed or evaporated during the experiment time course. There was no clear disease development observed on the leaf from 12 to 60 hpi (Figure 3.1a to e) and the leaves appeared green and healthy. Small water-soaked spots were observed at the inoculation site at 60 hpi. However, by 7 dpi (Figure 3.1f), dark brown lesions had spread across the leaves and were covered with aerial hyphae and sporangiophores. Leaf chlorophyll at this time point had almost completely disappeared.

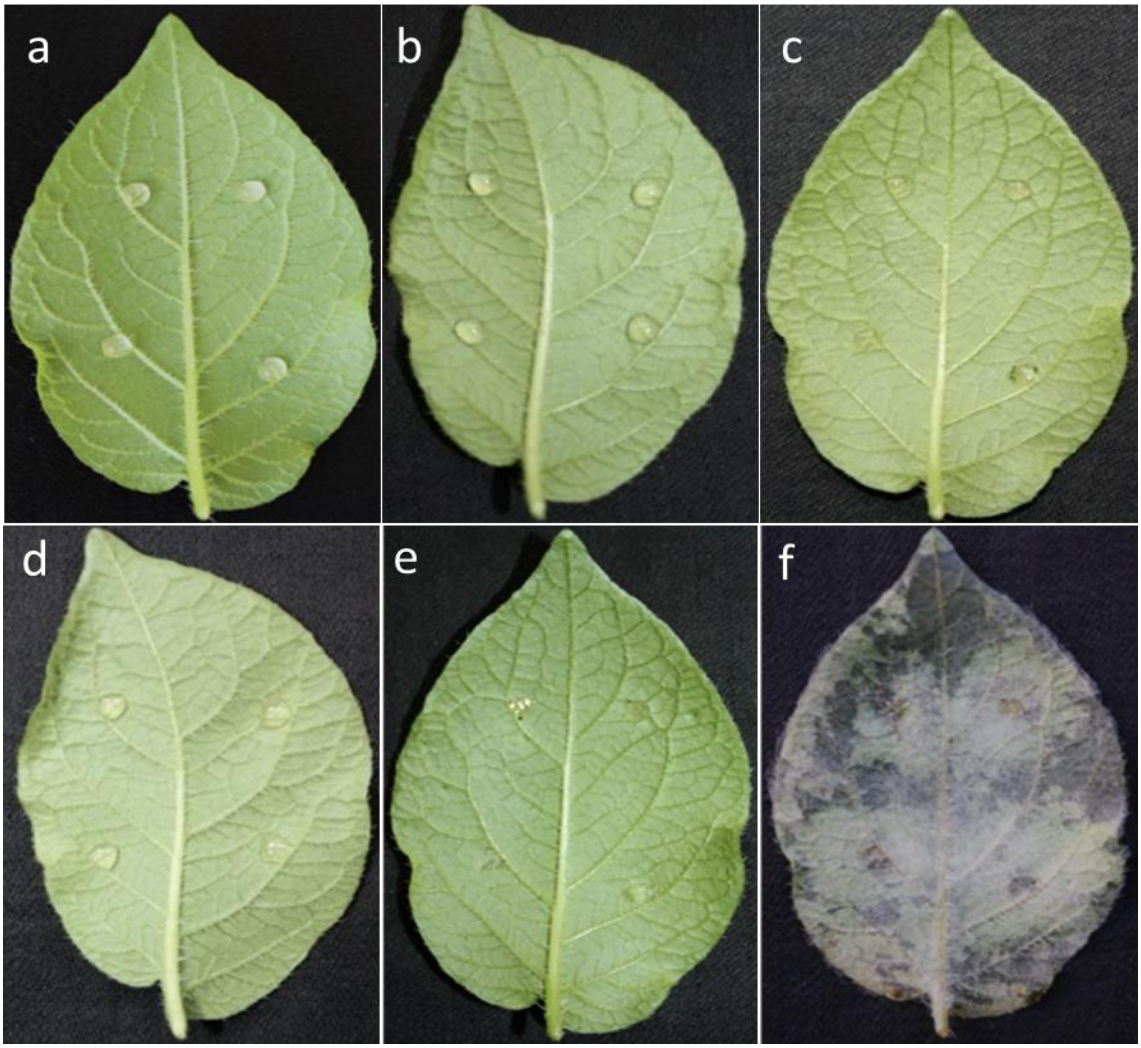

Figure 3.1 Digital images showing *P. infestans* inoculated leaf samples taken at 12 hpi (a), 24 hpi (b), 36 hpi (c), 48 hpi (d), 60 hpi (e), and 7 dpi (f). Clear disease development was observed by seven days (f).

3.2.2 Confocal microscopic examination of the *P. infestans* infection cycle

Microscopic examination of *P. infestans* infection was carried out using a Leica SP2 confocal microscope. At the earliest infection stage examined here (12 hpi), *P. infestans* (expressing the tandem dimer Tomato fluorescent protein; tdTomato) had already penetrated into the leaf tissue. Although some hyphae (in red) were located on the leaf surface and had not yet entered the leaf, haustoria were observed on some intercellular hyphae (indicated by arrow in Figure 3.2) indicating successful infection as early as 12 hpi. More extensive hyphal colonisation between host cells, along with haustoria, was

observed at 24 hpi. By 36 hpi, hyphae were highly branched and had extensively colonized mesophyll cells at the inoculation site. At 48 hpi extensive tissue colonisation was observed and disease development was further extended from the inoculation site and fewer new intercellular hyphae with haustoria were formed.

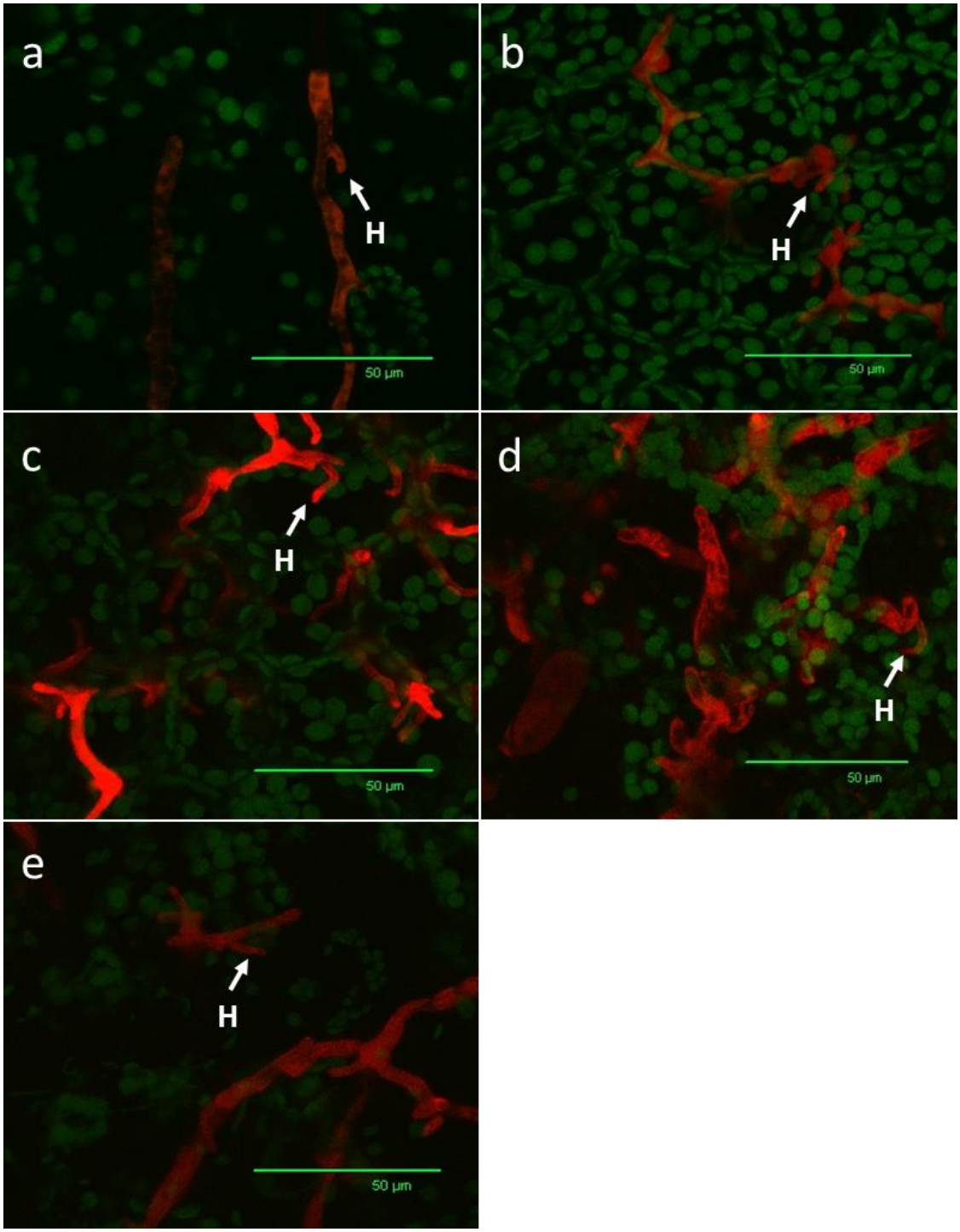

Figure 3.2 Confocal Z-stack images of infected leaf samples at 12 hpi (a), 24 hpi (b), 36 hpi (c), 48 hpi (d), and 60 hpi (e). Figures with the scale bar of 50µm show *P. infestans* (in red) and plant chlorophyll (in green). Haustorial (arrows followed by H) penetration was observed from early infection (12 hpi).

3.2.3 RNA extraction and quality control (spectrophotometry and bio-analyser), and cDNA synthesis

The quality and yield of the total RNA from *in vitro* stages of *P. infestans*, and infected and un-infected leaf samples showed acceptable quality for microarray experiments. The RNA integrity number (RIN) from the bio-analyser report with gel electrophoresis (see appendix 3a and 3b) for all biologically replicated samples, other than one replication of germinating cysts, was above the acceptable level of 6.60. Although the RIN number for one germinating cyst replicate was 1.20, no difference in the quality graphs were observed, compared to other samples.

3.2.4 Microarray analysis of *P. infestans* transformant 88069tdT10 leaf infection time course in *S. tuberosum*

The changes in the *P. infestans* transcriptome during early biotrophy were investigated by the use of Agilent single-colour microarrays. Microarray probes were designed to the total *P. infestans* transcriptome (Annex 3a); 18,024 predicted *P. infestans* transcripts are represented on the microarray. Of these, 15,264 were detected either in one or both of the two *in vitro* (sporangia and germinating cysts) stages, or any of the *in planta* (12, 24, 36, 48, and 60 hpi) infection stages (Annex 3b). 5,975 transcripts were detected in any and/or all of the *in planta* infection and non-infection (ni) stages (Annex 3c), according to the quality filter (the flag values that are present or marginal in two-thirds of the replicates) analysis. To determine the flag value, filtering was based on two factors; the percentile cut-off, and the filter criteria of a probe set having intensity values within the specified range. If the percentile cut-off was set as an intensity value of a probe below the 20th percentile in that particular sample, the gene is unlikely to be expressed in that sample. Probe sets were filtered such that they must have values within the range (above 20th percentile) in two of the three biological samples. Due to the possibility of interesting

genes being excluded, resulting in potentially interesting biological changes between experimental samples being missed, the stringency of the filter was set such that even if the gene was only expressed in two samples in the experiment, the probe set passes the filter to decrease the chances of excluding these changes.

Initially, a 'global' method was used for data normalisation, but it produced unexpected and inaccurate results for genes of known expression profile (e.g. *Hmp1*). Thus, 57 *P. infestans* genes were specifically selected for data normalisation (Table 3.1). These genes were selected due to their constitutive expression in different *in vitro* life stages of *P. infestans*, according to a previously published microarray study (Judelson *et al*., 2008). Results here also showed similar expression for all of the selected control genes in both *in vitro* stages (sporangia and germinating cysts) (Table 3.1), providing evidence that these genes may be used for the normalisation of the *P. infestans* infection time course microarray data. The genes in this control set encode functionally diverse proteins, including: functionally unannotated *Phytophthora* conserved hypothetical proteins (CHPs), hypothetical proteins (HPs), RNA metabolism related proteins, catalytic enzymes, nuclear genes, protein modification proteins, binding proteins (for stress responses), activator proteins (transcription factors), transferase proteins, signal transduction proteins, transmembrane proteins, and regulatory proteins.

Table 3.1 Control genes used in microarray data normalization. These genes were selected according to their constitutive expression in various *in vitro* life stages of *P. infestans* (Judelson *et al*., 2008). These genes are also constitutively expressed in both sporangia and germinating cysts. The table below shows the fold change (normalised value) of sporangia and germinating cysts.

Description	Primary accession	Sporangia	Germinating cysts
conserved hypothetical protein	PITG_21627T0	0.1643	0.1800
molybdenum cofactor sulfurase, putative	PITG_04515T0	0.2038	0.1964
conserved hypothetical protein	PITG_00025T0	0.2481	0.2285
notchless family protein	PITG_04722T0	0.2813	0.2798
nucleolar complex protein 3	PITG_12225T0	0.3166	0.3167
conserved hypothetical protein	PITG_15595T0	0.3711	0.4033
conserved hypothetical protein	PITG_08307T0	0.3732	0.4001
conserved hypothetical protein	PITG_09818T0	0.3896	0.4085
conserved hypothetical protein	PITG_08673T0	0.4515	0.4462
conserved hypothetical protein	PITG_09522T0	0.5023	0.5345
methylenetetrahydrofolate reductase, putative	PITG_05377T0	0.5070	0.5191
hypothetical protein	PITG_02323T0	0.5382	0.5745
folylpolyglutamate synthase, putative	PITG_01065T0	0.5481	0.5585
conserved hypothetical protein	PITG_02193T0	0.6121	0.5613
conserved hypothetical protein	PITG_02790T0	0.6584	0.6863
polycomb protein EZH2, putative	PITG_13838T0	0.6787	0.6916
conserved hypothetical protein	PITG_00995T0	0.7095	0.7302
conserved hypothetical protein	PITG_01740T0	0.7458	0.8184
conserved hypothetical protein	PITG_12576T0	0.7750	0.7845
methyltransferase	PITG_05300T0	0.7957	0.8346
conserved hypothetical protein	PITG_08084T0	0.8333	0.8604
conserved hypothetical protein	PITG_05128T0	0.8387	0.8766
conserved hypothetical protein	PITG_14816T0	0.8819	0.9285
hypothetical protein	PITG_15137T0	0.8987	0.9281
conserved hypothetical protein	PITG_02244T0	0.9302	0.9788
cytochrome Oxidase Biogenesis (Oxa1) Family	PITG_13344T0	0.9528	0.8706
hypothetical protein	PITG_00235T0	0.9715	0.9644
pre-mRNA-splicing factor ISY1	PITG_19064T0	0.9755	0.9674
conserved hypothetical protein	PITG_16388T0	1.0483	1.1133
DEAD/DEAH box RNA helicase, putative	PITG_02856T0	1.0565	1.0528
conserved hypothetical protein	PITG_09583T0	1.0597	1.0569
conserved hypothetical protein	PITG_03932T0	1.0691	1.1471
conserved hypothetical protein	PITG_13185T0	1.0732	1.1138
conserved hypothetical protein	PITG_11691T0	1.0782	1.1205
phosphoserine phosphatase	PITG_00166T0	1.1559	1.1718
conserved hypothetical protein	PITG_21219T0	1.1601	1.2154
conserved hypothetical protein	PITG_08183T0	1.1888	1.2168
conserved hypothetical protein	PITG_19237T0	1.2030	1.2839
HSF-type DNA-binding protein, putative	PITG_05353T0	1.2591	1.3262
mediator of RNA polymerase II transcription subunit, putative	PITG_14623T0	1.3300	1.3365

Table 3.1 **(continued)**

Description	Primary accession	Sporangia	Germinating cysts
hypothetical protein	PITG_19804T0	1.3323	1.4413
transmembrane protein, putative	PITG_07279T0	1.4183	1.5624
geranylgeranyl transferase, putative	PITG_19200T0	1.4352	1.3347
conserved hypothetical protein	PITG_01119T0	1.5271	1.4145
conserved hypothetical protein	PITG_19055T0	1.5540	1.6451
mannosyl-oligosaccharide alpha-1,2-mannosidase, putative	PITG_07365T0	1.6051	1.5590
conserved hypothetical protein	PITG_04699T0	1.7064	1.8304
ribosomal protein S6 kinase, putative	PITG_07055T0	1.8732	2.1465
conserved hypothetical protein	PITG_00456T0	1.9415	1.9579
H/ACA ribonucleoprotein complex subunit 3	PITG_18717T0	1.9996	2.1745
HSF-type DNA-binding protein, putative	PITG_03306T0	2.0258	1.9492
folylpolyglutamate synthase, putative	PITG_16937T0	2.0295	2.0843
3-hydroxyisobutyrate dehydrogenase, putative	PITG_17998T0	2.0389	2.0277
ubiquitin family protein, putative	PITG_03160T0	2.2736	2.3718
conserved hypothetical protein	PITG_00723T0	2.3806	2.5151
conserved hypothetical protein	PITG_20312T0	4.3683	4.7922
conserved hypothetical protein	PITG_20631T0	4.9761	5.3249

To perform statistical analyses, a set of 5,975 genes detected according to the presence and marginal flag values with statistically significant differences when grouped by 'Stage' were further analysed. Due to there being more than two conditions (five infection stages) for comparative analysis, the ANOVA statistical test was deemed robust for the microarray results (Cui and Churchill, 2003). A parametric test (one-way analysis of variance [Welch ANOVA] with p-value cut-off 0.05, multiple testing correction [Benjamini and Hochberg False Discovery Rate (FDR)]) was used to determine the significance level. Although about 5.0% of the identified genes would be expected to pass the restriction by chance, 1,707 transcripts (Annex 3d) were detected as differentially expressed in the *in planta* infection stages. All further data analyses are based on these 1,707 genes. Although many unannotated CHPs and HPs (448 transcripts) were in this group, there were a greater number of annotated genes (1,259) detected. Annotated transcripts included those encoding: spore and spore cleavage associated proteins (17), PAMPs and elicitors (11), enzyme inhibitor proteins (14), RxLR effectors (114), CRN

effectors (80), SCP family of extracellular proteins and small cysteine rich proteins (10), necrosis and cell wall-degrading enzymes (CWDEs), such as hydrolases, esterases (34), and NLPs such as, necrosis-inducing *Phytophthora* protein 1 (NPP1) (5) (Figure. 3.3). The remaining transcripts were related to the growth, development, and metabolism of *P. infestans*. As expected, the transgene for the tdTomato fluorescent protein was also readily detected.

The predicted transcriptome of *P. infestans* (18,142 transcripts) extracted from the *P. infestans* database (http://www.broadinstitute.org/annotation/genome/phytophthora_ infestans/MultiHome.html) was tested for genes encoding proteins with signal peptides. A set of 1,953 (10.7%) transcripts were predicted to encode secreted proteins using SignalP (ver4.1 by Peterson *et al*., 2011). In the ANOVA list of 1,707 transcripts from the microarray experiment described in this chapter, a total of 293 (Annex 3d) predicted secreted proteins were detected, accounting for 17.16% of the *P. infestans* transcripts within the ANOVA list. From the 9.4% (1,707 transcripts) of the entire transcriptome represented in the ANOVA list, these 293 secreted transcripts make up 15% of all *P. infestans* secreted proteins. In this list, there were 114 RxLR effectors detected as differentially expressed during the infection time course, out of which 108 RxLR effectors were predicted to encode a signal peptide for secretion. In addition, transcripts encoding PAMPs and elicitors (5), enzyme inhibitors (13), CRN effectors (12), SCP-like family and SCR proteins (5), CWDEs (9) and NPP1 protein like NLPs (4), were differentially expressed during infection (Figure 3.3). Several CHPs, HPs, (56) and metabolism-related proteins were also detected as secreted proteins in the ANOVA list.

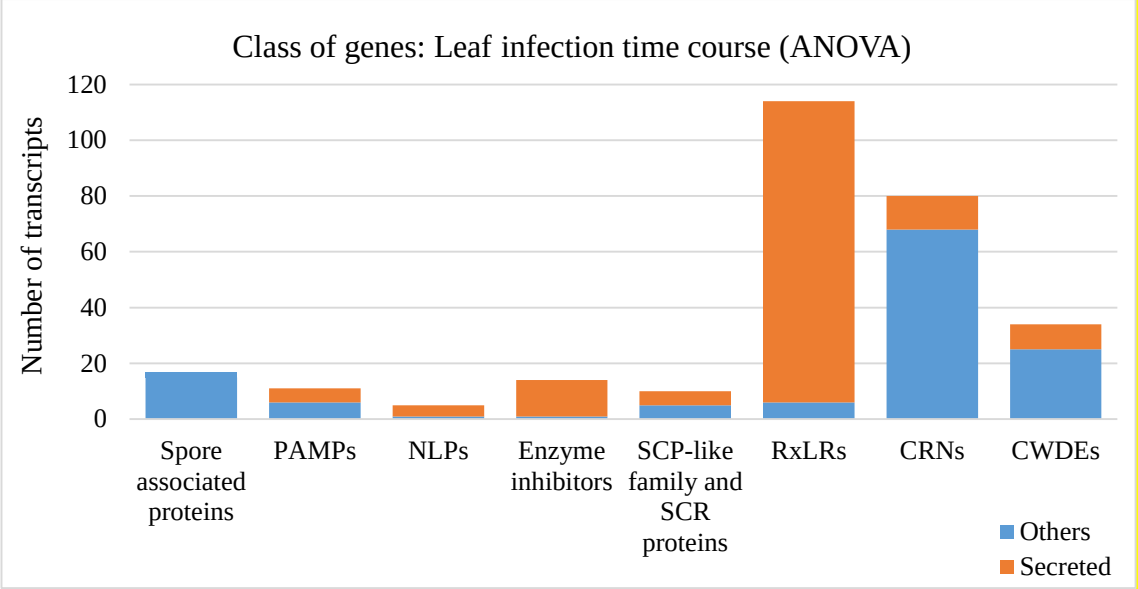

Figure 3.3 Class of differentially expressed genes (leaf infection: ANOVA) and the number of transcripts encoding secreted proteins in the selected groups. Blue represents non-secreted proteins while orange refers to secreted proteins. In the ANOVA list the majority of RxLR effectors and enzyme inhibitors were predicted as secreted proteins. However, low numbers of genes encoding secreted CRN effectors were predicted as secreted.

3.2.5 Flag values represent the detection of the individual genes at each different time point

The perfect match and mismatch probe pairs were measured by the microarray analysis software to find the difference in the hybridization signals in order to use statistical algorithms to determine the significant differences. This calculation signifies and labels each individual gene as 'Present', 'Marginal', and 'Absent'. To understand the significance level of the detection of each *P. infestans* transcript at each different infection time point (12, 24, 36, 48, and 60 hpi), data showing 'Present' flag value was extracted from each individual time point from the ANOVA list. For further analysis, a Venn diagram was developed in order to show the differentially expressed genes related to each different time point of infection (3.4a to d). At 12 hpi, 838 transcripts were detected according to the 'Present' flag value. At 24, 36, 48, and 60 hpi there were 659, 673, 911, and 1,176 transcripts detected, respectively. Although there were 133 transcripts specific to 12 hpi, a substantial number of transcripts (524) were detected at all infection time

points. This analysis was conducted in order to understand how differentially expressed genes are distributed among different infection time points.

Transcripts detected at individual time points were tested for signal peptide in order to find *Phytophthora* secreted proteins potentially necessary to establish biotrophic infection. At the earliest time point (12 hpi) tested, 98 (11.7%) out of 838 transcripts encoded a signal peptide in comparison to 88 (13.4%) out of 659, 103 (15.3%) out of 673, 155 (17%) out of 911, and 199 (16.9%) out of 1,176 at 24, 36, 48, and 60 hpi, respectively (Figure. 3.4c).

With the flag value analysis, the majority (98 out of 114) of the total RxLR effector encoding transcripts were detected at 60 hpi. However, there were nine, 25, 43, and 73 transcripts encoding RxLR effectors present at 12, 24, 36, and 48 hpi respectively. Among these differentially expressed RxLR effectors there were seven transcripts (PITG_08943, PITG_13093, PITG_14960, PITG_14965, PITG_15128, PITG_15278, and PITG_20934) shared across the infection time course, which included the well-characterised Avr protein Avr2 (PITG_08943). Other Avr protein-encoding transcripts were detected as early as 24 hpi and included *Avr3a* (PITG_14371), *Avrblb1* (PITG_21388) also named to *ipi01*, and the *Avrblb2* family (PITG_20300). A transcript for a single RxLR effector (PITG_04074) was detected only at 12 and 24 hpi, and not detected at any of the later time points sampled. Most of the RxLR effector coding transcripts (23 out of 25 transcripts), other than PITG_04074 and PITG_07741, detected at 24 hpi were also detected at 36 hpi. 38 out of 43 RxLR effector transcripts detected at 36 hpi were up-regulated by more than 2-fold. However, the normalised value at this time for the remaining five RxLRs were also more than 1.6 fold, which includes *Avrblb1* (1.9 fold). *Avr10* (unpublished; PITG_11484) was also significantly up-regulated at 36 hpi.

There were 73 transcripts encoding RxLR effectors significantly detected at 48 hpi including all *Avr* genes listed above. *Avrvnt1* (PITG_16294) was significantly up-regulated at 48 hpi. All RxLR effector transcripts detected at 48 hpi were also detected at 60 hpi. However, *AvrSmira2* (PITG_07558) was only detected at 60 hpi.

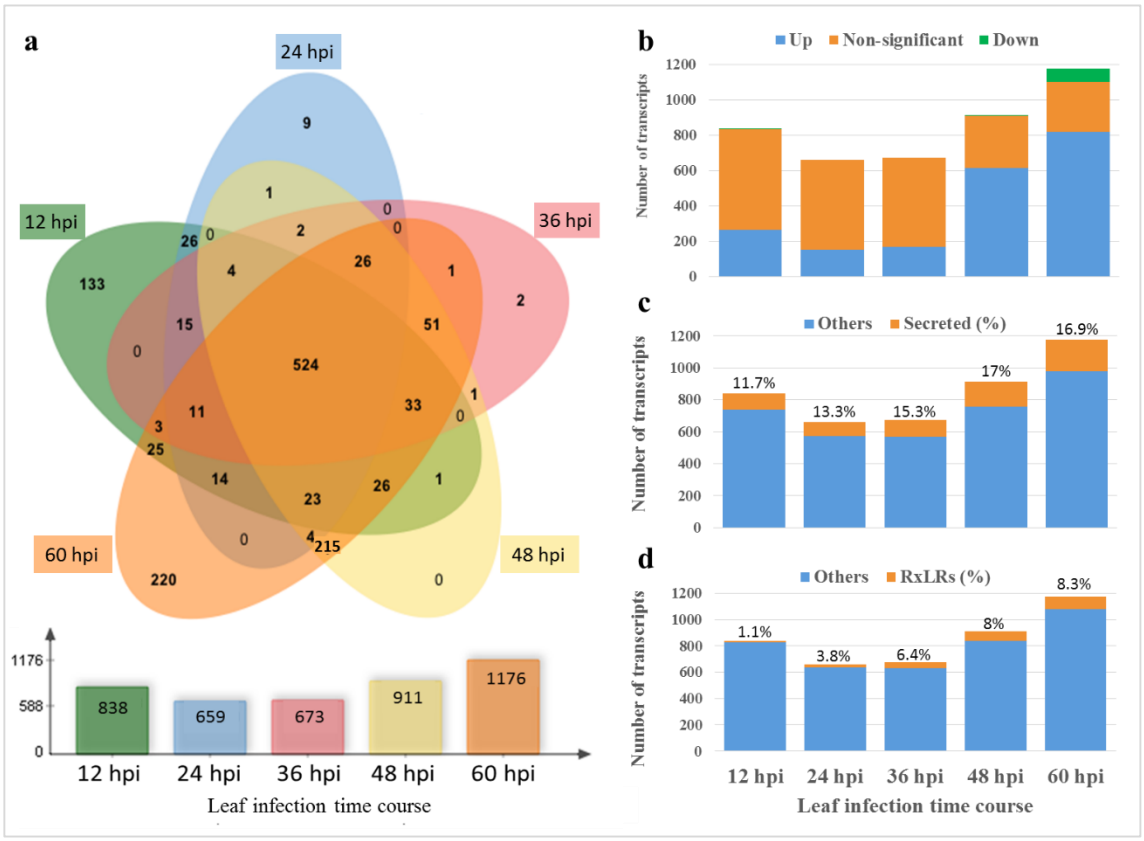

Figure 3.4 Analysis of detected differentially expressed (ANOVA list) *P. infestans* transcripts on the basis of 'Present' flag value during the infection time course from 12 to 60 hpi. Venn diagram (a) showing the significantly differentially distributed 1,707 total transcripts from the ANOVA group. 524 transcripts were detected as common in all infection time points. 133 transcripts were specific to 12 hpi compared to 220 transcripts at 60 hpi. Up-regulated transcripts (blue) (b) based on '2-fold or greater' were a higher proportion, compared to down-regulated transcripts (green). A higher number of transcripts showed non-significant change (between 0.5 and 2-fold) (orange) at early infection time points (12 to 36 hpi) (b). None of the differentially expressed transcripts were down-regulated at 24 and 36 hpi. As early as 12 hpi 11.7% (98) (orange) transcripts were predicted to encode proteins with a signal peptide (c) compared to 16.9% (199) transcripts detected at 60 hpi. Although the majority of transcripts (98; 8.3%) encoding RxLR effectors (orange) were detected at 60 hpi (d), there were 1.1% (9), 3.8% (25), 6.4% (43), and 8% (73) RxLR coding transcripts detected from 12, 24, 36, and 48 hpi respectively.

Transmembrane proteins (TPs) are essential for a multitude of vital cellular processes such as cell-cell communication, perception of chemical messengers, nutrient uptake, and cell wall synthesis. There are a total of 3,116 predicted TPs encoded in the *P. infestans* genome, and transcripts encoding 259 (Annex 3d) of these were detected on the microarray as being differentially expressed throughout the infection time course. At 12 hpi 13.7% of detected differentially expressed transcripts encoded predicted TPs. Similarly, 14.1%, 13.2%, 12.6%, and 13.7% of differentially expressed transcripts at 24, 36, 48, and 60 hpi respectively, encoded predicted TPs (Figure 3.5).

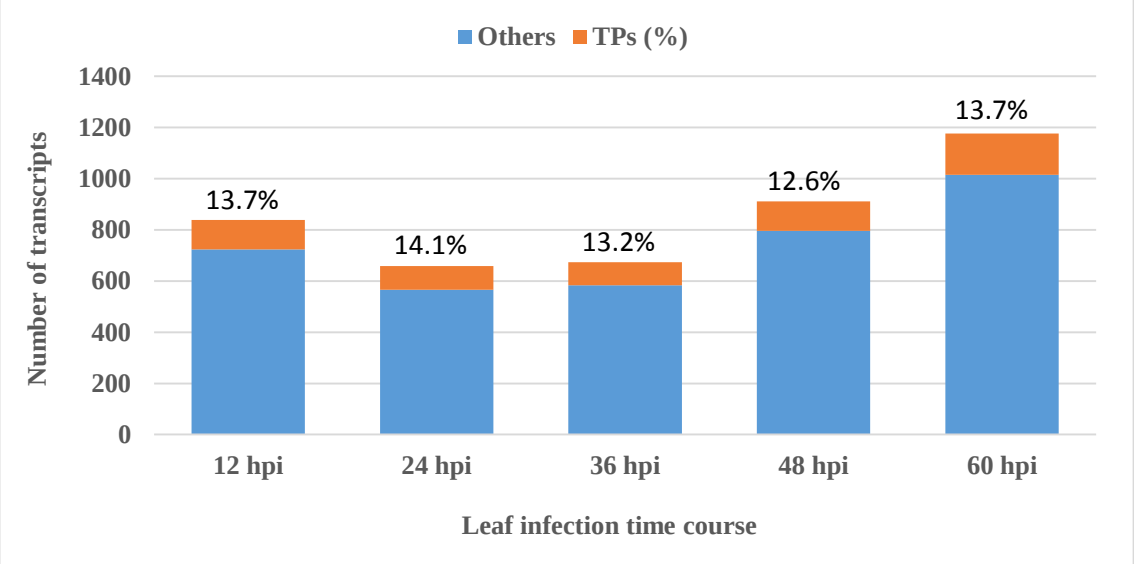

Figure 3.5 The proportion of differentially expressed transmembrane proteins (leaf infection: ANOVA) (percentage; orange) compared to the other proteins (blue) during the time course of infection. The proportion of membrane-bound proteins does not change markedly throughout the progression of infection.

In order to identify involvement of the proteins that determine and initiate the flow of genetic information from DNA to mRNA, the expression of transcription factors (TFs) detected on the microarray was assessed. There were 23 transcription factors differentially expressed during the time course of infection. Among these, four transcripts encoded myb-like DNA binding proteins. A MADS-box transcription factor, zinc finger

C2H2 type transcription factors, and several other transcription factors were also detected in the list.

3.2.6 Volcano plot analysis of transcriptional change during each infection stages

To understand the significant level of up and down-regulated genes in each infection time point, volcano plot analysis of self-stage comparison analysis was conducted. In order to reveal the grouping of gene expression involved in the early biotrophic interaction with the host plant, the genes that were specifically expressed during each different sampling time were analysed. Clusters of genes which were up and down-regulated at each sampling time were analysed on the basis of volcano plot built by comparing each stage (12 to 60 hpi) with itself from the ANOVA list. A Venn diagram was built in order to identify the differential expression during the infection time course (Figure 3.6a). The normalised value for differential expression was defined by 2 and the P-value cut-off was 0.05 (Annex 3e). These transcripts were differentially distributed among different time points of infection. However, some of them were present during different infection time points, allowing them to belong to more than one grouping. At 12 hpi there were 371 transcripts significantly expressed, and at 24, 36, 48 and 60 hpi there were 266, 244, 693, and 1050 transcripts respectively (Figure 3.6a).

Out of 371 transcripts significantly expressed at 12 hpi, analysed by volcano plot stage comparison of 12 hpi with itself, the majority of the transcripts (345 transcripts) were significantly up-regulated by 2 or more than 2-fold, and 26 transcripts were significantly down-regulated by 0.5 or less than 0.5 fold, defined by the normalised ratio (Figure 3.6b). Although 129 transcripts up-regulated at this time were listed as unannotated CHPs and HPs, 216 transcripts were annotated, according to the genome database. Among 216 up-regulated annotated transcripts, there were: spore associated proteins (13 transcripts)

including sporulation marker gene *Cdc14*, PAMPs and potential elicitors (three transcripts) including CBEL, CRN effectors (24 transcripts), and secreted RxLR effectors (two transcripts). Other protein coding transcripts such as for a secreted carbonic anhydrase (candidate effector), SCP-like extracellular proteins, enzyme inhibitor, ipiB1 family of glycine-rich proteins, glycoside hydrolase, transport proteins, and several other genes that are responsible for biotrophic interaction were also up-regulated during earliest infection stage of 12 hpi. Among down-regulated transcripts, there were 18 transcripts for RxLR effectors, two transcripts for CHPs, and one transcript each for protease inhibitor, SCR protein, glycoside hydrolase, and transglutaminase elicitor M81 protein were identified.

The 24 hpi stage was also analysed using the volcano plot pairwise comparison method to find significantly up-regulated and down-regulated genes at 24 hpi. Out of 266 transcripts, there were 265 transcripts up-regulated at this time point (Figure 3.6b). Although 106 transcripts up-regulated at this time point were unannotated CHPs and HPs, 160 transcripts were annotated including: spore associated proteins (eight transcripts), PAMPs (three transcripts) including CBEL, secreted RxLR effectors (two transcripts), and CRN effectors (15 transcripts). Other protein coding transcripts such as an SCP-like extracellular protein, enzyme inhibitor, ipiB1 family of glycine-rich proteins, glycoside hydrolase, transport proteins, and several other genes that are potentially responsible for biotrophic interaction were also up-regulated at 24 hpi. However, RxLR effector Avrblb2 (PITG_20301) was significantly down-regulated at this time point.

At 36 hpi, all detected 244 transcripts were significantly up-regulated (Figure 3.6b) by 2 or more than 2-fold. Transcripts encoding RxLR effectors (53 transcripts) including Avr proteins (Avr2, Avr3a, and Avrblb2) were significantly up-regulated at this stage.

Avrblb2 (PITG_20301), significantly down-regulated at 24 hpi was significantly up-regulated at this time. SCP-like extracellular proteins and enzyme inhibitors (six transcripts each), PAMPs including transglutaminase and elicitins (four transcripts), CRN effector (one transcript), and several other protein encoding transcripts such as NPP1 proteins, ipiB1 family of glycine-rich proteins, glycoside hydrolase, esterases, transport proteins, and several other proteins potentially involved in the biotrophic interaction were up-regulated at 36 hpi. The secreted effector candidate carbonic anhydrase (two transcripts) were also significantly up-regulated at this time point. Transcripts for 50 CHPs and HPs were also up-regulated at this time point.

At 48 hpi, 693 transcripts were detected as differentially expressed with the normalised value of 2 fold and above. 685 transcripts were significantly up-regulated (Figure 3.6b) at this time point, including those encoding: RxLR effectors (79 transcripts) including AVR proteins (Avr2, Avr3a, Avrblb1, and Avrblb2), CRN effectors (10 transcripts), enzyme inhibitors (13 transcripts), SCP-like extracellular proteins (five transcripts), cell wall degrading enzymes (18 transcripts), ipiB1 family of glycine-rich proteins, transport proteins, and several other proteins that may be responsible for biotrophic interaction. Transcripts for the secreted effector candidate carbonic anhydrase (two genes) were also up-regulated at this time point of infection. Among eight significantly down-regulated transcripts at this stage, there were three encoded for CHPs and HPs and one each for ipiB family of glycine rich protein, sorbitol dehydrogenases, Amt family of transporter protein, cutinase, and phosphatidylserine synthase.

Out of 1,050 transcripts differentially expressed at 60 hpi, 823 were significantly up-regulated and 227 transcripts were significantly down-regulated (Figure 3.6b). Up-regulated transcripts included those encoding: RxLR effectors (92 transcripts) including

Avr proteins (Avr2, Avr3a, Avrblb1, and Avrblb2), CRN effectors (14 transcripts), SCP-like extracellular proteins (six transcripts), enzyme inhibitors (12 transcripts), CWDEs (20 transcripts), elicitins (five transcripts), NLPs (three transcripts) and several other proteins that may be involved in biotrophic interactions. There were 154 CHPs and HPs up-regulated at this time. Among 227 significantly down-regulated at 60 hpi, 103 transcripts were CHPs and HPs. Transcripts encoding spore associated genes (10 transcripts) such as, sporulation marker gene *Cdc14*, nuclear LIM factor interactor, and sporangia and cleavage induced proteins were down-regulated at 60 hpi. One transcript each for RxLR effector (PITG_04074), SCP-like extracellular protein, and protease inhibitor (Epi11), and four transcripts of CRN effectors were also significantly down-regulated at this stage.

Using volcano plots, although several proteins were differentially expressed at more than one infection time point, at 12 hpi approximately 22.4% of transcripts (83) encoded predicted secreted proteins, followed by 20.7% (55) at 24 hpi, 34.4% (84) at 36 hpi, 21.1% (146) at 48 hpi, and 18.8% (198) at 60 hpi (Figure 3.6c).

Similarly, the proportion of genes encoding secreted RxLR effectors that were significantly differentially expressed, according to volcano plot analysis, up-regulated at 2-fold or more, and down-regulated less that 0.5 fold, at each infection time point were also analysed (Figure 3.6d). In comparison to the other genes, differentially expressed RxLR effectors comprised 21 (5.7%) transcripts at 12 hpi, out of which two transcripts were up-regulated and 19 transcripts were down-regulated.

Similar to the analysis based on flag value, transcripts for the majority of the total RxLR effectors detected (93 out of 114) were detected at 60 hpi. However, there were more transcripts encoding RxLR effectors (21) differentially expressed at 12 hpi in volcano

plot analysis compared to the RxLR coding transcripts (nine) that were detected by the flag value analysis method. This has happened as the flag value is only represented if the particular gene is detected as 'present' at specific time points, whereas volcano plot analysis evaluates each transcript with the significant normalised arbitrary value. Although there were only three transcripts for RxLR effectors differentially expressed at 24 hpi, compared to 25 transcripts detected using 'Present' flag value analysis, higher numbers of differentially expressed transcripts (52 and 79) were detected using volcano plots, compared to 43 and 73 transcripts detected by flag value analysis, at 36 and 48 hpi respectively. Interestingly, there were only four transcripts shared between all infection time points, compared to the flag value analysis (520 transcripts). These four transcripts are: RxLR effector (PITG_13452) up-regulated at 24, 36, 48, and 60 hpi, *Avrblb2* (PITG_20301) up-regulated at 36, 48, and 60 hpi, and two transcripts encoding CHPs. These CHPs were up-regulated at 12, 24 and 36 hpi, and were down-regulated at 48 and 60 hpi.

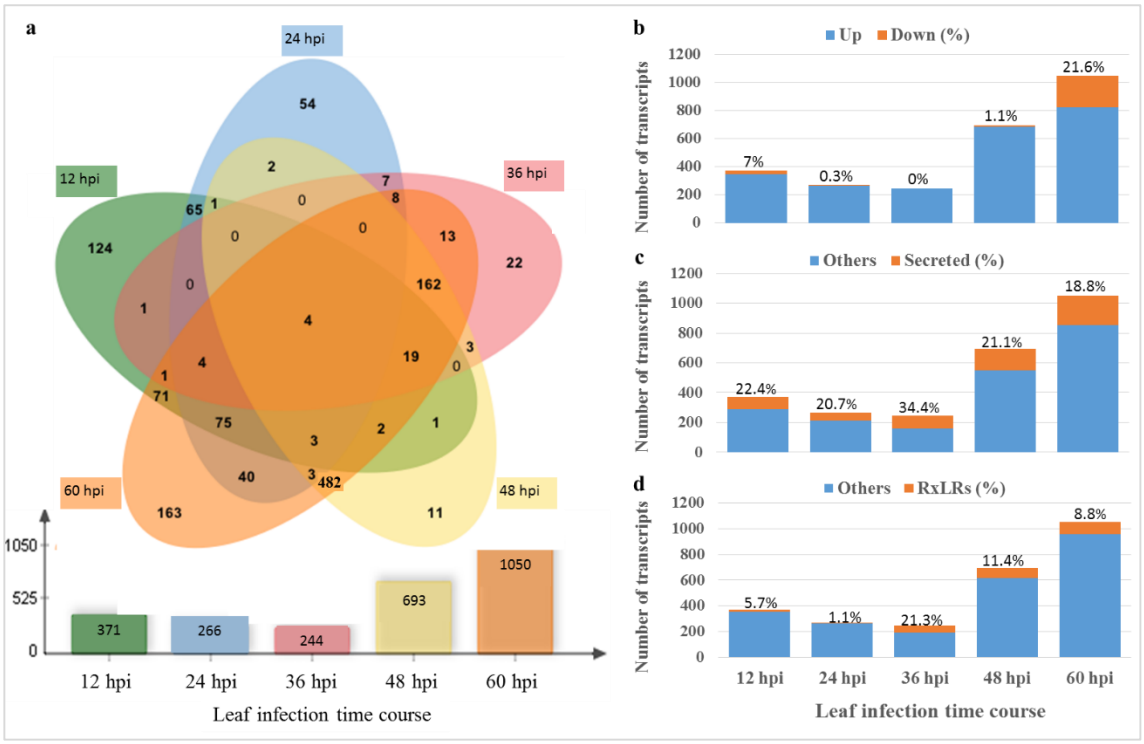

Figure 3.6 Volcano plot (leaf infection) built by comparing each stage (12, 24, 36, 48, and 60 hpi) with itself, in which transcripts differently expressed were defined by the normalised value of 2. Data were obtained from the 1,707 total differentially expressed transcripts from the ANOVA group (P-value cut-off: 0.05). Venn diagram (a) showing significantly differentially expressed transcripts at each different infection time point. Only four transcripts are common to each time point. Graph (b) showing numbers of transcripts significantly up-regulated (blue) at each different infection time point compared to down-regulation (orange). The analysis of genes encoding predicted secreted proteins (c) show more or less equally distributed proportions of transcripts for secreted proteins (orange) at each infection time point. Graph (d) shows the proportion (orange) of RxLR effector coding transcripts detected during each different time point of infection sampled. The greatest proportion of transcripts encoding RxLR effectors was at 36 hpi (21.3%).

3.2.7 Heatmap analysis of transcriptional change during infection

The set of 1,707 differentially expressed genes revealed by ANOVA (Annex 3d) were heatmap-clustered using Pearson's correlation approach, according to their expression profile (gene tree) (Figure 3.7).

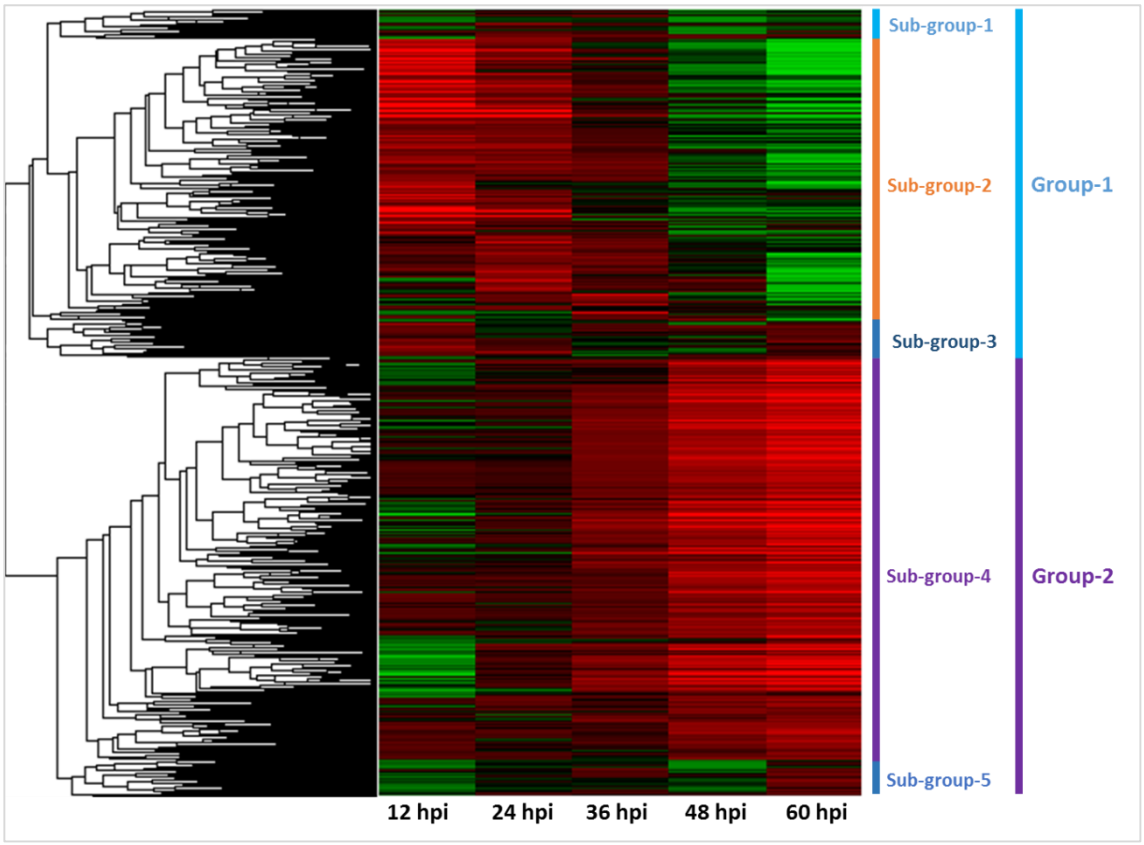

Figure 3.7 Heatmap clusters of differentially expressed genes from ANOVA were classified into two large 'overall' groups, and five sub-groups within those, according to their expression profiles across the five infection time points sampled (12, 24, 36, 48, and 60 hpi). Red represents up-regulation, whilst green represents down-regulation.

Clusters of differentially expressed genes were classified into two 'overall' groups, and five sub-groups according to their expression profiles (Figure 3.7; Annex 3d). Sub-group 1 and 3 were most similar to sub-group 2, in that they showed gradually down-regulation during infection. Sub-group 4 and 5 were similar to each other, in that they show overall up-regulation during infection. Thus, Sub-groups 1, 2, and 3 are encompassed by overall Group-1, where majority of the transcripts were detected early (12 and 24 hpi). Sub-groups 4 and 5 were encompassed by overall Group-2, mainly detected later in the infection time course (36 to 60 hpi). A similar analysis to that carried out for the transcripts at each time point was carried out to identify the proportion of transcripts encoding life stage specific (spore-associated proteins), and groups of proteins involved

in pathogenicity: PAMPs/elicitors, enzyme inhibitors, SCR proteins, RxLR effectors, CRN effectors, NPP1 proteins, CWDEs and esterases that are functionally annotated.

Sub-group-1 comprises a small set of 64 genes, including 21 (32.8%) uncharacterised CHPs and HPs. Although a low level of gene expression was observed in this group, the expression profile appears to show up-regulation particularly at 24, and 36 hpi (Figure 3.7). The levels of expression of two RxLR effector (PITG_09647, PITG_18981) encoding transcripts detected in this group were very low. Transporter genes such as ATP binding cassette (ABC), and major facilitator superfamily (MFS) transporters were 2- to 3-fold up-regulated in this group. PAMPs such as a transglutaminase elicitor, up-regulated at 36 hpi, was also detected in this group. Spore-associated proteins, enzyme inhibitors and ipiB family of extracellular proteins were not found in this sub-group.

The second largest sub-group (Sub-group-2), according to the heatmap clustering, comprised 613 transcripts, including 220 (35.9%) CHPs and HPs. The expression profile in this sub-group was characterised by high levels of transcript accumulation during the early stages (12, 24, with less at 36 hpi) of infection, and decreasing thereafter at 48 hpi and 60 hpi (Figure 3.7). Gene class analysis (Figure 3.8) showed that approximately 9.3% (57 transcripts) of the transcripts in this sub-group encoded CRN effectors. Although nine RxLR effectors were detected in this sub-group, only two (PITG_04074 and PITG_15753) were significantly (more than 2-fold) up-regulated. Transcripts encoding the other protein groups were present in comparatively low numbers: spore and cleavage-related proteins (15), PAMPs/elicitors (five), enzyme inhibitor (one), SCP-like family and SCR proteins (three), CWDEs such as hydrolase and esterase (seven), and all ipiB family and extracellular glycine-rich proteins (six). NLP-like NPP1 proteins were not found in

this sub-group. Several metabolic, transmembrane, and other proteins related to *P. infestans* growth and development were clustered in this sub-group.

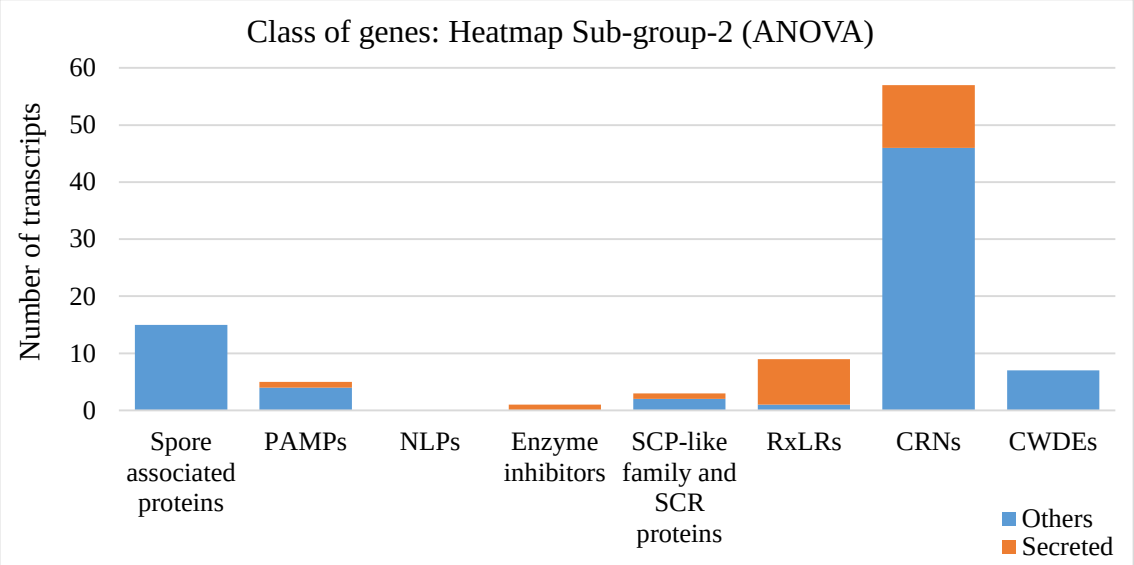

Figure 3.8 Numbers of annotated transcripts present in heatmap Sub-group 2 (cross reference to heatmap Figure 3.7). Apart from CRN effectors, spore associated transcripts are most highly presented in this sub-group.

A set of 75 transcripts (including 16 (21.3%) uncharacterised CHPs and HPs) comprised Sub-group 3. The majority of transcripts in this sub-group were not detected at 36 and 48 hpi (Figure 3.7). In this sub-group, genes encoding CRN effectors (four transcripts) were detected. However, transcripts encoding the other proteins such as spore and cleavage-related proteins, PAMPs/elicitors, RxLR effectors, enzyme inhibitors, SCP-like family and SCR proteins, ipiB family and extracellular glycine-rich proteins, and necrosis and CWDEs, such as hydrolase, esterase, and NLP proteins were absent.

Sub-group-4 was the largest expression group, comprising 875 transcripts, including those encoding 163 (18.6%) uncharacterised CHPs and HPs. The majority of transcripts were found to be up-regulated at 24, 36, 48 hpi, with all transcripts most highly up-regulated at 60 hpi (Figure 3.7). Among the 875 transcripts, class (Figure 3.9) analysis in this sub-group showed 10.6% (93 transcripts) encoded the RxLR class of cytoplasmic

effectors. These RxLR effectors were the largest proportion of the total of 114 that were differentially expressed during the infection time course. This included the avirulence effectors AvrSmira2 (PITG_07558), Avr2 (PITG_08943), Avr10 (PITG_11484), Avr3a (PITG_14371), Avrvnt1 (PITG_16294), Avrblb1 (PITG_21388) similar to ipi01, and Avrblb2 (PITG_20301). The biotrophic marker gene *Hmp1* (Avrova *et al.*, 2008) was also in this sub-group. Transcripts encoding CRN effectors (15), NLPs (five), CWDEs (21), and enzyme inhibitors (13) were among the largest protein classes detected in this sub-group. Other transcripts encoding PAMPs/elicitors (four) as well as SCP-like family and SCR proteins (six) were also detected. However, transcripts for the ipiB family of extracellular glycine-rich proteins were not found in this sub-group.

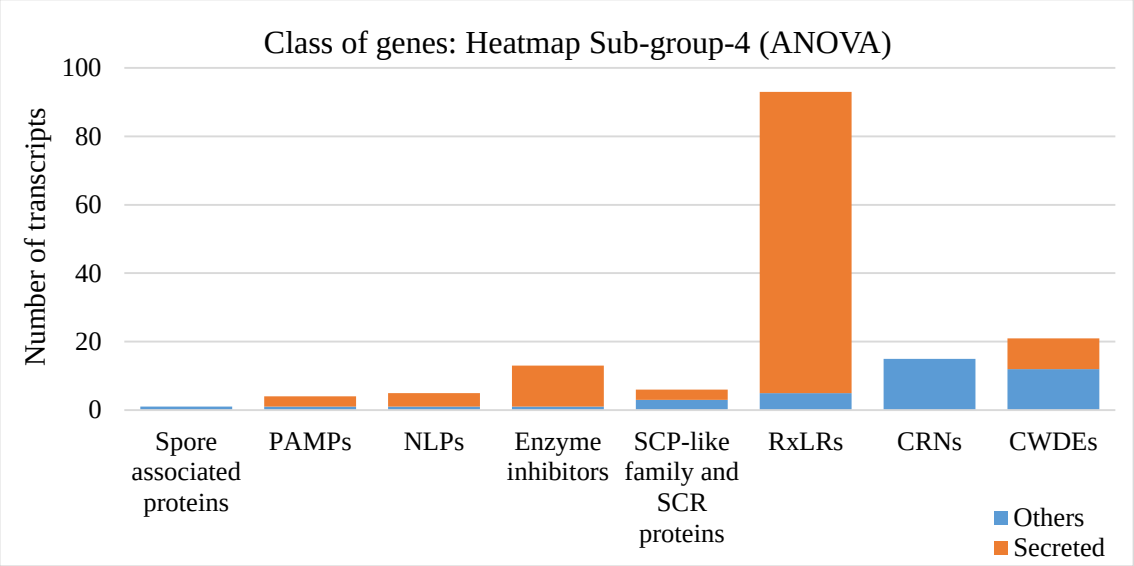

Figure 3.9 Numbers of annotated transcripts present in heatmap Sub-group 4 (cross reference to gene tree Figure 3.7). The majority of genes in this sub-group encode secreted RxLR effectors.

Expression sub-group five comprised 80 transcripts, including those encoding 28 (35%) uncharacterised CHPs and HPs. The expression profile of transcripts in this sub-group revealed up-regulation at 24, 36 and 60 hpi. Most of the transcripts in this sub-group were not detected at 12 and 48 hpi (Figure 3.7). This sub-group included transcripts for ten RxLR effector candidates, and two CRN effectors. Transcripts encoding NPP1 proteins,

enzyme inhibitors, spore-related proteins, SCP-like family and SCR proteins, and ipiB family of extracellular glycine-rich proteins were not detected in this sub-group.

Of the 114 RXLR effector coding transcripts showing differential expression during the infection time-course, 93 steadily increased in expression throughout infection (Sub-group 4), whereas 11 effectors (Sub-groups 1 and 2) were associated with the earliest infection time-points (up to 36 hpi) (Table 3.2).

Table 3.2 Transcripts encoding RXLR effectors significantly differentially expressed during potato leaf infection time course. According to heatmap groups, 114 RxLR effector transcripts, detected as differentially expressed, were classified into four sub-groups (sub-group 1, 2, 4, and 5) as listed in the table. The majority (93 transcripts) of RxLR effectors were clustered in sub-group 4. There were two, nine, and 10 transcripts encoding RxLR effectors in sub-groups 1, 2, and 5, respectively. Signal peptide analysis revealed 98 RxLRs were predicted to be secreted.

Description	Primary accession	Heatmap sub-group	Secreted protein	Cut-off value
RxLR	PITG_09647	1	Yes	0.75
RxLR	PITG_18981	1	Yes	0.71
RxLR	PITG_04074	2	Yes	0.751
RxLR	PITG_07741	2	Yes	0.855
RxLR	PITG_14960	2	Yes	0.678
RxLR	PITG_14965	2	Yes	0.678
RxLR	PITG_15753	2	Yes	0.84
RxLR	PITG_16409	2	Yes	0.584
RxLR	PITG_16424	2	Yes	0.584
RxLR	PITG_22825	2	Yes	0.768
RxLR	PITG_15128	2	No	
avr2 family	PITG_08278	4	Yes	0.525
avr2 family	PITG_08943	4	Yes	0.579
avr2 family	PITG_15972	4	Yes	0.537
avr2 family	PITG_19617	4	Yes	0.537
avr3a	PITG_14371	4	Yes	0.541
avr3a family	PITG_14368	4	Yes	0.573
avr3a family	PITG_14374	4	Yes	0.551
avr10	PITG_11484	4	Yes	0.843
avrblb1 (ipi01)	PITG_21388	4	Yes	0.819
avrblb2 family	PITG_04085	4	Yes	0.782
avrblb2 family	PITG_04090	4	Yes	0.731
avrblb2 family	PITG_18683	4	Yes	0.744
avrblb2 family	PITG_20300	4	Yes	0.731
avrblb2 family	PITG_20301	4	Yes	0.752
avrblb2 family	PITG_20303	4	Yes	0.784
avrSmira2	PITG_07558	4	Yes	0.914
avrvnt1	PITG_16294	4	Yes	0.827
PexRD2	PITG_14787	4	Yes	0.49
RxLR	PITG_20934	4	Yes	0.676
RxLR	PITG_21740	4	Yes	0.817
RxLR	PITG_22089	4	Yes	0.695
RxLR	PITG_22547	4	Yes	0.827
RxLR	PITG_22648	4	Yes	0.715
RxLR	PITG_22724	4	Yes	0.753
RxLR	PITG_22757	4	Yes	0.66
RxLR	PITG_22804	4	Yes	0.873
RxLR	PITG_22922	4	Yes	0.68

Table 3.2 **(Continued)**

Description	Primary accession	Heatmap sub-group	Secreted protein	Cut-off value
RxLR	PITG_22926	4	Yes	0.713
RxLR	PITG_23014	4	Yes	0.691
RxLR	PITG_23016	4	Yes	0.66
RxLR	PITG_23046	4	Yes	0.717
RxLR	PITG_23230	4	Yes	0.676
RxLR	PITG_00582	4	Yes	0.747
RxLR	PITG_01934	4	Yes	0.763
RxLR	PITG_02860	4	Yes	0.809
RxLR	PITG_03192	4	Yes	0.898
RxLR	PITG_04049	4	Yes	0.621
RxLR	PITG_04145	4	Yes	0.831
RxLR	PITG_04196	4	Yes	0.793
RxLR	PITG_04314	4	Yes	0.885
RxLR	PITG_05910	4	Yes	0.714
RxLR	PITG_05918	4	Yes	0.564
RxLR	PITG_06087	4	Yes	0.828
RxLR	PITG_06094	4	Yes	0.728
RxLR	PITG_06099	4	Yes	0.687
RxLR	PITG_07451	4	Yes	0.878
RxLR	PITG_07555	4	Yes	0.672
RxLR	PITG_07594	4	Yes	0.807
RxLR	PITG_07630	4	Yes	0.795
RxLR	PITG_09160	4	Yes	0.659
RxLR	PITG_09216	4	Yes	0.851
RxLR	PITG_09218	4	Yes	0.878
RxLR	PITG_09224	4	Yes	0.816
RxLR	PITG_09732	4	Yes	0.728
RxLR	PITG_09915	4	Yes	0.742
RxLR	PITG_09935	4	Yes	0.746
RxLR	PITG_10232	4	Yes	0.632
RxLR	PITG_10540	4	Yes	0.718
RxLR	PITG_10654	4	Yes	0.807
RxLR	PITG_11507	4	Yes	0.758
RxLR	PITG_12706	4	Yes	0.65
RxLR	PITG_12737	4	Yes	0.692
RxLR	PITG_13093	4	Yes	0.816
RxLR	PITG_13452	4	Yes	0.871
RxLR	PITG_13507	4	Yes	0.658
RxLR	PITG_14783	4	Yes	0.546
RxLR	PITG_14884	4	Yes	0.695
RxLR	PITG_15039	4	Yes	0.789
RxLR	PITG_15110	4	Yes	0.817
RxLR	PITG_15278	4	Yes	0.739

Table 3.2 **(Continued)**

Description	Primary accession	Heatmap sub-group	Secreted protein	Cut-off value
RxLR	PITG_15930	4	Yes	0.778
RxLR	PITG_16233	4	Yes	0.681
RxLR	PITG_16275	4	Yes	0.471
RxLR	PITG_16427	4	Yes	0.678
RxLR	PITG_16705	4	Yes	0.781
RxLR	PITG_16726	4	Yes	0.697
RxLR	PITG_17063	4	Yes	0.859
RxLR	PITG_17309	4	Yes	0.546
RxLR	PITG_17316	4	Yes	0.546
RxLR	PITG_18609	4	Yes	0.791
RxLR	PITG_18670	4	Yes	0.743
RxLR	PITG_18685	4	Yes	0.738
RxLR	PITG_19942	4	Yes	0.912
RxLR (Avh9.1)	PITG_05911	4	Yes	0.565
RxLR (Avh9.1)	PITG_05912	4	Yes	0.564
RxLR-3'	PITG_20336	4	Yes	0.676
RxLR-3'	PITG_22712	4	Yes	0.566
RxLR	PITG_00821	4	No	-
RxLR	PITG_04266	4	No	-
RxLR	PITG_04269	4	No	-
RxLR	PITG_13847	4	No	-
RxLR	PITG_16195	4	No	-
RxLR	PITG_16245	4	No	-
PexRD2 family	PITG_11383	5	Yes	0.749
PexRD2 family	PITG_22935	5	Yes	0.801
RxLR	PITG_09585	5	Yes	0.947
RxLR	PITG_10640	5	Yes	0.904
RxLR	PITG_13044	5	Yes	0.863
RxLR	PITG_13048	5	Yes	0.863
RxLR	PITG_15127	5	Yes	0.731
RxLR	PITG_15940	5	Yes	0.776
RxLR	PITG_23035	5	Yes	0.725
RxLR	PITG_23202	5	Yes	0.717

Differentially expressed genes were also grouped according to the normalised (fold change) value to identify the most highly up-regulated transcripts at each infection time sampled; the top 50 transcripts from each infection time are shown in Tables 3.3 to 3.7. Out of the top 50 up-regulated transcripts at 12 hpi (Table 3.3), 23 transcripts encoded secreted proteins. The most highly up-regulated transcripts in this list encode secreted RxLR effector PITG_04074, followed by three transcripts for non-secreted sorbitol dehydrogenases. The ipiB family of glycine-rich proteins, and SCP-like extracellular proteins, were also highly up-regulated at 12 hpi. All of these genes were listed in Sub-group 2 in the heatmap, including sporulation marker gene *Cdc14*, nuclear LIM factor, and CBEL PAMP. This list also includes seven transcripts for CHPs that encode secreted proteins.

At 24 hpi (Table 3.4), 23 transcripts out of the top 50 most up-regulated encoded secreted proteins. 27 transcripts up-regulated at 12 hpi, including those encoding an RxLR effector, SCP-like extracellular protein, ipiB1 family of glycine rich proteins, and three transcripts of sorbitol dehydrogenase were also up-regulated at this time point. An additional eight transcripts for secreted CHPs, and transcripts encoding transport proteins such as amino acid and auxin permease (AAAP), major facilitator superfamily (MFS), and ATP binding cassette (ABC) transporters, were also up-regulated at 24 hpi.

Out of the top 50 up-regulated transcripts at 36 hpi (Table 3.5), the majority (31 transcripts) of these, including six transcripts for CHPs, encoded secreted proteins. 18 transcripts for RxLR effectors, including one transcript each for Avr2 family protein (PITG_19617) and Avrblb2 (PITG_20303), were also up-regulated at 36 hpi. 23 transcripts, including 14 for RxLR effectors, up-regulated in this group were co-expressed with the biotrophy marker gene *Hmp1* (analysis described later in this chapter). Candidate

effectors such as catalase-peroxidase, and secreted carbonic anhydrase were also up-regulated at 36 hpi. Transcript encoding an NPP1 family protein (PITG_09716) was also up-regulated at this stage.

Out of the 50 most up-regulated transcripts at 48 hpi (Table 3.6), 41 transcripts encoded secreted proteins. The majority (31 transcripts) of up-regulated transcripts encoded RxLR effectors, including three transcripts for Avr2 family proteins, and six transcripts for Avrblb2 family proteins. Transcripts for catalase-peroxidase, NPP1, glycoside hydrolase, and pectinesterase were also up-regulated at this stage. 30 transcripts, including 20 RxLR effectors, were co-expressed with *Hmp1*. Five transcripts of CHPs detected at this stage encoded secreted proteins.

Among the 50 most up-regulated transcripts at 60 hpi (Table 3.7), 39 encoded secreted proteins. Among 29 RxLR effector coding transcripts up-regulated at this stage, there were two transcripts for Avr3a family proteins, and six for Avrblb2 family proteins. 38 of the top 50 transcripts up-regulated at 60 hpi were also up-regulated at 48 hpi. 28 transcripts, including 18 transcripts for RxLR effectors up-regulated in this group, were co-expressed with *Hmp1*. Four transcripts for CHPs up-regulated at this stage encoded secreted proteins.

Table 3.3 Top 50 transcripts up-regulated at 12 hpi. Transcripts in the table below were selected from the differentially expressed ANOVA list. P-value in the table refers to the significance level of each transcript differentially expressed during infection.

Description	Primary accession	Normalised value	P-value	Secreted protein
secreted RxLR effector peptide, putative	PITG_04074	51.2397	0.0018	Yes
sorbitol dehydrogenase, putative	PITG_04121	39.7445	0.0021	No
complement control module protein, putative	PITG_01333	38.8191	0.0017	Yes
sorbitol dehydrogenase, putative	PITG_04985	30.5301	0.0037	No
sorbitol dehydrogenase, putative	PITG_04989	28.8793	0.0018	No
SCP-like extracellular protein	PITG_10413	12.5534	0.0038	Yes
hypothetical protein similar to sexually induced protein 3	PITG_12878	11.9879	0.0102	Yes
AP-2 complex subunit alpha, putative	PITG_04335	10.7333	0.0140	No
sporangia induced hypothetical protein	PITG_00123	10.7269	0.0127	Yes
conserved hypothetical protein	PITG_18800	9.6267	0.0191	Yes
putative GPI-anchored serine-threonine rich hypothetical protein	PITG_17828	9.5327	0.0137	Yes
conserved hypothetical protein	PITG_11903	9.5200	0.0060	Yes
MtN3-like protein	PITG_04999	9.4883	0.0034	Yes
sporangia induced hypothetical protein	PITG_03875	7.8563	0.0097	No
protease inhibitor Epi11	PITG_07096	9.1443	0.0147	Yes
nuclear LIM factor interactor-interacting protein spore-specific form, putative	PITG_11241	7.7197	0.0021	No
AP-2 complex subunit sigma-1	PITG_04957	7.4001	0.0034	No
thrombospondin-like protein	PITG_16981	7.3370	0.0033	Yes
conserved hypothetical protein	PITG_02222	7.0295	0.0104	Yes
thioredoxin/dynein outer arm protein	PITG_15335	6.9594	0.0067	No
alcohol dehydrogenase, putative	PITG_10292	6.4735	0.0423	No
cleavage induced hypothetical protein	PITG_07355	6.2312	0.0086	No
cAMP-dependent protein kinase regulatory subunit	PITG_02671	6.1009	0.0114	No
transmembrane protein, putative	PITG_11863	6.0254	0.0424	No
conserved hypothetical protein	PITG_06741	5.8834	0.0142	Yes
CTD small phosphatase-like protein, putative	PITG_03933	5.8484	0.0044	No
conserved hypothetical protein	PITG_02399	5.8034	0.0114	Yes
protein kinase, putative	PITG_17577	5.7518	0.0148	No
cell 5A endo-1,4-betaglucanase, putative	PITG_08611	5.6197	0.0142	No
protein kinase, putative	PITG_20766	5.4575	0.0054	No
sporangia induced conserved hypothetical protein	PITG_13183	5.4463	0.0133	No
putative secreted protein	PITG_03583	5.4165	0.0124	Yes
cellulose binding elicitor lectin (CBEL), putative	PITG_03639	5.3750	0.0027	Yes
guanine nucleotide-binding protein G(I)/G(S)/G(T) subunit beta, putative	PITG_06376	5.1856	0.0033	No
ipiB1 family glycine-rich protein	PITG_22396	5.1809	0.0385	Yes
MADS-box transcription factor, putative	PITG_07059	5.1772	0.0060	No
outer dynein arm light chain 2	PITG_07793	5.1480	0.0246	No
dual specificity protein phosphatase, putative	PITG_18578	5.0051	0.0081	No
ammonium transporter (Amt) Family	PITG_10226	5.0036	0.0044	Yes
conserved hypothetical protein	PITG_18762	4.9794	0.0082	Yes
ammonium transporter (Amt) Family	PITG_20291	4.9793	0.0033	No
cleavage induced hypothetical protein	PITG_05296	4.9519	0.0077	No
transmembrane protein, putative	PITG_12771	4.8969	0.0426	No
ipiB1 family glycine-rich protein	PITG_22977	4.7937	0.0442	Yes
conserved hypothetical protein	PITG_12783	4.7922	0.0327	Yes
mucin-like protein	PITG_15968	4.7128	0.0129	Yes
sodium/potassium-transporting ATPase subunit alpha, putative	PITG_16061	4.5119	0.0018	No
bzip regulated hypothetical protein	PITG_17675	4.4683	0.0152	No

Table 3.3 **(continued)**

Description	Primary accession	Normalised value	P-value	Secreted protein
protein kinase, putative	PITG_00081	4.3640	0.0317	No
ipiB1 family glycine-rich protein	PITG_22976	4.3434	0.0473	Yes

Table 3.4 Top 50 transcripts up-regulated at 24 hpi. Transcripts in the table below were selected from the differentially expressed ANOVA list. P-value in the table refers to the significance level of each transcript differentially expressed during infection.

Description	Primary accession	Normalised value	P-value	Secreted protein
sorbitol dehydrogenase, putative	PITG_04121	23.71	0.0021	No
secreted RxLR effector peptide, putative	PITG_04074	21.40	0.0018	Yes
sorbitol dehydrogenase, putative	PITG_04985	19.44	0.0037	No
sorbitol dehydrogenase, putative	PITG_04989	17.60	0.0018	No
complement control module protein, putative	PITG_01333	8.37	0.0017	Yes
AP-2 complex subunit alpha, putative	PITG_04335	6.04	0.0140	No
Amino Acid/Auxin Permease (AAAP) Family	PITG_11283	5.47	0.0111	No
protein kinase, putative	PITG_17577	5.07	0.0148	No
M96 mating-specific protein, pseudogene	PITG_05904	4.97	0.0414	No
thrombospondin-like protein	PITG_16981	4.93	0.0033	Yes
conserved hypothetical protein	PITG_02009	4.88	0.0178	Yes
SCP-like extracellular protein	PITG_10413	4.88	0.0038	Yes
sporangia induced hypothetical protein	PITG_09287	4.69	0.0148	No
thioredoxin H-type	PITG_09722	4.67	0.0320	No
conserved hypothetical protein	PITG_07938	4.58	0.0270	Yes
glyceraldehyde-3-phosphate dehydrogenase, putative	PITG_19495	4.51	0.0389	No
putative GPI-anchored serine-threonine rich hypothetical protein	PITG_17828	4.38	0.0137	Yes
alcohol dehydrogenase, putative	PITG_10292	4.27	0.0423	No
protease inhibitor Epi11	PITG_07096	4.24	0.0147	Yes
U3 small nucleolar RNA-interacting protein, putative	PITG_03876	4.18	0.0466	No
conserved hypothetical protein	PITG_18762	4.11	0.0082	Yes
conserved hypothetical protein	PITG_00544	4.08	0.0365	Yes
Amino Acid/Auxin Permease (AAAP) Family	PITG_20230	4.02	0.0431	No
conserved hypothetical protein	PITG_02222	3.83	0.0104	Yes
sodium/potassium-transporting ATPase subunit alpha, putative	PITG_16061	3.70	0.0018	No
cleavage induced hypothetical protein	PITG_07355	3.58	0.0086	No
conserved hypothetical protein	PITG_19621	3.58	0.0383	Yes
nitrate reductase [NADPH], putative	PITG_13012	3.51	0.0278	No
conserved hypothetical protein	PITG_11903	3.45	0.0060	Yes
conserved hypothetical protein	PITG_05703	3.44	0.0087	Yes
sporangia induced hypothetical protein	PITG_03875	3.41	0.0097	No
ammonium transporter (Amt) Family	PITG_20291	3.40	0.0033	No
myosin-like protein	PITG_07985	3.37	0.0115	No
ATP-binding Cassette (ABC) Superfamily	PITG_08314	3.37	0.0399	No
ammonium transporter (Amt) Family	PITG_10226	3.34	0.0044	Yes
12-oxophytodienoate reductase, putative	PITG_14721	3.33	0.0114	No
transmembrane protein, putative	PITG_12771	3.31	0.0426	No
cAMP-dependent protein kinase regulatory subunit	PITG_02671	3.31	0.0114	No
WD domain-containing protein, putative	PITG_08121	3.30	0.0323	No
AP-2 complex subunit sigma-1	PITG_04957	3.29	0.0034	No
ipiB1 family glycine-rich protein	PITG_22396	3.24	0.0385	Yes
major facilitator superfamily (MFS)	PITG_22001	3.24	0.0109	No
hypothetical protein similar to sexually induced protein 3	PITG_12878	3.23	0.0102	Yes
conserved hypothetical protein	PITG_05945	3.22	0.0174	Yes
conserved hypothetical protein	PITG_17362	3.20	0.0229	Yes
conserved hypothetical protein	PITG_04381	3.18	0.0352	Yes
nitrite reductase [NAD(P)H], putative	PITG_13013	3.18	0.0089	No
sugar transporter, putative	PITG_07710	3.18	0.0114	No
ipiB1 family glycine-rich protein	PITG_22977	3.10	0.0442	Yes
CTD small phosphatase-like protein, putative	PITG_03933	3.09	0.0044	No

Table 3.5 Top 50 transcripts up-regulated at 36 hpi. Transcripts in the table below were selected from the differentially expressed ANOVA list. P-value in the table refers to the significance level of each transcript differentially expressed during infection.

Description	Primary accession	Normalised value	P-value	Secreted protein	Hmp1 co-expressed
Rab8 family GTPase, putative	PITG_06328	3.58	0.0091	No	No
NAD-specific glutamate dehydrogenase, putative	PITG_11116	3.52	0.0065	No	No
secreted RxLR effector peptide, putative	PITG_05918	3.43	0.0082	Yes	Yes
amino acid/auxin permease (AAAP) Family	PITG_11282	3.34	0.0088	No	No
major facilitator superfamily (MFS)	PITG_22001	3.17	0.0109	No	No
urocanase, putative	PITG_13490	3.08	0.0465	No	No
secreted RxLR effector peptide, putative	PITG_20934	2.99	0.0068	Yes	Yes
secreted RxLR effector peptide, putative	PITG_00582	2.99	0.0161	Yes	Yes
glucanase inhibitor protein 3	PITG_13671	2.89	0.0075	Yes	Yes
avrblb2 family secreted RxLR effector peptide, putative	PITG_20303	2.88	0.0033	Yes	No
secreted RxLR effector peptide, 3' partial	PITG_20336	2.87	0.0135	Yes	Yes
protease inhibitor Epi6	PITG_05440	2.80	0.0174	Yes	No
secreted RxLR effector peptide, putative	PITG_10654	2.80	0.0091	Yes	No
conserved hypothetical protein	PITG_17001	2.80	0.0426	Yes	No
sporangia induced hypothetical protein	PITG_03875	2.78	0.0097	No	No
catalase-peroxidase, putative	PITG_07143	2.74	0.0287	Yes	Yes
conserved hypothetical protein	PITG_11916	2.73	0.0127	Yes	Yes
avr2 family secreted RxLR effector peptide, putative	PITG_19617	2.73	0.0114	Yes	Yes
secreted RxLR effector peptide (Avh9.1), putative	PITG_05911	2.73	0.0119	Yes	Yes
secreted RxLR effector peptide, putative	PITG_12737	2.72	0.0029	Yes	Yes
GMP synthase [glutamine-hydrolyzing], putative	PITG_19656	2.71	0.0049	No	Yes
conserved hypothetical protein	PITG_12139	2.71	0.0023	Yes	Yes
secreted RxLR effector peptide, putative	PITG_14783	2.69	0.0210	Yes	Yes
carbonic anhydrase, putative	PITG_18284	2.63	0.0438	Yes	No
secreted RxLR effector peptide, putative	PITG_09160	2.62	0.0037	Yes	No
argininosuccinate synthase	PITG_05374	2.61	0.0068	No	No
elongation factor G, mitochondrial precursor	PITG_08681	2.60	0.0093	No	No
secreted RxLR effector peptide, putative	PITG_01934	2.59	0.0291	Yes	Yes
secreted RxLR effector peptide, putative	PITG_11507	2.56	0.0021	Yes	Yes
secreted RxLR effector peptide, putative	PITG_09216	2.56	0.0043	Yes	Yes
glycoside hydrolase, putative	PITG_18209	2.52	0.0142	No	No
hypothetical cleavage-induced protein	PITG_11588	2.52	0.0152	No	No
elicitin-like protein	PITG_22741	2.51	0.0055	Yes	No
secreted RxLR effector peptide, putative	PITG_11484	2.51	0.0032	Yes	Yes
conserved hypothetical protein	PITG_19621	2.49	0.0383	Yes	No
amino acid/auxin permease (AAAP) Family	PITG_11283	2.49	0.0111	No	No
PcF and SCR74-like cys-rich secreted peptide, putative	PITG_14645	2.49	0.0049	No	Yes
conserved hypothetical protein	PITG_06212	2.49	0.0399	Yes	No
amino acid/auxin permease (AAAP) Family	PITG_12808	2.47	0.0036	No	Yes
secreted RxLR effector peptide, putative	PITG_16195	2.47	0.0033	No	Yes
amino acid/auxin permease-like protein	PITG_17799	2.47	0.0115	No	Yes
conserved hypothetical protein	PITG_17362	2.46	0.0229	Yes	No
12-oxophytodienoate reductase, putative	PITG_14721	2.46	0.0114	No	No
sorbitol dehydrogenase, putative	PITG_04121	2.45	0.0021	No	No
NPP1-like protein	PITG_09716	2.45	0.0399	Yes	No
protease inhibitor EpiC3	PITG_14891	2.45	0.0291	Yes	No
SCP-like extracellular protein	PITG_10410	2.44	0.0091	Yes	No
secreted RxLR effector peptide, putative	PITG_14787	2.43	0.0134	Yes	Yes
periodic tryptophan protein 2	PITG_00052	2.41	0.0314	No	No
secreted RxLR effector peptide, putative	PITG_22089	2.41	0.0085	Yes	Yes

Table 3.6 Top 50 transcripts up-regulated at 48 hpi. Transcripts in the table below were selected from the differentially expressed ANOVA list. P-value in the table refers to the significance level of each transcript differentially expressed during infection.

Description	Primary accession	Normalised value	P-value	Secreted protein	Hmp1 co-expressed
NAD-specific glutamate dehydrogenase, putative	PITG_11116	10.16	0.0065	No	No
secreted RxLR effector peptide, putative	PITG_12737	8.92	0.0029	Yes	Yes
avrblb2 family secreted RxLR effector peptide, putative	PITG_20303	8.85	0.0033	Yes	No
secreted RxLR effector peptide, putative	PITG_11507	7.96	0.0021	Yes	Yes
Amino Acid/Auxin Permease (AAAP) Family	PITG_12808	7.37	0.0036	No	Yes
secreted RxLR effector peptide, putative	PITG_05918	7.26	0.0082	Yes	Yes
avrblb2 family secreted RxLR effector peptide, putative	PITG_04090	6.88	0.0063	Yes	Yes
secreted RxLR effector peptide, putative	PITG_11484	6.69	0.0032	Yes	Yes
avrblb2 family secreted RxLR effector peptide, putative	PITG_18683	6.57	0.0041	Yes	Yes
secreted RxLR effector peptide, putative	PITG_09160	6.45	0.0037	Yes	No
endoglucanase, putative	PITG_08944	6.36	0.0028	Yes	Yes
secreted RxLR effector peptide, putative	PITG_10654	6.30	0.0091	Yes	No
zinc (Zn2)-iron (Fe2) permease (ZIP) Family	PITG_00750	6.19	0.0041	No	Yes
avrblb2 family secreted RxLR effector peptide, putative	PITG_04085	5.93	0.0038	Yes	Yes
secreted RxLR effector peptide, putative	PITG_00582	5.87	0.0161	Yes	Yes
pectinesterase, putative	PITG_08912	5.81	0.0016	Yes	No
secreted RxLR effector peptide, putative	PITG_02860	5.67	0.0184	Yes	No
avrblb2 family secreted RxLR effector peptide, putative	PITG_20300	5.66	0.0025	Yes	No
secreted RxLR effector peptide, putative	PITG_22922	5.55	0.0114	Yes	No
secreted RxLR effector peptide (Avh9.1), putative	PITG_05912	5.48	0.0085	Yes	Yes
avrblb2 family secreted RxLR effector peptide, putative	PITG_20301	5.46	0.0026	Yes	No
catalase-peroxidase, putative	PITG_07143	5.44	0.0287	Yes	Yes
secreted RxLR effector peptide, putative	PITG_16195	5.43	0.0033	No	Yes
NPP1-like protein	PITG_09716	5.40	0.0399	Yes	No
secreted RxLR effector peptide (Avh9.1), putative	PITG_05911	5.32	0.0119	Yes	Yes
conserved hypothetical protein	PITG_04202	5.30	0.0019	Yes	No
secreted RxLR effector peptide, putative	PITG_16275	5.27	0.0033	Yes	Yes
glucanase inhibitor protein 3	PITG_13671	5.16	0.0075	Yes	Yes
secreted RxLR effector peptide, putative	PITG_09732	5.08	0.0148	Yes	Yes
conserved hypothetical protein	PITG_12139	5.04	0.0023	Yes	Yes
secreted RxLR effector peptide, putative	PITG_09216	4.96	0.0043	Yes	Yes
secreted RxLR effector peptide, putative	PITG_09224	4.95	0.0121	Yes	Yes
conserved hypothetical protein	PITG_18224	4.93	0.0026	Yes	Yes
glycoside hydrolase, putative	PITG_04135	4.73	0.0081	Yes	Yes
secreted RxLR effector peptide, putative	PITG_05910	4.66	0.0068	Yes	No
major facilitator superfamily (MFS)	PITG_13473	4.65	0.0044	No	No
amino acid/auxin permease-like protein	PITG_17799	4.59	0.0115	No	Yes
conserved hypothetical protein	PITG_11916	4.58	0.0127	Yes	Yes
avr2 family secreted RxLR effector peptide, putative	PITG_08278	4.56	0.0200	Yes	No
secreted RxLR effector peptide, putative	PITG_23014	4.56	0.0145	Yes	Yes
avr2 family secreted RxLR effector peptide, putative	PITG_19617	4.52	0.0114	Yes	Yes
secreted RxLR effector peptide, putative	PITG_04049	4.50	0.0053	Yes	Yes
secreted RxLR effector peptide, putative	PITG_22757	4.46	0.0491	Yes	Yes
conserved hypothetical protein	PITG_14583	4.45	0.0090	Yes	No
glutamate-rich WD repeat-containing protein	PITG_10015	4.42	0.0471	No	No
DNA-directed RNA polymerase I subunit RPA2, putative	PITG_02420	4.41	0.0146	No	No
Amino Acid/Auxin Permease (AAAP) Family	PITG_17803	4.40	0.0233	No	No
avr2 family secreted RxLR effector peptide, putative	PITG_15972	4.40	0.0030	Yes	No
secreted RxLR effector peptide, putative	PITG_06099	4.40	0.0018	Yes	Yes
secreted RxLR effector peptide, putative	PITG_18685	4.38	0.0142	Yes	No

Table 3.7 Top 50 transcripts up-regulated at 60 hpi. Transcripts in the table below were selected from the differentially expressed ANOVA list. P-value in the table refers to the significance level of each transcript differentially expressed during infection.

Description	Primary accession	Normalised value	P-value	Secreted protein	Hmp1 co-expressed
NAD-specific glutamate dehydrogenase, putative	PITG_11116	17.39	0.0065	No	No
avrblb2 family secreted RxLR effector peptide, putative	PITG_20303	16.59	0.0033	Yes	No
secreted RxLR effector peptide, putative	PITG_10654	12.69	0.0091	Yes	No
avrblb2 family secreted RxLR effector peptide, putative	PITG_04090	12.38	0.0063	Yes	Yes
secreted RxLR effector peptide, putative	PITG_12737	12.12	0.0029	Yes	Yes
pectinesterase, putative	PITG_08912	12.11	0.0016	Yes	No
conserved hypothetical protein	PITG_04202	11.49	0.0019	Yes	No
avrblb2 family secreted RxLR effector peptide, putative	PITG_18683	11.35	0.0041	Yes	Yes
avrblb2 family secreted RxLR effector peptide, putative	PITG_04085	11.34	0.0038	Yes	Yes
secreted RxLR effector peptide, putative	PITG_11507	10.96	0.0021	Yes	Yes
avrblb2 family secreted RxLR effector peptide, putative	PITG_20301	10.66	0.0026	Yes	No
avrblb2 family secreted RxLR effector peptide, putative	PITG_20300	10.54	0.0025	Yes	No
endoglucanase, putative	PITG_08944	9.89	0.0028	Yes	Yes
catalase-peroxidase, putative	PITG_07143	9.84	0.0287	Yes	Yes
secreted RxLR effector peptide, putative	PITG_05918	9.55	0.0082	Yes	Yes
secreted RxLR effector peptide, putative	PITG_09160	9.38	0.0037	Yes	No
conserved hypothetical protein	PITG_04213	9.24	0.0021	Yes	No
secreted RxLR effector peptide, putative	PITG_09732	9.10	0.0148	Yes	Yes
zinc (Zn2)-iron (Fe2) permease (ZIP) Family	PITG_00750	9.00	0.0041	No	Yes
Amino Acid/Auxin Permease (AAAP) Family	PITG_12808	8.94	0.0036	No	Yes
secreted RxLR effector peptide, putative	PITG_11484	8.85	0.0032	Yes	Yes
secreted RxLR effector peptide, putative	PITG_00582	8.58	0.0161	Yes	Yes
secreted RxLR effector peptide (Avh9.1), putative	PITG_05912	8.36	0.0085	Yes	Yes
amino acid/auxin permease-like protein	PITG_17799	8.14	0.0115	No	Yes
secreted RxLR effector peptide (Avh9.1), putative	PITG_05911	8.10	0.0119	Yes	Yes
conserved hypothetical protein	PITG_12139	8.03	0.0023	Yes	Yes
secreted RxLR effector peptide, putative	PITG_02860	7.55	0.0184	Yes	No
amino acid/auxin permease (AAAP) Family	PITG_17803	7.48	0.0233	No	No
secreted RxLR effector peptide, putative	PITG_18670	7.45	0.0034	Yes	No
glycoside hydrolase, putative	PITG_04135	7.35	0.0081	Yes	Yes
secreted RxLR effector peptide, putative	PITG_22922	7.23	0.0114	Yes	No
major facilitator superfamily (MFS)	PITG_13473	7.09	0.0044	No	No
conserved hypothetical protein	PITG_18224	6.84	0.0026	Yes	Yes
secreted RxLR effector peptide, putative	PITG_16195	6.73	0.0033	No	Yes
avr3a family secreted RxLR effector peptide, putative	PITG_14368	6.69	0.0047	Yes	No
secreted RxLR effector peptide, putative	PITG_09216	6.42	0.0043	Yes	Yes
beta-glucan synthesis-associated protein, putative	PITG_20896	6.29	0.0062	Yes	No
secreted RxLR effector peptide, putative	PITG_16275	6.21	0.0033	Yes	Yes
phosphoenolpyruvate carboxykinase	PITG_11189	6.17	0.0273	No	No
NPP1-like protein	PITG_09716	6.11	0.0399	Yes	No
protease inhibitor Epi6	PITG_05440	6.08	0.0174	Yes	No
glutamate-rich WD repeat-containing protein	PITG_10015	6.08	0.0471	No	No
secreted RxLR effector peptide, putative	PITG_05910	6.04	0.0068	Yes	No
secreted RxLR effector peptide, putative	PITG_13507	5.91	0.0034	Yes	Yes
secreted RxLR effector peptide, putative	PITG_09224	5.88	0.0121	Yes	Yes
major facilitator superfamily (MFS)	PITG_03540	5.87	0.0419	No	Yes
avr3a family secreted RxLR effector peptide, putative	PITG_14374	5.85	0.0049	Yes	Yes
secreted RxLR effector peptide, putative	PITG_22089	5.83	0.0085	Yes	Yes
secreted RxLR effector peptide, putative	PITG_09218	5.82	0.0037	Yes	No
PcF and SCR74-like cys-rich secreted peptide, putative	PITG_14645	5.80	0.0049	No	Yes

3.2.8 Co-expressed transcripts during infection by *P. infestans*

3.2.8.1 Sporulation marker (*Cdc14*) co-expressed genes

Ah-Fong and Judelson (2003) previously reported that the *Cdc14* gene is a key marker of sporulation, but is not expressed during hyphal growth in *P. infestans*. This same protein is also associated with flagella in *P. infestans* (Ah-Fong and Judelson, 2011) and is highly expressed in zoospores. The expression pattern of *Cdc14* (PITG_18578) was identified from the *in vitro* (sporangia and germinating cysts) and *in planta* (12 to 60 hpi) stages from the transcript list (after ANOVA) from the microarray experiment (Figure 3.10). *Cdc14* transcript was highly up-regulated (up to 17-fold) in sporangia, then decreased to 6-fold in germinating cysts. During infection this gene was 5-fold up-regulated at the earliest (12 hpi) infection time point. This could be due to the inoculation droplet still containing some un-germinated cysts or biflagellate zoospores on the surface of the leaf. *Cdc14* expression markedly decreased to 1-fold at 24 hpi, and decreased further by 36 hpi, 48 hpi, and 60 hpi, according to Pearson's correlation analysis.

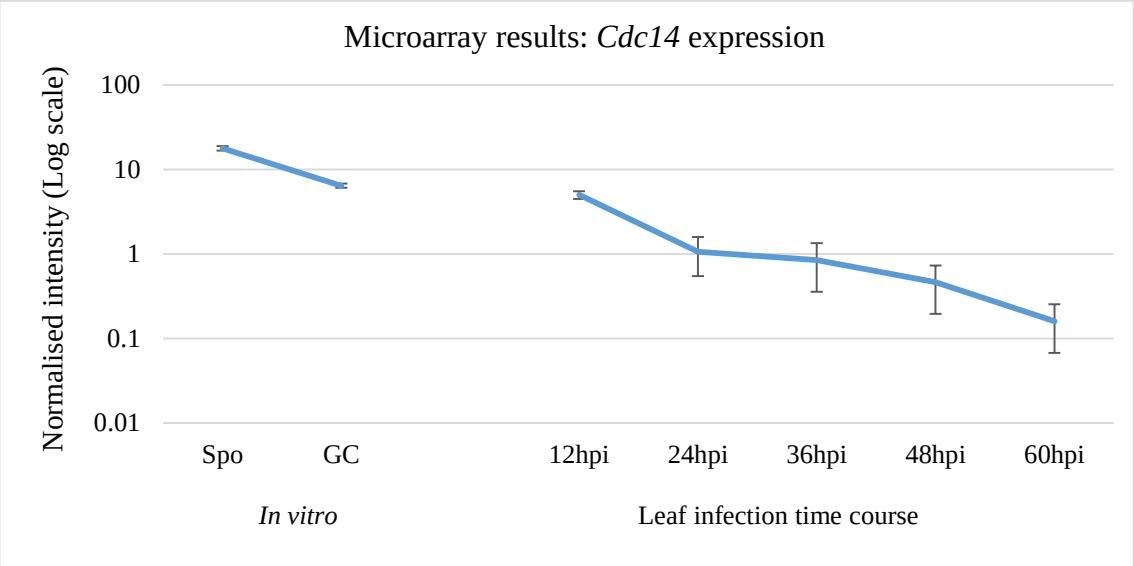

Figure 3.10 Sporulation marker *Cdc14* (PITG_18578) expression profile from normalised microarrays during *in vitro* and *in planta* infection stages (log scale). This graph shows the high expression of *Cdc14* in sporangia (Spo) and germinating cysts (GC) compared to *in planta* infection stages.

Genes co-expressed only during the *in planta* infection with sporulation marker *Cdc14* were clustered with a 95% probability rate of correlation coefficient (Figure 3.11). At this level of probability, 137 transcripts were co-expressed with *Cdc14* (Annex 3f). Although 42 transcripts in this set were unannotated CHPs and HPs, there were significant numbers of genes encoding proteins (Figure 3.12) related to *P. infestans* spore biology, such as sporangia-induced proteins, cleavage-induced proteins, and the spore-specific form of a nuclear LIM factor interacting protein (Judelson *et al*., 2008). In addition, genes encoding PAMPs such as cellulose binding elicitor lectin (CBEL) (Gaulin *et al*., 2002) were also represented in the *Cdc14*-co-expressed set, along with transcription factors such as a MADS-box transcription factor, and Myb-like DNA binding proteins, which were expressed highly at 12 hpi and then not detected for the remainder of the infection time course.

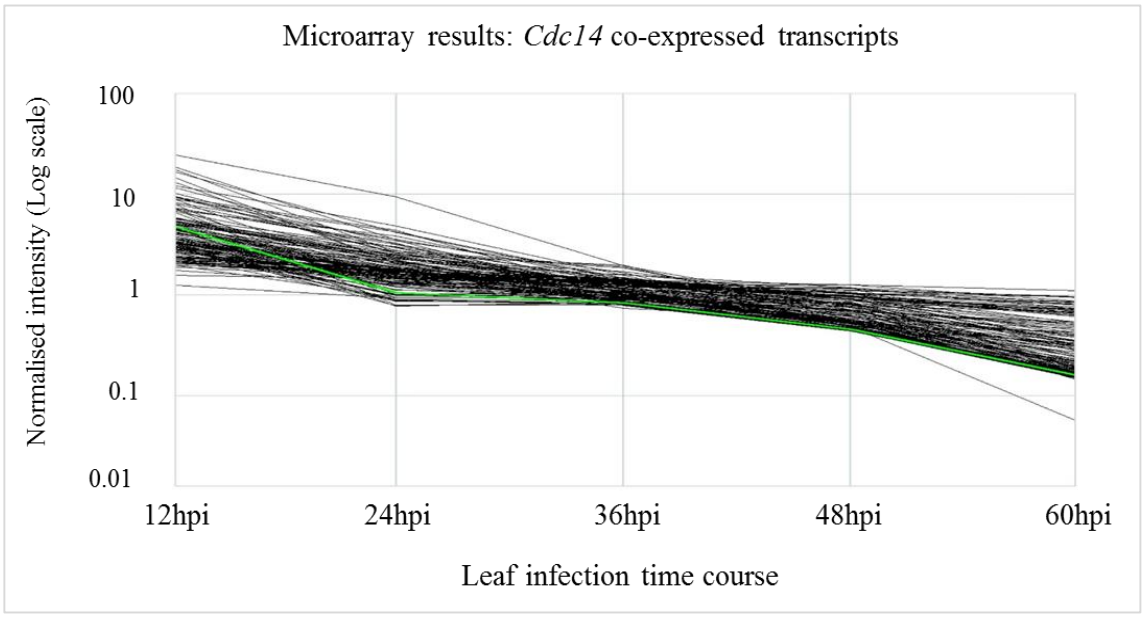

Figure 3.11 Expression (normalised intensity) of sporulation marker gene *Cdc14* (highlighted in green) co-expressed genes (95% probability; non-highlighted) during *in planta* infection stages (log scale). These genes are all down-regulated throughout the infection time course.

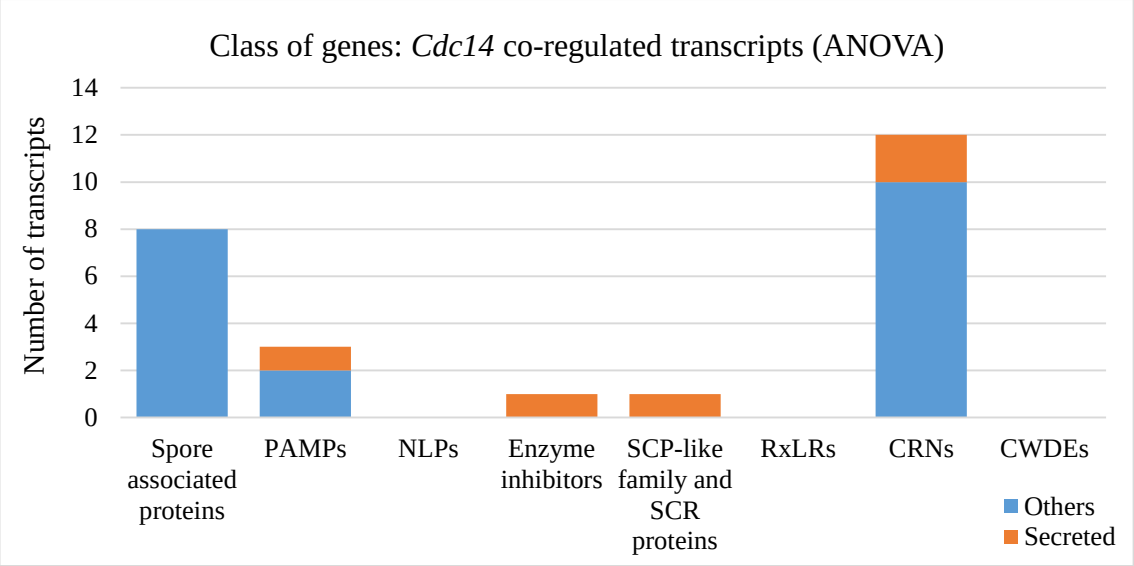

Figure 3.12 Class of differentially expressed genes among those co-expressed with *Cdc14* (PITG_18578). Transcripts encoding spore-associated proteins were co-expressed with this sporulation marker gene. 12 transcripts for CRN effectors also appeared to be co-expressed with *Cdc14*. Transcripts for an enzyme inhibitor and a SCP-like extracellular protein were also detected in this list. However, NLPs, RxLR effectors and CWDEs were not co-expressed with *Cdc14*. Blue represents non-secreted proteins while orange refers to secreted proteins.

3.2.8.2 Biotrophic marker (*Hmp1*) co-expressed genes

The haustorial membrane protein 1 (*Hmp1*) gene from *P. infestans* is a well-known marker of biotrophic infection stages. It has been reported to be up-regulated in germinating cysts (in comparison to sporangia) and during infection (Avrova *et al.*, 2008). Similar to the previous findings, in the microarray results described here, the transcript encoding this protein (PITG_00375) showed up-regulation in germinating cysts compared to sporangia, and was up-regulated throughout *in planta* infection (Figure 3.13).

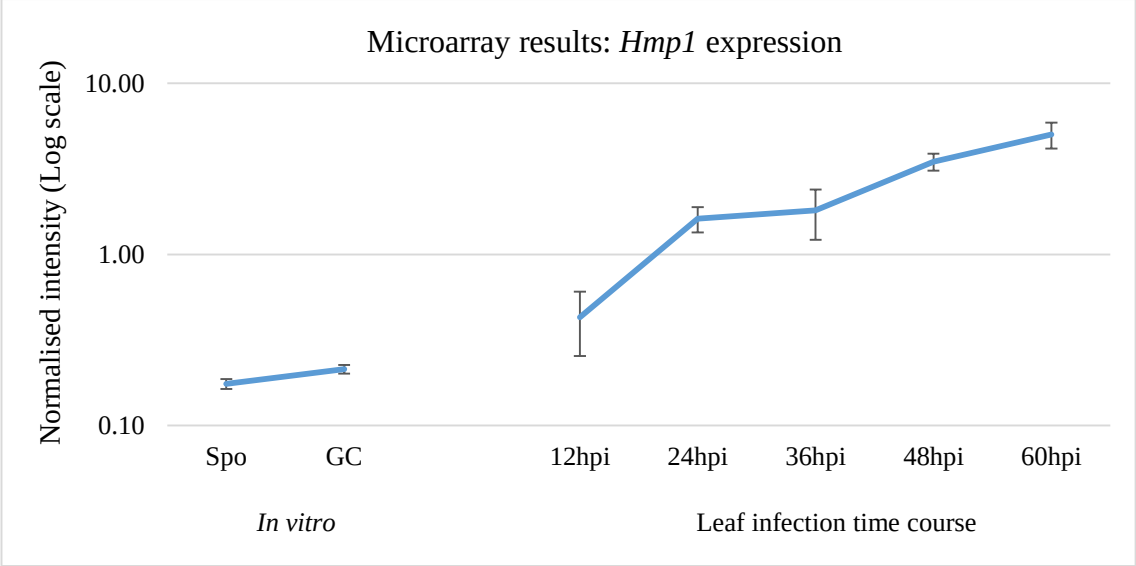

Figure 3.13 Expression profile of biotrophy marker gene *Hmp1* (PITG_00375) during *in vitro* and *in planta* infection stages (log scale; normalised microarray data). Expression of *Hmp1* was higher in germinating cysts (GC) compared to sporangia (Spo) and up-regulated *in planta* infection compared to *in vitro* stages.

A set of *Hmp1* co-expressed genes were extracted from the differentially expressed set of genes from the microarray results using the default setting of 95% probability rate (Figure 3.14). A set of 186 genes was co-expressed with *Hmp1 in planta* (Annex 3f). 36 transcripts were CHPs and HPs. Gene class analysis (Figure 3.15) among annotated transcripts co-expressed with *Hmp1* revealed the occurrence of numerous pathogenicity and potential biotrophy associated transcripts during early infection. The *Hmp1* co-expressed gene set contained 55 RxLR effectors, including well-known avirulence genes *Avr2* (Gilroy *et al*., 2011), *Avrblb1* (Vleeshouwers *et al*., 2008) (similar to *IpiO1*; van West *et al*., 1998), *Avrblb2* (Bozkurt *et al*., 2011), *Avr3a* (Armstrong *et al*., 2005), and *AvrVnt1* (Pel, 2010). Most of these avirulence proteins have previously been found to be secreted from haustoria or associated with haustoria to promote infection (Whisson *et al*., 2007; Gilroy *et al*., 2011; Bozkurt *et al*., 2011; van Poppel 2009). There were transcripts for nine secreted enzyme inhibitor proteins (protease inhibitors and glucanase inhibitors), eight CWDEs such as glycoside hydrolase and pectinesterase, two CRN effectors; two

transcription factors (C2H2 Zinc finger and S-II type), and one elicitin-like protein. No spore-related transcripts were co-expressed with *Hmp1*.

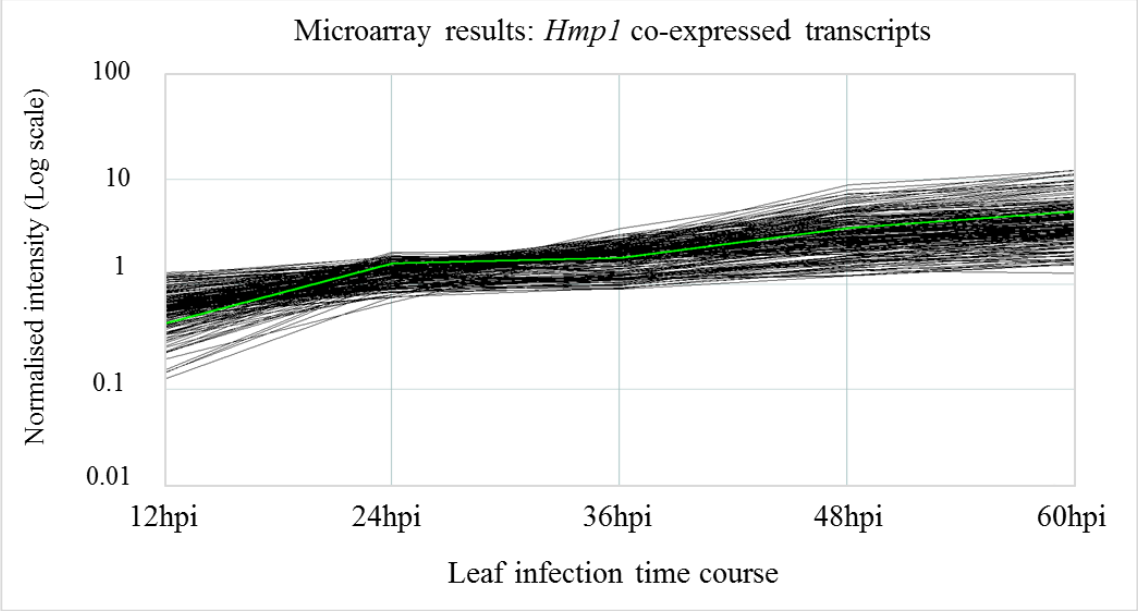

Figure 3.14 Expression profile of *Hmp1* (biotrophic marker gene - highlighted in green) co-expressed genes (95% probability; non-highlighted) derived from microarray results of *in planta* infection expression (log scale). These genes are up-regulated throughout the infection time course.

Out of 186 transcripts co-expressed with *Hmp1*, 45.7% (85 transcripts) comprised secreted proteins which includes the majority of the RxLR effectors in this group (53 out of 55 transcripts), followed by enzyme inhibitors (nine out of 10 transcripts), and CWDEs (six out of eight transcripts) (Figure 3.15). There were eight transcripts of CHPs encoding proteins with a predicted signal peptide.

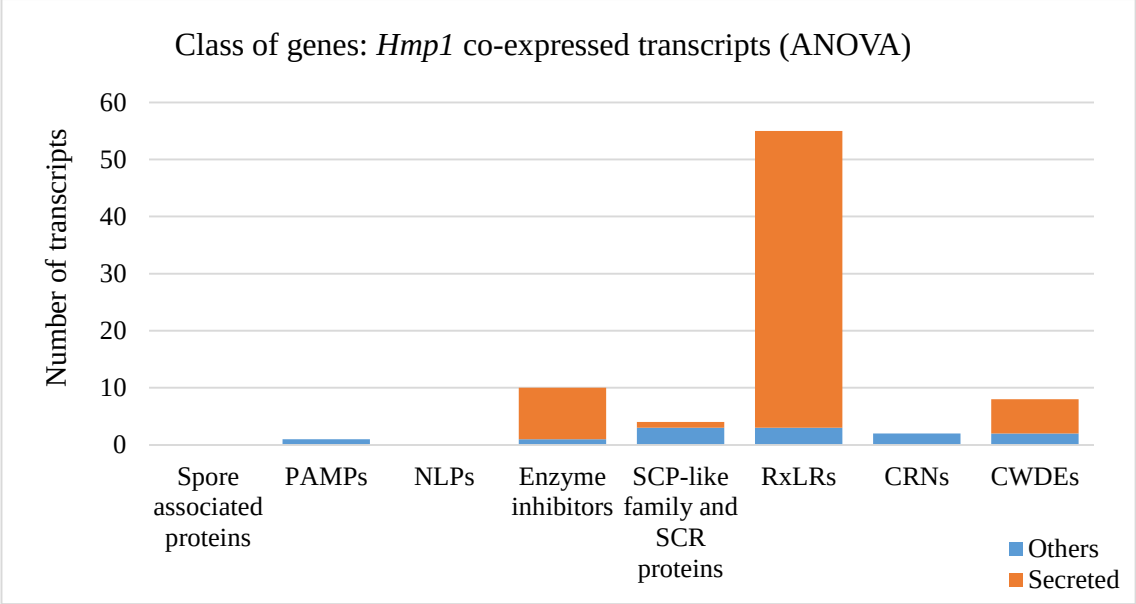

Figure 3.15 Class of differentially expressed genes among those co-expressed with *Hmp1*. A high number (55 transcripts) of cytoplasmic RxLR effectors were co-expressed with *Hmp1*. The majority of apoplastic effectors differentially expressed during leaf infection, such as enzyme inhibitors (glucanase and protease inhibitors) were also detected in the list. However, there were low numbers of genes encoding elicitins and CRN effectors co-expressed with *Hmp1*. Transcripts encoding secreted proteins (blue represents non-secreted proteins while orange refers to secreted proteins) showed the majority of RxLR effectors, enzyme inhibitors, and CWDEs co-expressed with *Hmp1* to be secreted proteins.

3.2.8.3 Necrotrophy marker (*NPP1*) co-expressed genes

Necrosis-inducing *Phytophthora* protein 1 (*NPP1*) is a potential inducer of the hypersensitive response in host cells (Fellbrich *et al*., 2002) and is a well-known necrotrophy marker gene in *Phytophthora*. Although the necrosis-inducing proteins constitute a large protein family in oomycetes, characterised secreted NPP1-like proteins (NCBI Reference Sequence: XP_002897301.1) in *Phytophthora* have two conserved cysteine residues followed by a hepta-peptide motif 'GHRHDWE' (Gijzen and Nürnberger, 2006). The necrotrophy marker gene *NPP1* (PITG_09716) used in this research to explore the expression profile during *in planta* infection stages also has the two conserved cysteine residues and known to induce necrosis (Cabral *et al*., 2012). However, this gene was slightly different in another conserved domain, the hepta-peptide motif; instead of 'GHRHDWE' this gene has 'GHRHGWE' (Figure 3.16). In contrast to

Hmp1, microarray results revealed that this gene was highly down-regulated during *in vitro* stages, especially in the germinating cyst stage, compared to sporangia, and highly up-regulated during later stages (48, and 60 hpi) of this infection time-course (Figure 3.17).

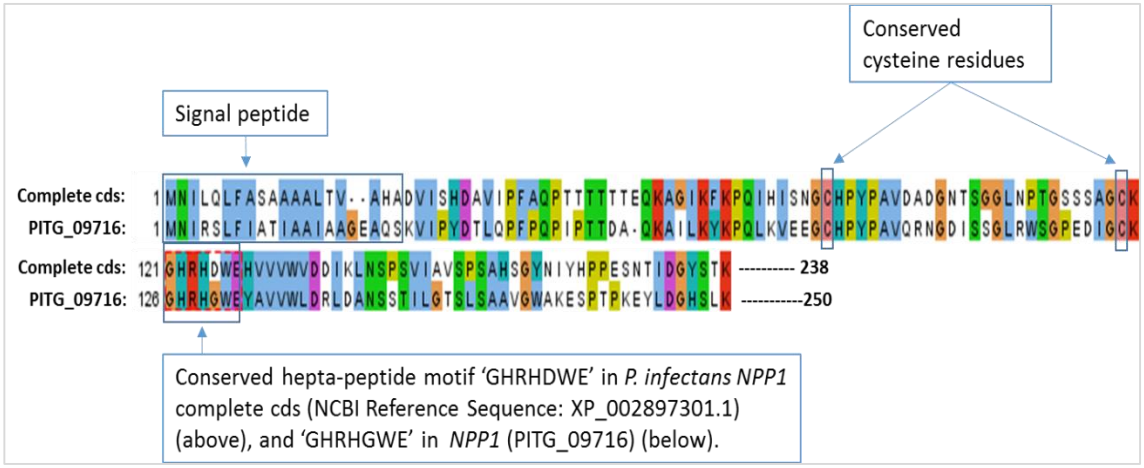

Figure 3.16 Comparison of NPP1-like sequences of *P. infestans*. Complete cds refers to the NPP1 like sequence (NCBI reference sequence XP_002897302.1), and differentially expressed NPP1-like protein (PITG_09716) revealed from the microarray (leaf infection) results. Both sequences have an N-terminal signal peptide, followed by the two cysteine residues. However, conserved hepta-peptide motifs were different with 'D' (aspartic acid) and 'G' (glycine).

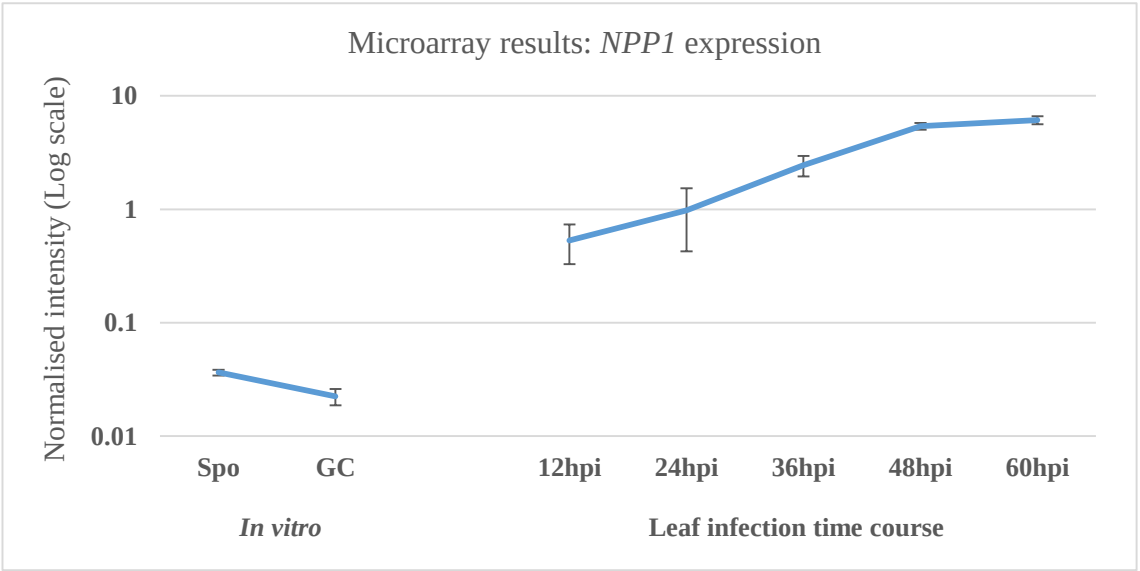

Figure 3.17 Normalised expression of the necrotrophy marker gene *NPP1* (PITG_09716). This graph shows the expression profile of *NPP1*, which is down-regulated in *in vitro* stages (Spo and GC) and induced from 24 hpi and highly up-regulated during 36, 48, and 60 hpi.

NPP1 co-expressed genes were also extracted from the microarray results of differentially expressed genes with the probability rate of 95% (Figure 3.18). 400 transcripts were co-expressed with the necrotrophy marker gene *NPP1* (Annex 3f). Although 65 transcripts co-expressed with *NPP1* genes were unannotated CHPs and HPs, there were many (62 transcripts) encoding RxLR effectors found in this group. This included avirulence proteins Avr2 family protein (PITG_08943), Avr3a (PITG_14371), and Avrblb2 family protein (PITG_20300, PITG_20301, and PITG_20303). There were also transcripts for three CRN effectors, seven enzyme inhibitors, two PAMPs/elicitors, and eight transcripts of CWDEs such as hydrolases and esterases in this group (Figure 3.19). There were 32.2% (129) transcripts overlapping between the gene sets identified for *NPP1* with *Hmp1* co-expressed genes. Transcript encoding berberine-like secreted protein (PITG_02930), which was not co-expressed with *Hmp1*, was also co-expressed with *NPP1*.

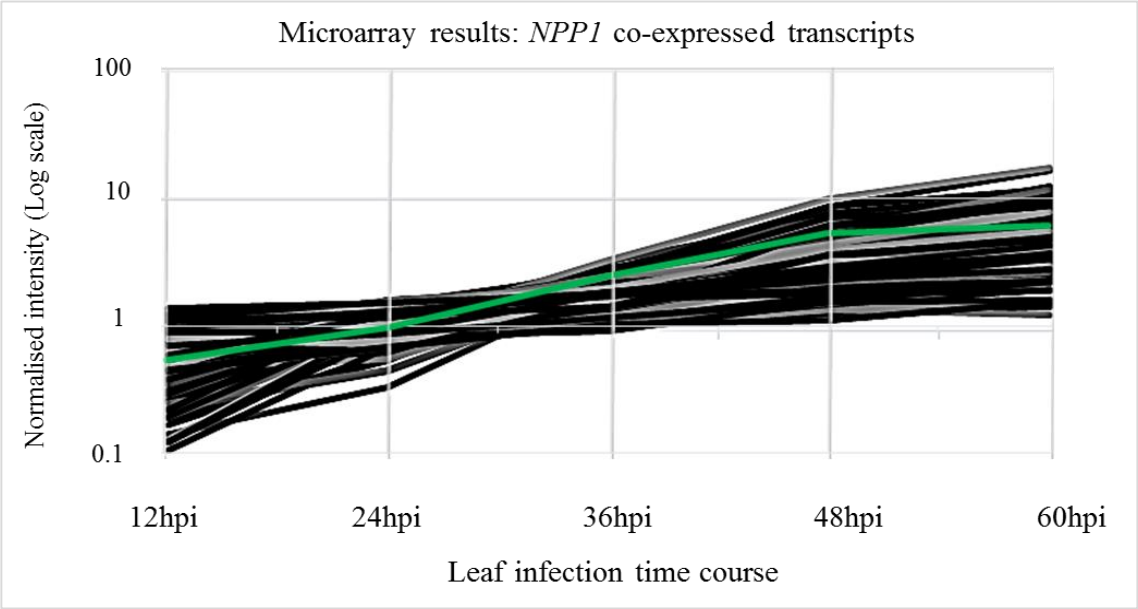

Figure 3.18 Expression profiles of *NPP1* (necrotrophy marker gene - highlighted in blue) co-expressed genes (95% probability: non-highlighted) derived from microarray results of *in planta* expression (log scale). These genes were highly up-regulated during later stages of the infection time course.

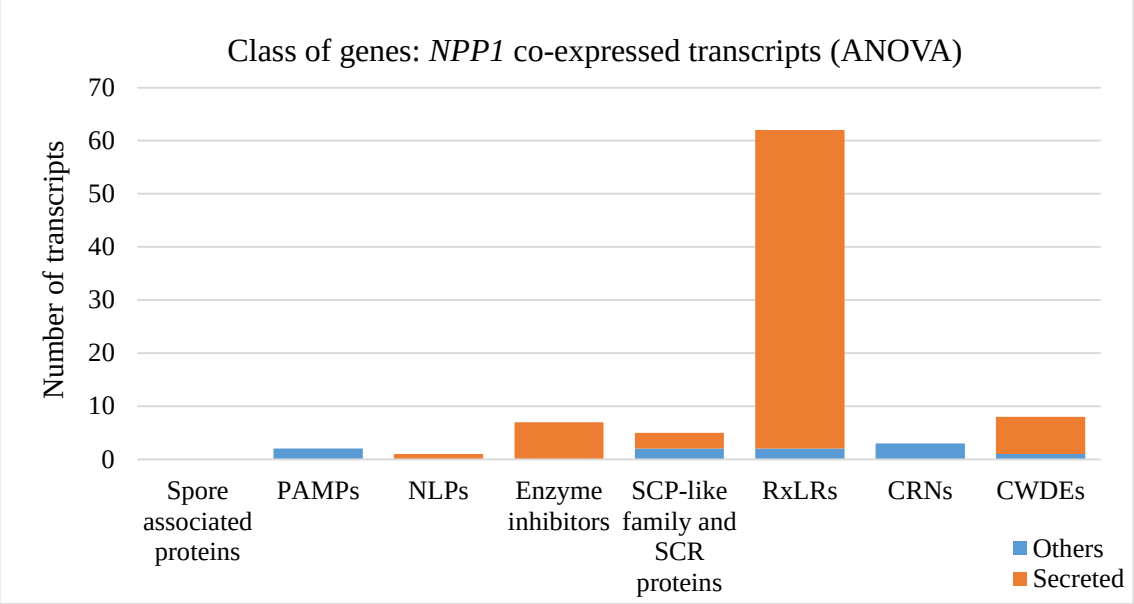

Figure 3.19 Class of differentially expressed genes among those co-expressed with *NPP1*. High numbers (62 transcripts) of cytoplasmic RxLR effectors were co-expressed with *NPP1*. The majority of apoplastic effectors differentially expressed during leaf infection, such as enzyme inhibitors (glucanase and protease inhibitors) were also detected in the list. However, there were low numbers of genes encoding elicitins and CRN effectors co-expressed with *NPP1*. Blue represents non-secreted proteins while orange refers to secreted proteins.

3.2.9 *In planta* infection-specific genes

A set of genes which were only expressed *in planta* were identified (Annex 3g) when compared with the results of the quality control (flag present and marginal) of *in vitro* and *in planta* gene groups from the microarray results. A set of 17 differentially expressed transcripts including ten (Figure 3.20) annotated transcripts were up-regulated specifically during *in planta* stages, including genes encoding cytoplasmic RxLR effectors (six transcripts) (PITG_04145, PITG_04314, PITG_10232, PITG_13044, PITG_13048, and PITG_15128). Although six transcripts encoding CHPs and HPs were detected as infection-specific, there was one transcript each for a glucanase inhibitor protein 1 (GIP1) (PITG_13638), elicitin-like protein (PITG_23188), a proton-dependant oligopeptide transporter (POT family) (PITG_09088), and pectinesterase (PITG_08911). All of these genes were either not detected or strongly down-regulated (up to 100-fold) in the *in vitro* stages.

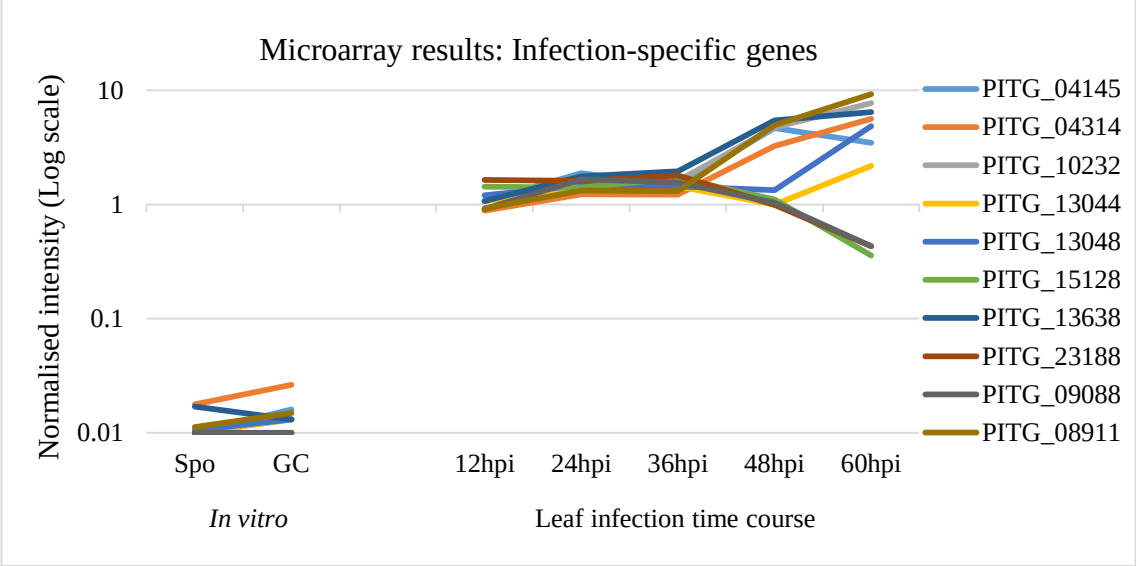

Figure 3.20 Microarray results of infection-specific transcripts not detected (according to flag value) *in vitro* (Spo and GC) compared to up-regulated *in planta* infection.

3.2.10 Microarray expression validation by QRT-PCR

3.2.10.1 Selection and validation of differentially expressed genes from the leaf infection time course (gene tree groups)

Selected genes from the microarray results were validated using QRT-PCR. The *P. infestans* actin A gene (*ActA*; PITG_15117) was used as a constitutively expressed endogenous control for expression normalisation. First, *ActA* expression was compared against the expression of constitutively expressed transgene *tdTomato* (*tdT*) (Figure. 3.21). Expression of *tdT* and *ActA* was used for normalization of expression for biotrophic marker gene *Hmp1*. The *tdT* gene encodes a red fluorescent marker transformed into *P. infestans* isolate 88069 to facilitate the cell biology study by confocal microscopy. It is constitutively expressed from the *Ham34* promotor. The expression profile of this gene on the microarray was less than one-fold different in all stages, including the infection time course. During validation, the expression level in sporangia (Spo) was set at one and a relative expression during the infection time-course was determined. The slightly lower relative expression for *tdT* is most likely due to the normalization against *ActA* in sporangia; *ActA* transcript is present at slightly elevated levels in sporangia (Vetukuri *et*

al., 2011). Expression of the biotrophy marker *Hmp1* was validated using both *ActA* and *tdT* in order to confirm the sufficiency of *ActA* for normalisation. Normalisation with *ActA* or *tdT* yielded equivalent expression profiles (Figure 3.22).

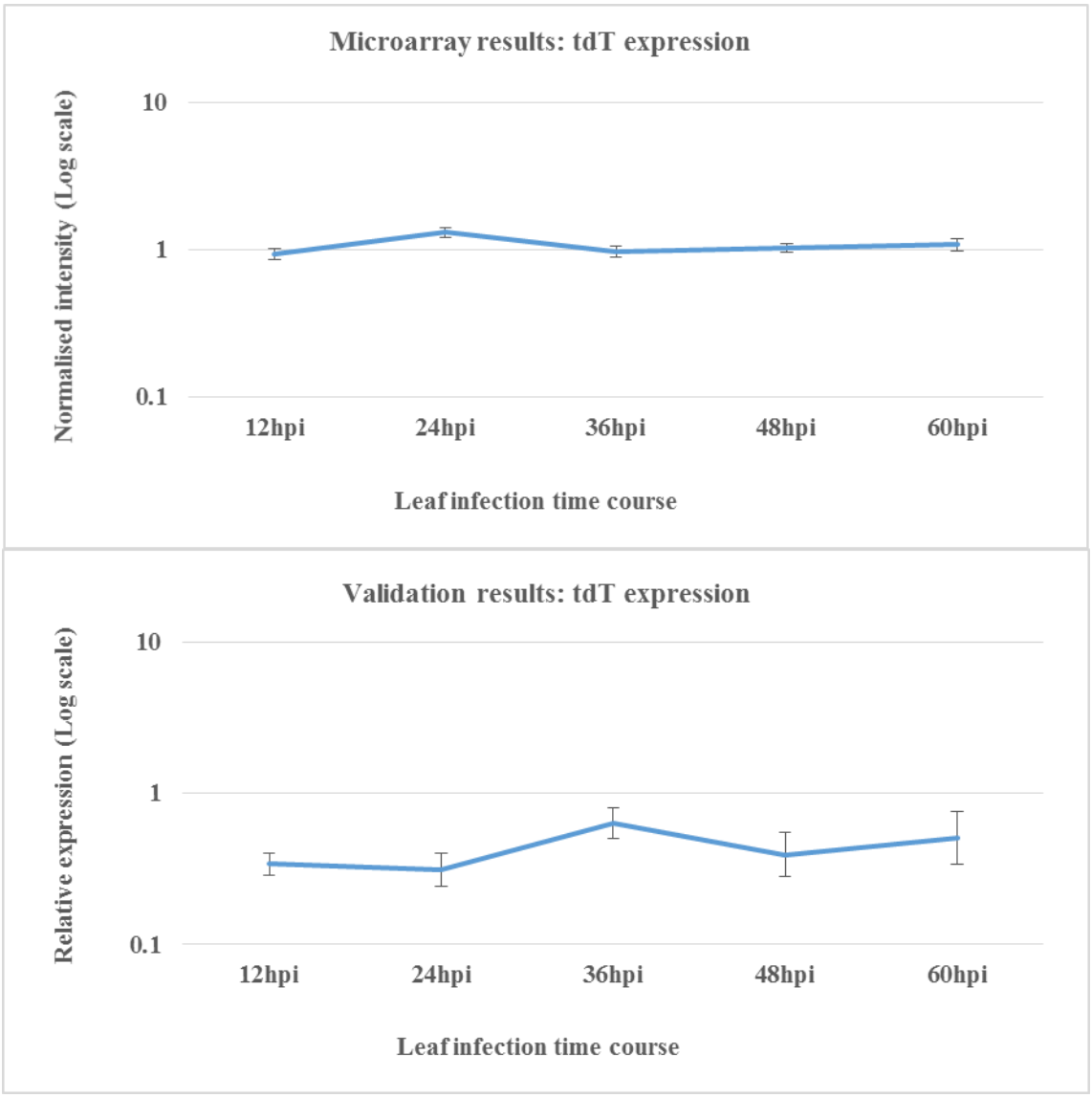

Figure 3.21 Comparison of the expression profiles of tdTomato (*tdT*) from microarray results (upper graph) and QRT-PCR validation (vs *ActA*) (lower graph). The graphs show similar expression profiles (less than 0.5-fold difference) *in planta* stages.

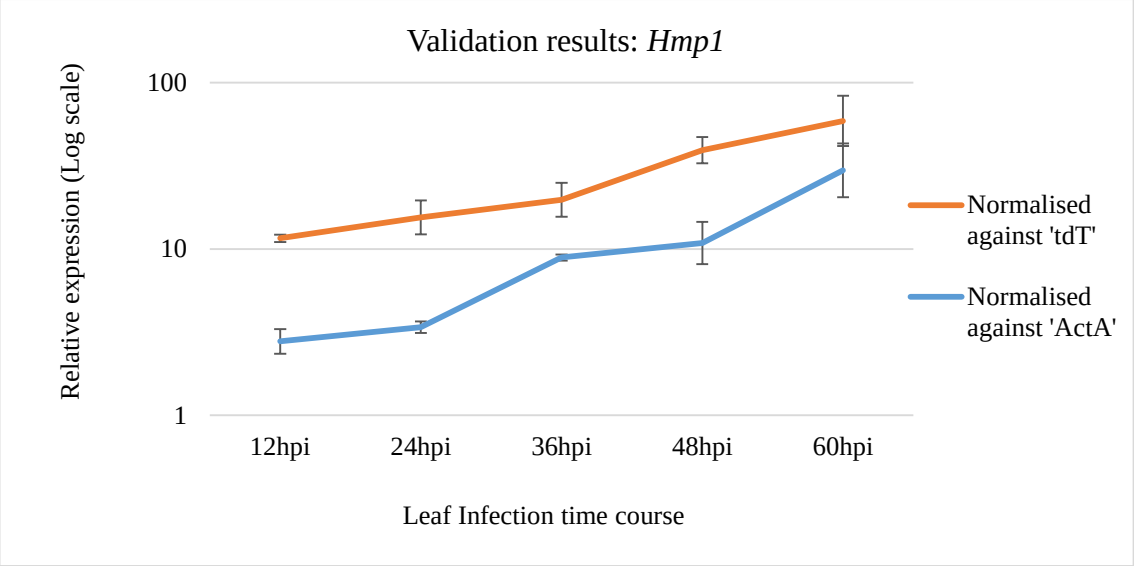

Figure 3.22 Comparison of *Hmp1* (PITG_00375) expression normalised using either *P. infestans ActA* or *tdT*. The graph shows a similar trend of *Hmp1* expression during *in planta* infection for each.

P. infestans genes (Table 3.8) encoding known functional proteins representing two major expression groups (Sub-groups 2 and 4) were selected from the microarray results of the *P. infestans* leaf infection time course for expression validation by QRT-PCR. Representative genes were taken from gene tree groups (Figure 3.7), *Cdc14* co-expressed genes (Figure 3.11), *Hmp1* co-expressed genes (Figure 3.14), *NPP1* co-expressed genes (3.18), infection specific genes, and some other genes detected but not significantly differentially expressed.

Table 3.8 The list of genes taken from the differentially expressed gene list (ANOVA), and additional genes detected from the microarray results, and QRT-PCR validation results. GC = germinating cysts, Spo = sporangia, Up = up-regulated, Down = down-regulated.

Description	Primary accession	In 'GC' compared to 'Spo'	Detection: *in planta* infection microarray	Heatmap Sub-group (ANOVA)	Co-expressed with	QRT-PCR validation (*In planta* infection)
Hmp1	PITG_00375	Up	Detected from 36 hpi	4	*Hmp1*	Up- throughout
Avr2 family	PITG_08943	Up	Detected throughout	4	*Hmp1*	Up- throughout
Avr3a	PITG_14371	Up	Detected throughout	4	*Hmp1*	Up- throughout
Avrblb1	PITG_21388	Equal	Detected throughout	4	*Hmp1*	Up- throughout
Avrblb2	PITG_20303	Down	Detected from 36 hpi	4	*NPP1*	Up- throughout
RxLR	PITG_02860	Down	Detected from 24 hpi	4	*NPP1*	Up- throughout
RxLR	PITG_03192	Up	Detected from 48 hpi	4	*Hmp1*	Up- throughout
RxLR	PITG_04074	Down	Absent from 36 hpi	2	None	Down- throughout
RxLR	PITG_04097	Absent	Absent throughout	None	None	Up- from 36 hpi
RxLR	PITG_04145	Absent	Detected from 48 hpi	4	None	Up- from 24 hpi
RxLR	PITG_04314	Absent	Detected at 60 hpi	4	None	Up- throughout
RxLR	PITG_04388	Down	Detected at 60 hpi	None	None	Up- throughout
RxLR	PITG_05146	Absent	Detected throughout	None	None	Up- from 24 hpi
RxLR	PITG_06308	Down	Detected at 60 hpi	None	None	Up- throughout
RxLR	PITG_06478	Up	Detected throughout	None	None	Up- from 24 hpi
RxLR	PITG_09585	Down	Detected at 60 hpi	5	None	Up- throughout
RxLR	PITG_09585	Down	Detected at 60 hpi	None	None	Up- from 24 hpi
RxLR	PITG_09680	Down	Detected at 60 hpi	None	None	Up- from 36 hpi
RxLR	PITG_09757	Absent	Detected throughout	None	None	Up- from 24 hpi
RxLR	PITG_10654	Down	Detected from 36 hpi	4	*NPP1*	Up- throughout
RxLR	PITG_13628	Absent	Absent throughout	None	None	Up- from 24 hpi
RxLR	PITG_13959	Absent	Absent throughout	None	None	Up- throughout
RxLR	PITG_15128	Absent	Detected throughout	2	None	Down- from 48 hpi
RxLR	PITG_15679	Absent	Detected at 60 hpi	None	None	Up- from 24 hpi
RxLR	PITG_18215	Absent	Absent throughout	None	None	Up- from 24 hpi
Cdc14	PITG_18578	Down	Absent from 24 hpi	2	*Cdc14*	Down- from 24 hpi
CBEL	PITG_03637	Up	Absent from 24 hpi	2	Cdc14	Down- from 24 hpi
Elicitin	PITG_03616	Up	Absent at 24, 36 hpi	None	None	Up- throughout
SNE1	PITG_13157	Up	Detected throughout	None	None	Up- throughout
EPI6	PITG_05440	Up	Detected from 36 hpi	4	*NPP1*	Up- throughout
EPIC4	PITG_00058	Down	Absent at 36 hpi	None	None	Down- at 36 hpi
Inf1	PITG_12551	Down	Detected throughout	None	None	Up- throughout
Inf4	PITG_21410	Down	Detected throughout	None	None	Up- from 24 hpi
Trans-gltaminase	PITG_05339	Up	Detected at 60 hpi	None	None	Up- throughout
GIP1	PITG_13638	Absent	Detected from 48 hpi	4	*Hmp1*	Up- from 24 hpi
NPP1	PITG_09716	Down	Detected from 36 hpi	4	None	Up- throughout
NPP1	PITG_23094	Absent	Detected at 60 hpi	None	None	Up- throughout
Pectinesterase	PITG_08912	Equal	Detected from 36 hpi	4	*NPP1*	Up- throughout
Glycoside hydrolase	PITG_04272	Absent	Detected throughout	None	None	Up- throughout
POT	PITG_09088	Absent	Detected throughout	2	None	Up- from 24 hpi

Table 3.8 **(continued)**

Description	**Primary accession**	**In 'GC' compared to 'Spo'**	**Detection: *in planta* infection microarray**	**Heatmap Sub-group (ANOVA)**	**Co-expressed with**	**QRT-PCR validation (*In planta* infection)**
MADS-box_TF	PITG_07059	Down	Absent from 24 hpi	2	*Cdc14*	Down- from 24 hpi
Myb_TF	PITG_14400	Down	Absent from 24 hpi	2	*Cdc14*	Down- from 24 hpi
Myb_TF	PITG_17567	Up	Absent from 24 hpi	2	*Cdc14*	Down- from 24 hpi

Functionally characterised genes were selected to validate the gene tree. Sporulation marker gene *Cdc14* and biotrophy marker gene *Hmp1* represent Sub-group 2 and Sub-group 4, respectively (Figure 3.7). These genes each confirmed the microarray results (Figure 3.23 and Figure 3.24).

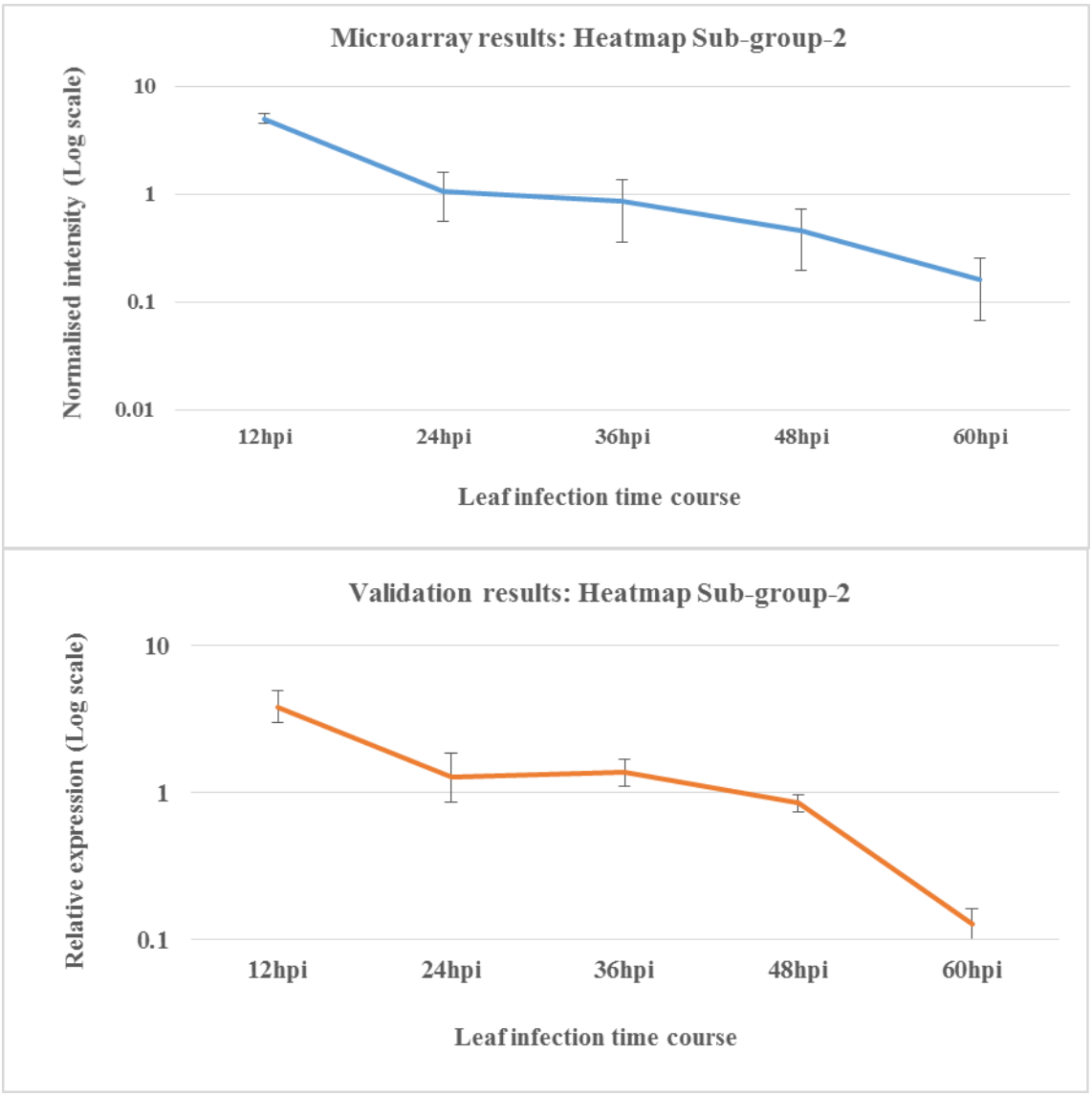

Figure 3.23 Validation of sporulation marker gene *Cdc14*. Sporulation marker gene *Cdc14* (PITG_18578), representing Group one (Sub-group 2) of heatmap clustering (upper graph; cross-reference Figure 3.7), and QRT-PCR validation of the same gene (lower graph). This gene was down-regulated during interaction with potato.

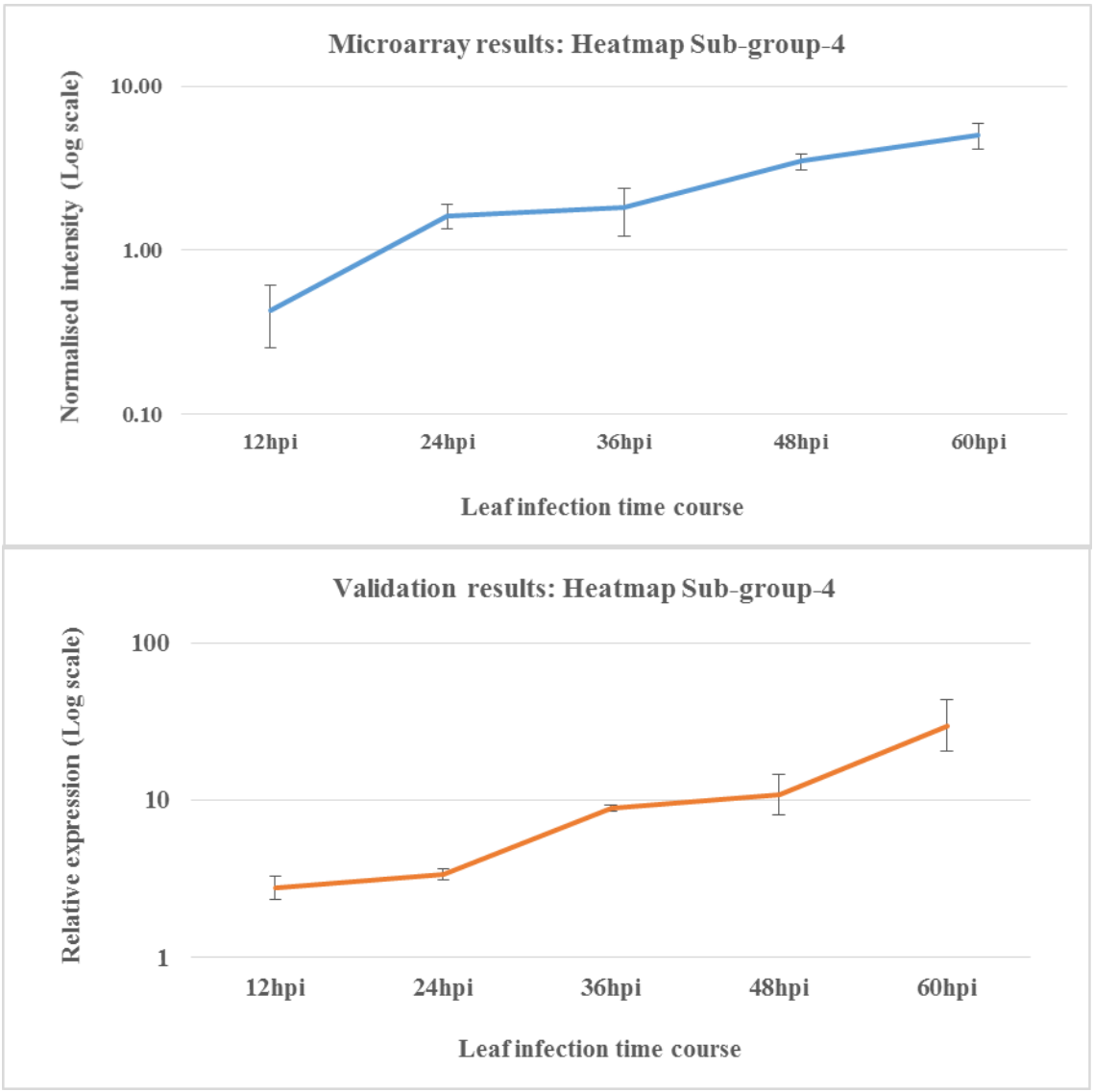

Figure 3.24 Validation of biotrophic marker gene *Hmp1*. Biotrophic marker *Hmp1* (PITG_00375), representing Group two (Sub-group 4) of heatmap clustering (upper graph; cross-ref Figure 3.7), and relative expression of the same gene (lower graph). A similar profile of expression was observed from the validation results.

3.2.10.2 Expression validation of co-expressed genes

The well characterised proteinaceous PAMP, CBEL (PITG_03637), was co-expressed with a close correlation coefficient (0.96) with sporulation marker gene *Cdc14*. Other genes such as MADS-box transcription factor (PITG_07059), and two transcription factor encoding transcripts (Myb-like DNA binding proteins) PITG_14400, and PITG_17567) were also co-expressed with *Cdc14* with a 0.99 correlation coefficient. Primers for these genes were designed and QRT-PCR validation was conducted (Figure 3.25).

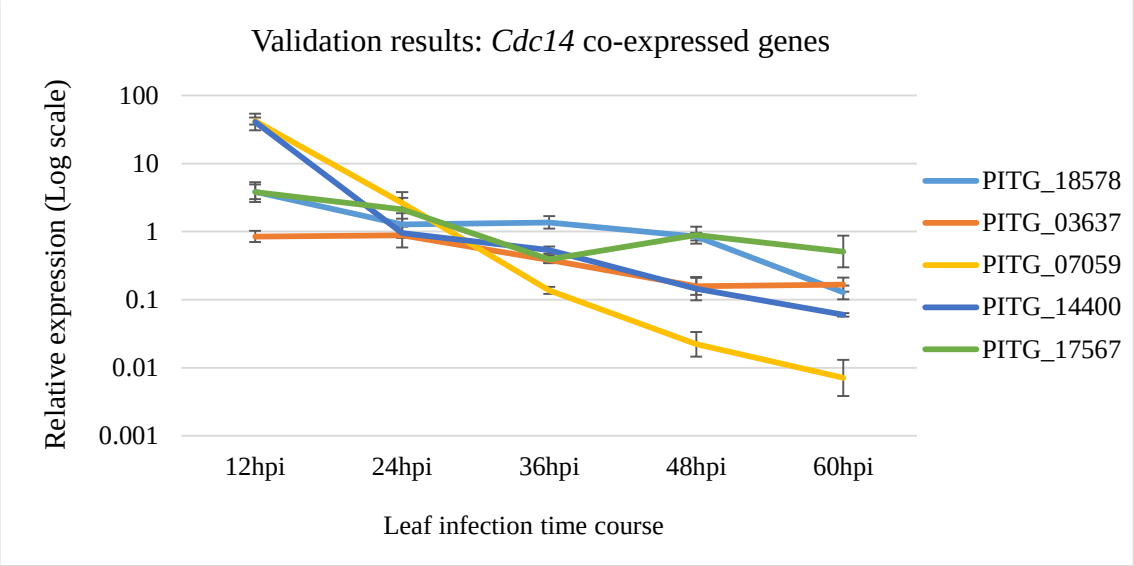

Figure 3.25 Relative expression of *Cdc14* (PITG_18578) and its co-expressed genes: *CBEL* family gene (PITG_03637), MADS-box transcription factor (PITG_07059), and two Myb-like DNA binding protein encoding transcripts (PITG_14400 and PITG_17567) during *in planta* infection stages. All genes were steadily down-regulated during infection when validated by QRT-PCR.

Genes encoding several Avr proteins, other RxLR effectors, CRN effectors, enzyme inhibitors, and SCR proteins potentially involved in the biotrophic interaction with hosts were co-expressed with biotrophic marker gene *Hmp1*. Four effector genes co-expressed with *Hmp1* (PITG_00375) were validated using QRT-PCR (Figure 3.26): *Avr2* (PITG_08943), *Avr3a* (PITG_14371), *Avrblb1* (PITG_21388), and another RxLR effector (PITG_ 03192) with published function (McLellan *et al*., 2013), with correlation coefficients of 0.98, 0.95, 0.99, and 0.96, respectively

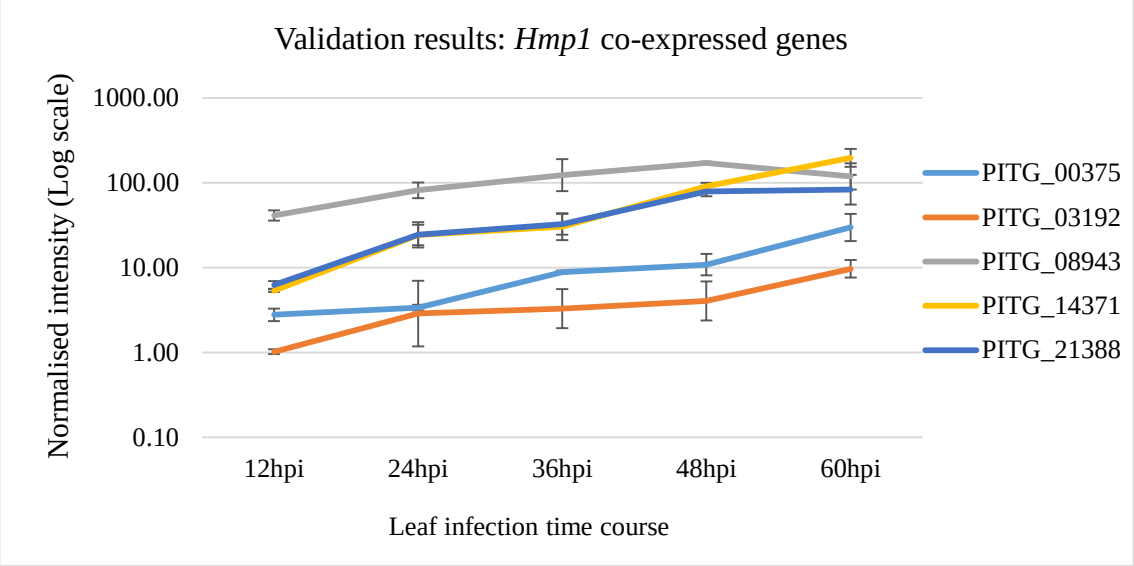

Figure 3.26 Relative expression of *Hmp1* (PITG_00375) and its co-expressed genes: an RxLR effector (PITG_03192), *Avr2* (PITG_08943), *Avr3a* (PITG_14371), and *Avrblb1* (PITG_21388). All genes shown in the graphs were steadily up-regulated during the infection time course.

The expression levels of the selected *NPP1* (PITG_09716) and its co-expressed genes such as *pectinesterase* (PITG_08912), *EPI6* (PITG_05440), and *RxLR* effector (PITG_02860 and PITG_10654) with correlation coefficients of 0.98, 0.99, 0.99 and 0.99, respectively, were confirmed with the QRT-PCR validation (Figure 3.27). Expression for PITG_08912 showed an apparent decrease in expression at 60 hpi, but still exhibited strong up-regulation at this time point.

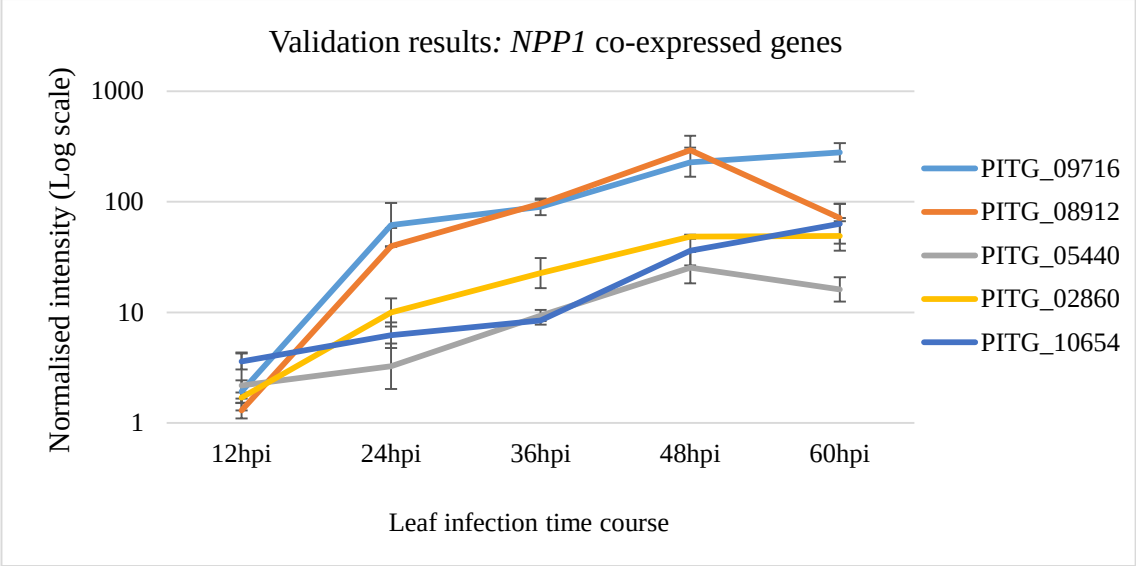

Figure 3.27 Relative expression of an *NPP1* (PITG_09716) and co-expressed genes such as *pectinesterase* (PITG_08912), *EPI6* (PITG_05440), and *RxLR* effectors (PITG_02860, and PITG_10654). All of the genes were up-regulated during later time points of *in planta* infection.

3.2.10.3 Expression validation of selected infection-specific genes

Infection-specific *P. infestans* genes were those that were not detected on the microarray or were strongly down-regulated *in vitro*, but expressed and up-regulated during potato leaf infection. For the validation of infection specific genes, in addition to cDNA from the leaf infection time course (12, 24, 36, 48, and 60 hpi) and *in vitro* sporangia, cDNA from *in vitro* grown vegetative mycelium was also used.

The expression profiles of the selected infection-specific genes were typically similar to the microarray results (Figure 3.28). Transcripts for all of the infection specific genes identified from the microarray were detected in the *in vitro* stages using QRT-PCR. This is probably due to the increased detection sensitivity of the QRT-PCR assay. However, all tested genes were more strongly expressed during infection than in the *in vitro* stages. Selected genes included: a proton-dependent oligopeptide transporter (*POT*) (PITG_09088), a glucanase inhibitor protein 1 (*GIP1*) (PITG_13638), and an RxLR effector (PITG_15128). Using QRT-PCR, all of the selected genes were down-regulated

in vegetatively grown mycelium (*in vitro* grown hyphae harvested at 60 hpi), compared to sporangia, and were up-regulated during infection. Although most of the infection-specific genes were found to be down-regulated in germinating cysts (data not shown) when compared to sporangia, upon validation, some individual genes such as an *NPP1* homolog also showed up-regulation. However, these genes were more strongly up-regulated during infection compared to *in vitro*.

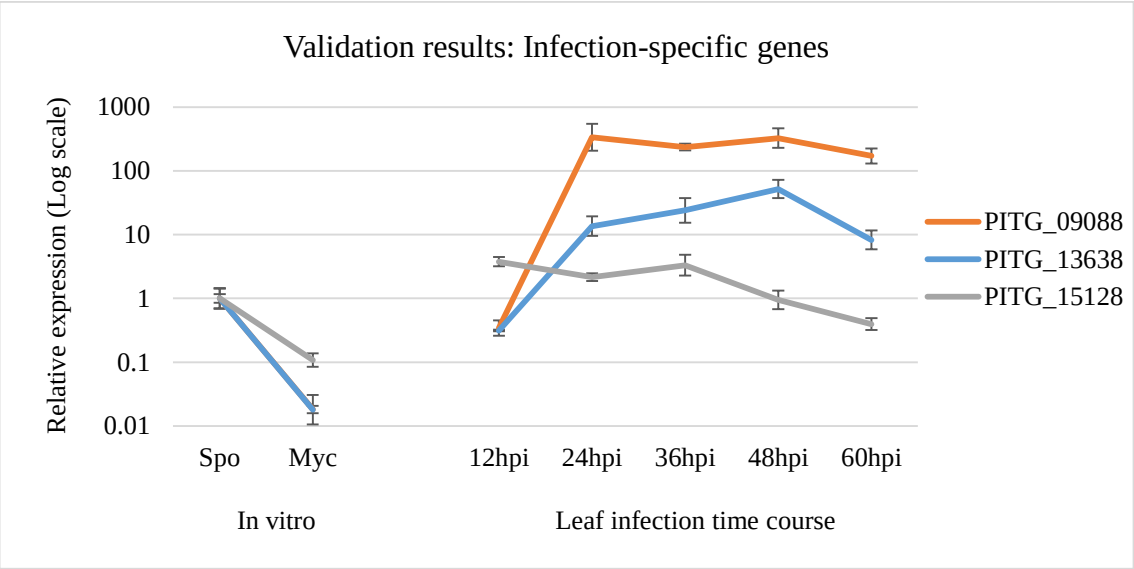

Figure 3.28 QRT-PCR validation of the selected infection-specific genes: *POT* (PITG_09088), *GIP1* (PITG_13638), and an *RxLR* effector (PITG_15128) identified from the microarray results of infection specific gene set. These genes were down-regulated in vegetative hyphae (Myc) grown in nutrient-rich media. All three genes confirmed the microarray results.

3.2.11 Gene expression analysis of selected genes detected in the microarray leaf infection (not differentially expressed)

Several genes that were below thresholds of detection for statistical analyses, but indicated potential changes in raw reads throughout the infection time course, were expression profiled by QRT-PCR. Several RxLR effector-encoding transcripts (PITG_04097, PITG_04388, PITG_05146, PITG_06308, PITG_06478, PITG_09585, PITG_09680, PITG_09757, PITG_13628, PITG_13959, PITG_15679, and PITG_18215) (cross ref Table 3.3) were selected, as these effectors were thought to be

important for pathogenicity and functional characterisation of these genes has been in progress in the James Hutton Institute *Phytophthora* laboratory. For example, an RxLR effector (PITG_13628) which potentially targets a map-4-kinase (MAP4Ks), implementing early signal transduction (Zheng *et al*., 2014) was not detected by the microarray. However, QRT-PCR gene expression analysis showed early (24 hpi) up-regulation (Figure 3.29).

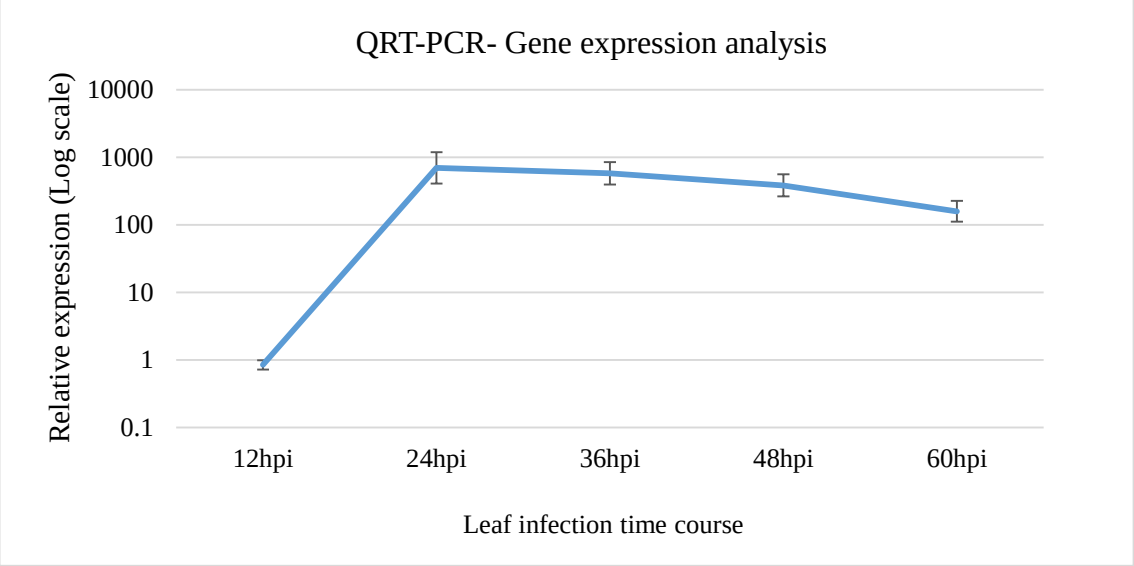

Figure 3.29 QRT-PCR gene expression analysis of RxLR effector coding gene PITG_13628. This gene was not detected in leaf infection microarray.

In addition, *P. infestans* PAMP-encoding transcripts such as *INF1* (PITG_12551), *INF4* (PITG_21410), and transglutaminase M81-like protein (containing the PAMP Pep13) (PITG_05339) were also previously well-characterised but did not pass the ANOVA for differential expression in this analysis. A transcript encoding protease inhibitor (*EPIC4*) (PITG_00058) was also detected during early infection time points, but was not in the ANOVA list. QRT-PCR of this gene also validated patterns seen in the microarray. Similarly, QRT-PCR of other genes encoding secreted proteins such as glycoside hydrolase (PITG_04272) and the elicitor NLP (PITG_23094), also excluded from the ANOVA list, validated the normalised expression patterns in the microarray. Finally, the

suppressor of necrosis (*SNE1*) (PITG_13157) gene also revealed a similar QRT-PCR expression profile to the microarray results.

3.3 Discussion

3.3.1 Study of cell biology revealed early biotrophic interaction with the host

P. infestans, a hemi-biotrophic pathogen, can colonise entire host leaves within a week and completes its life cycle by emerging from stomata as sporangiophores and aerial hyphae on the host leaf surface (Figure 3.1f). Similar to previous studies (for example Avrova *et al*., 2007), the cell biology study by confocal microscopy showed penetration of the leaf and formation of haustoria in plant cell cytoplasm as early as 12 hpi. This indicates that penetration of the host by *P. infestans* has occurred within 12 hpi and enough time had elapsed for haustoria to form and deliver effectors. The initial formation of haustoria from intercellular hyphae can occur within three hours (Avrova *et al*., 2008). The presence of haustoria during the early stage of infection was also validated by the QRT-PCR expression of a biotrophy marker gene, *Hmp1*, which showed up-regulation at 12 hpi and throughout the infection time course. The presence of haustoria at each of the time-points studied in the microarray provides evidence that the transcriptomic study presented here represents the biotrophic phase of infection. This is further supported by the lack of obvious macroscopic disease symptoms; from 12 hpi to 60 hpi the leaf tissues appeared healthy but the presence of haustoria inside the plant cell cytoplasm confirmed the biotrophic phase of infection, rather than the later necrotrophic and sporulation phases.

3.3.2 A whole-transcriptome microarray approach reveals transcriptional changes during *P. infestans* infection of potato leaves

It was essential to identify the temporal transcriptional changes during the early biotrophic interaction in order to understand how the pathogen establishes disease. The microarray analysis encompassing the first 60 hours of infection revealed dramatic changes in the transcriptome of *P. infestans*, with 1,707 differentially expressed transcripts, including 293 predicted secreted proteins. Transcripts for several well-known *Avr* genes, other RxLR effectors, elicitors and PAMPs, and CWDEs were differently expressed during these early stages. Among all detected genes at 12 hpi, according to the volcano plot (pairwise comparison), 22.4% (cross ref Figure 3.6c) were predicted to be secreted proteins, and are candidate effectors used by *P. infestans*, supporting the hypothesis that a diverse battery of effectors are deployed from the earliest stage of infection to establish biotrophy during potato infection.

By analysing the transcripts that exhibited the most dramatic change in normalised expression at each time point, it was clear that a large proportion of the transcripts encoded secreted candidate effectors proteins. This further highlights the importance to *P. infestans* of deploying effectors to interact with plant targets and promote infection.

3.3.3 Comparative studies of the differentially expressed transcripts revealed biotrophy as an essential stage in host colonization

The 1,707 transcripts differentially expressed from 12 to 60 hpi allowed comparison with previous studies, in which detection of transcripts was only possible from 48 hpi to 7 days post-inoculation with *P. infestans* strains 3928A and T30-4 (Haas *et al*., 2009; Cooke *et al*., 2012). 293 transcripts of 88069tdT isolate were predicted to encode secreted proteins involved in early infection stages, which is a greater percentage (17.2%) in relation to the differentially expressed genes than detected in 3928A (8.6%). In T30-4, 22.4% of the

differentially expressed transcripts encoded secreted proteins. However, the total number of differentially expressed transcripts in T30-4 was comparatively low at 683 transcripts, compared to 88069 (1,707 transcripts).

In 88069tdT, 114 RxLR effector-encoding transcripts (108 transcripts predicted to encode secreted RxLRs) were detected as differentially expressed, which is a similar number (115 transcripts) of transcripts detected in 3928A (from 2 dpi). However, comparatively few transcripts encoding RxLR effectors were detected as differentially expressed in T30-4 (86 transcripts) infection (Cooke *et al*., 2012). Although expression of 50 secreted RxLR effectors were in common among all isolates, there were 37 secreted RxLR effectors up-regulated or detected only in the 88069tdT infection time course (Figure 3.30). This could partly be due to detection of RxLRs involved only in the earlier stages sampled here (12-36 hpi), which may be no longer needed in the later stages of biotrophy (48 and 60 hpi), or due to those cytoplasmic effectors that are specific to 88069 isolate. For example, RxLR effectors (PITG_00821, PITG_04074, PITG_07741, PITG_08943 (Avr2), PITG_14960, PITG_14965, and PITG_20934) detected early (12 hpi) and differentially expressed throughout the infection time course were only detected in 88069. Similarly, the PexRD2 family of RxLR effectors (PITG_11383) was also only detected early in 88069. Both of these effectors are present in the reference genome for T30-4 (Haas *et al*., 2009).

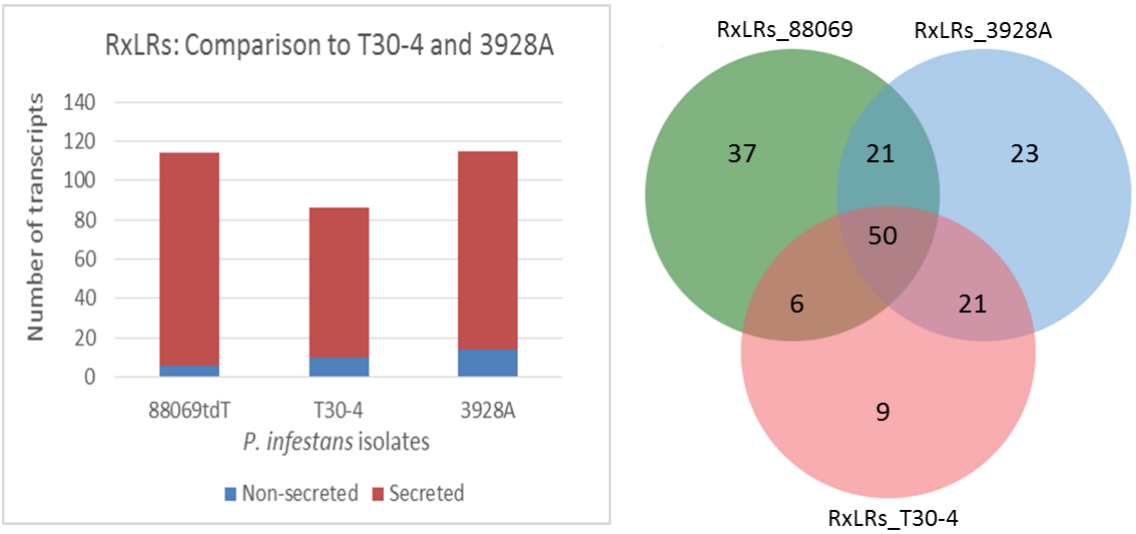

Figure 3.30 A comparison of RxLR effector coding genes of *P. infestans* isolate 88069tdT differentially expressed during infection, with previously published T30-4 and 3928A (Cooke *et al*., 2012). The graph on the left shows the comparative numbers of total secreted RxLR proteins detected by microarray in three different isolates; 88069tdt, T30-4, and 3928A. The Venn diagram on the right shows the numbers of expressed RxLR effectors that were detected and distributed among three isolates.

Although only greater than 2-fold up-regulated expression data were presented in a further, separately conducted microarray experiment using isolate T30-4 (Haas *et al*., 2009), those data revealed a comparatively lower number (494 transcripts) of differentially expressed transcripts involved in pathogenicity when compared to 1,343 transcripts in 88069tdT that were 2-fold up-regulated and differentially expressed during the time course of infection. This could either be due to the detection sensitivity of the different microarray platforms, leading to lower detection of genes in T30-4, or the characteristics of different isolates such as genuine up-regulation of more genes during infection by 88069. There were 242 secreted protein encoding transcripts that were >2-fold up-regulated in 88069tdT compared to 131 transcripts in T30-4. More RxLRs (91 transcripts) were detected to be >2-fold up-regulated in 88069tdT compared to T30-4 (62 transcripts), with an overlap of 40 RxLRs in between both isolates (Figure 3.31). Taken together, these results highlight the sensitivity of the Agilent microarray system used here, and underline its potential for studying transcriptional changes during early (12 to 36 hpi)

plant-pathogen interactions. An alternative strategy to analyse transcriptome-wide change is to use sequencing of mRNAs (RNAseq). The number of differentially expressed genes identified in the microarray study described here is comparable to two available studies where RNAseq has been used for oomycete plant infection. In one study using *Pseudoperonospora cubensis*, 2383 differentially expressed genes were identified during an eight day infection sampling (Savory *et al*., 2012). Similarly, RNAseq analysis of *Phytophthora phaseoli* infection on Lima bean identified 1284 differentially expressed genes after six days of infection (Kunjeti *et al*., 2012).

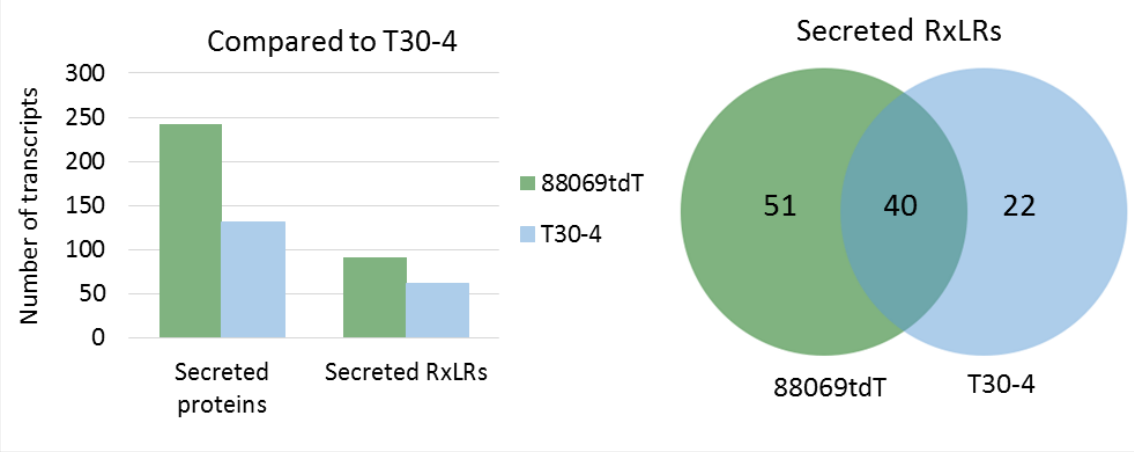

Figure 3.31 A comparison of total transcripts differentially expressed (>2 fold up-regulated) during infection for *P. infestans* isolates T30-4 (Haas *et al*., 2009), and 88069tdT. The graph on the left shows the comparative numbers of total predicted secreted proteins, and secreted RxLR effector proteins in two different isolates; 88069tdt and T30-4. The Venn diagram on the right shows the number of secreted RxLR effectors that were shared and those that were unique between the two isolates.

3.3.4 Genes co-expressed with stage-specific marker genes confirm stages during the infection process

Previously identified *P. infestans* genes, such as sporulation marker *Cdc14* (Ah-Fong *et al*., 2003), biotrophy marker gene *Hmp1* (Avrova *et al*., 2008), and necrotrophy marker gene *NPP1* (Cabral *et al*., 2012) were used as reference genes. The expression profiles of these marker genes were used to identify co-expressed genes, thus revealing genes that are likely to be involved in the same stage of infection, and disease progression and

development. Transcripts for *Cdc14* were still detected at 12 hpi, probably due to some un-germinated spores, and potentially zoospores, still being present on the surface of the leaf. However, *Cdc14* expression subsequently subsided in later time points of infection, suggesting that the infection was fully initiated by 24 hpi. Genes co-expressed with *Cdc14* included those encoding *P. infestans* PAMPs (CBEL), several spore-related proteins, and spore cleavage-related proteins. This supports the assertion that un-germinated spores are still present at 12 hpi, but the infection has fully commenced by 24 hpi. *P. infestans* spore germination is asynchronous, and sporangia and cysts can germinate over a period of many hours. As an example, in Avrova *et al*. (2008), a mixture of germinating cysts and sporangia can be seen on the surface of a potato leaf, but at different stages of germination and development.

Biotrophy marker gene *Hmp1* was detected at 12 hpi and was continuously up-regulated throughout the infection time course. Hmp1 is located at the *P. infestans* haustorial membrane interface, which has also been determined as the secretion site for RxLR effector proteins that are essential for the biotrophic interaction with the host. Genes co-expressed with *Hmp1* included those encoding many characterised RxLR effectors (Avr2, Avr3a, ipiO1/Avrblb1, AvrVnt1 and PITG_03192; Haas *et al*., 2009; Gilroy *et al*., 2011a; Armstrong *et al*., 2005; van West *et al*., 1998; Vleeshouwers *et al*., 2008; Pel, 2010; McLellan *et al*., 2013), suggesting that these proteins are produced and delivered at the same time as haustorium formation to establish biotrophy. To date, only a small number of RxLR effectors have been tested to identify where they are delivered from. All of those tested (Avr3a, Avr2, Avrblb1, Avr4) are delivered from haustoria (Whisson *et al*., 2007; van Poppel, 2008; Gilroy *et al*., 2011). With the exception of Avr4, all of these are in the Hmp1 co-expressed list. Although functional characterisation has to be conducted on more effectors, the *Hmp1* co-expressed gene set revealed a novel criterion for the

candidate effectors and other related genes that might be functionally involved in delivery from the haustorium, or indeed involvement in its formation.

Interestingly, a number of apoplastic effectors, including protease and glucanase inhibitors, were also co-expressed with *Hmp1*, suggesting haustoria as a potential site for secretion of these proteins. Moreover, the bi-functional catalase-peroxidases (KatG) was also co-expressed with *Hmp1*. Although it is not functionally characterised in oomycetes, an equivalent secreted catalase-peroxidase characterised in *Magnaporthe grisea* is suggested to detoxify the oxidative burst generated as a defence response by the host (Tanabe *et al*., 2011). In addition, there were genes encoding several other proteins (CWDEs, SCP-like extracellular proteins) found to be co-expressed with *Hmp1*, suggesting multiple strategies of the pathogen to modify the host.

Expression of the necrotrophy marker gene NPP1 (secreted protein) potentially revealed the initiation of necrosis during later stages of infection from 36 hpi onward. It is interesting that an overlap was observed between *HMP1* and *NPP1* co-expressed genes, perhaps due to the simultaneous requirement to release nutrients whilst suppressing defences. Interestingly, a transcript encoding a berberine-like protein (secreted protein), co-expressed with NPP1, might have an inhibitory effect on programmed cell death. Berberine proteins (also called berberine bridge enzymes) are involved in the synthesis of the alkaloid berberine, which can inhibit thymocyte apoptosis in animals (Miura *et al*., 1997). It could be speculated that *P. infestans* secreted berberine-like proteins might also contribute to inhibiting programmed cell death in infected host plant cells.

In a similar study to this chapter, Jupe *et al*. (2013) demonstrated that there were distinct transcriptional stages in *P. capsici* infection, and also used the orthologous *PcHmp1*, *PcNPP1*, and *PcCdc14* genes to define biotrophic, necrotrophic, and sporulation stages

in a microarray experiment of *P. capsici* infection of tomato. In comparison, the *P. infestans* infection used for microarray analysis in this chapter remained within biotrophy. This was highly successful in identifying pathogen genes that were differentially expressed from the earliest stages of infection when the outcome of the interaction is determined, and before any macroscopic symptoms were visible. However, it did not define the end of biotrophy and transition to necrotrophy or sporulation. Thus, had additional infection time points been included, such as 72 hpi and 96 hpi, a more complete transcriptional profile of the entire *P. infestans* infection cycle could have been revealed in a single experiment.

3.3.5 The microarray experiment revealed infection-specific genes

The identification of numerous infection-specific genes has provided new insights into the infection process. Infection-specific genes are described as those genes which are either absent, or very low expression *in vitro* life stages compared to high expression *in planta* infection. To date, there is still a lack of published research on infection-specific genes in plant-pathogens. Previously, a single sequence family in *P. infestans*, *Phytophthora infestans* non-coding infection-specific 1 (*Pinci*1), identified from a combination of suppression subtraction hybridization and sequencing of *P. infestans* bacterial artificial chromosome (BAC) clones, was identified (Whisson *et al*., 2001; Avrova *et al*., 2007). cDNA libraries constructed from the interaction of plant and pathogen can contain both host and pathogen sequences (Bittner-Eddy *et al*., 2003) and may be a useful source of infection-specific genes. A gene encoding an apoplastic effector, glucanase inhibitor protein 1 (*GIP1*), was co-expressed with *Hmp1* during the *in planta* infection and was absent in the *in vitro* stages. Damasceno *et al*. (2008) have reported that this gene was not expressed in the tomato apoplast and *in vitro* grown

mycelium, but was induced during tomato leaf infection. Results here support the evidence that this gene might be specifically induced in response to the host cell in order to defend *P. infestans* from preformed or early plant defences, and its protein may be secreted from haustoria. However, functional analysis is necessary to confirm these preliminary results. This category also included several RxLR effectors, and CWDEs such as a pectinesterase. The preliminary expression analysis suggests that these genes are involved in establishing a biotrophic interaction and are not needed for growth *in vitro*, as QRT-PCR results of three genes showed an absence of expression in vegetatively-grown hyphae.

Chapter 4. Comparison of leaf and tuber infection by *Phytophthora infestans* in *Solanum tuberosum* (cv. Bintje)

4.1 Introduction

It is known that the behaviour of a pathogen and its morphological development depend on many host characteristics, such as tissue type, preformed barriers to infection, antimicrobial compounds, available nutrients, and an ability to suppress host defence responses. *P. infestans* infects both potato foliage and tuber tissues. The symptoms of foliar blight are easily visible in the field whereas tuber blight can only be seen after harvest and/or during storage. It has been reported (de Bary, 1861) that tubers in the field are infected mostly by sporangia that are washed off the infected leaves or transferred from the stem to the soil, and occasionally from neighbouring diseased tubers (Sato, 1980). Whilst the periderm in the potato tuber provides a defensive barrier to *P. infestans* (Toxopeus, 1961), weak points exists such as lenticels, buds, or wounds, which allow this pathogen to invade the tuber (Pathak and Clarke, 1987). Therefore, harvested tubers can be infected if they come into contact with contaminated soil or diseased tissue (Murphy and Mckay, 1925).

Most of the research on potato late blight (*P. infestans*) has been focused on foliar blight, and wild Mexican potato species such as *S. demmisum* have been used as sources to introduce foliar resistance into cultivated potato (Reddick, 1939; Birch and Whisson, 2001; Fry 2008). Tuber blight has not been investigated to the same extent. Previous research suggested that the function of the resistance (*R*) genes in tubers may only be important if *P. infestans* was able to penetrate to the medulla cells primarily located at the centre of tubers (Flier *et al*., 2001). However, *P. infestans* can invade tubers via cuts or damaged areas and, therefore, resistance genes are important to help protect against this

disease (Millett *et al*., 2009). A report on chemical spray (phosphonic acid) of potato foliage showed reduced susceptibility of potato tubers to *P. infestans* (Cooke and Little, 2002) suggesting that phosphonate, transported into the tubers, not only acts as an antimicrobial compound but also activates systemic plant defences.

There have been numerous transcriptomic analyses between various *P. infestans* isolates and potato foliage (e.g. Haas *et al*., 2009; Cooke *et al*., 2012). However, tuber infection is poorly studied, with few analyses of disease responses in tuber tissues (Garas *et al*., 1979; Henfling *et al*., 1980; Doke and Tomiyama 1980; Doke, 1983; Doke and Miura 1995; Fernández *et al*., 2012; Rastogi and Pospisil, 2012). None of these studies have focussed on transcriptomic dynamics of host or pathogen during *P. infestans* infection of tubers. Only recently has there been a transciptome study of potato tubers infected by *P. infestans* (Gao *et al*., 2013). This study revealed that transgenic resistance to late blight, mediated by the *RpiBlb1* gene, was only effective in tubers if expressed at unusually high levels. Tuber resistance was accompanied by rapid induction of known defense genes and other differentially expressed host genes.

It is important to understand the pathogenic behaviour of *P. infestans* in both foliar and tuber tissue of potato so that the role of pathogen molecules such as PAMPs and effectors can be characterised. From the study of *P. infestans* infection of potato leaves it is clear that there is a dynamic exchange of signals between plant and pathogen, leading to large scale transcriptome and proteome change in both pathogen (Chapter 3) and plant (Gyetvai *et al*., 2012). During successful host-leaf colonisation, many RxLR and other secreted effectors are up-regulated and co-expressed with a biotrophic marker gene (*Hmp1*) (Chapter 3). It is unknown if the differentially expressed genes identified in Chapter 3

(PAMPS, elicitors, effectors, and cell wall degrading enzymes) have similar expression profiles during colonisation of different host tissues (here leaf vs. tuber tissues).

To understand *P. infestans* pathogenicity and disease development in tubers, it is important to determine if there is a biotrophic interaction during early infection in tuber tissue. The formation of haustoria is indicative of the biotrophic stage of infection, since RxLR effectors are known to be delivered from these structures by *P. infestans* (Whisson *et al*., 2007; Gilroy *et al*., 2011). It is also important to investigate similarities and differences by comparative studies of the same pathogen in different tissues from the same host so that multiple pathogenic behaviours can be identified. Identification of a biotrophic stage of tuber colonisation, and its detailed molecular characterisation, will inform breeders about the potential for resistance genes to work as effectively in this tissue as they do in leaves.

P. infestans, isolated from the same host plant species, can exist as a population comprising numerous different genotypes (Cooke *et al*., 2012). This could be due to the pathogen strategies for evolving to overcome disease resistance during the pathogen-host arms race. If a single genotype of *P. infestans* can use different strategies to colonise different host tissues, then it is necessary to understand these interactions and effector gene expression to find the best solution for disease resistance in all host tissues. In this chapter, hypotheses to be addressed are (i) that *P. infestans* does establish a biotrophic interaction with potato tuber tissue and express effectors, and (ii) that there are differences in *P. infestans* gene expression in tuber tissue compared to leaves.

4.2 Results

4.2.1 Macroscopic symptoms on potato tubers

Phenotypic changes during disease progression were recorded using digital photography (Figure 4.1a to f). The *P. infestans* inoculation droplet on the cut tuber surface was slowly absorbed or evaporated during the experiment time course. There was no clear macroscopic disease development observed on the tuber slices from 12 hpi (Figure 4.1a) to 48 hpi (Figure 4.1d). However, small water-soaked brown spots (four spots indicated by arrows) were observed at the inoculation site at 60 hpi (Figure 4.1e). By 7 dpi (Figure 4.1f), dark brown lesions had appeared on the cut tubers which were covered with aerial hyphae and sporangiophores.

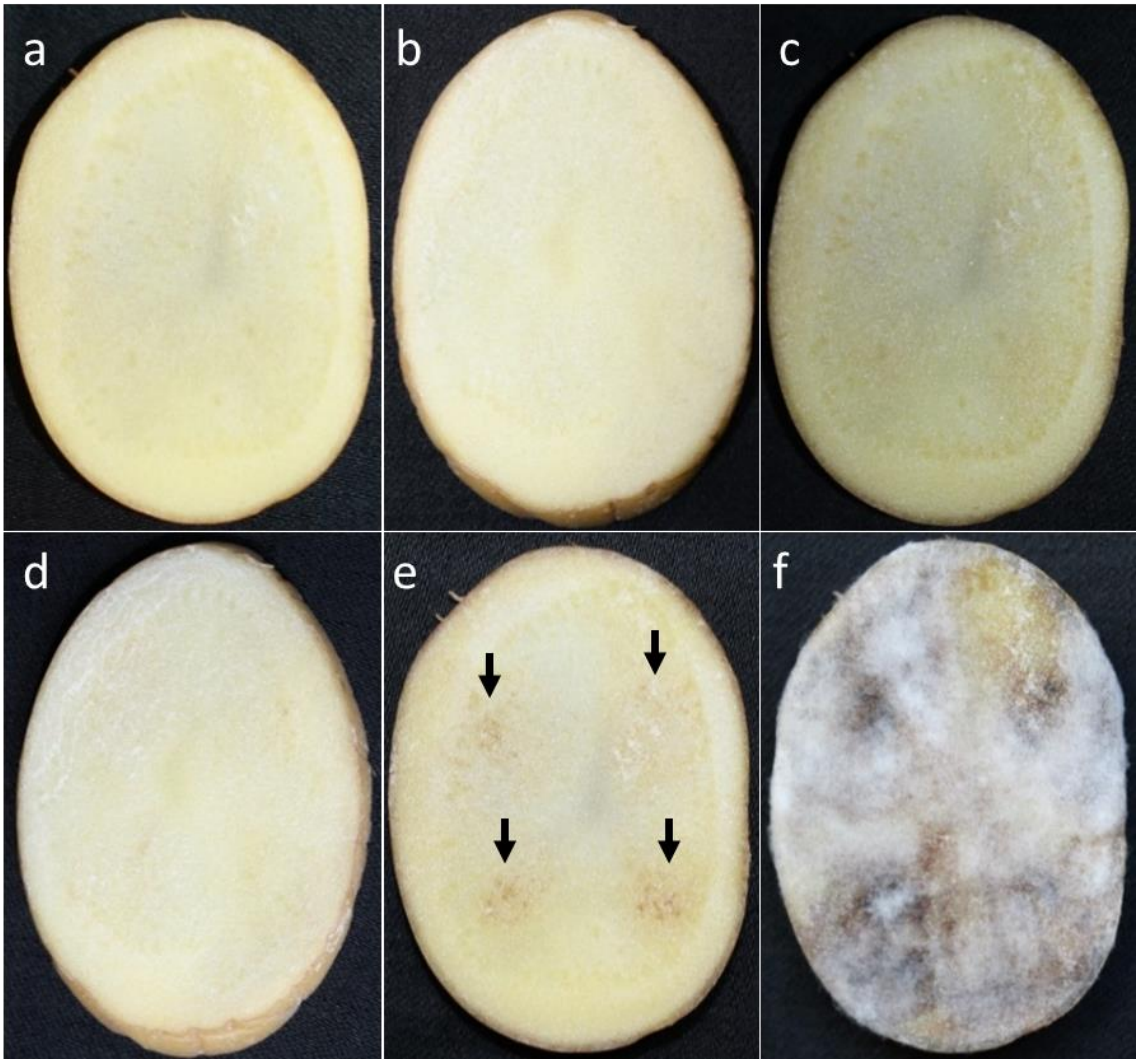

Figure 4.1 Digital image showing *P. infestans* inoculated tuber slices at 12 hpi (a), 24 hpi (b), 36 hpi (c), 48 hpi (d), 60 hpi (e), and 7 dpi (f). Dead cells in and around inoculated sites (indicated by arrows) in tuber slices were observed from 60 hpi (e) and clear phenotypic disease development producing aerial hyphae and sporangia was observed by 7 dpi (f).

4.2.2 Microscopic examination of *P. infestans* infection in potato tuber slices

Since the *P. infestans* strains used were tagged with either cytoplasmic GFP and Hmp1-mRFP (88069-2c5mRFP11; Avrova *et al*., 2008), or cytoplasmic tandem dimer Tomato fluorescent protein (tdTomato) (88069tdT10), microscopic examination of infection in potato tuber tissues were carried out using a Leica SP2 confocal microscope. A preliminary examination of infection on tuber slices (Tesco organic potato tubers) using 2c5mRFP11 was conducted on 48 hpi samples (Figure 4.2a to c). The observation of

green hyphae with Hmp1-mRFP (red) at haustoria (indicated by arrow followed by H) confirmed the occurrence of biotrophy during tuber infection.

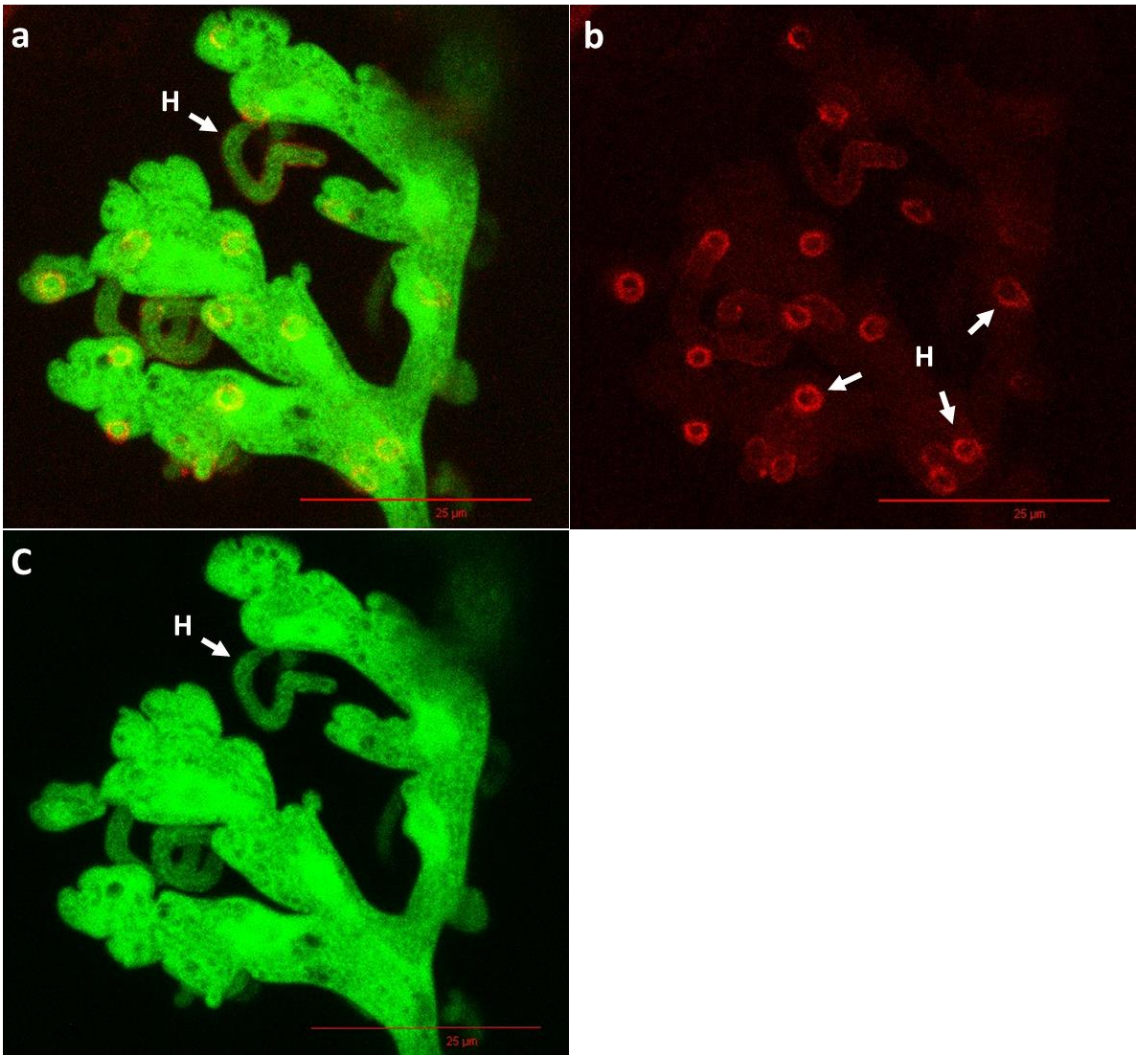

Figure 4.2 Confocal Z-stack image of 2c5mRFP11 infected tuber slices at 48 hpi. Overlay (a) and single colour (b and c) projection images of Hmp1-mRFP (red) which accumulates predominantly at the base of haustoria (arrows followed by H) in a *P. infestans* strain that co-expresses cytoplasmic GFP, showed haustorial formation during tuber infection. Scale bar represents 25 µm.

The experiments on biologically replicated samples to confirm biotrophy during infection of tuber tissue, and to compare the infections with leaf tissues were conducted using the same pathogen (88069tdT) and host (cv. Bintje) as in Chapter 3. At the earliest infection stage examined here (12 hpi), *P. infestans* had already penetrated into the tuber tissue, although some hyphae (fluorescing red) were located on the surface of the tuber slice and

had not yet penetrated into the tuber tissue. Haustorium-like structures were observed on some intercellular hyphae (indicated by a white arrow in Figure 4.3), indicating successful infection at 12 hpi (Figure 4.3a). More extensive hyphal growth, along with haustoria, was observed at 24, 36, 48, and 60 hpi (Figure 4.3b to e respectively). Hyphae were highly branched and had extensively colonized tuber cells at the inoculation sites during later infection time points. Although not quantified, at 48 hpi (Figure 4.3d) and 60 hpi (Figure 4.3e) *P. infestans* hyphae appeared more elongated, curved, and thicker, compared to the early infection time points.

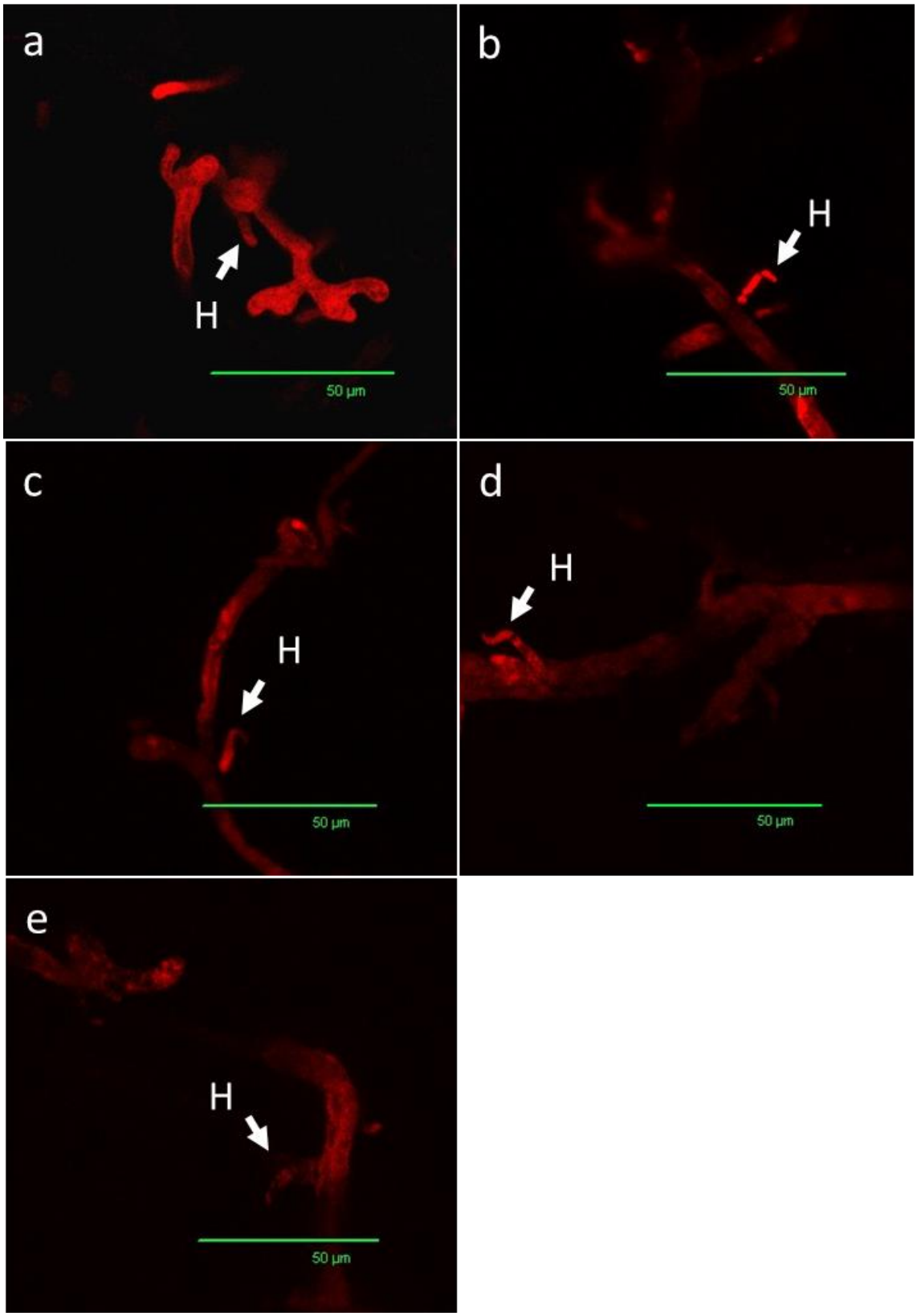

Figure 4.3 Confocal projections of tuber slices, infected with the 88069tdT strain, at 12 hpi (a), 24 hpi (b), 36 hpi (c), 48 hpi (d), and 60 hpi (e). Figures show *P. infestans* (in red). Haustoria (shown by arrows followed by H) were observed from early infection (12 hpi) and were detected throughout the infection. Scale bar represents 50 µm.

4.2.3 RNA extraction, quality control (spectrophotometry), and cDNA synthesis

RNA was extracted from sporangia, germinating cysts, and a tuber infection time course (12, 24, 36, 48, and 60 hpi). The quality and yield of the total RNA from *in vitro* stages of *P. infestans*, and infected tuber samples was acceptable for QRT-PCR experiments. Integrity of the isolated RNA was confirmed using agarose gel electrophoresis. These RNA samples were used to prepare cDNA as templates for expression analysis.

4.2.4 Gene expression analysis of *P. infestans* PAMPs, elicitors, necrosis-inducing proteins, and cytoplasmic effectors during a tuber infection time course

Previously described and published *P. infestans* genes detected in the leaf infection microarray, such as the sporulation marker *Cdc14*, biotrophy marker *Hmp1*, a PAMP (CBEL family protein), the elicitor/necrosis inducing protein (NPP1), and a cytoplasmic RxLR effector (*Avrblb1*), were selected for gene expression analysis by QRT-PCR.

The gene expression profile of sporulation marker gene *Cdc14* (PITG_18578), in comparison to sporangia when normalised to *P. infestans* actin, was down-regulated throughout the tuber infection time course (Figure 4.4).

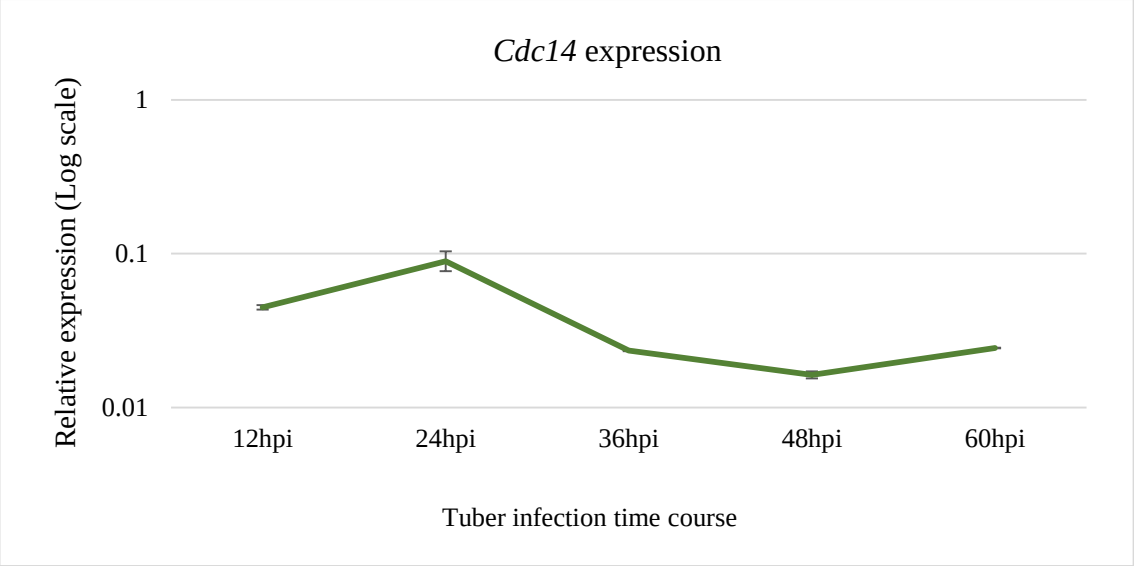

Figure 4.4 The gene expression profile for sporulation marker gene *Cdc14* (PITG_18578) during tuber infection time course. Relative expression of this gene showed down-regulation throughout the infection time course from 12 to 60 hpi in comparison to sporangia (given a value of 1).

The proteinaceous PAMP, cellulose binding elicitor lectin-like family protein (CBEL; PITG_03637), was used to examine whether, as observed in leaf colonisation, this PAMP is down-regulated during tuber colonisation. Gene expression analysis showed this CBEL gene to be 6-fold up-regulated at 12 hpi in tuber infection compared to the level of this transcript in sporangia, consistent with it playing a role during appressorium-mediated host penetration (Grenville-Briggs *et al*., 2010). The transcript was found to be down-regulated from 24 hpi, and remained down-regulated for the rest of the infection time course (Figure 4.5).

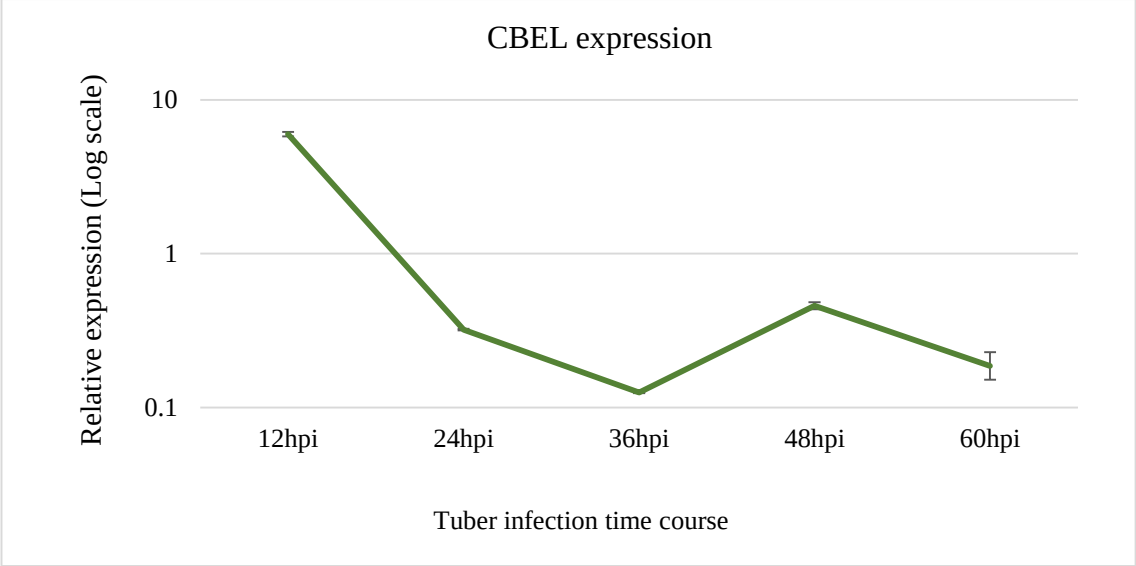

Figure 4.5 The gene expression profile for proteinaceous PAMP CBEL (PITG_03637) during tuber infection time course. Relative expression of this gene showed 6-fold up-regulation at 12 hpi followed by down-regulation from 24 to 60 hpi in comparison to sporangia.

The expression of biotrophy marker gene *Hmp1* (PITG_00375) was investigated in the tuber infection time course to test whether a biotrophic interaction was being established. In comparison to sporangia, the gene expression profile of *Hmp1* showed strong up-regulation (up to 58-fold) at 12 hpi, a reduction to 15-fold at 24 hpi, and steady up-regulation across 36, 48, and 60 hpi (53, 289, and 302-fold, respectively) (Figure 4.6).

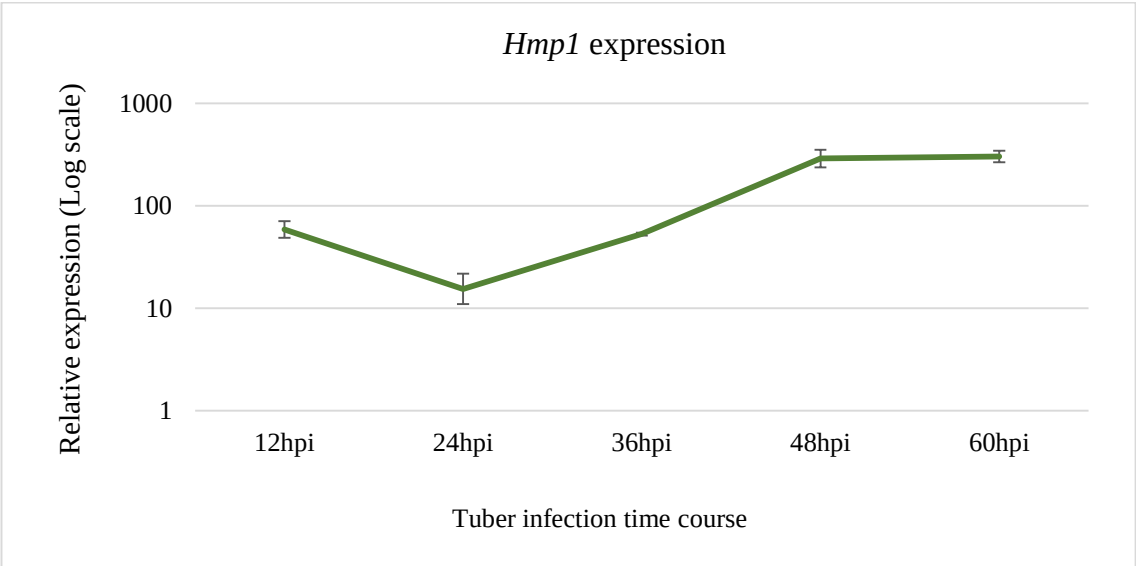

Figure 4.6 The gene expression profile for biotrophy marker gene *Hmp1* (PITG_00375) during tuber infection time course. Relative expression of this gene showed up-regulation at 12 hpi and throughout the infection time course in comparison to sporangia.

The expression of the gene encoding the cytoplasmic RxLR effector *Avrblb1* (PITG_21388) was analysed during tuber infection time course. Expression of *Avrblb1* (also called *ipiO1*) has previously been shown to be associated with invading *P. infestans* hyphae (van West *et al.*, 1998). Gene expression analysis revealed a similar expression profile to *Hmp1*, showing up-regulation at 12 hpi (35-fold), a drop at 24 hpi (to 9-fold) and greater up-regulation at 36, 48, and 60 hpi (26, 45, and 76-fold, respectively) (Figure 4.7).

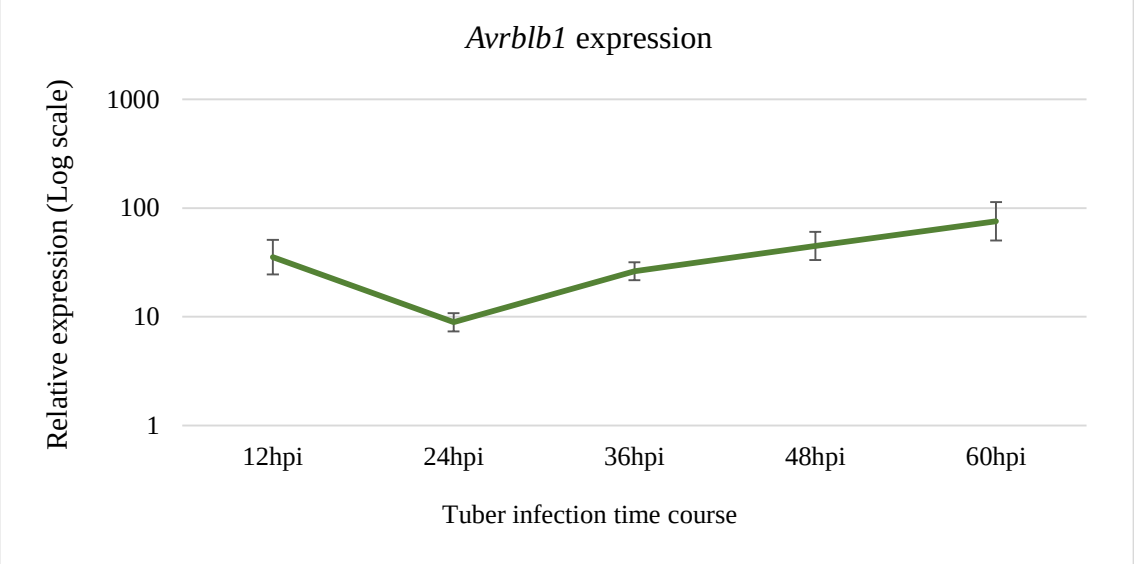

Figure 4.7 The expression profile for cytoplasmic RxLR effector coding gene *Avrblb1* (PITG_21388) during tuber infection time course. Similar to the expression profile for *Hmp1* (see Figure 4.5), the relative expression of *Avrblb1* was up-regulated at 12 hpi and throughout the infection time course when compared to the expression level in sporangia.

The NPP1 protein belongs to the large family of NLPs (necrosis-like proteins), which in oomycetes have two characteristic cysteine residues at the N-terminus (Gijzen and Nürnberger 2006; Feng and Li 2013).

During tuber infection, the NPP1-family protein PITG_09716 was highly expressed at 12 hpi (576-fold), compared to 24 hpi (86-fold) (Figure 4.8). This gene had a similar gene expression profile to *Hmp1* and *Avrblb1*.

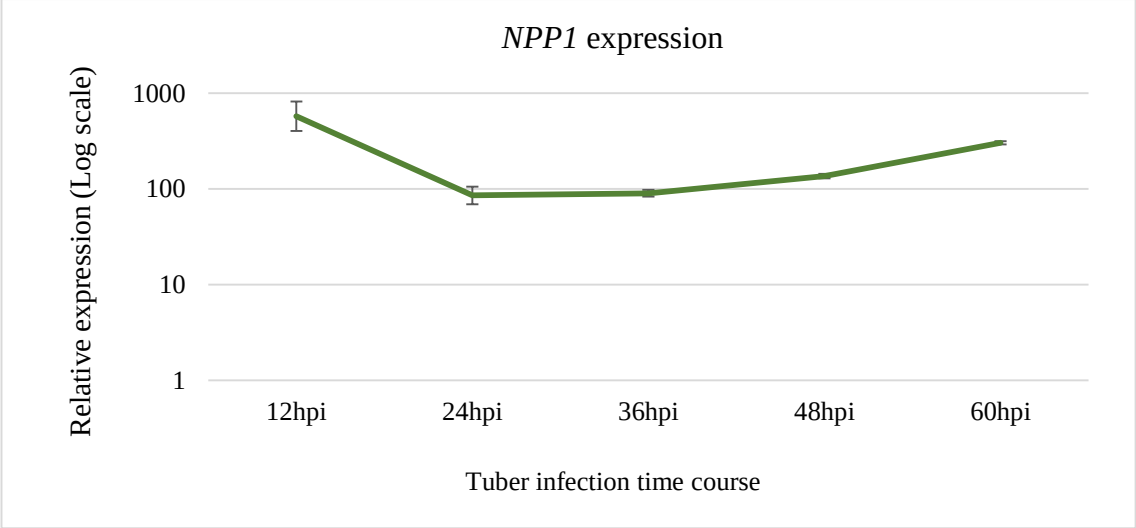

Figure 4.8 The expression profile for necrosis-inducing family gene (NPP1 family) PITG_09716 during tuber infection time course. The relative expression of this NPP1 family member was very highly up-regulated at 12 hpi compared to 24, 36, 48, and 60 hpi, when compared to the expression level in sporangia.

4.2.5 Gene expression analysis of selected infection-specific genes identified from the leaf infection microarray

The expression profiles for selected infection-specific genes from the leaf microarray (from Chapter 3) were determined during the tuber infection time course. This group of genes were analysed to determine if these genes were generally infection-specific (any tissue type) or only leaf infection-specific. The selected genes, encoding a glucanase inhibitor protein (PITG_13638), an NLP family protein (PITG_23094), a proton-dependant oligopeptide transporter protein (PITG_09088), and two cytoplasmic RxLR effector proteins (PITG_09757 and PITG_15679) were also up-regulated during tuber infection (Figure 4.9). However, genes encoding a glycoside hydrolase protein (PITG_04272), and two other RxLR effectors (PITG_05146 and PITG_15128) were not detected in the tuber infection time course. All of the selected genes were down-regulated in vegetatively grown mycelium (*in vitro* grown hyphae harvested at 60 hpi), compared to sporangia (Figure 4.9).

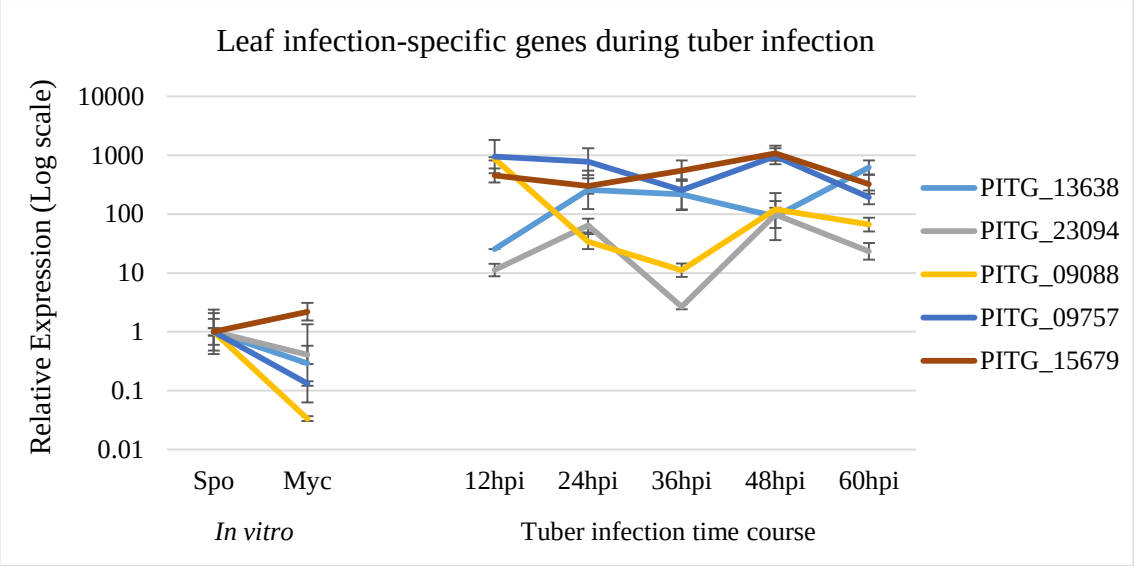

Figure 4.9 The expression profiles for the selected leaf infection-specific genes during tuber infection relative to *P. infestans* actin. Out of eight genes validated in the leaf infection time course, only five genes were detected during the tuber infection time course: glucanase inhibitor protein (PITG_13638), NLP protein (PITG_23094), proton-dependant oligopeptide transporter protein (PITG_09088), and two cytoplasmic RxLR effector proteins (PITG_09757 and PITG_15679).

4.3 Discussion

4.3.1 The cell biology of tuber infection revealed a biotrophic interaction

The cell biology study by confocal microscopy showed haustorial structures formed in the tuber tissue as early as 12 hpi. However, these results originated from *P. infestans* inoculated onto the cut surface of tuber slices. Future work will focus on inoculation of the tuber skin surface, as preliminary results (not shown) did indicate some penetration of the pathogen through the epidermis. Nevertheless, the observation here of haustorium formation indicates that *P. infestans* had penetrated host tuber tissue by 12 hpi or earlier, and potentially established a biotrophic interaction. The *P. infestans* transformant (hmp1-mRFP + cytoplasmic GFP) expresses the Hmp1-mRFP fusion driven by the native *Hmp1* promotor, so that the red fluorescence will only appear at the time that the gene is activated (Avrova *et al*., 2008). The presence of haustoria during the early stage of tuber infection was also corroborated by the QRT-PCR expression analysis of the endogenous

biotrophic marker gene, *Hmp1*, which showed up-regulation at 12 hpi and throughout the infection time course. Haustoria have been identified previously in potato tuber tissue infected with *P. infestans* (Hohl and Stössel, 1976). That study used transmission electron microscopy to examine tuber infection. While haustoria were identified, it was not possible to determine if they were functionally equivalent to those found in infected leaf tissue. The presence of Hmp1 surrounding haustoria in tubers (this chapter) signifies that these are indeed functionally equivalent.

4.3.2 Down-regulation of expression for the PAMP (CBEL) and sporulation marker gene (*Cdc14*) during early initiation of tuber infection

In comparison to sporangia, the sporulation marker gene *Cdc14* was significantly down-regulated from 12 hpi and throughout the infection time course. This expression pattern is consistent with the earliest stages of leaf infection, in which sporulation-associated genes are down-regulated (Chapter 3). In comparison to the biotrophic marker gene *Hmp1* and cytoplasmic effector *Avrblb1*, low levels of expression for CBEL (PITG_03637) at 12 hpi suggests that suppression of this PAMP occurs soon after initial penetration, again consistent with the establishment of a biotrophic interaction between the pathogen and potato tuber tissues. The results may suggest that the pathogen also generally suppresses PAMPs during tuber infection. However, this requires expression profiling of genes encoding the PEP13 and INF1 PAMPs in future. It could be speculated that *Hmp1* and *Avrblb1* (and likely other effector genes) were highly up-regulated at 12 hpi to suppress PTI activated during tuber colonisation. In agreement with this, Gao *et al*. (2013) noted suppression of defence related genes in tuber tissue infected with *P. infestans*.

4.3.3 A similar pattern of gene expression in both leaf and tuber infection suggests a biotrophic stage is also important in tuber tissue infection

Although cytoplasmic effectors and the necrosis-inducing proteins were highly up-regulated at 12 hpi along with biotrophic marker gene *Hmp1*, overall the pattern of gene expression trends were similar in leaf and tuber hosts. More obvious differences were the level of relative gene expression (up-regulation) in tuber infection which was higher than in leaf infection. This could be due to the different cellular structures, defence mechanisms, and the available nutrients in leaves and tubers. Alternatively, the differences in relative up-regulation of the genes tested could reflect differences in the speed of infection development between leaf and tuber tissue.

4.3.4 Comparative studies of previously identified infection-specific transcripts revealed leaf infection-specific genes

Among eight leaf infection-specific genes identified from Chapter 3, two cytoplasmic RxLR effectors (PITG_05146 and PITG_15128) and a glycoside hydrolase protein (PITG_04272) were not detected by QRT-PCR during tuber infection. The remaining five genes were up-regulated in both leaf and tuber infections. These five genes could be associated specifically with *P. infestans* biotrophy on any host tissue, as they were equally up-regulated in both leaf and tuber infection, but were down-regulated in vegetatively-grown hyphae.

Finally, the comparison of gene expression in leaf and tuber tissues reflects the dynamics of biotrophy in both tissues. The genes that were specific only to *P. infestans* infection of leaf tissue appear to be dispensable for establishing infection in tubers. The specificity of expression for these genes also reveals that there are different signals perceived by *P. infestans* in leaf and tuber tissue and that these signals activate different sets of genes.

Although there is evidence shown here that suggests biotrophy and effector delivery are important to *P. infestans* for promoting disease development in tubers, in the future it would be informative to test lines of *P. infestans*, silenced for specific effectors (Avrova *et al*., 2008; Bos *et al*., 2010; McLellan *et al*., 2013), for their ability to infect tuber tissue. This would reveal if effectors are genuinely required for tuber infection, or whether the effector gene expression observed here only reflects *P. infestans* following a pre-set transcriptional programme.

Chapter 5. Transcriptional change in *P. infestans* during growth in apoplastic fluid from *N. benthamiana*

5.1 Introduction

The dynamic of pathogen signal perception and response can vary from host to host, condition to condition, and time to time. To understand the varieties of pathogen strategies to colonise a host, the changes in mRNA levels during different conditions and stages can be assessed.

To determine the molecular events in the interaction of the hemi-biotrophic pathogen *P. infestans* during early infection of host plants, in order to understand its pathogenicity and disease development, it is important to study pathogenic behaviour in intercellular spaces. During infection, the majority of *P. infestans* hyphal growth is in the intercellular spaces, the apoplast. In comparison, haustoria that are formed inside host cells, represent a smaller proportion of pathogen biomass during infection. The apoplast is also where the primary defence mechanisms of host cells lie. It is critical that protein-protein interactions occur in host apoplast, as in this intercellular space the host recognizes conserved pathogen molecules (PAMPs) (Doehlemann and Hemetsberger, 2013). Additionally, there is evidence that pathogen effectors, such as protease inhibitors, interact with plant proteases in apoplastic fluid (Song *et al*., 2009). It is also important to understand if the genes that are up-regulated during host interaction also share expression similarities during different growth circumstances such as nutrient-rich medium (feeding stages), and sterile distilled water (starvation stages) so that core components for pathogenicity can be identified.

Previous microarray studies have only been sensitive enough to detect a proportion of the transcriptome during host infection, and yet QRT-PCR studies reveal that transcriptional

changes of well-characterised biotrophy-related proteins occur before they are detectable by microarray. Research in this chapter was initiated from microscopic observations that revealed haustorium-like structures are formed when *P. infestans* was grown in apoplastic fluid from *N. benthamiana*. The microarray analysis here was to enable a detailed transcriptome study of pathogen hyphal growth in plant apoplastic fluid, nutrient-rich pea broth media, and starvation in water, to test the hypothesis that infection-related genes are upregulated in response to soluble chemical signals present in apoplastic fluid.

5.2 Results

Overview

Initially, the formation of haustoria-like structures when grown in *N. benthamiana* apoplastic fluid (AF) was confirmed by microscopy, in comparison with pea broth (PB) (nutrient-rich medium), and sterile distilled water (SW) (during starvation). A microarray experiment was conducted to include *P. infestans* growth in the above media, and sampled at 24 and 48 hpi. This experiment also included *P. infestans* zoospores, which were used to inoculate the three growth media. Similar to the experiments in Chapter 3, the fluorescently tagged strain of *P. infestans* (88069tdT) was used for these experiments.

From the microarray, genes were grouped according to the level and pattern of their expression, and include stage-specific marker genes encoding PAMP proteins, avirulence proteins, other RxLR effectors, NLP proteins, and other genes which are involved in infection and differentially expressed during the interaction time course (from Chapter 3). Transcripts that were only present during growth in AF, PB, and SW were also identified. Transcript accumulation from a selection of genes from all groupings was validated using quantitative real-time RT-PCR (QRT-PCR).

5.2.1 Microscopic examination of *P. infestans* (bright-field microscopy) grown in apoplastic fluid

Microscopic examination of *P. infestans* growth in apoplastic fluid, pea broth, and sterile distilled water was carried out using a bright-field microscope. At 24 hpi, empty *P. infestans* sporangia, germinating cysts, as well as some hyphae, were observed in all AF, PB, and SW inoculations (image not shown). Numerous branched hyphae were observed at 48 hpi in AF (Figure 5.1a). However, the growth density of accumulated hyphae in pea broth and sterile distilled water were comparatively low (Figure 5.1b and c). In addition, mycelium in sterile distilled water looked very unhealthy and the hyphae were very thin. In apoplastic fluid, haustorium-like structures were also observed on some hyphae (arrow in Figure 5.1a). Haustorium-like structures were not observed in PB or SW.

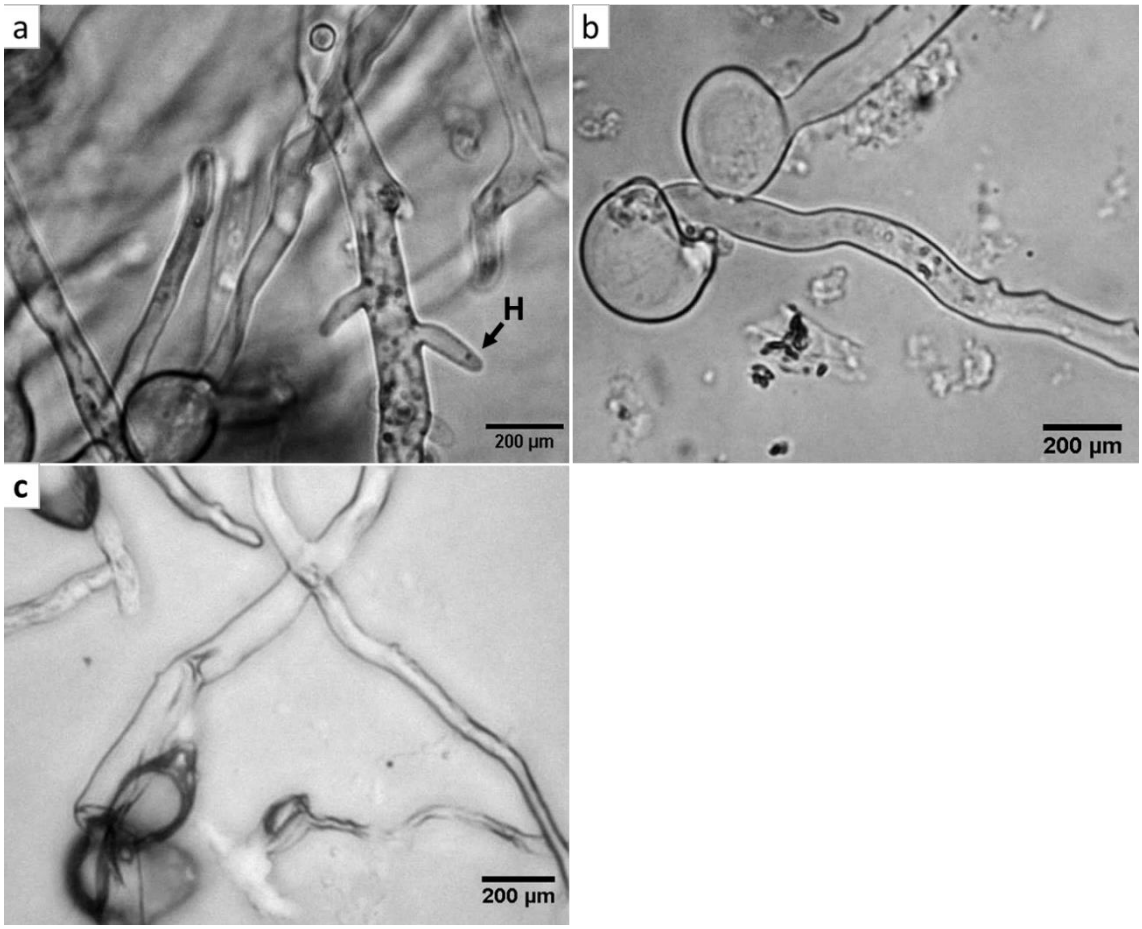

Figure 5.1 Bright-field images of *in vitro* grown *P. infestans* mycelia taken from the Nikon microscope. Images showing *P. infestans* mycelia grown in apoplastic fluid of *N. benthamiana* (a), nutrient-rich pea broth medium (b), and sterile distilled water (c). At 48 hpi, haustoria-like structures (arrow followed by H) were occasionally observed in apoplastic fluid (a). There were no such structures of *P. infestans* observed in pea broth medium, or in sterile distilled water at this time point. Scale bar 200µm.

5.2.2 RNA extraction and quality control (spectrophotometry and bio-analyser), and cDNA synthesis

The quality and yield of the total RNA from *P. infestans* zoospores, and hyphae grown in apoplastic fluid, pea broth, and sterilised distilled water inoculated samples showed acceptable quality for microarray experiments. The RNA integrity number (RIN) from the bio-analyser report with gel electrophoresis (Appendix 5a and 5b) for all biologically replicated samples were above 7.20.

5.2.3 Microarray analysis of *P. infestans* transformant 88069tdT10 grown in apoplastic fluid (*N. benthamiana*), pea broth media, and sterile distilled water

The changes in the *P. infestans* transcriptome during the growth in apoplastic fluid, nutrient-rich pea broth media, and sterile distilled water at two time points (24 and 48 hpi) were investigated using Agilent single-colour microarrays. Microarray probes were designed to the total *P. infestans* transcriptome according to the information provided in Chapter 3 (cross reference Annex 3a); 18,024 predicted transcripts are represented on the microarray. Of these, 15,513 were detected either in one or more of *P. infestans* zoospores, or zoospore inoculated apoplastic fluid, pea broth, or sterile distilled water sampled at 24 and 48 hpi (Annex 5a), according to the quality filter (flag values; present or marginal in two-thirds of the replicates) analysis. *P. infestans* zoospores were included since the different media were inoculated with this spore type. This allowed a direct comparison of transcriptional changes in the transition from motile spore to growing hyphae in the first 24 h of the experiment. Similar to the leaf infection microarray in Chapter 3, the same 57 *P. infestans* genes were specifically selected for data normalisation (cross reference Chapter 3, Table 3.1).

To perform statistical analyses, the set of 15,513 genes detected as described above were subjected to a one-way analysis of variance (Welch ANOVA) with p-value cutoff of 0.05. The multiple testing correction (Benjamini and Hochberg False Discovery Rate (FDR)) was used to determine the significance level. That is, 5.0% of the identified genes would be expected to pass the restriction by chance. This revealed 13,819 transcripts (Annex 5b) detected as differentially expressed in the experiment (all sample conditions). All further data analyses are based on these 13,819 genes.

5.2.4 Flag values represent the detection of the individual genes in each different inoculation condition and time point

To understand the expression specificity of each *Phytophthora* transcript in each different condition (AF, PB, and SW) and time points (24, and 48 hpi), and *P. infestans* zoospores (Zo), data showing 'Present' flags were extracted from the ANOVA list (Annex 5c). A Venn diagram was developed to show the differentially expressed genes related to each different time point of infection (Figure 5.2). For zoospores, 12,868 transcripts were detected according to a 'Present' flag. In the AF, PB, and SW, 12,554, 12,377, and 12,867 transcripts were detected respectively either in one of the inoculation time points (24 and 48 hpi), or both. Although a substantial number (11,712) of transcripts were detected at all conditions and time points, there were few (572, 65, 8, and 98) transcripts detected as specific to Zo, AF, PB, and SW respectively (Figure 5.2). This analysis was conducted to understand how differentially genes are distributed among the different growth conditions tested.

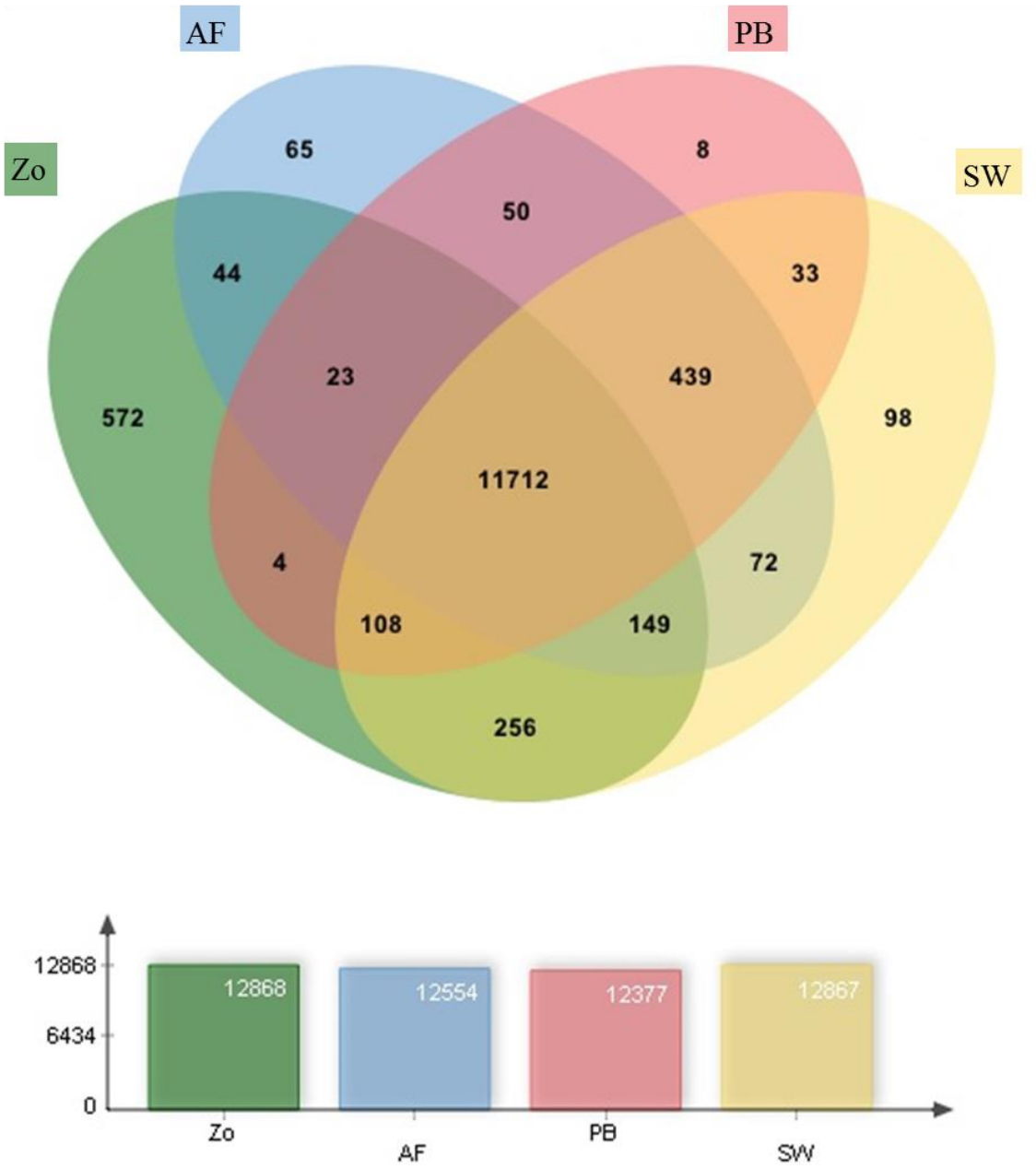

Figure 5.2 Analysis of detected *P. infestans* transcripts ('Present' flag) *in vitro*: zoospores (Zo), and during growth in apoplastic fluid (AF), pea broth (PB), and sterile distilled water (SW). The Venn diagram was constructed from the 13,819 total transcripts from the ANOVA group. 11,712 transcripts were detected as common to all conditions. Altogether, 572, 65, 8, and 98 transcripts were specific to ZO, AF, PB, or SW, respectively.

Although the majority of transcripts (7824 transcripts) detected as significantly differentially expressed were unannotated CHPs and HPs, there were 5,995 annotated transcripts in this group. Among annotated transcripts there were genes encoding spore and cleavage associated proteins (116). In addition, there were many genes associated with plant interactions, such as PAMPs and elicitors (36), enzyme inhibitor proteins (32),

RxLR effectors (322), CRN effectors (354), SCP family of extracellular proteins and small cysteine rich proteins (55), cell wall-degrading enzymes (CWDEs), such as hydrolases, esterases (81), and NLPs such as NPP1 (37) (Figure 5.3). The remaining differentially expressed transcripts were related to the growth, development, and metabolism of *P. infestans*. As expected, the transgene for the tdTomato fluorescent protein was also readily detected.

In the ANOVA list of 13,819 transcripts from the microarray experiment a total of 1,419 (Annex 5b) predicted secreted proteins were detected, accounting for 10.3% of the *P. infestans* transcripts within the ANOVA list. These 1,419 transcripts encode approximately 73% of all *P. infestans* predicted secreted proteins. In the entire ANOVA list, there were transcripts encoding 322 RxLR effectors detected as differentially expressed, of which 298 RxLR effectors were predicted to be secreted proteins, based on the presence of an annotated signal peptide. In addition, transcripts for secreted PAMPs and elicitors (23), enzyme inhibitors (25), CRN effectors (40), SCP-like family and SCR proteins (27), CWDEs (29) and NLP proteins (21), were differentially expressed during infection. There were several CHPs, HPs (504 transcripts), and other growth, development, and metabolism-related proteins (459 transcripts) predicted as secreted proteins in the ANOVA list.

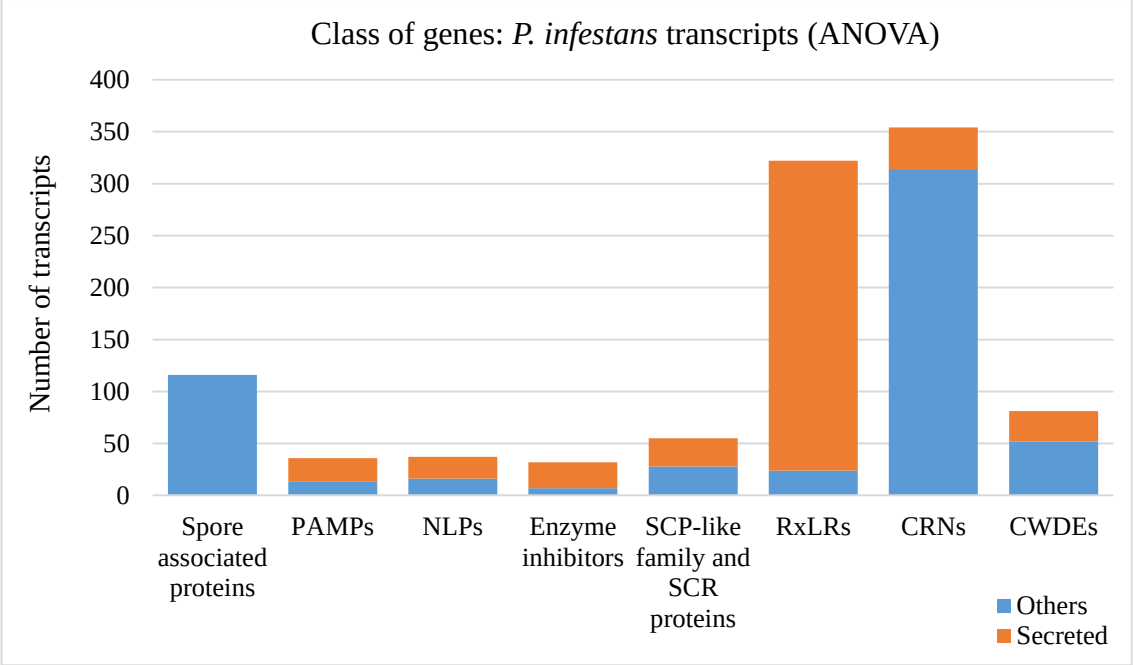

Figure 5.3 Class of differentially expressed genes in the microarray (ANOVA) experiment and the number of transcripts encoding secreted proteins in the selected groups. Groupings encompass genes found to be differentially expressed among any of the biologically replicated samples (apoplastic fluid, pea broth, sterile distilled water, and zoospores). The majority of effectors (CRNs and RxLRs) were detected as significantly differentially expressed in either one or all of the sample conditions including *P. infestans* zoospores. Blue represents non-secreted proteins while orange represents secreted proteins. The majority of RxLR effectors and enzyme inhibitors were predicted to be secreted.

Transcripts detected for individual growth conditions and time points were also assessed for predicted signal peptides to determine if there were significant differences in the proportion of secreted proteins encoded by the transcripts in each condition. This analysis may yield insight into the proportion of *P. infestans* secreted proteins necessary to establish growth in the plant apoplast, vegetative growth, or respond to starvation. There were 1,221 (9%) transcripts detected in the zoospore microarray that were predicted to encode secreted proteins. However, signal peptide analysis on the differentially expressed genes during growth in AF, PB, and SW showed a proportion of approximately 10% for all conditions (Figure 5.4).

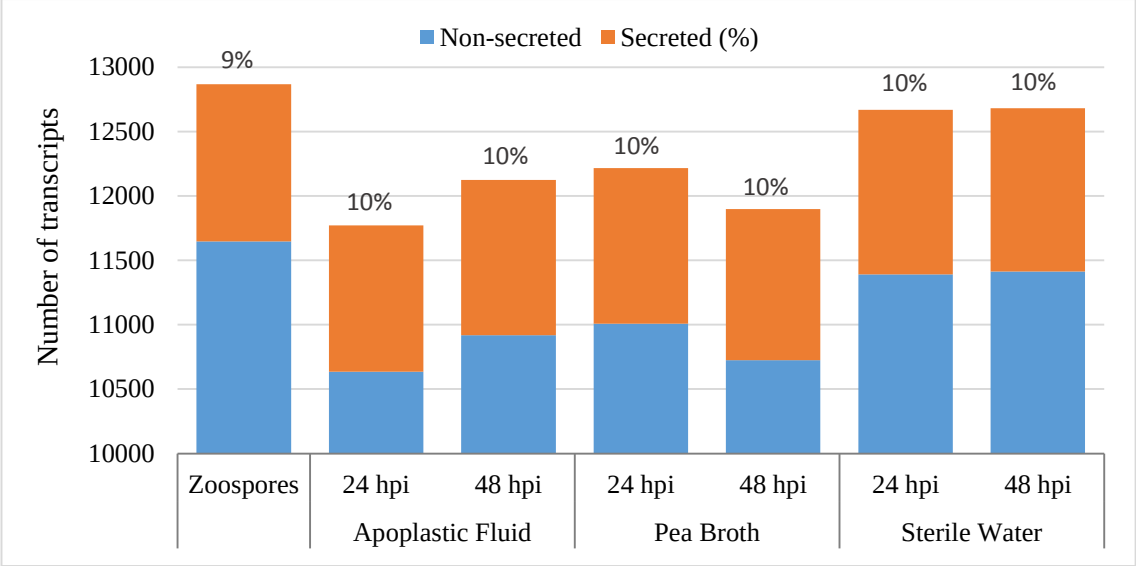

Figure 5.4 Analysis of detected *P. infestans* transcripts conducted on the basis of 'Present' flag from the microarray results of Zo, AF, PB, and SW. Approximately 9% of the detected transcripts in zoospores were predicted to encode secreted proteins, and 10% of detected transcripts were predicted to encode secreted proteins in apoplastic fluid, pea broth, and sterile distilled water at 24 and 48 hpi.

With the flag analysis, the total RxLR effectors (322 transcripts) detected by the microarray were distributed across all conditions: 236, 227, 265, 254, 239, 273, and 272 transcripts were detected in ZO, AP (24 and 48 hpi), PB (24 and 48 hpi), and SW (24 and 48 hpi), respectively. The proportion of RxLR-coding transcripts, compared to the total number of detected transcripts for ZO, AP (24 and 48 hpi), PB (24 and 48 hpi), and SW (24 and 48 hpi) was 1.8%, 1.9%, 2.2%, 2.1%, 2%, 2.1%, and 2.1%, respectively (Figure 5.5).

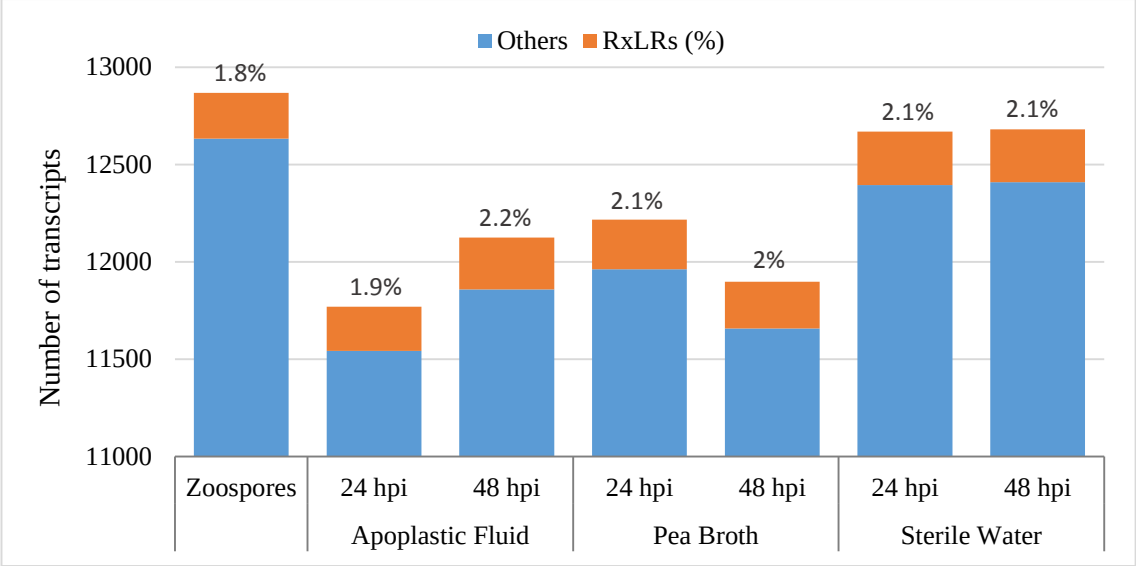

Figure 5.5 The proportion of differentially expressed RxLR effector proteins (percentage; orange) compared to the other proteins (blue) detected as 'Present' Zo, AF, PB, and SW. The proportion of transcripts encoding RxLR effector proteins does not change markedly in any condition.

Flag (Present) analysis, combined with normalization, allows determination of the proportion of the transcripts that are up-regulated (more than 2-fold), non-significant change (in between 0.5 and 2 fold), and down-regulated (less than 0.5 fold) in a given condition. Analysis of up-regulated, non-significant change, and down-regulated transcripts in each condition and time point revealed marked transcriptional changes in *P. infestans* (Figure 5.6). Out of 12,868 transcripts detected in zoospores, 4,643 transcripts (36.8%) were significantly up-regulated (Table 5.1). A comparatively low number of transcripts were detected as up-regulated in AF, PB, and SW. Out of 11,770 and 12,124 transcripts detected at 24 and 48 hpi in AF, respectively, 480 transcripts (4.1%), and 1,021 transcripts (8.4%) were up-regulated, respectively. Out of 12,216 and 11897 transcripts detected at 24 and 48 hpi in PB, respectively, 211 transcripts (1.7%), and 356 transcripts (2.9%) were up-regulated, respectively. Out of 12,668, and 12,681 transcripts detected at 24 and 48 hpi in SW, respectively, 490 transcripts (3.9%), and 662 transcripts (5.2%) were up-regulated, respectively. Transcripts that were detected but not significantly changed were 6,350, 11,248, 9,830, 11,985, 11,137, 12,105, and 11,961 in

zoospores, AF 24 hpi, AF 48 hpi, PB 24 hpi, PB 48 hpi, SW 24 hpi, and SW 48 hpi, respectively. Similarly, there was a higher number (1,875; 14.6%) of transcripts down-regulated in zoospores, followed by 1,273 transcripts (10.5%) in AF (48 hpi), and 404 transcripts (3.4%) in PB (48 hpi). There were less than 1 % of transcripts detected as down-regulated in the other samples.

Table 5.1 Flag value analysis of detected *P. infestans* transcripts from the ANOVA list of microarray data. Number and percentages (%) of transcripts detected as up-regulated, non-significant change, and down-regulated in *P. infestans* zoospores (Zo), and *P. infestans* grown in apoplastic fluid of *N. benthamiana* (AF), nutrient-rich pea broth media (PB), and sterile distilled water (SW).

Samples	**Total transcripts**	**Up- regulated**		**Non-significant**		**Down- regulated**	
		transcripts	**(%)**	**transcripts**	**(%)**	**transcripts**	**(%)**
Zoospores	12868	4643	36.1	6350	49.3	1875	14.6
AF 24 hpi	11770	480	4.1	11248	95.6	42	0.4
AF 48 hpi	12124	1021	8.4	9830	81.1	1273	10.5
PB 24 hpi	12216	211	1.7	11985	98.1	20	0.2
PB 48 hpi	11897	356	3.0	11137	93.6	404	3.4
SW 24 hpi	12668	490	3.9	12105	95.6	73	0.6
SW 48 hpi	12681	662	5.2	11961	94.3	58	0.5

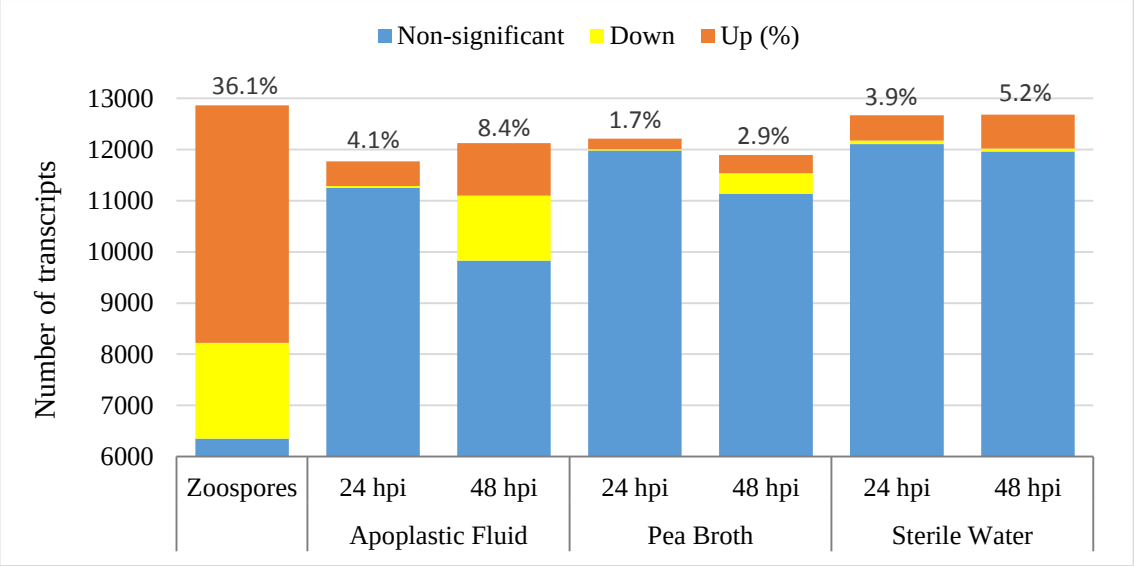

Figure 5.6 The proportion of differentially expressed non-significant change (blue), down-regulated (yellow), and up-regulated (percentage; orange) detected during Zo, AF, PB, and SW. Analysis of detected transcripts was conducted on the basis of 'Present' flag and normalized expression value. Although the normalised expression level of more than 6,000 transcripts were assessed as non-significant change in all samples (more than 0.5 fold and less than 2 fold), 36.1% of the total detected transcripts in zoospores were up-regulated (more than 2 fold). In apoplastic fluid (AF) 4.1%, and 8.4% transcripts were up-regulated, which was more than in pea broth (PB) (1.7%, 2.9%), and sterile distilled water (SW) (3.9%, 5.2%) at 24 and 48 hpi, respectively. 15.6% of the detected transcripts were down-regulated (less than 0.5 fold) in zoospores, followed by 10.5% in apoplastic fluid (48 hpi), and 3.4% in pea broth (48 hpi). In all other conditions and times, there were less than 1% transcripts detected as down-regulated.

Out of 3,116 total predicted transmembrane proteins (TPs) encoded in the *P. infestans* genome, there were 2,590 transcripts (Annex 5b) detected as differentially expressed in any one of the sample conditions. In the ANOVA list, 2,387 transcripts encoding TPs were detected in zoospores. Similarly, high numbers of transcripts (2,178, 2,273, 2,281, 2,223, 2,359, and 2,366) encoding TPs were detected in AF 24 hpi, AF 48 hpi, PB 24 hpi, PB 48 hpi, SW 24 hpi and SW 48 hpi, respectively (Figure 5.7).

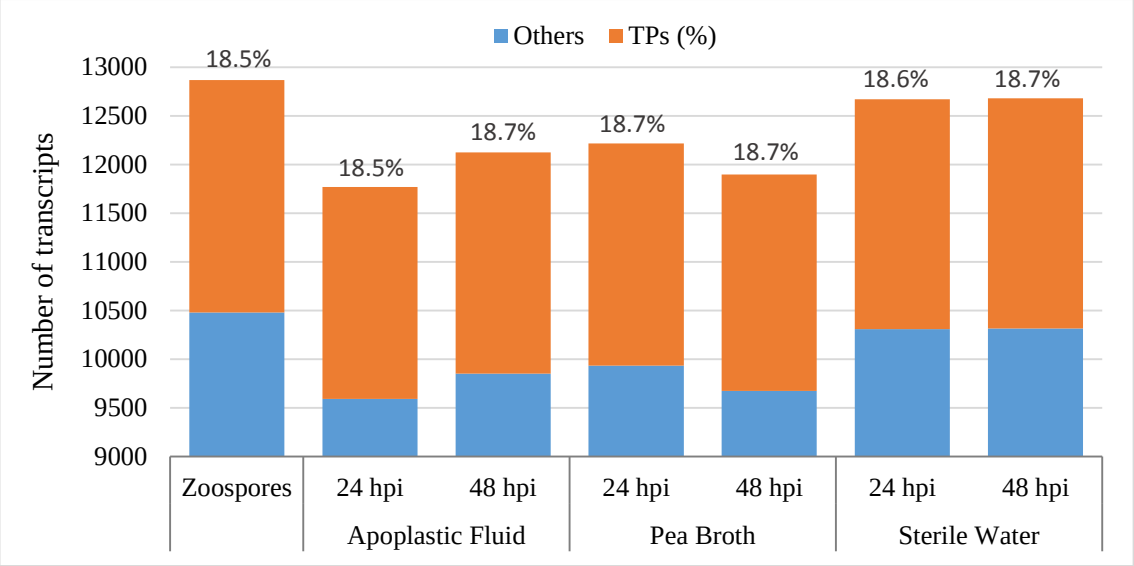

Figure 5.7 The proportion of differentially expressed *P. infestans* transcripts encoding transmembrane proteins (percentage; orange) compared to other transcripts (blue) detected in Zo, AF, PB, and SW. Approximately 18.5% of the detected transcripts in zoospores encoded transmembrane proteins (TPs). The expression of genes encoding membrane bound proteins does not change markedly in any sample type.

In order to identify involvement of the proteins that determine and initiate the flow of genetic information from DNA to mRNA, the expression of transcription factors (TFs) detected on the microarray was assessed. There were 74 transcription factors differentially expressed in the zoospores stage, and during growth in apoplastic fluid, pea broth, and sterile distilled water. Among these, 25 transcripts encoded myb-like DNA binding proteins, followed by bzip transcription factors (12 transcripts). However, a MADS-box transcription factor, calmodulin-binding transcriptional activator, CCAAT-binding transcription factor, TFIIH basal transcription factor, and several other transcription factor types were also detected.

5.2.5 Volcano plot analysis of transcriptional change during different growth conditions

To understand the significant changes in gene expression involved in growth in AF, PB, and SW, the genes that were detected/specifically expressed during each different sampling time and condition were analysed. Clusters of genes which were differentially

expressed at each sampling time and condition were analysed on the basis of volcano plot built by comparing each condition (AF, PB, and SW) and timing (24 and 48 hpi) with itself using the ANOVA list (cut-off at 0.05) (Annex 5d). The normalised value was defined as 2 and a P-value cut-off was at 0.05. The transcripts were differentially distributed among different samples. However, some were present during different conditions and time points, allowing them to be distributed into more than one grouping. In the AF 24 hpi sample, there were 105 transcripts identified, and for AF 48 hpi , PB 24 hpi, PB 48 hpi, SW 24 hpi, and SW 48 hpi, there were 2,291, 155, 701, 556 and 710 transcripts respectively (Figure 5.8a).

Out of 105 transcripts detected for AF 24 hpi by volcano plot stage comparison, the majority of the transcripts (95 transcripts) were up-regulated by more than 2-fold (Figure 5.8b). 58 transcripts were listed as unannotated CHPs and HPs, and 37 transcripts were previously annotated. Among the 37 annotated transcripts, four encode secreted RxLRs. Other transcripts coded for: spore associated protein and enzyme inhibitor (one transcript each), serine protease family (five transcripts), glycoside hydrolase (four transcripts), and transport proteins (11 transcripts). There were ten transcripts down-regulated in this condition encoding: transglutaminase elicitor, sulfatase like protein, and polygalacturonase (one transcript each), catalase peroxidase and protein kinase (two transcripts each), and CHPs (three transcripts).

The analysis of the AF 48 hpi growth stage was also analysed using the volcano plot pairwise comparison method to find the significantly up- and down-regulated genes at this stage. Out of 2,291 transcripts, there were 1,021 transcripts up-regulated at this time point (Figure 5.8b). Although 460 transcripts up-regulated at this time point encoded unannotated CHPs and HPs, 561 transcripts were annotated, including: RxLR effectors

(85 transcripts), CRN effectors (two transcripts), PAMPs and elicitors (ten transcripts), CWDEs and necrosis inducing proteins (24 transcripts), SCP-like extracellular proteins (three transcripts), and enzyme inhibitors (two transcripts). Candidate effectors such as secreted carbonic anhydrases (three transcripts) were also up-regulated at this stage. Other protein coding transcripts, such as serine protease family proteins, polygalacturonase proteins, polysaccharide lyase proteins, transport proteins, and several other proteins including Hmp1 and well characterised Avr proteins, that are responsible for biotrophic interactions with host plants and *P. infestans* growth and development were also up-regulated at this stage. However, many genes (1,270 transcripts) encoding CHPs and HPs (763 transcripts), spore associated proteins (56 transcripts) including sporulation marker gene (*Cdc14*), CRN effectors (38 transcripts), RxLR effectors (13 transcripts including *Avrblb1*), enzyme inhibitors (three transcripts), and SCR proteins (four transcripts) were significantly down-regulated. Other protein encoding transcripts such as ipiB1 family of glycine rich proteins, carbonic anhydrase, catalase peroxidase, and other protein coding transcripts that might not be necessary for growth in apoplastic fluid were also down-regulated at this stage.

P. infestans transcripts detected as significantly differentially expressed in nutrient-rich PB medium after 24 hpi were analysed by volcano plot analysis. This set of 155 transcripts included 47 CHPs and HPs. Among the 155 transcripts, 137 were up-regulated, including 39 transcripts encoding CHPs and HPs (Figure 5.8b). Among the 98 annotated transcripts up-regulated at this stage, there were seven transcripts encoding RxLR effectors. Although there were six transcripts for hydrolytic enzymes such as pectinesterases and a glycoside hydrolase, no transcripts encoding NLP proteins were detected. Transcripts for a protease inhibitor and for the sporulation marker gene *Cdc14* were also up-regulated at this stage. A set of 18 transcripts, including eight CHPs, were

significantly down-regulated. Among ten annotated transcripts, there were two transcripts for CBEL, and one transcript each for serine protease, protein kinase, sulfatase-like protein, and polygalacturonase. Two transcripts for transporters were also down-regulated at this stage.

A set of 701 *P. infestans* transcripts, including 323 transcripts of CHPs and HPs, were significantly differentially expressed at 48 hpi in nutrient-rich PB medium (Figure 5.8b). Of these, 332 transcripts, including 92 CHPs and HPs, were found to be up-regulated more than two-fold. Among 240 annotated transcripts up-regulated at this stage, there were 15 transcripts for RxLR effectors, 13 transcripts for CWDEs, and six transcripts for PAMPs and elicitors. A transcript each for a glucanase inhibitor, and an SCP-like extracellular protein were also up-regulated at this stage. A set of 369 transcripts, including 231 CHPs and HPs, were significantly down-regulated at this stage. Among 138 annotated transcripts down-regulated, 12 transcripts encoded RxLR effectors, three transcripts for CRN effectors, and a transcript each for elicitin, glucanase inhibitor, and an SCP-like extracellular protein were detected. The majority (25) of transcripts encoding spore-associated proteins were significantly down-regulated at this stage.

A set of 556 *P. infestans* transcripts, including 309 CHPs and HPs, were significantly differentially expressed at 24 hpi in SW (starvation stage) (Figure 5.8b). Of these, 483 transcripts, including 282 CHPs and HPs, were significantly up-regulated at this stage. Out of 201 annotated and up-regulated transcripts, there were 38 transcripts for RxLR effectors, five transcripts for PAMPs and elicitors, six transcripts for enzyme inhibitors, five transcripts for SCP-like extracellular and SCR proteins, 12 transcripts for CWDEs, and three transcripts for spore associated proteins. Candidate effectors such as secreted carbonic anhydrase (three transcripts) and catalase-peroxidase (one transcript) were also

detected as up-regulated in the list. A set of 73 transcripts, including 27 transcripts of CHPs and HPs, were significantly down-regulated at this stage. Among 46 annotated down-regulated transcripts, three transcripts coded for RxLR effectors, and one transcript for an enzyme inhibitor (protease inhibitor) were detected.

A set of 710 *P. infestans* transcripts, including 424 CHPs and HPs, were significantly differentially expressed at 48 hpi in SW (Figure 5.8b). 652 transcripts, including 409 CHPs and HPs, were significantly up-regulated at this stage. Among 243 annotated up-regulated transcripts there were 40 transcripts for RxLR effectors, five transcripts for CRN effectors, four transcripts each for PAMPs and elicitors, SCP-like extracellular proteins, and six transcripts for CWDEs. Effector candidates such as secreted carbonic anhydrase (two transcripts) were also detected as up-regulated. At this stage, 58 transcripts that included 15 CHPs and HPs, were significantly down-regulated. Among 43 annotated down-regulated transcripts, there were two transcripts for RxLR effectors, and a transcript each for a protease inhibitor and a pectinesterase.

Similarly, the proportion of genes encoding secreted RxLR effectors that were detected and differently expressed, up-regulated two-fold or more, and down-regulated less than 0.5-fold were also analysed across the experiment (AF, PB, SW; volcano plot analysis) (Figure 5.8d). There were four transcripts for a gene family encoding RxLR effectors (PITG_05911, PITG_05912, PITG_05918, and PITG_22089) significantly up-regulated in growth in AF at 24 hpi that were specific to this stage. Out of 98 transcripts encoding RxLR effectors expressed at 48 hpi in AF, 85 were significantly up-regulated. This list included well characterised RxLR effectors such as Avr2 (PITG_08943), Avr3a (PITG_14371), Avr4 (PITG_07387), PexRD1 (PITG_15287) and PexRD36 (PITG_23132). 13 transcripts for RxLR effectors were significantly down-regulated at

this stage. This list included the well characterised *Avr* gene *Avrblb1* (PITG_21388). Two transcripts for paralogs of PexRD8 (PITG_14738 and PITG_17838) were also down-regulated at this stage. Out of seven transcripts encoding RxLR effectors expressed at 24 hpi in PB, all of them were significantly up-regulated. Out of 25 RxLR effector coding transcripts detected at 48 hpi in PB, 13 were significantly up-regulated and 12 were down-regulated. There were 42 transcripts encoding RxLR effectors detected at 24 hpi in SW, out of which 38 transcripts were up-regulated and four transcripts were down-regulated. Similarly, out of 42 RxLR transcripts detected at 48 hpi in SW, 40 transcripts were significantly up-regulated compared to two transcripts that were down-regulated.

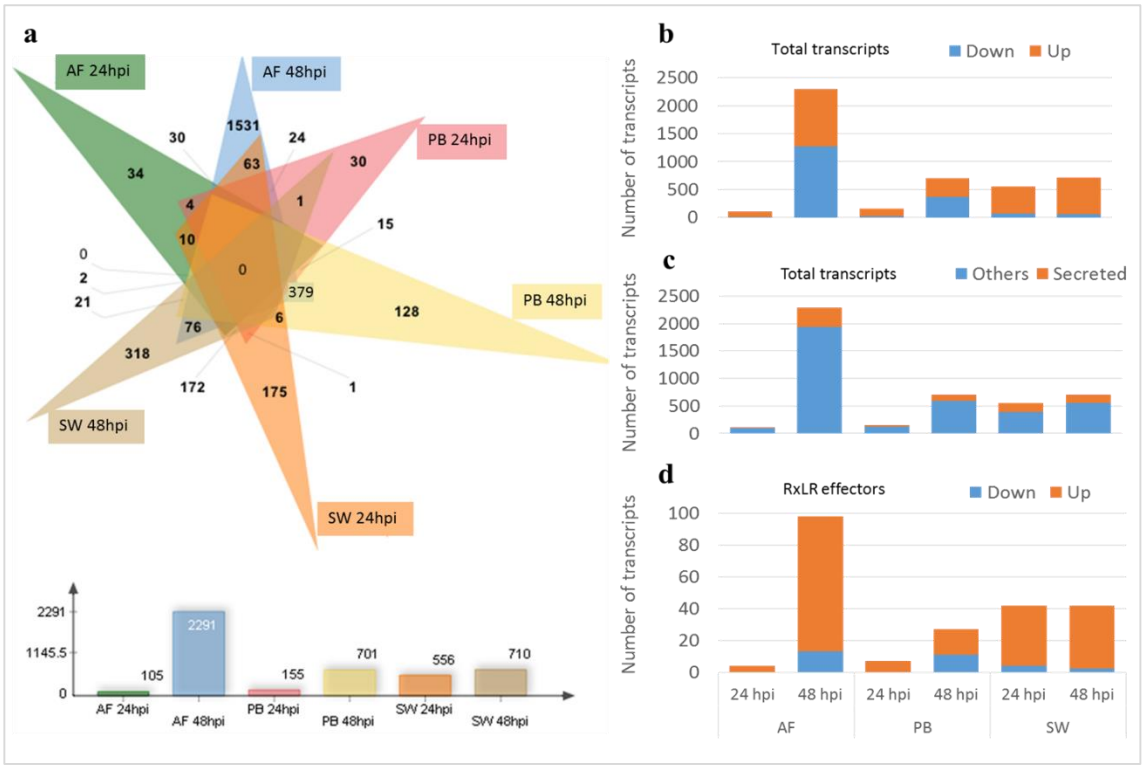

Figure 5.8 Volcano plot built by comparing each stage (AF 24 hpi, AF 48 hpi, PB 24 hpi, PB 48 hpi, SW 24 hpi, and SW 48 hpi) with itself, in which transcripts were differently expressed as defined by the normalised expression value of 2. Data was obtained from the differentially distributed 13,819 total transcripts from the ANOVA (P-value cut-off: 0.05). Venn diagram (a) showing significantly differentially expressed transcripts distributed among each different growth condition. Graph (b) showing comparative numbers of transcripts significantly up-regulated (orange) during each different stages compared to down-regulation (blue). The analysis of the genes encoding proteins with a signal peptide (c) shows a higher number of secreted proteins in AF 48 hpi, followed by SW 24 hpi, SW 48 hpi, and PB 48 hpi. Fewer transcripts encoded proteins with a signal peptide in AF 24 hpi and PB 24 hpi. Graph (d) shows the number of transcripts encoding RxLR effectors detected during each different growth condition. At AF 48 hpi, the greatest number of transcripts for RxLR effectors (85 transcripts) were up-regulated, compared to other conditions and time points.

According to the volcano plot analysis, 151 RxLR effector genes showing differential expression in *P. infestans* stage (zoospores), and different growth conditions (AF, PB, and SW) were identified (Table 5.2) from the microarray experiment. 139 out of 151 RxLR effectors were predicted secreted proteins.

Table 5.2 RxLR effectors significantly differentially expressed in *in vitro* zoospores, and during growth in AF, PB, and SW. According to volcano plot, 151 RxLRs detected as differentially expressed were classified into each condition as listed in the table. The majority (68 transcripts) of transcript for RxLR effectors were significantly/solely up-regulated during growth in AF at 24 (four transcripts), and 48 (64 transcripts) hours. Out of 23 transcripts specific to growth in SW, 11 were up-regulated at 24 hpi and 12 transcripts were up-regulated at 48 hpi. Few transcripts (one each for 24 and 48 hpi) were specific to growth in PB. Signal peptide analysis revealed the majority (139 transcripts) of the RxLR effectors were predicted to be secreted. Up= up-regulated, Down= down-regulated.

Description	Primary accession	Secreted	Detected in	Expression	P-value
RxLR (Avh9.1)	PITG_05911	Yes	AF 24 hpi	Up	0.000322
RxLR (Avh9.1)	PITG_05912	Yes	AF 24 hpi	Up	0.000947
avr2 family	PITG_07499	Yes	AF 48hpi	Up	0.0141
avr2 family	PITG_07500	Yes	AF 48hpi	Up	0.0086
avr2 family	PITG_08278	Yes	AF 48hpi	Up	6.24E-05
avr2 family	PITG_08943	Yes	AF 48hpi	Up	1.22E-05
avr2 family	PITG_15972	Yes	AF 48hpi	Up	4.62E-05
avr2 family	PITG_19617	Yes	AF 48hpi	Up	7.58E-05
avr2 family	PITG_13940	Yes	SW 48hpi	Up	0.00031
avr2 family	PITG_13956	Yes	SW 48hpi	Up	0.000128
avr2 family	PITG_21949	Yes	SW 48hpi	Up	2.37E-05
avr3a	PITG_14371	Yes	AF 48hpi	Up	8.42E-06
avr3a family	PITG_14368	Yes	AF 48hpi	Up	2.07E-06
avr3a family	PITG_14374	Yes	AF 48hpi	Up	5.80E-06
avr4	PITG_07387	Yes	AF 48hpi	Up	0.000224
avrblb1 (ipi01)	PITG_21388	Yes	AF 48hpi, & SW 48hpi	Down in AF 48 hpi	2.53E-05
PexRD1	PITG_15287	Yes	AF 48hpi	Up	0.00151
PexRD36	PITG_23132	Yes	AF 48hpi	Up	0.00639
PexRD8 family	PITG_14736	Yes	SW 24hpi, & SW 48hpi	Up	6.09E-05
PexRD8 family	PITG_14737	Yes	AF 48hpi, SW 24hpi, & SW 48hpi	Up	0.000133
PexRD8 family	PITG_14738	Yes	AF 48hpi, SW 24hpi, & SW 48hpi	Up	9.90E-05
PexRD8 family	PITG_17838	Yes	AF 48hpi, SW 24hpi, & SW 48hpi	Up	0.000306
RxLR	PITG_00366	Yes	SW 24hpi & SW 48 hpi	Up	1.35E-06
RxLR	PITG_00821	Yes	AF 48hpi, PB 48hpi, SW 24hpi, & SW 48hpi	Down in PB 48 hpi	1.11E-05
RxLR	PITG_01724	No	AF 48hpi, & PB 48hpi	Up	0.00236
RxLR	PITG_02830	Yes	AF 48hpi	Up	0.000506
RxLR	PITG_02860	Yes	AF 48hpi, PB 24hpi, & PB 48hpi	Up	4.52E-06
RxLR	PITG_04049	Yes	SW 24hpi	Up	0.000312
RxLR	PITG_04063	Yes	AF 48hpi	Down	0.000158
RxLR	PITG_04074	Yes	AF 48hpi	Down	0.000163
RxLR	PITG_04167	No	AF 48hpi	Up	5.25E-05
RxLR	PITG_04169	Yes	AF 48hpi	Up	7.40E-05
RxLR	PITG_04178	Yes	AF 48hpi	Up	0.000102
RxLR	PITG_04203	Yes	AF 48hpi	Up	0.000159
RxLR	PITG_04266	No	AF 48hpi	Up	0.000101
RxLR	PITG_04269	No	AF 48hpi	Up	0.000117
RxLR	PITG_04276	No	AF 48hpi	Up	0.000244
RxLR	PITG_04314	Yes	SW 48hpi	Down	3.38E-05
RxLR	PITG_04373	Yes	PB 48hpi	Down	1.69E-05
RxLR	PITG_04388	Yes	AF 48hpi, & SW 48hpi	Up	0.000277
RxLR 3' partial	PITG_05074	Yes	AF 48hpi	Up	0.000237
RxLR	PITG_05750	Yes	SW 24hpi	Up	0.000237

Table 5.2 **(Continued)**

Description	Primary accession	Secreted	Detected in	Expression	P-value
RxLR	PITG_05846	Yes	AF 48hpi	Up	0.00108
RxLR	PITG_05910	Yes	AF 48hpi	Up	6.40E-05
RxLR	PITG_05918	Yes	AF 24 hpi	Up	0.0127
RxLR	PITG_05983	Yes	AF 48hpi	Up	0.000964
RxLR	PITG_06092	Yes	SW 24hpi, & SW 48hpi	Up	4.66E-07
RxLR	PITG_06099	Yes	AF 48hpi	Up	0.000141
RxLR	PITG_06246	Yes	AF 48hpi	Up	0.000882
RxLR	PITG_06308	Yes	AF 48hpi	Up	0.00168
RxLR	PITG_06413	Yes	SW 24hpi, & SW 48hpi	Up	0.000607
RxLR	PITG_06478	Yes	AF 48hpi	Up	0.000128
RxLR	PITG_07451	Yes	AF 48hpi	Up	0.00018
RxLR	PITG_07550	Yes	SW 24hpi, & SW 48hpi	Up	3.20E-05
RxLR	PITG_07556	Yes	SW 24hpi, & SW 48hpi	Up	0.00017
RxLR	PITG_07594	Yes	AF 48hpi	Up	1.77E-05
RxLR	PITG_07630	Yes	AF 48hpi	Up	5.16E-05
RxLR	PITG_07766	Yes	SW 24hpi	Up	0.0189
RxLR	PITG_09160	Yes	AF 48hpi	Up	1.31E-06
RxLR	PITG_09216	Yes	AF 48hpi, & PB 48hpi	Up	3.22E-06
RxLR	PITG_09218	Yes	SW 24hpi	Up	4.88E-05
RxLR	PITG_09316	Yes	AF 48hpi, & PB 48hpi	Up	0.000309
RxLR	PITG_09503	Yes	SW 24hpi, & SW 48hpi	Up	0.000233
RxLR	PITG_09689	Yes	AF 48hpi	Down	0.000195
RxLR	PITG_09837	Yes	SW 48hpi	Up	0.000444
RxLR	PITG_09838	Yes	SW 48hpi	Up	0.000111
RxLR	PITG_09861	Yes	AF 48hpi	Up	0.000107
RxLR	PITG_09915	Yes	SW 48hpi	Up	0.00962
RxLR	PITG_09935	Yes	SW 48hpi	Up	0.000116
RxLR	PITG_10116	Yes	PB 48hpi	Down	0.000463
RxLR	PITG_10339	Yes	SW 48hpi	Up	1.85E-06
RxLR	PITG_10341	Yes	AF 48hpi	Up	0.000335
RxLR	PITG_10396	Yes	AF 48hpi, & PB 48hpi	Up	2.36E-06
RxLR	PITG_10640	Yes	SW 24hpi	Up	1.81E-05
RxLR	PITG_10808	Yes	AF 48hpi	Up	0.000423
RxLR	PITG_10818	Yes	AF 48hpi, & PB 48hpi	Up	3.69E-06
RxLR	PITG_10835	No	AF 48hpi	Up	3.90E-05
RxLR	PITG_11947	Yes	SW 24hpi, & SW 48hpi	Up	5.30E-05
RxLR	PITG_12276	Yes	AF 48hpi	Down	0.00228
RxLR	PITG_12721	Yes	PB 48hpi	Down	0.000198
RxLR	PITG_12722	Yes	PB 48hpi	Down	0.000182
RxLR	PITG_12737	Yes	AF 48hpi	Up	3.31E-05
RxLR	PITG_13044	Yes	AF 48hpi, PB 24hpi, & PB 48hpi	Up	0.000506
RxLR	PITG_13045	Yes	AF 48hpi	Up	1.85E-05
RxLR	PITG_13047	Yes	AF 48hpi	Up	0.000161
RxLR	PITG_13048	Yes	AF 48hpi, PB 24hpi, & PB 48hpi	Up	0.000114
RxLR	PITG_13093	Yes	AF 48hpi, & SW 48hpi	Up	1.62E-05
RxLR	PITG_13452	Yes	AF 48hpi, PB 48hpi, SW 24hpi, & SW 48hpi	Down in PB 48 hpi	8.94E-06
RxLR	PITG_13509	Yes	SW 24hpi	Up	0.000142
RxLR	PITG_13529	Yes	PB 24hpi	Up	0.00458
RxLR	PITG_13543	Yes	AF 48hpi	Up	0.0291
RxLR	PITG_14054	Yes	AF 48hpi	Up	0.000257
RxLR	PITG_14093	Yes	AF 48hpi, SW 24hpi, & SW 48hpi	Up	0.000228
RxLR	PITG_14294	Yes	SW 48hpi	Up	0.000174
RxLR	PITG_14360	Yes	PB 48hpi, & SW 24hpi	Down in PB 48 hpi	3.26E-06

Table 5.2 **(Continued)**

Description	Primary accession	Secreted	Detected in	Expression	P-value
RxLR	PITG_14662	Yes	AF 48hpi	Up	5.00E-05
RxLR	PITG_14684	Yes	AF 48hpi	Up	0.00146
RxLR	PITG_14782	No	SW 24hpi, & SW 48hpi	Up	0.000136
RxLR	PITG_14783	Yes	AF 48hpi, PB 48hpi, SW 24hpi, & SW 48hpi	Down in PB 48 hpi	2.30E-05
RxLR	PITG_14787	Yes	AF 48hpi, PB 48hpi, SW 24hpi, & SW 48hpi	Down in PB 48 hpi	7.09E-06
RxLR	PITG_14788	Yes	PB 48hpi, SW 24hpi, & SW 48hpi	Down in PB 48 hpi	2.48E-05
RxLR	PITG_14965	Yes	PB 48hpi	Down	0.0398
RxLR	PITG_14983	Yes	AF 48hpi	Up	0.00281
RxLR	PITG_14984	Yes	AF 48hpi	Up	0.00011
RxLR	PITG_15105	Yes	AF 48hpi	Down	0.000279
RxLR	PITG_15123	Yes	AF 48hpi, PB 24hpi, PB 48hpi, & SW 24hpi	Down in SW 24 hpi	2.10E-05
RxLR	PITG_15125	Yes	AF 48hpi, PB 24hpi, PB 48hpi, & SW 24hpi	Down in SW 24 hpi	6.59E-06
RxLR	PITG_15127	Yes	AF 48hpi, PB 48hpi, & SW 24hpi	Down in SW 24 hpi	0.000127
RxLR	PITG_15278	Yes	AF 48hpi	Up	1.44E-05
RxLR	PITG_15930	Yes	AF 48hpi	Up	9.27E-05
RxLR	PITG_15940	Yes	AF 48hpi, & SW 48hpi	Up	0.000126
RxLR	PITG_16705	Yes	AF 48hpi	Up	4.49E-05
RxLR	PITG_16713	No	SW 48hpi	Up	0.000455
RxLR	PITG_16726	Yes	AF 48hpi	Up	0.00018
RxLR	PITG_16737	Yes	PB 48hpi, SW 24hpi, & SW 48hpi	Down in PB 48 hpi	1.29E-05
RxLR	PITG_17214	Yes	SW 24hpi, & SW 48hpi	Up	0.000134
RxLR	PITG_17217	Yes	SW 24hpi, & SW 48hpi	Up	0.000303
RxLR	PITG_18325	Yes	AF 48hpi, PB 48hpi, & SW 48hpi	Down in SW 48 hpi	3.86E-06
RxLR	PITG_18405	Yes	SW 24hpi	Up	4.06E-05
RxLR	PITG_18487	Yes	SW 24hpi, & SW 48hpi	Up	0.000184
RxLR	PITG_18609	Yes	AF 48hpi	Up	1.19E-05
RxLR	PITG_19232	Yes	AF 48hpi	Up	0.00269
RxLR	PITG_19655	Yes	AF 48hpi	Up	0.00215
RxLR	PITG_19996	Yes	SW 48hpi	Up	4.28E-05
RxLR	PITG_20144	Yes	AF 48hpi	Up	0.00289
RxLR	PITG_20857	Yes	SW 24hpi, & SW 48hpi	Up	0.000343
RxLR	PITG_20922	No	AF 48hpi	Up	1.48E-06
RxLR	PITG_20940	Yes	SW 24hpi, & SW 48hpi	Up	1.71E-05
RxLR	PITG_21648	No	AF 48hpi	Up	8.97E-05
RxLR	PITG_22089	Yes	AF 24 hpi	Up	0.0026
RxLR	PITG_22375	Yes	AF 48hpi, & PB 48hpi	Up	1.07E-05
RxLR	PITG_22675	Yes	SW 24hpi	Up	8.50E-06
RxLR	PITG_22722	Yes	AF 48hpi	Down	1.86E-05
RxLR	PITG_22724	Yes	SW 24hpi	Up	0.00053
RxLR	PITG_22757	Yes	AF 48hpi, & SW 24hpi	Down in AF 48 hpi	0.000395
RxLR	PITG_22798	Yes	AF 48hpi	Up	6.46E-05
RxLR	PITG_22802	Yes	PB 24hpi, & SW 24hpi	Up	7.03E-05
RxLR	PITG_22804	Yes	AF 48hpi	Up	0.000245
RxLR	PITG_22825	Yes	AF 48hpi	Up	1.93E-05
RxLR	PITG_22894	Yes	SW 24hpi	Up	0.000968
RxLR	PITG_22900	Yes	PB 48hpi	Up	0.00153
RxLR	PITG_22926	Yes	AF 48hpi	Up	0.000293
RxLR	PITG_22945	No	AF 48hpi, & PB 48hpi	Up	3.15E-05
RxLR	PITG_23014	Yes	AF 48hpi, & SW 24hpi	Down in SW 24 hpi	0.000139

Table 5.2 **(Continued)**

Description	Primary accession	Secreted	Detected in	Expression	P-value
RxLR	PITG_23016	Yes	AF 48hpi	Up	2.02E-05
RxLR	PITG_23036	Yes	AF 48hpi	Up	0.000731
RxLR	PITG_23092	Yes	AF 48hpi	Up	0.000161
RxLR	PITG_23129	No	AF 48hpi	Up	0.00556
RxLR	PITG_23137	Yes	SW 24hpi	Up	0.000675
RxLR	PITG_23206	Yes	AF 48hpi	Up	0.000667
RxLR	PITG_23226	Yes	SW 48hpi	Up	0.00721

5.2.6 Gene co-expression during growth of *P. infestans*

5.2.6.1 Sporulation marker (*Cdc14*) co-expressed genes

Ah-Fong *et al*. (2011) previously reported that the *Cdc14* gene is highly expressed in zoospores and sporangia. As this microarray experiment was conducted using *P. infestans* zoospores and zoospore inoculated AF, PB, and SW, it is necessary to identify the transcripts associated with zoospores, in order to more accurately highlight the transcriptome changes in each different growth condition. The microarray revealed that *Cdc14* (PITG_18578) was significantly expressed (up-regulated) in zoospores (30-fold) and decreased to two-fold in AF and PB 24 hpi, and 1.8-fold in SW 24 hpi. Its expression was then significantly down-regulated (less than 0.5-fold) at 48 hpi in AF, PB, and SW (Figure 5.9). These results suggest that this gene is not switched off during hyphal growth in *P. infestans*, or that some residual spores remain in the samples used for the microarray.

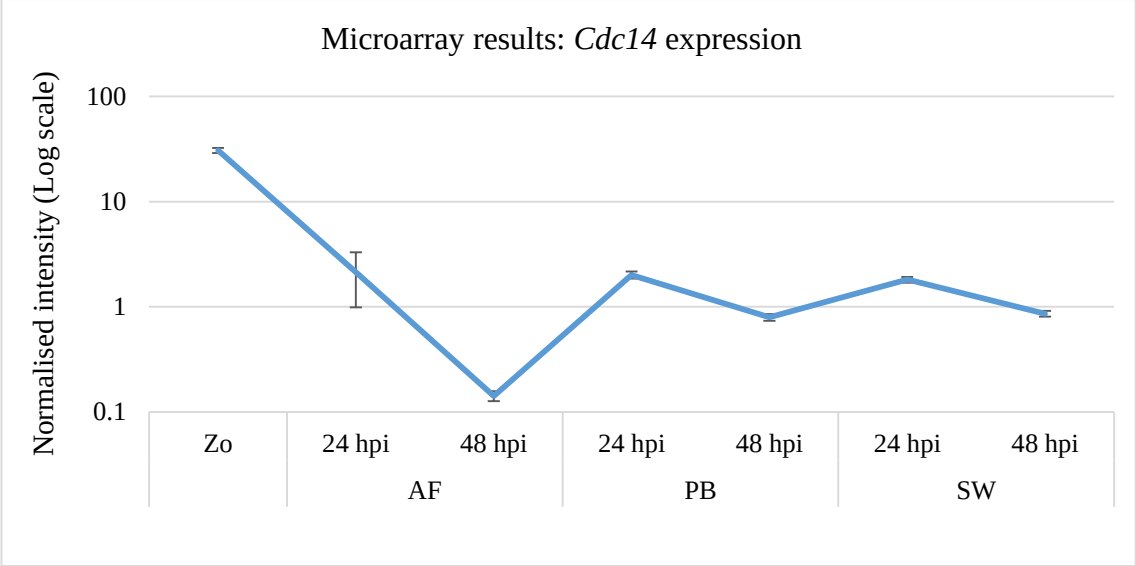

Figure 5.9 Sporulation marker *Cdc14* (PITG_18578) expression profile in Zo, AF, PB, and SW from normalised microarrays (log scale). This graph shows the high expression of *Cdc14* in zoospores compared to inoculation time course in AF, PB, and SW. This gene was most significantly down-regulated at 48 hpi in AF.

Genes co-expressed with sporulation marker *Cdc14* were clustered with a 95% probability rate of correlation coefficient (Figure 5.10). At this level of probability, 813 transcripts were co-expressed with *Cdc14* (Annex 5b). Although 514 transcripts in this set were unannotated CHPs and HPs, out of 299 annotated transcripts, there were significant numbers (45 transcripts) of genes (Figure 5.11) encoding proteins related to *P. infestans* spores, such as sporangia-induced proteins, cleavage-induced proteins, and the spore-specific form of a nuclear LIM factor interacting protein (Judelson *et al*., 2008). In addition, the gene encoding *PiGPA1* (PITG_03612), previously reported as an essential factor of zoospore motility and virulence in *P. infestans* (Latijnhouwers *et al*., 2004; Dong *et al*., 2004) was also highly up-regulated (20-fold) in zoospores and represented in the *Cdc14*-co-expressed set with the correlation coefficient of 0.98.

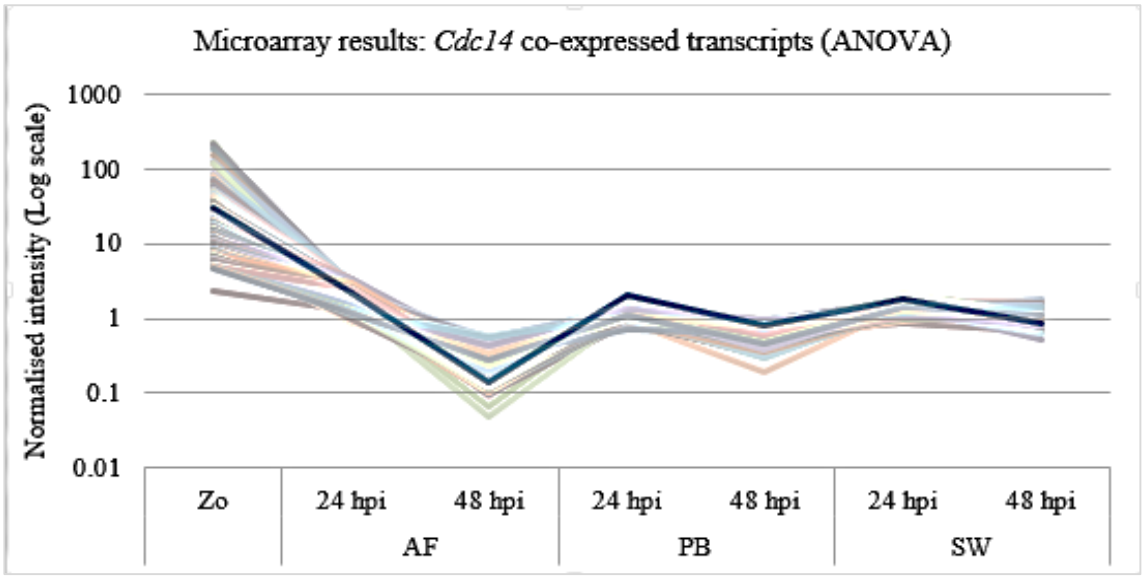

Figure 5.10 Expression (normalised intensity) of sporulation marker *Cdc14* (highlighted in blue) and co-expressed (95% probability; non-highlighted) genes in zoospores, AF (24 and 48 hpi), PB (24 and 48 hpi), and SW (24 and 48 hpi) (log scale) extracted from the microarray results (ANOVA). These genes are up-regulated in zoospores and down-regulated during the inoculation time course in AF, PB, and SW.

Out of 813 transcripts co-expressed with *Cdc14*, 7.9% (65 transcripts) comprised secreted proteins which included transcripts for six RxLR effector candidates, two transcripts each for elicitors, CWDEs, and SCR74 cysteine rich proteins, and one transcript each for a CRN effector, NLP, and an enzyme inhibitor (Figure 5.11). Signal peptides were predicted for 30 CHPs.

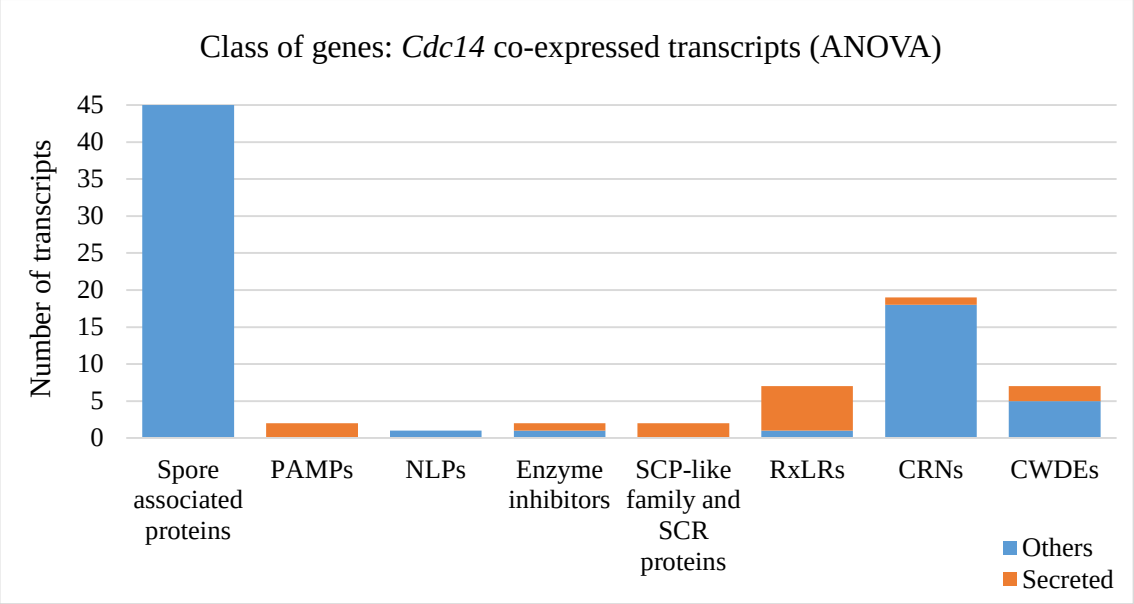

Figure 5.11 Class of differentially expressed genes co-expressed with *Cdc14* (PITG_18578). A high number (45 transcripts) of spore associated transcripts were co-expressed with *Cdc14*. The next largest group of co-expressed transcripts (19 transcripts) encoded CRN effectors. Some RxLR effectors and CWDEs also appeared to be co-expressed with *Cdc14*. Two transcripts each for elicitors, enzyme inhibitors and SCP-like extracellular proteins were also detected in this list. Blue represents non-secreted proteins while orange refers to secreted proteins.

5.2.6.2 Biotrophic marker (*Hmp1*) co- expressed genes

The biotrophy marker gene, haustorial membrane protein 1 (*Hmp1*) (PITG_00375) gene from *P. infestans* was assessed to investigate its expression profile during all sample conditions. Results from the flag value analysis revealed 'Present' in all samples but volcano plot analysis did not show significant up-regulation or down-regulation in any sampled condition (Figure 5.12).

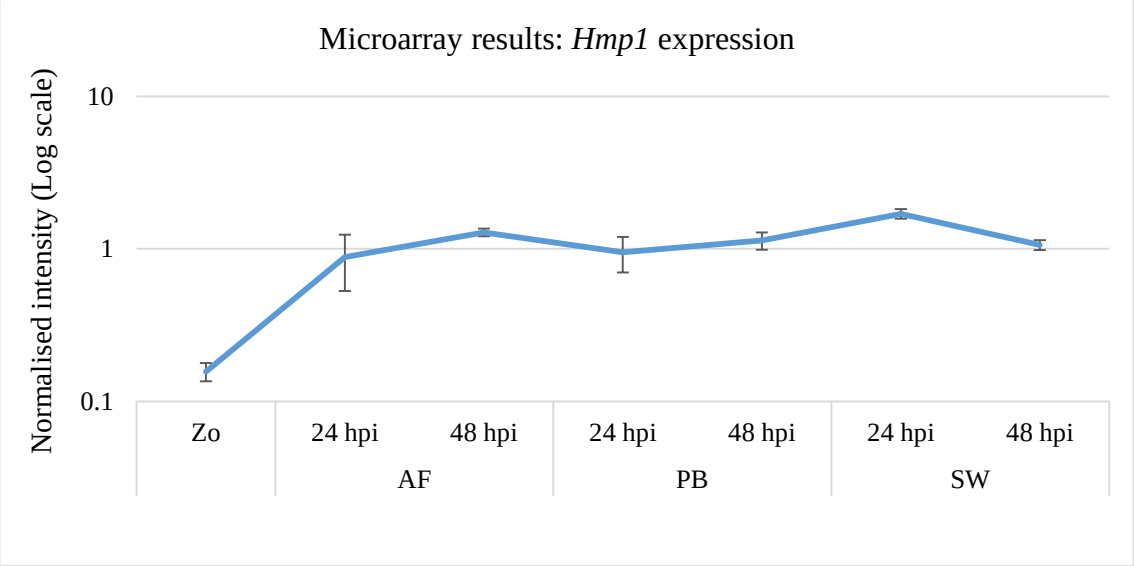

Figure 5.12 Expression profile of biotrophy marker gene *Hmp1* (PITG_00375) in zoospores, and growth in AF, PB, and SW (log scale; normalised microarray data). Expression of *Hmp1* was significantly down-regulated in zoospores and appeared to be slightly induced at AF 48 hpi, and SW 48 hpi. This gene was slightly down-regulated at AF 24 hpi, PB 24 and 48 hpi, and SW 48 hpi.

Since haustorium-like structures are occasionally formed during growth in AF, and *Hmp1* is associated with haustoria, it is important to identify the genes co-expressed with this marker of biotrophy. A set of *Hmp1* co-expressed genes (288 transcripts) (Annex 5b) were extracted from the differentially expressed set of genes from the microarray results using the default setting of 95% probability rate (Figure 5.13). The majority of *Hmp1* co-expressed transcripts (146 transcripts) were unannotated CHPs and HPs. Among 142 annotated transcripts, 20 encoded RxLR effectors, including five transcripts for the PexRD2 (PITG_11350, PITG_11383, PITG_11384, PITG_21422, and PITG_22935) family. RxLR effectors such as PITG_04089 (Zheng *et al*., 2014) were also co-expressed with *Hmp1*. Other transcripts such as elicitors (four transcripts), enzyme inhibitors (three transcripts), and a CRN effector and a small cysteine rich protein (one transcript each) were also found to be co-expressed with *Hmp1*. A transcript for cellulose synthase 4 (PITG_16984) was co-expressed with *Hmp1*, suggesting the formation of infection structures such as appressoria (Grenville-Briggs *et al*., 2008) in apoplastic fluid. No

spore-related transcripts were co-expressed with *Hmp1*. Gene class analysis (Figure 5.14) of genes co-expressed with *Hmp1* revealed the majority (19 transcripts) were possibly not related to biotrophic interaction with host, as these effectors were not detected during leaf infection. However, one transcript of an RxLR (PITG_22648) was co-expressed with *Hmp1* in both apoplastic fluid and during leaf infection, suggesting this effector might be involved in pre- and early biotrophic stages. The 20 transcripts of effectors were also induced in SW at 24 hpi indicating that these are potentially generally necessary for cyst germination, or they encode proteins required in the earliest stage of infection.

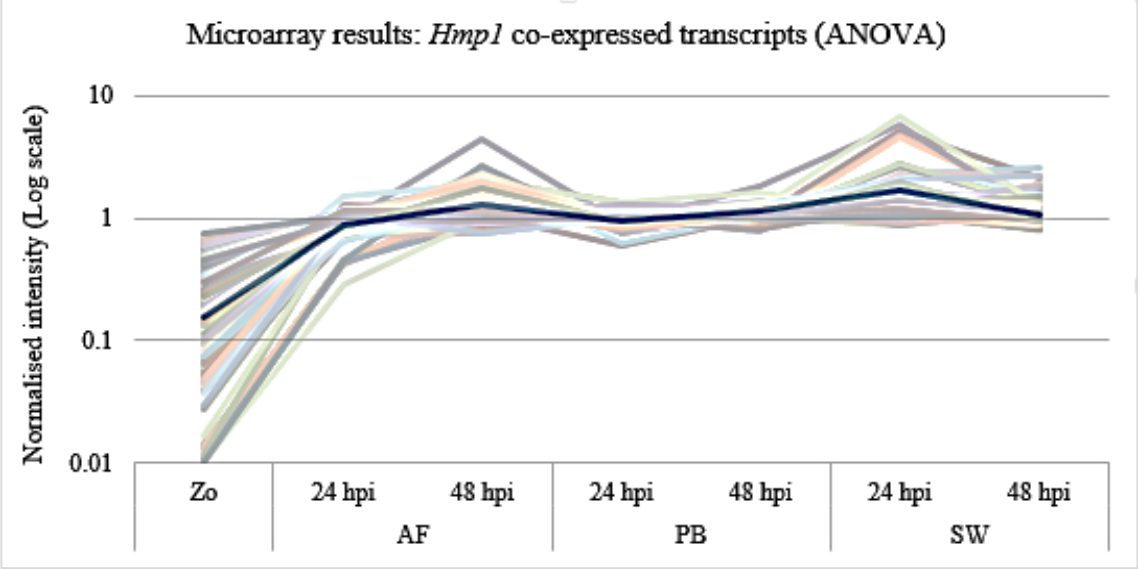

Figure 5.13 Expression profile of transcripts derived from microarray results of zoospores, and growth in AF, PB, and SW (log scale). Expression (normalised intensity) of *Hmp1* (biotrophy marker gene, highlighted) and co-expressed (95% probability; non-highlighted) genes in zoospores, AF (24 and 48 hpi), PB (24 and 48 hpi), and SW (24 and 48 hpi) (log scale) extracted from the microarray results (ANOVA). These genes are down-regulated in zoospores.

Out of 288 transcripts co-expressed with *Hmp1*, 19.8% (57 transcripts) comprised secreted proteins which included 20 RxLR effectors, followed by enzyme inhibitors (three transcripts), elicitors (two transcripts), and SCRs (one transcript) (Figure 5.14). Transcripts for 18 CHPs were predicted to encode secreted proteins.

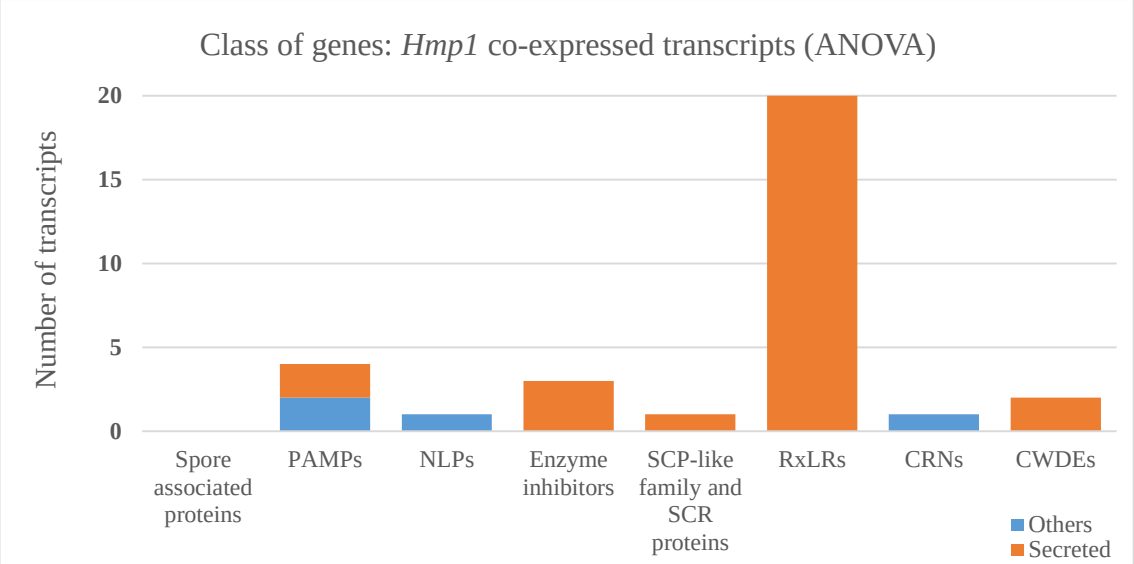

Figure 5.14 Class of differentially expressed genes co-expressed with *Hmp1* (PITG_00375) in Zo, and *P. infestans* grown in AF, PB, and SW. 20 transcripts for cytoplasmic RxLR effectors were co-expressed with *Hmp1*. Four transcripts for elicitors, and three transcripts for protease inhibitors were detected in the list. There was one transcript each for a CRN effector and a SCR protein also co-expressed with *Hmp1*. All of the RxLR effectors and enzyme inhibitors co-expressed with Hmp1 were secreted proteins (blue represents non-secreted proteins while orange refers to secreted proteins).

5.2.6.3 Avirulence gene *Avr3a* co-expressed genes

P. infestans gene *Avr3a* is one of the best characterised cytoplasmic effectors (Armstrong *et al.*, 2005) and reported to be secreted from haustoria (Whisson *et al.*, 2007). In this microarray analysis, *Avr3a* was induced at 24 hpi and was significantly (2.9-fold) up-regulated at 48 hpi during growth in AF. This gene was not significantly induced (less than two-fold) in PB. *Avr3a* was found to be down-regulated at 24 and 48 hpi during growth in SW (Figure 5.15).

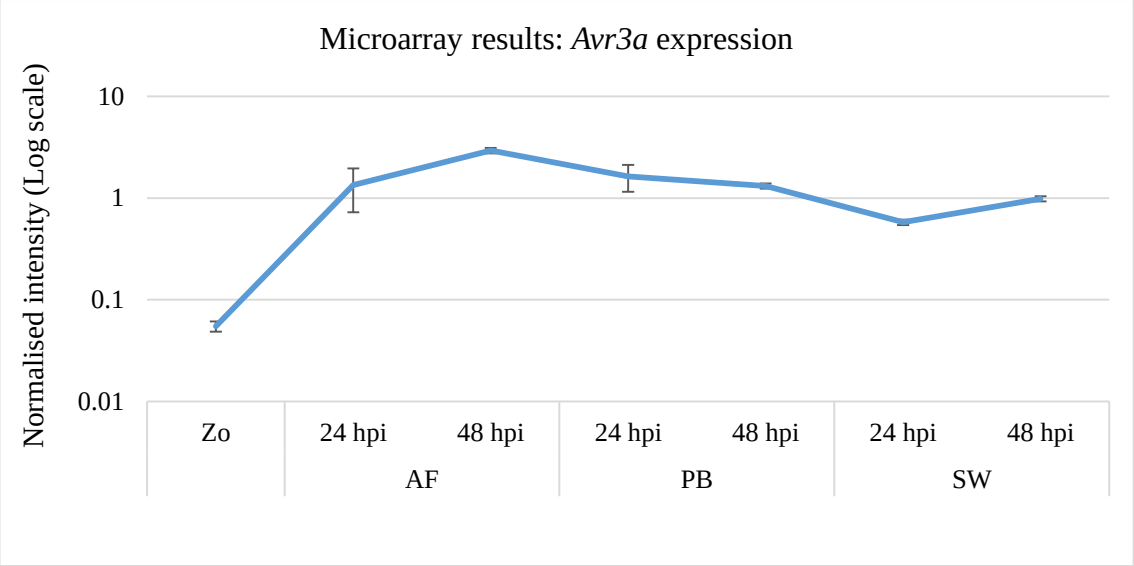

Figure 5.15 Expression profile for avirulence gene *Avr3a* (PITG_14371) in zoospores, and growth in AF, PB, and SW (log scale; normalised microarray data). Expression of *Avr3a* was significantly down-regulated in zoospores compared to up-regulation in AF at 48 hpi. This gene was slightly down-regulated at SW 24 and 48 hpi.

Although the biotrophy marker gene *Hmp1* was not significantly (two-fold or more) up-regulated in AF, PB, or SW, cytoplasmic effector *Avr3a*, secreted through haustoria (Whisson *et al*., 2007), was significantly up-regulated at 48 hpi in AF. This indicates that expression of this effector is potentially enhanced by signals present in the plant apoplast. Therefore, it was important to identify the genes co-expressed with this avirulence marker gene in order to discover the group of genes that are also induced in the same way. This might lead to the understanding of pathogen behaviour in establishing biotrophic relations with host plants.

A set of *Avr3a* co-expressed genes (416 transcripts) (Annex 5b) were identified from the differentially expressed genes from the microarray results using the default setting of 95% probability rate (Figure 5.16). The largest group of *Avr3a* co-expressed transcripts (186 transcripts) were unannotated CHPs and HPs. Gene class analysis (Figure 5.17) showed that, out of 216 annotated transcripts, 51 encoded RxLR effectors co-expressed with *Avr3a*. These included well characterised effectors *Avr2* (PITG_08943), *Avr4*

(PITG_07387), *Avrblb2* (PITG_20301), and *Avr10* (PITG_11484), with the correlation coefficient of 0.97 for each of *Avr2*, *Avr4*, and *Avrblb2*, and 0.98 for *Avr10*. Five transcripts of RxLRs (PITG_04167, PITG_04178, PITG_14363, PITG_14374, and PITG_23016), including two related transcripts of *Avr3a* paralogs (PITG_14363 and PITG_14374), were highly co-expressed (correlation coefficient of 1) with *Avr3a*. Other transcripts that were co-expressed with *Avr3a* included apoplastic effectors (*SCR74* cysteine-rich protein PITG_14645, protease inhibitors *Epi1* and *Epi6* [PITG_22681 and PITG_05440 respectively]), and PAMPs (elicitin-like protein encoding genes such as *INF1*, *INF4*, and *INF6* [PITG_12551, PITG_21410, and PITG_12556 respectively], and transglutaminase elicitor-like protein [PITG_22117]). Interestingly, a transcript encoding a necrosis-inducing protein *NPP1* (PITG_09716) (highlighted as necrotrophy marker gene in Chapter 3) was also co-expressed with *Avr3a*.

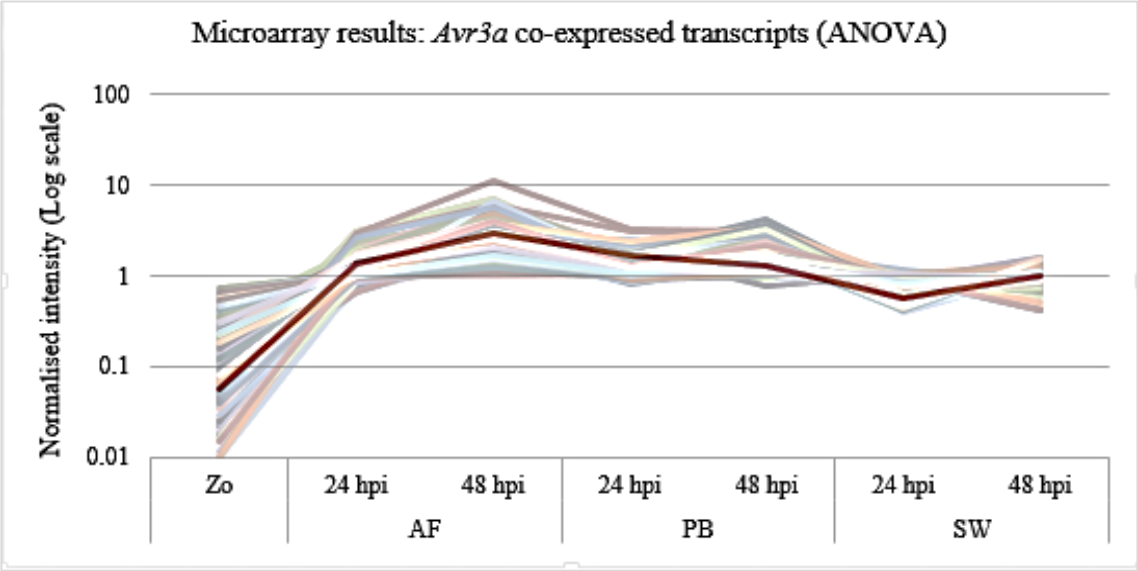

Figure 5.16 Expression profile of *Avr3a* (highlighted) co-expressed (95% probability, non-highlighted) genes derived from microarray results of zoospores (Zo), and growth in apoplastic fluid (AF), pea broth (PB), and sterile distilled water (SW) (log scale). These genes are down-regulated in zoospores, and up-regulated at 48 hpi in AF compared to PB, and SW.

Out of 402 transcripts co-expressed with *Avr3a*, 25.12% (101 transcripts) encoded predicted secreted proteins which included 49 RxLR effectors (out of 51 transcripts), followed by elicitors (five out of eight transcripts), NLPs (three out of four) and enzyme inhibitors (two out of three transcripts) (Figure 5.17). 19 transcripts for CHPs were predicted to encode secreted proteins. One transcript for SCR, and two transcripts of CWDEs co-expressed with *Avr3a* were not secreted proteins.

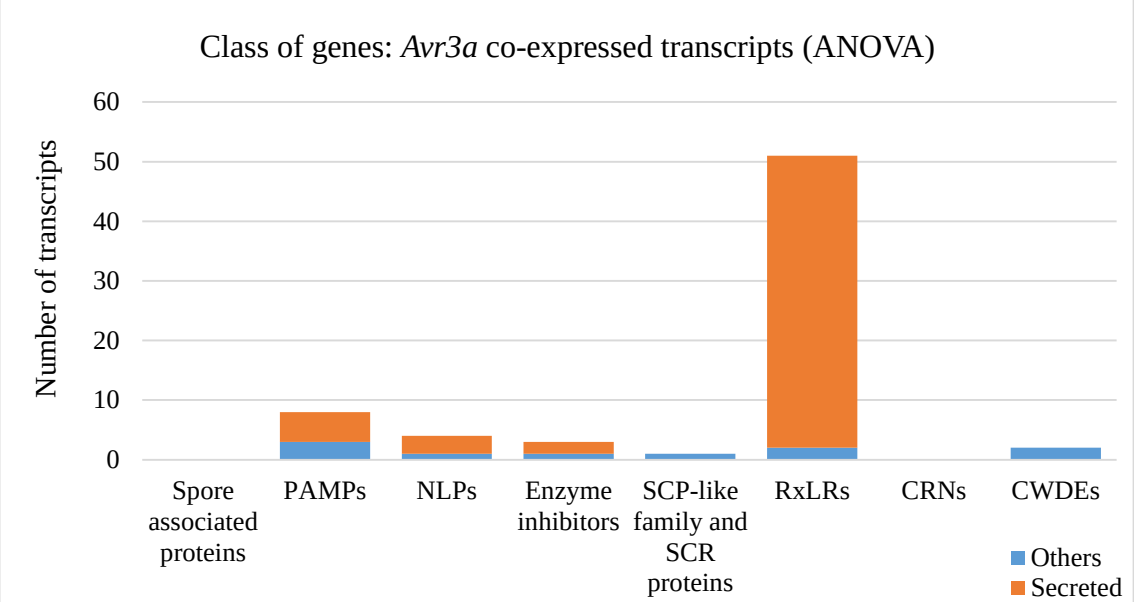

Figure 5.17 Differentially expressed genes, annotated as infection-related, that are co-expressed with *Avr3a* (PITG_14371). A high number (51 transcripts) of cytoplasmic RxLR effectors were co-expressed with *Avr3a*. Four transcripts for elicitors, and three transcripts for protease inhibitors, and one transcript each for an SCR protein (non-secreted) were also co-expressed with *Avr3a*. Transcripts encoding secreted protein (blue represents non-secreted proteins while orange refers to secreted proteins) showed that most of the RxLR effectors, enzyme inhibitors, and NLPs detected were predicted secreted proteins.

5.2.7 Quantitative RT-PCR (QRT-PCR) validation of microarray expression profiles

5.2.7.1 Selection and validation of differentially expressed genes significantly up-regulated in Zo, AF, PB, and SW

Microarray validation was conducted using genes which were significantly and differentially expressed in one of the following: zoospores, AF, PB, and SW. QRT-PCR

was carried out on cDNA samples prepared from total RNA isolated from *P. infestans* samples as described in methods Chapter 2. Selected genes from the microarray results in this chapter were validated using QRT-PCR (Table 5.3). The *P. infestans* actin A gene (*ActA*) was used as a constitutively expressed endogenous control for expression normalisation. The levels of expression of each gene were compared to sporangia (set at the relative expression value of 1).

Table 5.3 List of genes selected from the microarray results of differentially expressed genes in Zo, AF, PB, and SW, and QRT-PCR validation results. Zo = zoospores, AF = apoplastic fluid, PB= pea broth, SW= sterile distilled water, Up = up-regulated.

Primary accession	Description	Microarray expression	Co-expressed with	QRT-PCR validation
PITG_07134	*ABC transporter*	Up in AF	None	Validated
PITG_13063	*purine-cytosine permease*	Up in AF	None	Validated
PITG_13661	*transmembrane protein*	Up in AF	None	Validated
PITG_02860	*RxLR*	Up in AF and PB	*Avr3a*	Validated
PITG_10396	*RxLR*	Up in AF and PB	*Avr3a*	Validated
PITG_22375	*RxLR*	Up in AF and PB	*Avr3a*	Validated
PITG_16866	*NPP1*	Up in AF and PB	None	Validated
PITG_14787	*RxLR*	Up in AF and SW	None	Validated
PITG_07283	*threonine dehydratase catabolic*	Up in PB	None	Validated
PITG_11940	*Chitin-binding protein*	Up in SW	None	Validated
PITG_22916	*NPP1*	UP in SW	None	Validated
PITG_11239	*LIM factor-spore specific*	Up in Zo	None	Validated
PITG_18428	*cleavage induced protein*	Up in Zo	None	Validated
PITG_18578	*Cdc14*	Up in Zo	*Cdc14*	Validated

Fourteen differentially expressed transcripts were either specific or highly expressed in one or more of the Zo, AF, PB, and SW samples. Sporulation marker gene *Cdc14* was down-regulated in AF, PB, and SW and highly up-regulated in Zo. Similarly, spore associated proteins such as LIM factor (PITG_11239), and a cleavage induced protein (PITG_18428) also validated the microarray results (Figure 5.18). Out of four RxLR effectors selected for validation, three (PITG_02860, PITG_10396, and PITG_22375) were validated as co-expressed with *Avr3a* (Figure 5.19). One RxLR effector (PITG_14787) was validated as highly up-regulated in AF and SW compared to PB

(Figure 5.20). Genes encoding an ABC transporter, purine-cytosine permease, and a transmembrane protein (PITG_07013, PITG_13063, and PITG_13661, respectively) were validated as specific to AF and were highly up-regulated during growth in AF (Figure 5.21). For example, transmembrane protein PITG_13661 was 6-fold up-regulated at 24 hpi in AF followed by 12-fold at 48 hpi, but were down-regulated in PB, and in SW. A similar expression pattern was observed for the ABC transporter and purine-cytosine permease. The enzyme threonine dehydratase (PITG_07283) was specifically and significantly up-regulated during growth in PB (Figure 5.22). The NLP family protein NPP1- like protein (PITG_16866) was up-regulated in AF and PB. Although this gene was not significantly up- or down-regulated in SW according to the microarray results, QRT-PCR validation results revealed that it is also up-regulated in SW, although the level of expression in SW was comparatively lower than in AF and PB (Figure 5.23). Although the precise biological function of the gene encoding a chitin-binding protein (PITG_11940) in *P. infestans* is unknown, this transcript is highly up-regulated in SW. Transcript encoding a different NLP (PITG_22916) was also significantly up-regulated in SW compared to down-regulation in AF and PB (Figure 5.24).

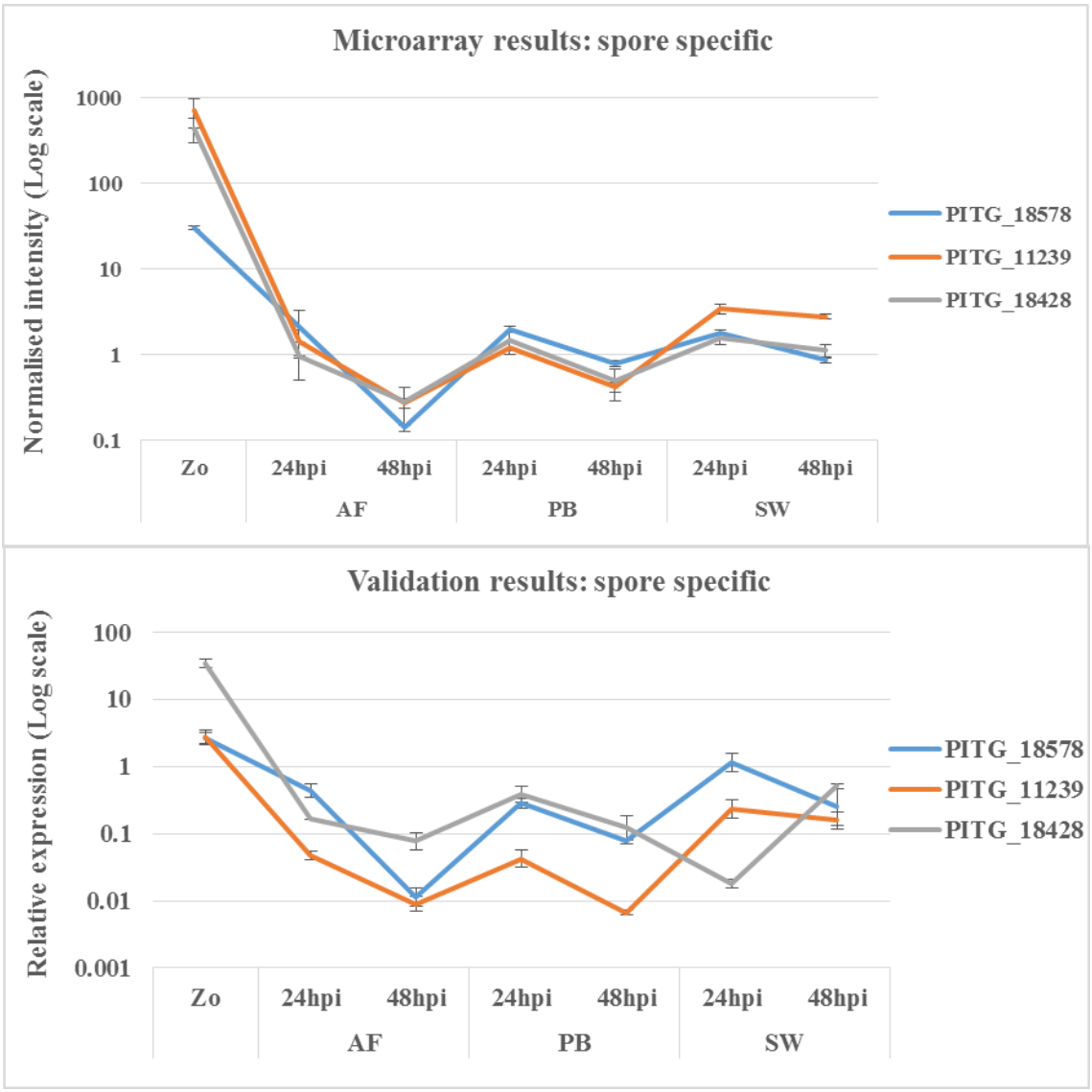

Figure 5.18 Microarray results (left) and QRT-PCR validation (right) of sporulation marker gene *Cdc14* (PITG_18578), and transcripts encoding spore associated proteins such as nuclear LIM factor interactor (PITG_11239), and cleavage induced protein (PITG_18428). All of the genes in the figure showed up-regulation in zoospores, compared to down-regulation during growth in apoplastic fluid (AF), pea broth (PB), and sterile distilled water (SW).

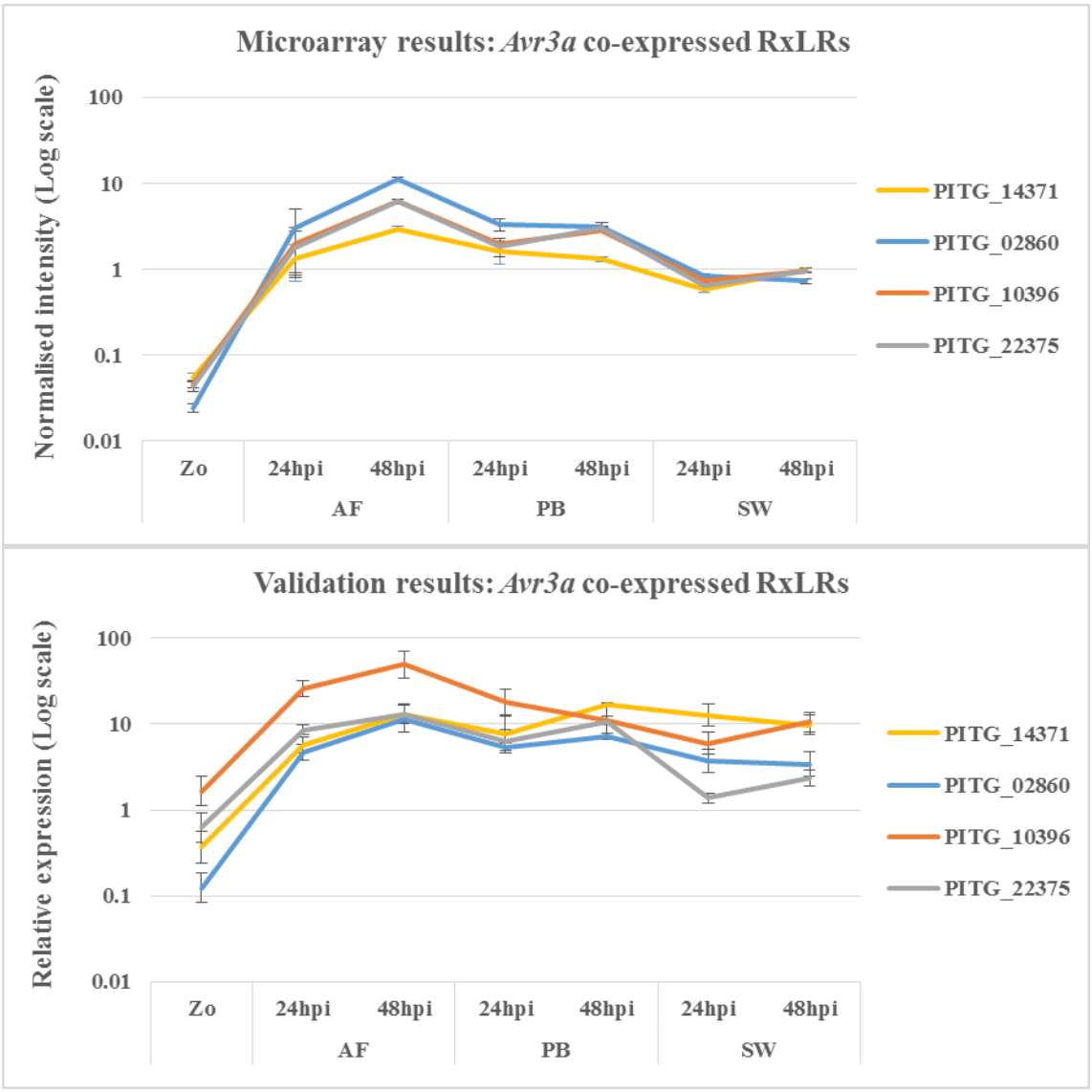

Figure 5.19 Microarray results (upper graph) and QRT-PCR validation (lower graph) of secreted RxLR effectors (PITG_02860, PITG_10396, and PITG_22375). These genes were co-expressed with avirulence gene *Avr3a* (PITG_14371). All of the genes in the figure showed down-regulation in zoospores compared to up-regulation during growth (24, and 48 hpi) in apoplastic fluid (AF) and pea broth (PB). Comparatively low expression was observed during growth in sterile distilled water (SW).

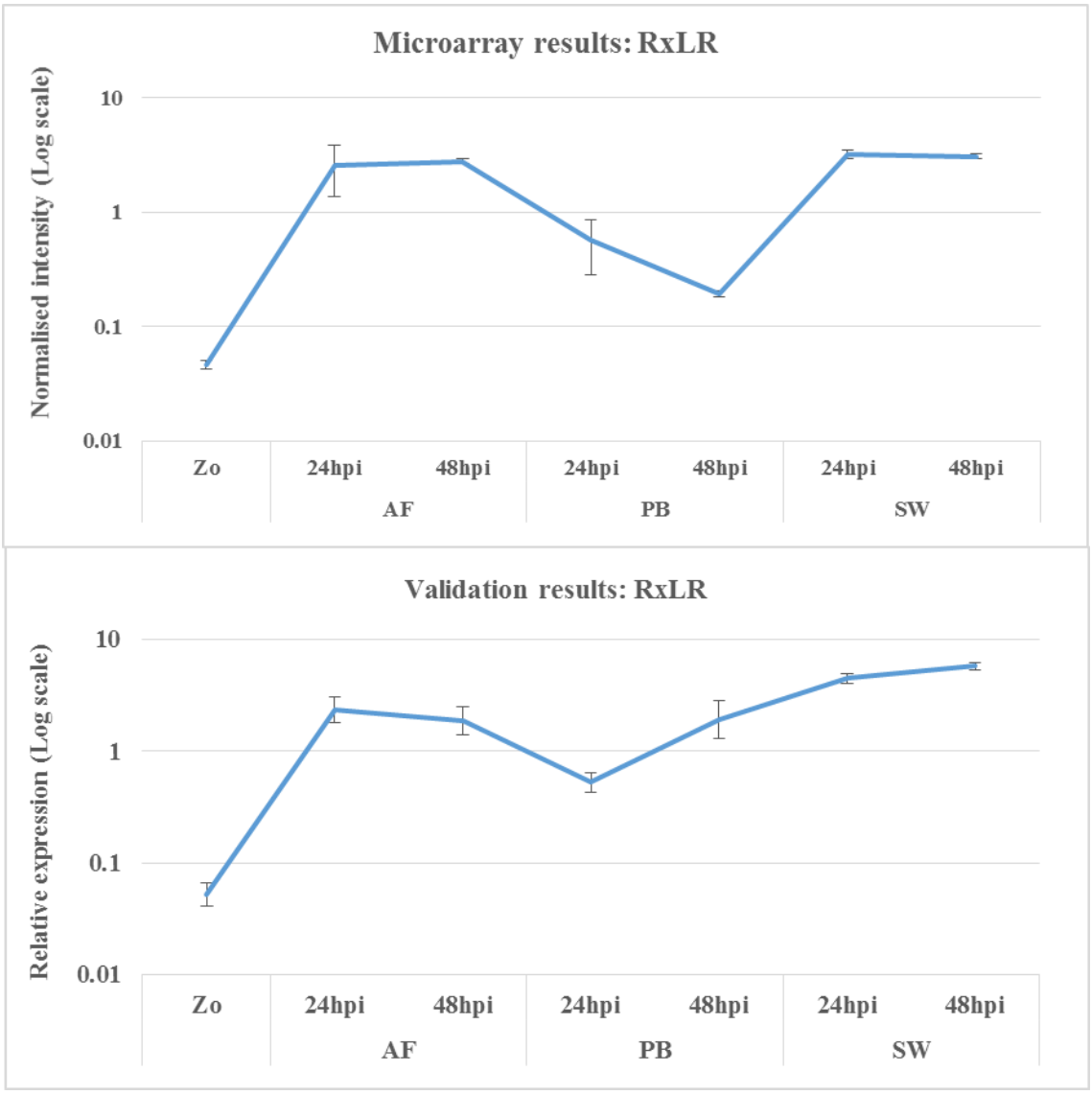

Figure 5.20 Microarray results (upper graph) and QRT-PCR validation (lower graph) of secreted RxLR effector (PITG_14787). This RxLR effector was up-regulated during growth in apoplastic fluid (AF) and sterile distilled water (SW) compared to down-regulated during growth in pea broth (PB).

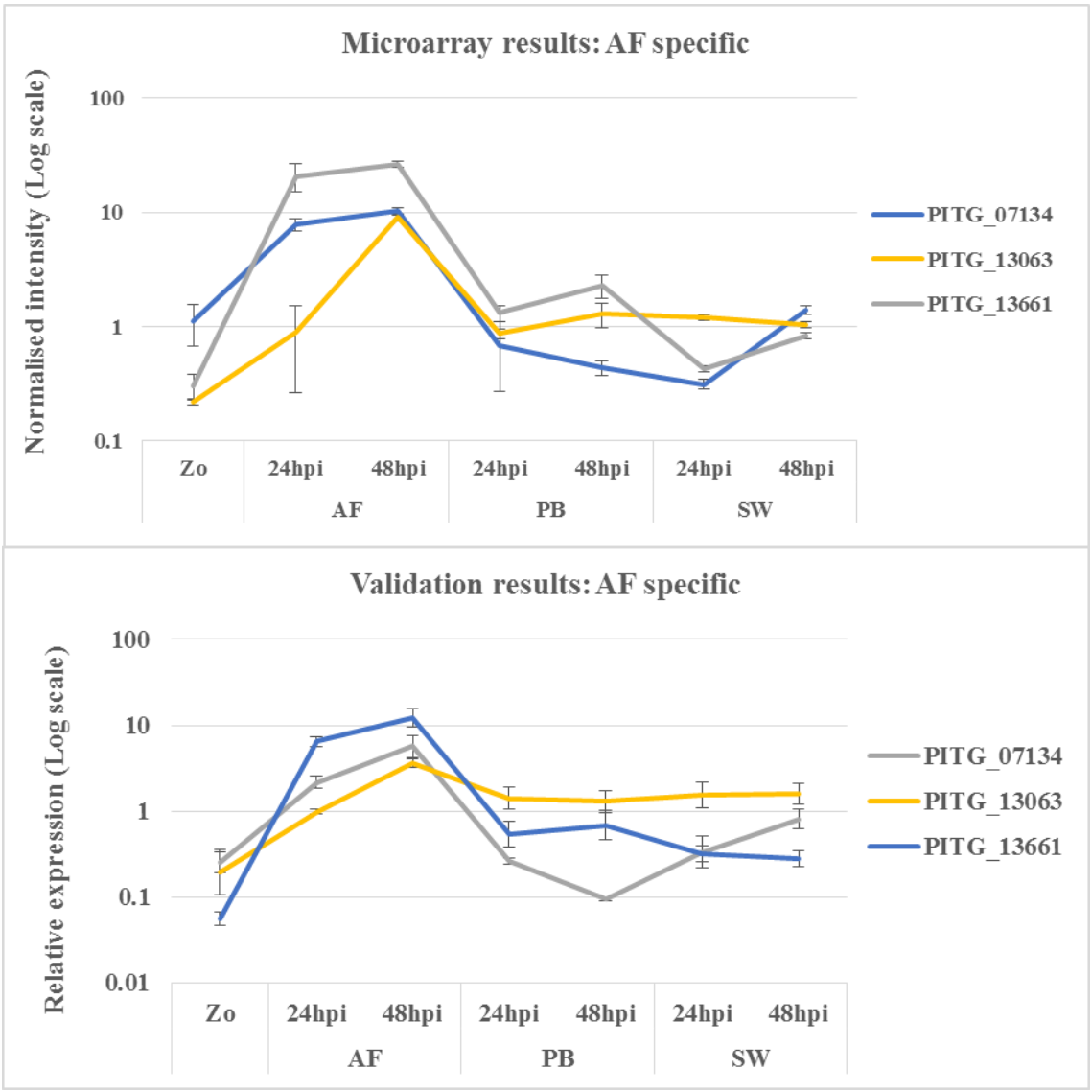

Figure 5.21 Microarray results (upper graph) and QRT-PCR validation (lower graph) of selected transcripts encoding an ABC transporter (PITG_07134), a purine-cytosine permease (PITG_13063), and a transmembrane protein (PITG_13661). These genes showed up-regulation during growth in apoplastic fluid (AF), compared to down-regulation during growth in pea broth (PB), and sterile distilled water (SW).

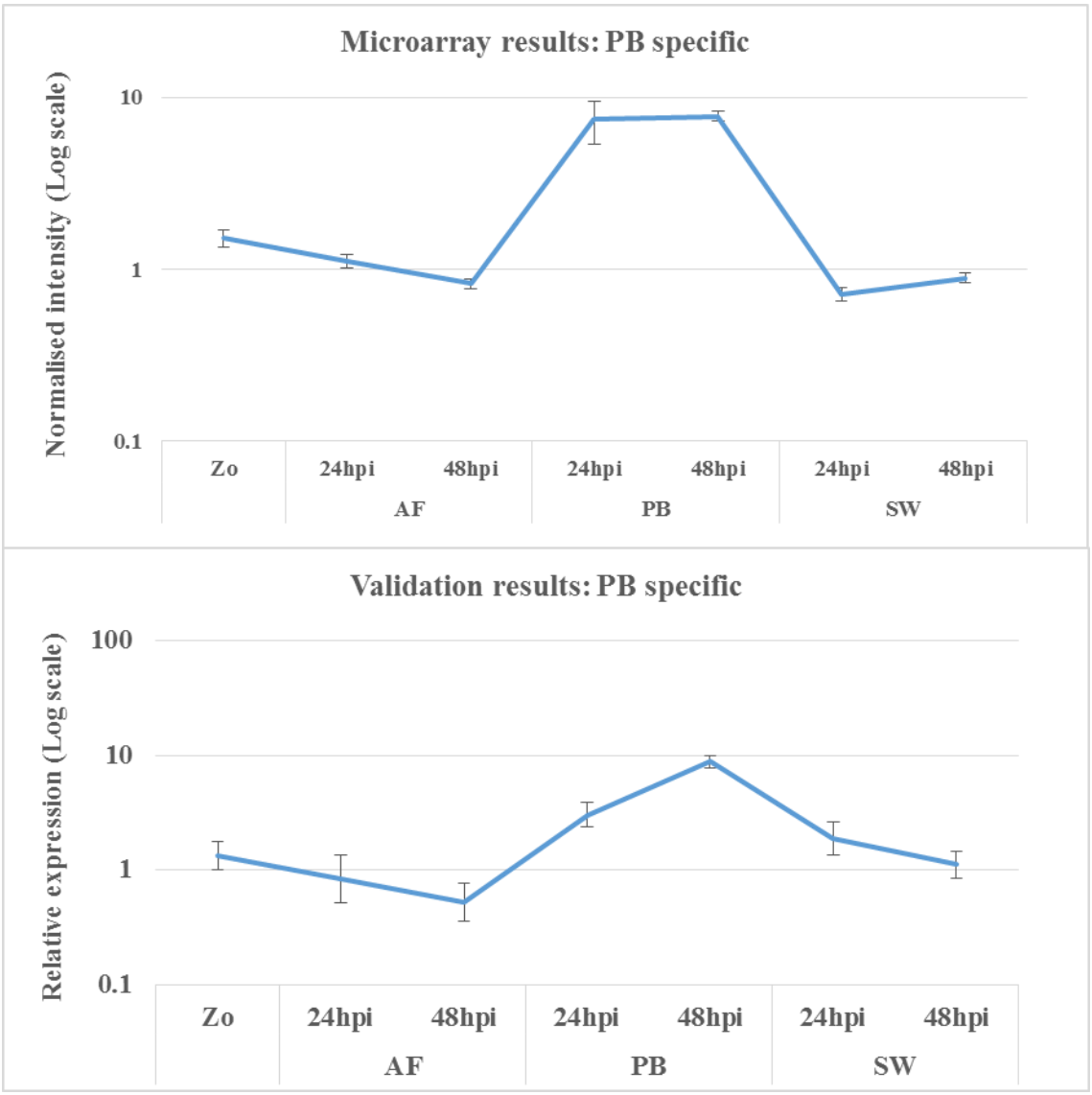

Figure 5.22 Microarray results (upper graph) and QRT-PCR validation (lower graph) of catabolic enzyme, threonine dehydratase (PITG_07283) expression. The gene was significantly up-regulated in pea broth (PB) compared to down-regulated in apoplastic fluid (AF), and pea broth (PB).

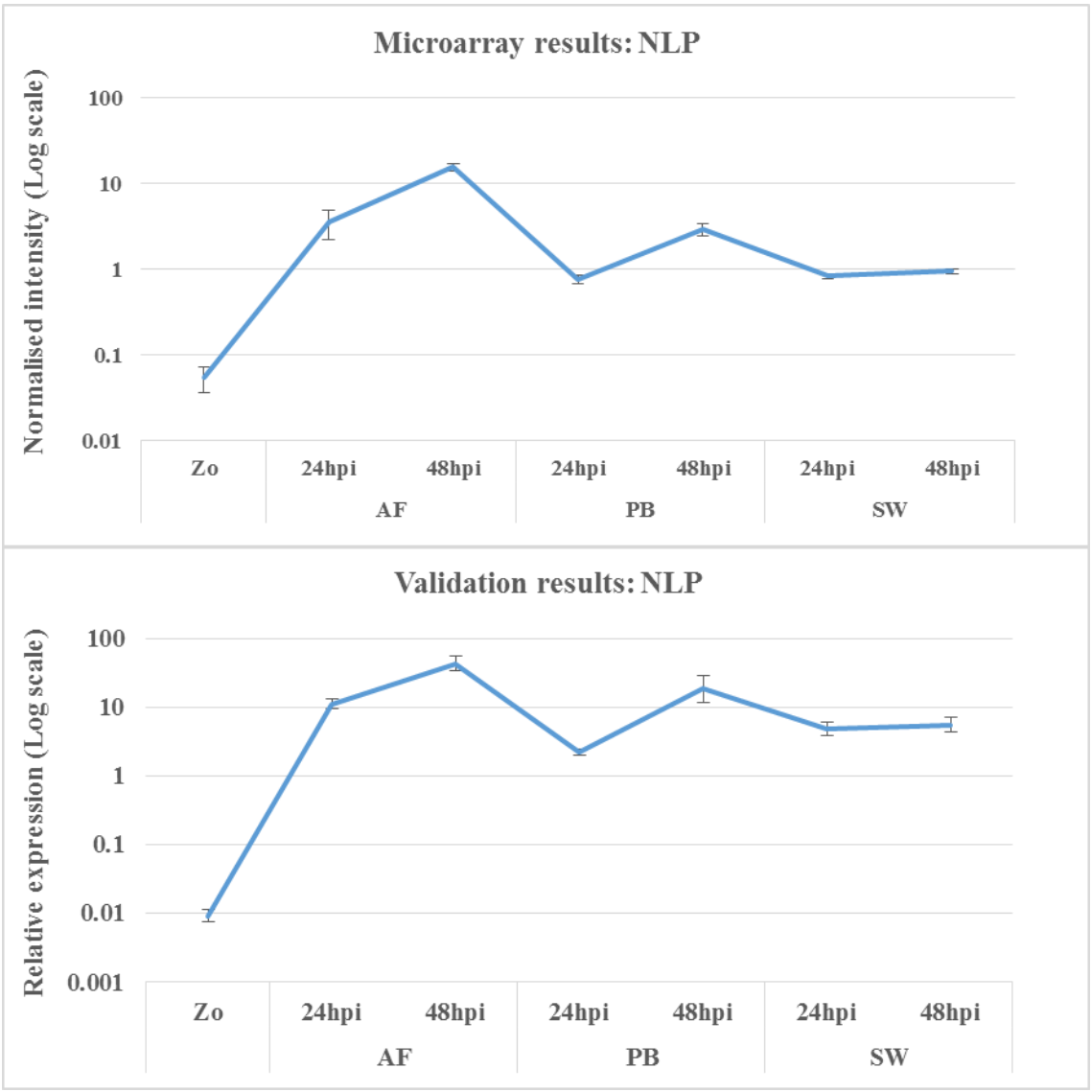

Figure 5.23 Microarray results (upper graph) and QRT-PCR validation (lower graph) of an NLP (PITG_16866) gene expression. A similar expression profile was observed in apoplastic fluid (AF), pea broth (PB), and sterile distilled water (SW) interaction, although the relative expression levels were typically higher for the QRT-PCR analysis.

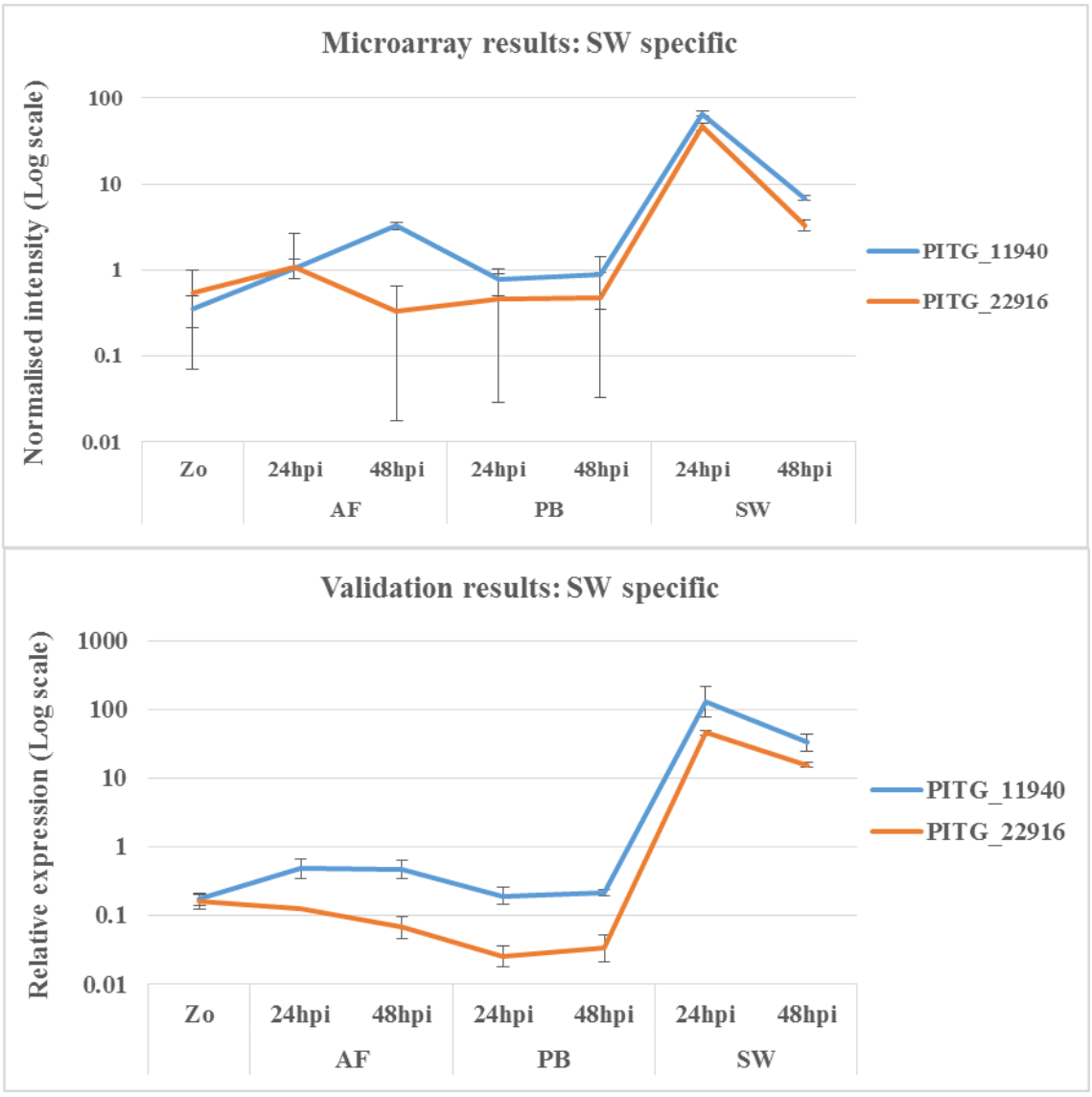

Figure 5.24 Microarray results (upper graph) and QRT-PCR validation (lower graph) of chitin-binding protein (PITG_11940), and a necrosis inducing protein (NLP) (PITG_22916) expression. Both genes showed up-regulation in sterile distilled water (SW) compared to down-regulation during growth in apoplastic fluid (AF), and pea broth (PB).

5.2.7.2 Expression analysis (QRT-PCR) of genes differentially expressed during growth in AF, PB, and SW compared with leaf and tuber infection

Out of 14 transcripts used for AF, PB, and SW microarray validation, eight transcripts were assessed for gene expression comparison with leaf and tuber infection. In this list there were four transcripts for RxLR effectors (PITG_02860, PITG_10396, PITG_14787, and PITG_22375), and one transcript each for sporulation marker (*Cdc14*) (PITG_18578), ABC transporter (PITG_07134), transmembrane protein (PITG_13661),

and an NLP (PITG_22916). The expression of two RxLR effectors (PITG_02860 and PITG_14787) highly up-regulated in AF compared to PB and SW, were comparatively highly up-regulated in leaf infection and tuber infection. However, the expression levels of the other two RxLRs (PITG_10396 and PITG_22375) were comparatively lower than in AF (Figure 5.25).

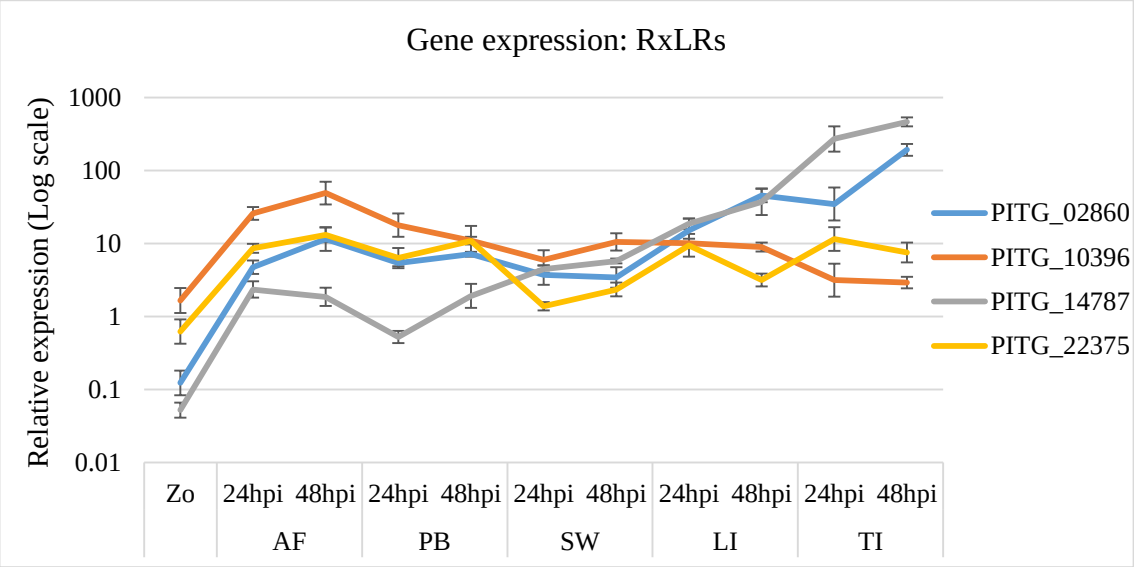

Figure 5.25 Relative expression of RxLR effectors during growth in apoplastic fluid (AF), pea broth (PB), and sterile distilled water (SW), in comparison to leaf (LI) and tuber (TI) infection (24 and 48 hpi). Two patterns of gene expression were observed during *in planta* infection; PITG_02860 and PITG_14787 were more highly expressed *in planta* compared to PITG_10396, and PITG_22375.

Sporulation marker gene, *Cdc14* (PITG_18578) was down-regulated during both leaf infection and tuber infection (Figure 5.26), most markedly at 48 hpi. *Cdc14* expression was readily detected at 24 hpi in all samples, probably due to the presence of some un-germinated zoospores or sporangia. However, this gene was down-regulated or non-significantly expressed in all conditions except in Zo compared to sporangia. The genes encoding the ABC transporter (PITG_07134) and a transmembrane protein (PITG_13661) specific to AF from the microarray results/validation were also significantly up-regulated *in planta*. The NLP protein encoding transcript (PITG_22916), which was not detected in the leaf infection microarray was also down-regulated in QRT-

PCR gene expression analysis. However this gene was up-regulated in SW and tuber infection (Figure 5.27).

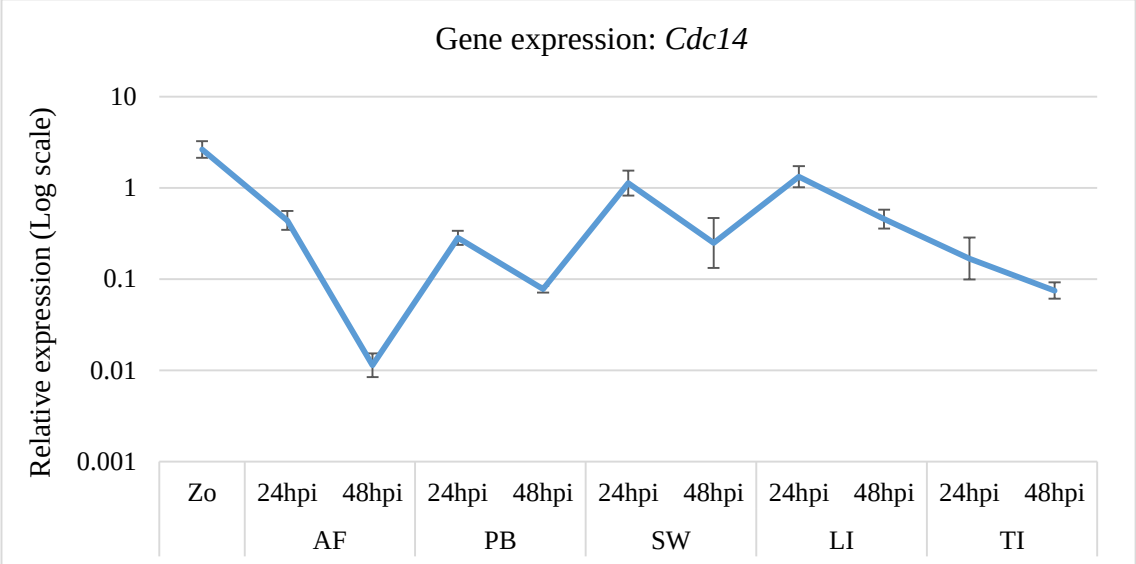

Figure 5.26 Relative expression of *Cdc14* (PITG_18578) in zoospores (Zo), and during growth in apoplastic fluid (AF), pea broth (PB), and sterile distilled water (SW), compared to leaf (LI) and tuber (TI) infection. *Cdc14* was up-regulated in Zo compared to down-regulation in the rest of the samples.

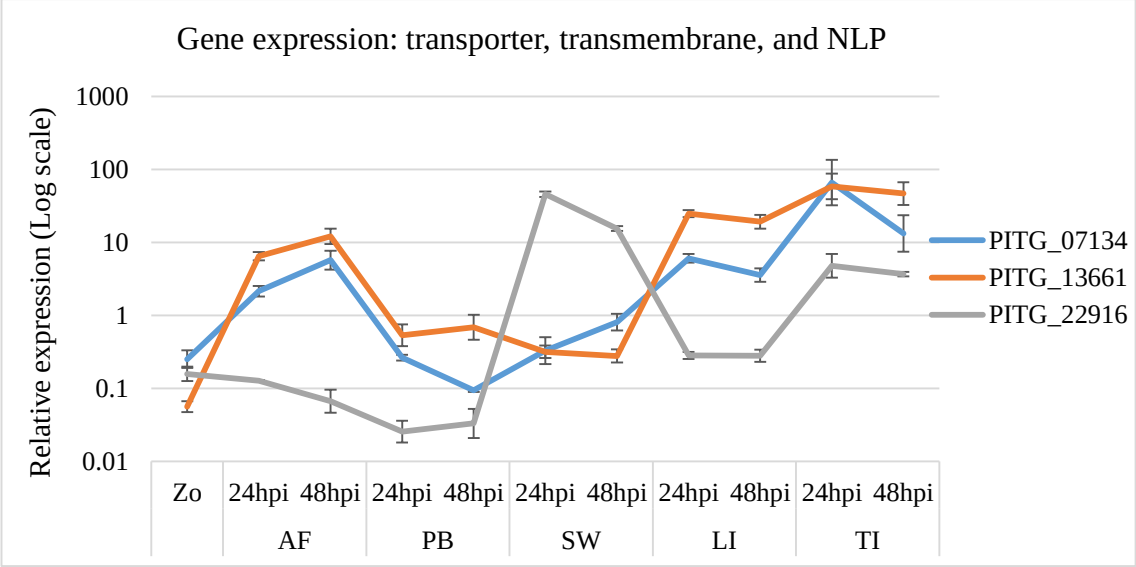

Figure 5.27 Relative expression of transcripts for ABC transporter (PITG_07134), transmembrane protein (PITG_13661), and NPP1 (PITG_22916) during growth in apoplastic fluid (AF), pea broth (PB), and sterile distilled water (SW), in comparison to leaf and tuber infections. PITG_07134 and PITG_13661 were highly expressed in apoplastic fluid and *in planta* infection, whereas PITG_22916 was up-regulated in sterile distilled water and down-regulated during leaf infection.

5.3 Discussion

The plant apoplast is the initial site where pathogen growth takes place, and because of this it plays a critical role in both the initiation and management of the plant defence responses (Bolwell *et al*., 2001; Rico and Preston, 2008). The primary commitment to live on the host or to exit is made by the pathogen during the initial stage of infection that occurs in the intercellular space. This is the crucial cite for the molecular interaction between plant and pathogen (Doehlemann and Hemetsberger 2013). Rico and Preston (2008) found that pathogens take advantage of the nutrients within the apoplastic fluid to grow and multiply; for example the hemi-biotrophic bacterial pathogen *P. syringae* grows well in tomato apoplast extracts. Similarly, there is evidence that the biotrophic fungus *C. fulvum* enters tomato leaves via stomata and remains apoplastic throughout its life cycle (Joosten, 2012). In this case, it can be anticipated that molecular communication between this fungal pathogen and its host is largely apoplastic during biotrophy. Furthermore, De Wit and Spikman (1982) found that the *C. fulvum* effectors (then elicitors of necrosis) are found in tomato apoplast colonised by the pathogen; *C. fulvum* effector *Avr9* was also recognised by *Cf-9* in the tomato apoplast (Jones *et al*., 1994). Thus, it can also be anticipated that some elements of these pathogenic behaviours are shared in the hemi-biotrophic oomycete pathogen *P. infestans.* During molecular interaction with the host, Bolwell *et al*. (2001) found that pathogen elicitors triggering oxidative reactions in the plant apoplast were linked to strengthening the cell walls. Furthermore, they found the potential involvement of plant cell wall generating H_2O_2 for their defence strategies. Similarly, there is also evidence that initially *S. lycopersici* grows in the intercellular spaces of *N. benthamiana* during colonisation (Martin-Hernandez *et al*., 2000). Given that enzymatic hydrolysis proteins such as tomatinase are generated in the plant apoplast by the pathogen *S. lycopersici*, suppression of plant defence is likely to

begin in the apoplast (Bouarab *et al*., 2002). Further, plant-derived proteases and glucanases can also attack pathogen molecules and require inhibition by the pathogen for successful infection (Bozkurt *et al*., 2011; Damasceno *et al*., 2008; Tian *et al*., 2004, 2007). Given all the above mentioned evidence it is important to identify the pathogenic components of *P. infestans* that are likely to function specifically in the apoplast. Several pathogen transcripts that are differentially expressed in apoplastic fluid compared to zoospores, pea broth, and sterile water revealed additional information about the *P. infestans* transcriptome.

5.3.1 Microscopy revealed the formation of haustorium-like structures during hyphal growth in host apoplastic fluid

Although haustorium-like structures were not detected by microscopy at 24 hpi in plant apoplastic fluid, haustoria-like structure were identified by 48 hpi. That these structures were not identified during growth in pea broth or water suggests that plant signals that trigger changes in pathogen development are present in the apoplast. The presence of haustoria in apoplastic fluid was supported by the QRT-PCR analysis of expression for a biotrophy marker gene, *Hmp1*, which showed up-regulation at 24 and 48 hours after inoculation. However, QRT-PCR results also showed that *Hmp1* was also up-regulated during pathogen growth in sterile distilled water. This is in agreement with Avrova *et al*. (2008) where it was shown that Hmp1 is produced in vesicles in cysts germinating in water, and also immediately prior to infection. Therefore, transcripts co-expressed with biotrophic marker gene *Hmp1* in apoplastic fluid and sterile water are likely to be associated with and/or contribute to haustorium formation.

5.3.2 A microarray experiment reveals transcriptome-wide changes during growth in apoplastic fluid, pea broth and sterile distilled water

Hemi-biotrophic pathogens can use multiple strategies to establish biotrophy in order to colonise host plants. It is believed that pathogens regulate different molecules in order to complete their life cycle and at the same time they also regulate host molecules that are necessary for establishing a biotrophic interaction. To establish a biotrophic relation with a host, pathogens must secrete and transport several classes of effector molecules to different host locations so that they can alter host immunity. This means that the expression of effectors requires a trigger, but this has remained elusive for most pathogens. The formation of haustorium-like structures in apoplastic fluid suggests that such a chemical trigger for expression of infection-related genes is present in apoplastic fluid. The microarray analysis of *P. infestans* zoospores, inoculated apoplastic fluid, pea broth, and sterile distilled water samples revealed the drastic changes in the transcriptome of *P. infestans*, with 13,819 differentially expressed transcripts identified, including 1,419 predicted secreted proteins. While many of the differentially expressed transcripts were associated with zoospores, thousands of transcripts were found to respond to growth in the three different media. These findings are in general agreement with an earlier microarray study that showed that *P. infestans* has a highly dynamic transcriptome (Judelson *et al*., 2008). Transcripts for several well-known *Avr* genes, other RxLR effectors, elicitors and PAMPs, NLPs, and CWDEs were differentially expressed in each sample. Furthermore, volcano plot analysis (pairwise comparison) of differentially expressed transcripts from the microarray results revealed significant up-regulation of secreted candidate effectors in apoplastic fluid (Figure 5.8, Table 5.1). These findings further support the hypothesis that the apoplast contains host signals that influence pathogen development. Many of the genes that showed up-regulation in apoplastic fluid

were also detected when *P. infestans* was grown in pea broth, but were expressed at a lower level. This could be due to pea broth being a plant extract, and may still be inducing the expression of some infection-related genes. The specific induction of infection related genes in apoplastic fluid could be further determined through examining the transcriptome of *P. infestans* when grown in a chemically defined medium. Although further analysis is essential, infection-specific genes such as glucanase inhibitor protein 1 (PITG_13628) determined from Chapter 3 were not detected in any of the *in vitro* stages, supporting the evidence that these genes might only be necessary for biotrophy. However, there were infection-specific genes also up-regulated in sterile water, indicating a wide range of regulatory factors controlling up-regulation of infection-associated genes. Surprisingly, these genes were not all up-regulated in AF, suggesting there might be other factors contributing their regulation.

5.3.3 Comparative studies of gene expression in apoplastic fluid and *in planta* infection revealed common expression profiles

Among 13,819 transcripts differentially expressed in zoospores, apoplastic fluid, pea broth, and sterile distilled water, expression of eight transcripts, including four RxLR effectors, and one transcript each for *Cdc14*, ABC transporter, transmembrane, and necrosis-inducing proteins was compared with expression during leaf and tuber infection (cross reference Figure 5.26, 5.27 and 5.28). The RxLR effectors highly up-regulated during growth in apoplastic fluid were also highly expressed during *in planta* infection, suggesting that expression of these genes is genuinely induced by chemical cues from the plant apoplastic environment. Similarly, transcripts encoding an ABC transporter protein and a transmembrane protein that were up-regulated in apoplastic fluid were also up-regulated during *in planta* infection. This is the evidence that some non-secreted transmembrane protein coding genes such as ABC transporters, and transmembrane

proteins are not needed during vegetative pathogen growth or response to starvation, but are necessary for host infection. Thus, the microarray experiment performed here will serve as a valuable resource for identifying infection-related genes from *P. infestans* that were not detected in the infection microarray experiment from Chapter 3. However, not all infection related genes were expressed when *P. infestans* was grown in apoplastic fluid, as the infection-specific genes identified in Chapter 3 were not expressed or not/up-regulated during growth in apoplastic fluid. This indicates that there are cues from the apoplastic fluid that induce *P. infestans* gene expression during infection, but separate cues induce the expression of other sets of infection related genes. A set of 55 RxLR effectors co-expressed with *Hmp1* during *in planta* infection from Chapter 3 included widely recognised avirulence genes including *Avr2*, *Avr3a*, *Avrblb1* (*ipi01*), and *Avrblb2*, which are likely to be associated with haustoria. Interestingly, most of these transcripts were detected during growth in apoplastic fluid. However, none of them were co-expressed with *Hmp1*. Following the leaf analysis in Chapter 3, with the more extensive analysis *in vitro*, including apoplastic fluid, it is promising that genes such as *Avr2* (PITG_08943), *Avr3a* (PITG_14371), and RD2 family (PITG_14787) that were highly up-regulated in apoplastic fluid were also detected from 12 hpi *in planta* infection, and associated with early infection. Out of 85 transcripts significantly up-regulated in apoplastic fluid, 18 transcripts including the above mentioned genes were significantly up-regulated during *in planta* infection. Interestingly, out of five transcripts encoding RxLR effectors (PITG_01394, PITG_04145, PITG_15128, PITG_10232, and PITG_18685) undetected in the apoplastic fluid, pea broth and sterile water, four of them (excluding PITG_18685) were also found to be absent in sporangia and germinating cysts. However, the same four transcripts were only detected *in planta* infection

indicating that these effectors might have similar regulation characteristics to the other infection-specific genes.

Chapter 6. General discussion and future directions

6.1 General discussion

The potato crop is of great significance with regard to its global socio-economic value and contribution to food security (Birch *et al*., 2012). Unfortunately the demands of meeting future food security objectives are impeded due to the continuing and devastating impact of the pathogen *P. infestans.* In order to boost potato production there has been a two-pronged approach: efforts to improve potato yields as well as efforts to limit *P. infestans*' ability to inflict massive crop losses. According to Hansen *et al.* (2007), the Green Revolution resulted in environmentally harmful fungicides being liberally used to reduce crop losses to disease, and still today farmers rely on these fungicides to help protect their crops by spraying them throughout the growing period. However, by using molecular biology techniques to identify pathogen strategies to overcome resistance genes, it is potentially possible to minimize the amount of fungicides being used by identifying novel ways to prevent infection.

Whilst new discoveries and advances in knowledge have led to a deeper understanding of the *P. infestans* infection cycle and the mechanisms involved at the molecular level, such as the roles of PAMPs and effectors in triggering and suppressing PTI, the identification and manipulation of *R* genes to activate ETI, this has not transferred yet to result in improvements to conventional breeding approaches (Vleeshouwers *et al.*, 2011). The uptake of new approaches and technologies, such as focusing on core effectors in order to identify plant resistances (Birch *et al.,* 2008), provides a great opportunity to improve potato crop production, but requires a revolutionary shift in thinking beyond the current traditional breeding programmes that still dominate within agricultural systems. However, there remains much to be understood regarding pathogen gene expression

during infection, necessary for elucidating how the biotrophic phase of infection is established with its host. Without detailed knowledge of this process, the above mentioned approaches are not likely to deliver durable disease control.

It is important to understand the dynamic exchange of signals between plant and pathogen that leads to large-scale transcriptome and proteome changes in both organisms during infection. One approach to understand the molecular interplay during infection is to assess the change in mRNA levels for characterised genes that are associated with specific infection stages, such as the biotrophic interaction. In recent years research has provided insights into the general life cycle and behaviour of oomycete pathogens, either by providing a deeper understanding of cell biology (Gubler and Hardham, 1988; Jackson and Hardham, 1998; Hardham, 2001, 2006, 2007; Ah-Fong and Judelson, 2003, 2011; Ah-Fong *et al*., 2007; Avrova *et al*., 2008) and/or by increased knowledge of transcriptome dynamics (Tyler *et al*., 2006; Judelson *et al*., 2008; Haas *et al*., 2009; Lévesque *et al*., 2010; Cooke *et al*., 2012; Tripathy *et al*., 2012). However, there are few reports that have used the latest and most sensitive microarray technology to reveal detailed transcriptomic knowledge of pathogen strategies for early biotrophic colonisation (Jupe *et al*., 2013). The research in this thesis aimed to use transcriptomic analyses of *P. infestans* to address hypotheses on gene expression during the biotrophic stage of infection, linking transcriptome changes to disease development, the establishment of a biotrophic stage in disease development in tubers, and infection-related gene expression induced by growth in a cell-free apoplastic fluid extract from a solanaceous host plant. These studies provide additional knowledge of *P. infestans* pathogenicity and disease development.

6.1.1 Cell biology of haustoria in leaf and tuber infection

Chapter 3 and 4 of this thesis provided more extensive cell biology knowledge of haustorium formation during leaf and tuber infection. The presence of haustoria in leaf and tuber infection at 12 hpi indicate that host penetration and a biotrophic interaction had occurred by this early time point. The formation of haustoria in leaf tissue is well documented, but is not well described in tuber infection. Haustoria formed in tuber tissue appeared to be much longer that those formed in leaf infections. Previously, Hmp1 has been reported as an essential protein that is localised to haustoria. It appears to localise predominantly to the base of haustoria, from where the haustoria elongate from the intercellular hyphae to translocate effectors (Whisson *et al*., 2007). The use of a transgenic line of *P. infestans* that expresses an Hmp1-mRFP fusion protein from the native *Hmp1* promotor showed that haustoria formed in infected tuber tissue were likely to be functionally equivalent to those formed in leaf tissue.

6.1.2 Transcriptome studies of leaf infection

Chapter 3 provides a detailed study of the transcriptomic changes occurring during biotrophic infection of potato leaf tissue by *P. infestans*. The presence of haustoria during the entire infection time course, and the lack of macroscopic cell death, provides evidence that the transcriptomic study presented here represent the biotrophic phase of infection. That the interaction studied was entirely biotrophic was supported by the QRT-PCR expression of the biotrophy marker gene, *Hmp1*, showing up-regulation at 12 hpi and throughout the infection time course. That this study gathered transcriptome data from as early as 12 hpi and remained within biotrophy (60 hpi), sets it apart from all other studies into *Phytophthora* infection. Other recent studies have only begun analysis at 48 hpi (Haas *et al*., 2009; Cooke *et al*., 2012), or have sampled from an early time point through

into necrotrophy (Jupe *et al*., 2013). The significance is that effector expression could be broadly placed into two groups. One group of effectors is expressed at a high level at the earliest stages of infection, with expression decreasing during later infection stages, while others are expressed at increasing levels throughout the infection. Only by sampling the earliest stages could these observations be made.

In Chapter 3 a comparison with previous microarray studies (Haas *et al*., 2009; Cooke *et al*., 2012) on different genotypes of *P. infestans* identified additional core effector components contributing to pathogenicity. This set of common effectors is likely to contain the essential effectors needed for *P. infestans* infection. Microarray analysis of *P. infestans* (88069) used in this research was sensitive enough to reveal dynamic changes in the transcriptome that trigger (PAMPs; PTI) and suppress (effectors; ETS) immune responses in potato. Combined with ongoing research that aims to determine effector function and PAMP activity in *P. infestans* (Bos *et al*., 2010; McLellan *et al*., 2013; Zheng *et al*., 2014), the microarray data in this thesis can be used in future to develop a model of molecular events during disease development.

6.1.3 Expression of genes co-expressed with stage-specific marker genes

Relatively few *Phytophthora* genes have been functionally linked with specific developmental stages. For example, expression of the *Cdc14* gene is associated with sporulation and spores, and *Hmp1* expression is associated with haustorium formation. In a transcriptomic experiment, such as a microarray, identification of additional genes that are co-expressed with stage specific marker genes can identify other genes that contribute to that stage. In Chapters 3 and 5, the expression profile of sporulation marker gene *Cdc14* (PITG_18578) (Ah-Fong *et al*., 2007) was assessed to identify co-expressed genes. The expression pattern of *Cdc14* and co-expressed genes showed up-regulation in sporangia

or zoospores, and down-regulation after inoculation on plant leaf tissue, or into apoplastic fluid as a proxy for intercellular growth in leaves. This suggested a transition to a different morphological stage, such as hyphal growth or infection. As expected, *Cdc14* co-expressed genes included spore-related proteins, but also included PAMPs (e.g. CBEL), verifying a potential pathogen strategy to avoid PTI, as reported previously (Haas *et al* 2009).

Chapter 3 also expands the initial discovery of the biotrophy marker gene *Hmp1* (PITG_00375) (Avrova *et al*., 2008) to include 185 genes that are >95 % co-expressed with it during infection. This set of genes potentially includes those transcripts that encode proteins essential for formation of haustoria and establishment of a biotrophic interaction with host cells. The largest grouping of transcripts co-expressed with *Hmp1* encoded RxLR effectors, including well-characterised *Avr* genes, such as *Avr3a* (Armstrong *et al*., 2005), *Avr2* (Haas *et al*., 2009, Gilroy *et al*., 2011), *Avrblb1* (also called *IpiO1*; van West *et al*., 1998), *Avrblb2* (Bozkurt *et al*., 2011), *AvrVnt1* (Pel, 2010), and other characterised RxLR effectors such as PITG_03192 (McLellan *et al*., 2013). The early timing of expression for *Hmp1* and co-expressed genes suggests that establishing a biotrophic interaction with its host is critical from the earliest stage of infection. The tight co-expression of 55 RxLR genes with *Hmp1* is consistent with the encoded effectors being secreted from haustoria. Intriguingly, apoplastic effectors such as SCR74 and both protease and glucanse inhibitors were co-expressed with *Hmp1*. It will be interesting to discover whether they are secreted from haustoria. However, not all RxLR effectors were co-expressed with *Hmp1*, such as RD2, which suppresses activation of a MAP3 kinase (King *et al*., 2014). Whether it is secreted by haustoria, it is unlikely to be present throughout the period when haustoria are likely formed.

Many of the genes co-expressed with *NPP1* (PITG_09716) have roles during biotrophy. This was unexpected, as NPP1 family members are associated with necrotrophy. Nevertheless, either this member of the family does not promote cell death, or these associated effectors, and indeed Hmp1, are indicative of the pathogen suppressing PTI in response to NPP1. A further intriguing possibility is that this NPP1 family member is secreted from haustoria and is associated in some way with effector uptake, perhaps through lysis of endocytic vesicles inside plant cells to release effectors into the cytosol.

6.1.4 Infection-specific genes

A small number of transcripts were identified from the microarrays that were highly up-regulated only during infection. These transcripts were not detected in any other lifecycle stages, during starvation, or hyphal growth in rich medium (pea broth) or apoplastic fluid. Transcripts verified by QRT-PCR as infection-specific encoded proteins such as POT (PITG_09088), GIP1 (PITG_13638), and an RxLR effector (PITG_15128). The verification that there are genuinely infection specific transcripts in the *P. infestans* microarray data generated in this thesis suggests that further QRT-PCR validation will uncover additional genes in this group. The biological significance is that genes that are expressed only during infection can only have roles during infection. Moreover, their regulation must be based solely on plant-derived cues. Further functional analysis will be needed to determine if the infection-specific genes contribute to establishing a biotrophic relationship with the host plant.

6.1.5 Expression of stage-specific marker genes (*Cdc14*, and *Hmp1*), PAMPs, effectors, and infection specific genes during tuber infection

Most studies of *P. infestans* infection have focussed on leaf colonisation. Studies into tuber infection have typically not addressed pathogen gene expression and, where they

have, it has been at late stages of infection (Judelson *et al*., 2009). Expression of candidate pathogenicity genes has not been examined during tuber infection previously. Tuber tissue is very different in composition to leaf tissue, and thus it was uncertain whether infection would require similar pathogen gene expression. Unlike Chapter 3, microarray analysis of *P. infestans* genes was not carried out for tuber infection. Instead, genes were selected from the study in Chapter 3, and used in qRT-PCR assays of tuber infection. The selected genes displayed similar expression profiles to those observed in leaf infection. Similar to leaf infection *Cdc14* (PITG_18578) and CBEL (PITG_03637) were down-regulated throughout the infection time course (cross reference Chapter 4), again suggesting suppression of PAMP expression during early stages of infection. *Hmp1* (PITG_00375) was highly up-regulated during early (12 hpi) infection suggesting that the pathogen has already penetrated the host cells and formed haustoria to translocate effector proteins. As stated earlier, confocal microscopy using a transgenic *P. infestans* line expressing an Hmp1-mRFP fusion protein showed formation of haustoria.

Among the genes tested by QRT-PCR in tuber infection were five genes shown to be infection specific in Chapter 3. The expression profiles of these selected genes in tubers were also infection specific. The formation of haustoria, expression of biotrophy related genes, and effectors strongly suggests that suppression of host defences and establishment of biotrophy is important during tuber infection.

6.1.6 Expression of infection-related genes in apoplastic fluid from the model solanaceous plant, *Nicotiana benthamiana*

From many previous studies (Whisson *et al*., 2007; Avrova *et al*., 2008), and seen here in Chapters 3 and 4, much of the pathogen infection biomass is located in the intercellular spaces as hyphae. It is unclear as to what signals are perceived by *P. infestans* to initiate

gene expression during infection, or to initiate formation of haustoria. An initial observation that haustoria-like structures are occasionally formed when *P. infestans* is grown in fresh apoplastic fluid extract from the model solanaceous host *N. benthamiana* suggested that molecules present in the apoplast may induce infection-associated gene expression in *P. infestans*. Other studies, primarily with plant pathogens including oomycetes, have shown plant extracts to induce expression of infection-related genes (Yamakawa *et al*., 1998; Bolwell *et al*., 2001; Zipfel *et al*., 2004; Jha *et al*., 2005; Tian *et al*., 2005; Marina *et al*., 2008). Similarly, Vieira *et al*., (2011) have reported that the plant apoplast is an important destination compartment for nematode protein secretion during early migration. In Chapter 5, a microarray experiment demonstrated that most of the highly up-regulated genes in zoospores (used to inoculate the apoplastic fluid, rich medium, and sterile water) were down-regulated by 48 hpi in all *in vitro* samples. The major group of these genes were spore-associated genes such as *Cdc14* (PITG_18578).

Similar analyses for gene-co-expression as carried out in Chapter 3 were also performed for gene expression in apoplastic fluid. *Hmp1* was not strongly differentially expressed in apoplastic fluid, probably reflecting the very low numbers of haustorium-like structures formed. Despite this, many of the transcripts (20) co-expressed with *Hmp1* encoded secreted RxLR effectors, as in Chapter 3. This include five transcripts of Pex-RD2 family of RxLRs. Pex-RD2 (PITG_14787) is characterised as necessary for suppression of host immunity during early infection (King *et al*., 2014) suggesting that the Pex-RD2 family of RxLRs co-expressed with *Hmp1* might be the earliest pathogen responses triggered particularly by the apoplastic fluid following penetration. Interestingly, all of the RxLRs except one transcript (PITG_22648), including RD2, that were co-expressed with *Hmp1* in apoplastic fluid were not co-expressed with *Hmp1* during leaf infection. It is possible that *Hmp1* is initially induced by signals in apoplastic fluid after pathogen penetration,

and that all of the associated 20 RXLR genes up-regulated with it in AF are also activated by this signal. We can expect that the constituents of AF will alter during infection and it is possible that at least some of the RxLR genes co-expressed with *Hmp1* throughout biotrophy in leaves are actually responding to additional signals generated at later stages of infection.

There were 109 transcripts of RxLRs detected in the leaf infection microarray that were also detected in the pathogen grown in apoplastic fluid. Out of these, 10 and 85 transcripts including Pex-RD2 (PITG_14787) (King *et al*., 2014) were significantly up-regulated in AF at 24 and 48 hpi respectively, indicating *P. infestans* effector regulation is triggered in AF. *Avr3a* was significantly differentially expressed in AF, and transcripts co-expressed with it included many RxLR effectors and other infection related genes. However, infection-specific genes that were characterised in Chapter 3 and 4 were either not expressed, or poorly expressed, in AF. Taken together, the results signify that there are molecules in cell-free apoplastic fluid that induce infection gene expression in *P. infestans*, but there are additional signals for infection gene expression that originate from intact, living plant cells during infection. Quantitative RT-PCR of selected genes validated the expression profiles found in the apoplastic fluid. Crucially, genes that were up-regulated in apoplastic fluid were also up-regulated at similar times and levels during leaf and tuber infection. This also suggests that the microarray data in Chapter 5 may be a useful resource for identification of additional pathogenicity genes and processes in *P. infestans*. For example, genes encoding an ABC transporter, purine-cytosine permease, and a transmembrane protein (PITG_07013, PITG_13063, and PITG_13661, respectively) were specifically and highly up-regulated at AF and during infection *in planta*.

Overall, these results suggest that transcriptomic studies of early infection stages *in planta* and in cell-free systems are important to understand disease development and pathogenicity.

6.2 Future prospects

6.2.1 How specific are the *Cdc14*, *Hmp1*, and *NPP1* co-expressed genes?

Apart from PAMPs (CBEL), other *Cdc14* co-expressed transcripts encoding CRN effectors (12 transcripts), candidate effectors such as carbonic anhydrase (PITG_14412), and protease inhibitor EPI11 (PITG_07096). Are these candidate effectors co-expressed with *Cdc14* because they are required at the earliest contact with the host plant? More temporally defined analysis of their expression, and functional analysis of these effectors for their localization and role in infection has to be carried out to address this question.

Apoplastic effectors such as protease and glucanase inhibitors were also co-expressed with *Hmp1*, implicating haustoria as a potential site also for secretion of these proteins. Many RxLR effectors (55 transcripts) were co-expressed with *Hmp1* during leaf infection. This included Avr3a, which is known to be secreted through haustoria (Armstrong *et al*., 2005). Are these RxLRs functionally co-regulated with Hmp1? Are they all necessary to invade the host plant? For example, RNAi of *Avr3a* and PITG_03192 has shown that silencing these genes was enough to reduce pathogenicity (Bos *et al*., 2010; McLellan *et al*., 2013 respectively). Several other questions have been raised, for example, regarding the role of a bi-functional catalase-peroxidase (KatG) co-expressed with *Hmp1*, which is essential for detoxifying the ROS mediated oxidative bursts in other pathosystems (Tanabe *et al*., 2011). It would be interesting to investigate if this gene is behaving in a similar way to detoxify ROS in the *P. infestans*-potato pathosystem.

A set of 62 RxLR effector encoding transcripts were co-expressed with *NPP1* (PITG_09716) and 39 transcripts out of these were also co-expressed with *Hmp1*. It would be an interesting avenue of research to determine if these common effectors are required for a longer period of the *P. infestans* infection cycle. In addition to these co-expressed genes was one encoding a secreted berberine-like protein. In mammalian systems, this inhibits thymocyte apoptosis (Miura *et al*., 1997). A question that arises is, does the equivalent protein in *P. infestans* have an effect of inhibiting programmed cell death in infected host plant cells?

6.2.2 What are the role of common and isolate specific RxLR effectors?

Comparative studies using microarray data revealed 50 transcripts encoding RxLR effectors in common between *P. infestans* isolates 88069, 3928A, and T30-4 during infection. However, there were 37, 23, and 9 transcripts of RxLR effectors only detected in 88069, 3928A, and T30-4 respectively. Comparatively, there were more RxLR effectors detected in 88069 than other isolates. To fully understand if these genes are in fact specific to these individual isolates, or are a result of different rates of infection progression, more precise measurements of their gene expression, possibly normalised to pathogen biomass, will be revealing.

6.2.3 What are the roles of infection-specific genes?

It is interesting to determine if these genes are essential for successful potato and tomato infection. Genes that were up-regulated during leaf infection were not detected in pathogen grown in apoplastic fluid, and some of them were also absent in tuber infection. Functional analysis of these genes could be carried out by using gene silencing or more recently developed mutational analysis approaches such as the CRISPR system for genome engineering (Wilkinson and Wiedenheft, 2014).

Chapter 7. References

Abramovitch, R. B., Anderson, J. C., and Martin, G. B. (2006). Bacterial elicitation and evasion of plant innate immunity. *Nature Reviews Molecular Cell Biology*. 7: 601−611.

Ah-Fong, A. M. V., and Judelson, H. S. (2003). Cell cycle regulator Cdc14 is expressed during sporulation but not hyphal growth in the fungus-like oomycete *Phytophthora infestans*. *Molecular Microbiology*. 50 (2): 487–494.

Ah-Fong, A. M., Xiang, Q., and Judelson, H. S. (2007). Architecture of the sporulation-specific *Cdc14* promoter from the oomycete *Phytophthora infestans*. *Eukaryotic Cell*. 6 (12): 2222–2230.

Ah-Fong, A. M., and Judelson, H. S. (2011). New role for Cdc14 phosphatase: localization to basal bodies in the oomycete *Phytophthora* and its evolutionary coinheritance with eukaryotic flagella. *PloS One*. 6 (2): e16725.

Alberts, B., Johnson, A., Lewis, J., Raff, M., Roberts, K., and Walter, P. (2008). *Molecular Biology of the Cell*. Garland Science, NY, USA.

Andrivon, D., Giorgetti, C., Baranger, A., Calonnec, A., Cartolaro, P., Faivre, R., Guyader, S., Lauri, P. E., Lescourret, F., Parisi, L., Ney, B., Tivoli, B., and Sache, I. (2013). Defining and designing plant architectural ideotypes to control epidemics? *European Journal of Plant Pathology*. 135 (3): 611–617.

Armstrong, M. R., Whisson, S. C., Pritchard, L., Bos, J. I. B., Venter, E., Avrova, A. O., Rehmany, A. P., Bohme, U., Brooks, K., Cherevach, I., Hamlin, N., White, B., Fraser, A., Lord, A., Quail, M. A., Churcher, C., Hall, N., Berriman, M., Huang, S., Kamoun, S., Beynon, J. L., and Birch, P. R. J. (2005). An ancestral oomycete locus contains late blight avirulence gene *Avr3a*, encoding a protein that is recognized in the host cytoplasm. *PNAS*. 102 (21): 7766–7771.

Aronson, J. M., Cooper, B. A., and Fuller, M. S. (1967). Glucans of oomycete cell wall. *Science*. 155 (3760): 332–335.

As-sadi, F., Carrere, S., Gascuel, Q., Hourlier, T., Rengel, D., Le Paslier, M. C., Bordat, A., Boniface, M. C., Brunel, D., Gouzy, J., Godiard, L., and Vincourt, P. (2011). Transcriptomic analysis of the interaction between *Helianthus annuus* and its obligate parasite *Plasmopara halstedii* shows single nucleotide polymorphisms in CRN sequences. *BMC Genomics*. 12 (1): 498.

Ausubel, F. M., Brent, R., Kingston, R. E., Moore, D. D., Seidman, J. G., Smith, J. A., and Struhl, K. (1995). *Current Protocols in Molecular Biology*. John Wiley and Sons. NY, USA.

Avrova, A. O., Whisson, S. C., Pritchard, L., Venter, E., De Luca, S., Hein, I., and Birch, P. R. J. (2007). A novel non-protein-coding infection-specific gene family is clustered throughout the genome of *Phytophthora infestans*. *Microbiology*. 153: 747–759.

Avrova, A. O., Boevink, P. C., Young, V., Grenville-Briggs, L. J., van West, P., Birch, P. R. J., and Whisson, S. C. (2008). A novel *Phytophthora infestans* haustorium- specific membrane protein is required for infection of potato. *Cellular Microbiology*. 10 (11): 2271–2284.

Bai, Y., Pavan, S., Zheng, Z., Zappel, N. F., Reinstädler, A., Lotti, C., De Giovanni, C., Ricciardi, L., Lindhout, P., Visser, R., Theres, K., and Panstruga, R. (2008). Naturally occurring broad-spectrum powdery mildew resistance in a central American tomato accession is caused by loss of Mlo function. *Molecular Plant-Microbe Interactions*. 21 (1): 30–39.

Baldauf, S. L., Roger, A. J., Wenk-Siefert, I., and Doolittle, W. F. (2000). A kingdom-level phylogeny of eukaryotes based on combined protein data. *Science*. 290 (5493): 972–977.

Baldauf, S. L. (2008). An overview of the phylogeny and diversity of eukaryotes. *Journal of Systematics and Evolution*. 46 (3): 263–273.

Ballvora, A., Ercolano, M. R., Weiss, J., Meksem, K., Bormann, C. A., Oberhagemann, P., Salamini, F., and Gebhardt, C. (2002) The *R1* gene for potato resistance to late blight (*Phytophthora infestans*) belongs to the leucine zipper/NBS/LRR class of plant resistance genes. *Plant Journal*. 30: 361–371.

Bartoletti, S. C. (2001). Black potatoes: the story of the great Irish famine, *1845-1850*. Houghton Mifflin Company, NY, USA.

Baxter, L., Tripathy, S., Ishaque, N., Boot, N., Cabral, A., Kemen, E., Thines, M., Ah-Fong, A., Anderson, R., Badejoko, W., Bittner-Eddy, P., Boore, J. L., Chibucos, M. C., Coates, M., Dehal, P., Delehaunty, K., Dong, S., Downton, P., Dumas, B., Fabro, G., Fronick, C., Fuerstenberg, S. I., Fulton, L., Gaulin, E., Govers, F., Hughes, L., Humphray, S., Jiang, R. H. Y., Judelson, H., Kamoun, S., Kyung, K., Meijer, H., Minx, P., Morris, P., Nelson, J., Phuntumart, V., Qutob, D., Rehmany, A., Rougon-Cardoso, A., Ryden, P., Torto-Alalibo, T., Studholme, D., Wang, Y., Win, J., Wood, J., Clifton, S. W., Rogers, J., Van den Ackerveken, G., Jones, J. D. G., McDowell, J. M., Beynon, J., and Tyler, B. M. (2010). Signatures of adaptation to obligate biotrophy in the *Hyaloperonospora arabidopsidis* genome. *Science*. 330 (6010): 1549–1551.

Beakes, G. W., and Sekimoto, S. (2009). The evolutionary phylogeny of oomycetes – insights gained from studies of holocarpic parasites of algae and invertebrates. *Oomycete Genetics and Genomics*. Wiley- Blackwell. 1: 1–24.

Beakes, G. W., Glockling, S. L., and Sekimoto S. (2012). The evolutionary phylogeny of the oomycete "fungi". *Protoplasma*. 249 (1): 3–19.

Belkhadir, Y., Jaillais, Y., Epple, P., Balsemao-Pires, E., Dangl, J. L., and Chory, J. (2012). Brassinosteroids modulate the efficiency of plant immune responses to microbe-associated molecular patterns. *PNAS*. 109: 297–302.

Bernoux, M., Ellis, J. G., and Dodds, P. N. (2011). New insights in plant immunity signalling activation. *Current Opinion in Plant Biology*. 14: 512–518.

Billon-Grand, G., Marais, M. F., Joseleau, J. P., Girard, V., Gay, L., & Fèvre, M. (1997). A novel 1, 3-β-glucan synthase from the oomycete *Saprolegnia monoica*. *Microbiology*. 143 (10): 3175–3183.

Birch, P. R. J., and Whisson, S. C. (2001). *Phytophthora infestans* enters the genomic era. *Molecular Plant Pathology*. 2 (5): 257–263.

Birch, P. R. J., Rehmany, A. P., Pritchard, L., Kamoun, S., Beynon, J. L., (2006). Trafficing arms: oomycetes effectors enter host plant cells. *Trends in Microbiology*. 14 (1): 8–11.

Birch, P. R., Boevink, P. C., Gilroy, E. M., Hein, I., Pritchard, L., and Whisson, S. C. (2008). Oomycete RXLR effectors: delivery, functional redundancy and durable disease resistance. *Current Opinion in Plant Biology*. 11 (4): 373–379.

Birch, P. R. J., and Avrova, A. O. (2009). Gene expression profiling. *Oomycete Genetics and Genomics*. Wiley- Blackwell. 24: 477–492.

Birch, P. R. J., Bryan G., Fenton, B., Gilroy E. M., Hein I., Jones, J. T., Prashar A., Taylor M. A., Torrance L., and Toth, I. K. (2012). Crops that feed the world 8: Potato: are the trends of increased global production sustainable? *Food Security*. 4, 477–508.

Bittner-Eddy, P. D., Allen, R. L., Rehmany, A. P., Birch, P., and Beynon, J. L. (2003). Use of suppression subtractive hybridization to identify downy mildew genes expressed during infection of *Arabidopsis thaliana*. *Molecular Plant Pathology*. 4 (6): 501–507.

Block, A., Li, G., Fu, Z. Q., and Alfano, J. R. (2008). Phytopathogen type III effector weaponry and their plant targets. *Current Opinion in Plant Biology*. 11 (4): 396–403.

Boissy, G., O'Donohue, M., Gaudemer, O., Perez, V., Pernollet, J. C., and Brunie, S. (1999). The 2.1 Å structure of an elicitin-ergosterol complex: a recent addition to the sterol carrier protein family. *Protein Science*. 8 (6): 1191–1199.

Boller, T., and Felix, G. (2009). A renaissance of elicitors: perception of microbe-associated molecular patterns and danger signals by pattern-recognition receptors. *Annual Review of Plant Biology*. 60: 379–406.

Bolwell, P. P., Page, A., Piślewska, M., and Wojtaszek, P. (2001). Pathogenic infection and the oxidative defences in plant apoplast. *Protoplasma*. 217 (1-3): 20–32.

Bos, J. I., Armstrong, M., Whisson, S. C., Torto, T. A., Ochwo, M., Birch, P. R. J., and Kamoun, S. (2003). Intraspecific comparative genomics to identify avirulence genes from *Phytophthora*. *New Phytologist*. 159 (1): 63–72.

Bos, J. I., Chaparro-Garcia, A., Quesada-Ocampo, L. M., Gardener, B. B., and Kamoun, S. (2009). Distinct amino acids of the *Phytophthora infestans* effector AVR3a condition

activation of *R3a* hypersensitivity and suppression of cell death. *Molecular Plant-Microbe Interactions*. 22: 269–281.

Bos, J. I., Armstrong, M. R., Gilroy, E. M., Boevink, P. C., Hein, I., Taylor, R. M., Zhendong, T., Engelhardt, S., Vetukuri, R. R., Harrower, B., Dixelius, C., Bryan, G., Sadanandom, A., Whisson, S. C., Kamoun, S., and Birch, P. R. J. (2010). *Phytophthora infestans* effector AVR3a is essential for virulence and manipulates plant immunity by stabilizing host E3 ligase CMPG1. *PNAS*. 107 (21): 9909- 9914.

Bouarab, K., Melton, R., Peart, J., Baulcombe, D., and Osbourn, A. (2002). A saponin-detoxifying enzyme mediates suppression of plant defences. *Nature*. 418 (6900): 889–892.

Bozkurt, T. O., Schornack, S., Win, J., Shindo, T., Ilyas, M., Oliva, R., Cano, L. M., Jones, A. M. E., Huitema, E., van deer Hoorn, R. A. L., and Kamoun, S. (2011). *Phytophthora infestans* effector AVRblb2 prevents secretion of a plant immune protease at the haustorial interface. *PNAS*. 108 (51): 20832–20837.

Brunner, F., Rosahl, S., Lee, J., Rudd, J. J., Geiler, C., Kauppinen, S., Rasmussen, G., Scheel, D., and Nurnberger, T. (2002), Pep-13, a plant defense-inducing pathogen-associated pattern from *Phytophthora* transglutaminases. *EMBO Journal*. 21: 6681–6688.

Burki, F., Shalchian-Tabrizi, K., Minge, M., Skjæveland, Å., Nikolaev, S. I., Jakobsen, K. S., and Pawlowski, J. (2007). Phylogenomics reshuffles the eukaryotic supergroups. *PloS One*. 2 (8): e790.

Burki, F., Shalchian-Tabrizi, K., and Pawlowski, J. (2008). Phylogenomics reveals a new 'megagroup' including most photosynthetic eukaryotes. *Biology Letters*. 4 (4), 366-369.

Cabral, A., Oome, S., Sander, N., Küfner, I., Nürnberger, T., and Van den Ackerveken, G. (2012). Nontoxic Nep1-like proteins of the downy mildew pathogen *Hyaloperonospora arabidopsidis*: Repression of necrosis-inducing activity by a surface-exposed region. *Molecular Plant-Microbe Interactions*. 25 (5): 697–708.

Caillaud, M. C., Piquerez, S. J., Fabro, G., Steinbrenner, J., Ishaque, N., Beynon, J., and Jones, J. D. (2012). Subcellular localization of the Hpa RxLR effector repertoire identifies a tonoplast-associated protein HaRxL17 that confers enhanced plant susceptibility. *The Plant Journal*. 69 (2): 252–265.

Cao, H., Glazebrook, J., Clarke, J. D., Volko, S., and Dong, X. (1997). The *Arabidopsis NPR1* gene that controls systemic acquired resistance encodes a novel protein containing ankyrin repeats. *Cell*. 88 (1): 57–63.

Casimiro, S., Tenreiro, R., and Monteiro, A. A. (2006). Identification of pathogenesis-related ESTs in the crucifer downy mildew oomycete *Hyaloperonospora parasitica* by high-throughput differential display analysis of distinct phenotypic interactions with *Brassica oleracea*. *Journal of Microbiological Methods*. 66 (3): 466–478.

Caten, C. E., and Jinks, J. L. (1968). Spontaneous variability of single isolates of *Phytophthora infestans*. I. Cultural variation. *Canadian Journal of Botany*. 46 (4): 329–348.

Cavalier-Smith, T., and Chao, E. E. (2006). Phylogeny and megasystematics of phagotrophic heterokonts (kingdom Chromista). *Journal of Molecular Evolution*. 62 (4): 388–420.

Chaparro-Garcia, A., Wilkinson, R. C., Gimenez-Ibanez, S., Findlay, K., Coffey, M. D., Zipfel, C., Rathjen, J. P., Kamoun, S., and Schornack, S. (2011). The receptor-like kinase SERK3/BAK1 is required for basal resistance against the late blight pathogen *Phytophthora infestans* in *Nicotiana benthamiana*. *PLoS One*. 6 (1): e16608.

Chen, L., Song, Y., Li, S., Zhang, L., Zou, C., and Yu, D. (2012). The role of WRKY transcription factors in plant abiotic stresses. *Biochimica et Biophysica Acta (BBA)-Gene Regulatory Mechanisms*. 1819 (2): 120–128.

Cheung, F., Win, J., Lang, J. M., Hamilton, J., Vuong, H., Leach, J. E., Kamoun, S., Lévesque, C. A., Tisserat, N., and Buell, C. R. (2008). Analysis of the *Pythium ultimum* transcriptome using Sanger and pyrosequencing approaches. *BMC genomics*. 9 (1): 542.

Chisholm, S. T., Coaker, G., Brad, D., and Staskawicz, B. J. (2006). Host-microbe interactions: shaping evolution of the plant immune response. *Cell*. 124: 803–814.

Chu, Z., Yuan, M., Yao, J., Ge, X., Yuan, B., Xu, C., Li, X., Fu, B., Li, Z., Bennetzen, J. L., Zhang Q., and Wang, S. (2006). Promoter mutations of an essential gene for pollen development result in disease resistance in rice. *Genes and Development*. 20 (10): 1250–1255.

Coburn, B., Sekirov, I., and Finlay, B. B. (2007). Type III secretion systems and disease. *Clinical Microbiology Reviews*. 20 (4): 535–549.

Coffey, M. D., and Gees, R. (1991). The cytology of development. *Advances in Plant Pathology, Vol. 7 Phytophthora infestans, the Cause of Late Blight of Potato* (eds D.S. Ingram and P.H. Williams), Academic Press, London. 31–51.

Cooke, L. R., and Little, G. (2002). The effect of foliar application of phosphonate formulations on the susceptibility of potato tubers to late blight. *Pest Management Science*. 58 (1): 17-25.

Cooke, D. E. L., and Lees, A. K. (2004). Markers, old and new, for examining *Phytophthora infestans* diversity. *Plant Pathology*. 53 (6): 692-704.

Cooke, D. E., Cano, L. M., Raffaele, S., Bain, R. A., Cooke, L. R., Etherington, G. J., Deahl, K. L., Farrer, R. A., Gilroy, E. M., Goss, E. M., Grünwald, N. J., Hien, I., MacLean, D., McNicol, J. W., Randall, E., Oliva, R. F., Pel, M. A., Shaw, D. S., Squires, J. N., Taylor, M. C., Vleeshouwers, V. G. A. A., Birch, P. R. J., Lees, A., and Kamoun, S. (2012). Genome analyses of an aggressive and invasive lineage of the Irish potato famine pathogen. *PLoS Pathogens*. 8 (10): e1002940.

Cornelis, G. R. (2006). The type III secretion injectisome. *Nature Reviews Microbiology*. 4 (11): 811-825.

Cournoyer, P., and Dinesh-kumar, S. P. (2011). NB-LRR immune receptors in plant virus defence. *Recent advances in plant virology. Caister Academic Press, Norfolk*. 149-176.

Cui, X., and Churchill, G. A. (2003). Statistical tests for differential expression in cDNA microarray experiments. *Genome Biology*. 4 (4): 210.

Dai, G. H., Andary, C., Mondolot-Cosson, L., and Boubals, D. (1995). Histochemical studies on the interaction between three species of grapevine, *Vitis vinifera*, *V. rupestris* and *V. rotundifolia* and the downy mildew fungus, *Plasmopara viticola*. *Physiological and Molecular Plant Pathology*. 46 (3): 177-188.

Damasceno, C. M., Bishop, J. G., Ripoll, D. R., Win, J., Kamoun, S., and Rose, J. K. (2008). Structure of the glucanase inhibitor protein (GIP) family from *Phytophthora* species suggests coevolution with plant endo-β-1, 3-glucanases. *Molecular Plant-Microbe Interactions*. 21 (6): 820-830.

Davidse, L. C., Looijen, D., Turkensteen, L. J. and van der Wal, D. (1981) Occurrence of Metalaxyl-resistant strains of *Phytophthora* infestans in Dutch potato fields. *Netherlands Journal of Plant Pathology*. 87: 65-68.

Deahl, K. L., Goth, R. W., Young, R., Sinden, S. L., and Gallegly, M. E. (1991). Occurrence of the A2 mating type of *Phytophthora infestans* in potato fields in the United States and Canada. *American Potato Journal*. 68 (11): 717-725.

De Bary, A. H. (1876). Researches into the nature of the potato fungus, *Phytophthora infestans*. *Journal of the Royal Agriculture Society of England*. 2 (12): 23 –269.

del Castillo-Múnera, J., Cárdenas, M., Pinzón, A., Castañeda, A., Bernal, A. J., and Restrepo, S. (2013). Developing a taxonomic identification system of *Phytophthora* species based on microsatellites. *Revista Iberoamericana de Micología*. 30 (2): 88-95.

Deslandes, L., Olivier, J., Peeters, N., Feng, D. X., Khounlotham, M., Boucher, C., Somssich, I., Genin, S., and Marco, Y. (2003). Physical interaction between RRS1-R, a protein conferring resistance to bacterial wilt, and PopP2, a type III effector targeted to the plant nucleus. *PNAS*. 100 (13): 8024-8029.

Dewdney, J., Reuber, T. L., Wildermuth, M. C., Devoto, A., Cui, J., Stutius, L. M., Drummond, E. P., and Ausubel, F. M. (2000). Three unique mutants of *Arabidopsis* identify *eds* loci required for limiting growth of a biotrophic fungal pathogen. *The Plant Journal*. 24 (2): 205-218.

De Wit, P. J., and Spikman, G. (1982). Evidence for the occurrence of race and cultivar-specific elicitors of necrosis in intercellular fluids of compatible interactions of *Cladosporium fulvum* and tomato. *Physiological Plant Pathology*. 21 (1): 1-11.

Dodds, P. N., Lawrence, G. J., Catanzariti, A. M., Ayliffe, M. A., and Ellis, J. G. (2004). The *Melampsora lini AvrL567* avirulence genes are expressed in haustoria and their products are recognized inside plant cells. *The Plant Cell*. 16 (3): 755-768.

Doehlemann, G., and Hemetsberger, C. (2013). Apoplastic immunity and its suppression by filamentous plant pathogens. *New Phytologist*. 198 (4): 1001-1016.

Doke, N., and Tomiyama, K. (1980). Effect of hyphal wall components from *Phytophthora infestans* on protoplasts of potato tuber tissues. *Physiological Plant Pathology*. 16 (2): 169-176.

Doke, N. (1983). Involvement of superoxide anion generation in the hypersensitive response of potato tuber tissues to infection with an incompatible race of *Phytophthora infestans* and to the hyphal wall components. *Physiological Plant Pathology*. 23 (3): 345-357.

Doke, N., and Miura, Y. (1995). *In vitro* activation of NADPH-dependent O_2-generating system in a plasma membrane-rich fraction of potato tuber tissues by treatment with an elicitor from *Phytophthora infestans* or with digitonin. *Physiological and Molecular Plant Pathology*. 46 (1): 17-28.

Dyrløv Bendtsen, J., Nielsen, H., von Heijne, G., and Brunak, S. (2004). Improved prediction of signal peptides: SignalP 3.0. *Journal of Molecular Biology*. 340 (4): 783-795.

Elmore, J. M., Lin, Z. J. D., and Coaker, G. (2011). Plant NB-LRR signaling: upstreams and downstreams. *Current Opinion in Plant Biology*. 14 (4): 365-371.

Engelhardt, S., Boevink, P. C., Armstrong, M. R., Ramos, M. B., Hein, I., and Birch, P. R. (2012). Relocalization of late blight resistance protein R3a to endosomal compartments is associated with effector recognition and required for the immune response. *The Plant Cell*. 24 (12): 5142-5158.

Erwin, D. C., and Ribeiro, O. K. (1996). *Phytophthora Disease Worldwide*. St. Paul, Minnesota, USA: The American Phytopathological Society.

Eulgem, T., Rushton, P. J., Schmelzer, E., Hahlbrock, K., and Somssich, I. E. (1999). Early nuclear events in plant defence signalling: rapid gene activation by WRKY transcription factors. *The EMBO Journal*. 18 (17): 4689-4699.

Fellbrich, G., Romanski, A., Varet, A., Blume, B., Brunner, F., Engelhardt, S., Felix, G., Kemmerling, B., Krzymowska, M., and Nurnberger, T. (2002). NPP1, a *Phytophthora*-associated trigger of plant defense in parsley and *Arabidopsis*. *The Plant Journal*. 32: 375-390.

Feng, B. Z., and Li, P. Q. (2013). Molecular characterization and functional analysis of the *Nep1-like* protein-encoding gene from *Phytophthora capsici*. *Genetics and Molecular Research*. 12 (2): 1468.

Fernández, M. B., Pagano, M. R., Daleo, G. R., and Guevara, M. G. (2012). Hydrophobic proteins secreted into the apoplast may contribute to resistance against *Phytophthora infestans* in potato. *Plant Physiology and Biochemistry*. 60: 59-66.

Flier, W. G., Grünwald, N. J., Fry, W. E., and Turkensteen, L. J. (2001). Formation, production and viability of oospores of *Phytophthora infestans* from potato and *Solanum demissum* in the Toluca Valley, central Mexico. *Mycological Research*. 105 (8): 998-1006.

Forbes, G. A., Goodwin, S. B., Drenth, A., Oyarzun, P., Ordoñez, M. E., and Fry, W. E. (1998). A global marker database for *Phytophthora infestans*. *Plant Disease*. 82 (7): 811-818.

Fry, W. E., Goodwin, S. B., Dyer, A. T., Matuszak, J. M., Drenth, A., Tooley, P. W., Sujkowski, L. S., Koh, Y. J., Cohen, B. A., and Spielman, L. J. (1993). Historical and recent migrations of *Phytophthora infestans*: chronology, pathways, and implications. *Plant Disease*. 77: 653-661.

Fry, W. E., and Goodwin, S. B. (1997). Re-emergence of potato and tomato late blight in the United States. *Plant Disease*. 81 (12): 1349-1357.

Fry, W. (2008). *Phytophthora infestans*: the plant (and R gene) destroyer. *Molecular Plant Pathology*. 9: 385–402.

Fry, W. E., Grunwald, N. J., Cooke, D. E. L., McLeod, G., Forbes, A., and Cao, K. (2009). Population genetics and population diversity of *Phytophthora infestans*. In Lamour, K., and Kamoun, S. (eds). *Oomycete genetics and genomics*. Wiley-Blackwell, NJ, USA, 7, 139-164.

Fu, L., Wang, H. Z., Feng, B. Z., and Zhang, X. G. (2013). Cloning, expression, purification and initial analysis of a novel pectate lyase Pcpel1 from *Phytophthora capsici*. *Journal of Phytopathology*. 161 (4): 230-238.

Gao, L., Tu, Z. J., Millett, B. P., and Bradeen, J. M. (2013). Insights into organ-specific pathogen defense responses in plants: RNA-seq analysis of potato tuber-*Phytophthora infestans* interactions. *BMC Genomics*. 14 (340): 1–12.

Garas, N. A., Doke, N., and Kuć, J. (1979). Suppression of the hypersensitive reaction in potato tubers by mycelial components from *Phytophthora infestans*. *Physiological Plant Pathology*. 15 (2): 117-126.

Gaulin, E., Jauneau, A., Villalba, F., Rickauer, M., Esquerré-Tugayé, M. T., and Bottin, A. (2002). The CBEL glycoprotein of *Phytophthora parasitica* var. *nicotianae* is involved in cell wall deposition and adhesion to cellulosic substrates. *Journal of Cell Science*. 115 (23): 4565-4575.

Gaulin, E., Drame, N., Lafitte, C., Torto-Alalibo, T., Martinez, Y., meline-Torregrosa, C., Khatib, M., Mazarguil, H., Villalba-Mateos, F., Kamoun, S., Mazars, C., Dumas, B., Bottin, A., Esquerre-Tugaye, M. T., and Rickauer, M. (2006). Cellulose binding domains of a *Phytophthora* cell wall protein are novel pathogen-associated molecular patterns. *Plant Cell*. 18: 1766–1777.

Gaulin, E., Madoui, M. A., Bottin, A., Jacquet, C., Mathé, C., Couloux, A., Wincker, P., and Dumas, B. (2008). Transcriptome of *Aphanomyces euteiches*: new oomycete putative pathogenicity factors and metabolic pathways. *PLoS One*. 3 (3): e1723.

Gawehns, F., Cornelissen, B. J., and Takken, F. L. (2013). The potential of effector-target genes in breeding for plant innate immunity. *Microbial Biotechnology*. 6 (3): 223-229.

Gees, R., and Hohl, H. R. (1988). Cytological comparison of specific (R3) and general resistance to late blight in potato leaf tissue. *Phytopathology*. 78 (3): 350-357.

Ghimire, S. R., Hyde, K. D., Hodgkiss, I. J., Shaw, D. S., and Liew, E. C. Y. (2003). Variations in the *Phytophthora infestans* population in Nepal as revealed by nuclear and mitochondrial DNA polymorphisms. *Phytopathology*. 93 (2): 236-243.

Gijzen, M., and Nürnberger, T. (2006). Nep1-like proteins from plant pathogens: recruitment and diversification of the NPP1 domain across taxa. *Phytochemistry*. 67 (16): 1800-1807.

Gilroy, E. M., Breen, S., Whisson, S. C., Squires, J., Hein, I., Kaczmarek, M., Turnbull, D., Boevink, P. C., Lokossou, A., Cano, L. M., Morales, J., Avrova, A. O., Pritchard, L., Randall, E., Lees, A., Govers, F., van West, P., Kamoun, S., Vleeshouwers, V. G., Cooke, D. E., and Birch P. R. J. (2011a). Presence/absence, differential expression and sequence polymorphisms between PiAVR2 and PiAVR2-like in *Phytophthora infestans* determine virulence on *R2* plants. *New Phytologist*. 191: 763–776.

Gilroy, E. M., Taylor, R. M., Hein, I., Boevink, P., Sadanandom, A., and Birch, P. R. J. (2011b). CMPG1- dependent cell death follows perception of diverse pathogen elicitors at the host plasma membrane and is suppressed by *Phytophthora infestans* RXLR effector AVR3a. *New Phytologist*. 190: 653–666.

Gisi, U., and Cohen, Y. (1996). Resistance to phenylamide fungicides: a case study with *Phytophthora infestans* involving mating type and race structure. *Annual Review of Phytopathology*. 34 (1): 549-572.

Glazebrook, J. (2005). Contrasting mechanisms of defense against biotrophic and necrotrophic pathogens. *Annual Review of Phytopathology*. 43: 205-227.

Gómez-Alpizar, L., Carbone, I., and Ristaino, J. B. (2007). An Andean origin of *Phytophthora infestans* inferred from mitochondrial and nuclear gene genealogies. *PNAS.* 104 (9): 3306-3311.

Goodwin, S. B., Spielman, L. J., Matuszak, J. M., Bergeron, S. N., and Fry, W. E. (1992). Clonal diversity and genetic differentiation of *Phytophthora infestans* populations in northern and central Mexico. *Phytopathology*. 82 (9): 955-961.

Goodwin, S. B., Cohen, B. A., Deahl, K. L., and Fry, W. E. (1994). Migration from northern Mexico as the probable cause of recent genetic changes in populations of *Phytophthora infestans* in the United States and Canada. *Phytopathology*. 84 (6): 553-558.

Govers, F. (2009). Forword. In Lamour, K., and Kamoun, S. (eds). *Oomycete genetics and genomics*. Wiley-Blackwell, NJ, USA: ix- xi.

Grenville-Briggs, L. J., Anderson, V. L., Fugelstad, J., Avrova, A. O., Bouzenzana, J., Williams, A., Wawra, S., Whisson, S. C., Birch, P. R. J., Bulone, V., and van West, P. (2008). Cellulose synthesis in *Phytophthora infestans* is required for normal appressorium formation and successful infection of potato. *The Plant Cell.* 20 (3): 720-738.

Grenville-Briggs, L. J., Avrova, A. O., Hay, R. J., Bruce, C. R., Whisson, S. C., and van West, P. (2010). Identification of appressorial and mycelial cell wall proteins and a survey of the membrane proteome of *Phytophthora infestans*. *Fungal Biology*. 114 (9): 702–723.

Groves, C. T., and Ristaino, J. B. (2000). Commercial fungicide formulations induce *in vitro* oospore formation and phenotypic change in mating type in *Phytophthora infestans*. *Phytopathology*. 90 (11): 1201-1208.

Grünwald, N. J., and Flier, W. G. (2005). The biology of *Phytophthora infestans* at its center of origin. *Annual Review of Phytopathology.* 43: 171-190.

Gubler, F., and Hardham, A. R. (1988). Secretion of adhesive material during encystment of *Phytophthora cinnamomi* zoospores, characterized by immunogold labelling with monoclonal antibodies to components of peripheral vesicles. *Journal of Cell Science*. 90 (2): 225-235.

Gururani, M. A., Venkatesh, J., Upadhyaya, C. P., Nookaraju, A., Pandey, S. K., and Park, S. W. (2012). Plant disease resistance genes: Current status and future directions. *Physiological and Molecular Plant Pathology*. 78; 51-65.

Gyetvai, G., Sønderkær, M., Göbel, U., Basekow, R., Ballvora, A., Imhoff, M., Kersten, B., Nielsen, K. L., and Gebhardt, C. (2012).The transcriptome of compatible and incompatible interactions of potato (*Solanum tuberosum*) with *Phytophthora infestans* revealed by DeepSAGE analysis. *PLoS One*. 7 (2): e31526

Haas, B. J., Kamoun, S., Zody, M. C., Jiang, R. H. Y., Handsaker, R. E., Cano, L. M., Grabherr, M., Kodira, C. D., Raffaele, S., Torto-Alalibo, T., Bozkurt, T. O., Ah-Fong, A. M. V., Alvarado, L., Anderson, V. L., Armstrong, M. R., Avrova, A., Baxter, L., Beynon, J., Boevink, P. C., Bollmann, S. R., Bos, J. I. B., Bulone, V., Cai, G. H., Cakir, C., Carrington, J. C., Chawner, M., Conti, L., Costanzo, S., Ewan, R., Fahlgren, N., Fischbach, M. A., Fugelstad, J., Gilroy, E. M., Gnerre, S., Green, P. J., Grenville-Briggs, L. J., Griffith, J., Grunwald, N. J., Horn, K., Horner, N. R., Hu, C. H., Huitema, E., Jeong, D. H., Jones, A. M. E., Jones, J. D. G., Jones, R. W., Karlsson, E. K., Kunjeti, S. G., Lamour, K., Liu, Z. Y., Ma, L. J., MacLean, D., Chibucos, M. C., McDonald, H., McWalters, J., Meijer, H. J. G., Morgan, W., Morris, P. F., Munro, C. A., O'Neill, K., Ospina-Giraldo, M., Pinzon, A., Pritchard, L., Ramsahoye, B., Ren Q. H., Restrepo, S., Roy S., Sadanandom, A., Savidor, A., Schornack, S., Schwartz, D. C., Schumann, U. D., Schwessinger, B., Seyer, L., Sharpe, T., Silvar, C., Song, J., Studholme, D. J., Sykes, S., Thines, M., van de Vondervoort, P. J. I., Phuntumart, V., Wawra, S., Weide, R., Win, J., Young, C., Zhou, S. G., Fry, W., Meyers, B. C., van West, P., Ristaino, J., Govers, F., Birch, P. R. J., Whisson, S. C., Judelson, H. S., and Nusbaum, C. (2009) Genome sequence and analysis of the Irish potato famine pathogen *Phytophthora infestans*. *Nature*. 461 (17): 393–398.

Halim, V. A., Hunger, A., Macioszek, V., Landgraf, P., Nürnberger, T., Scheel, D., and Rosahl, S. (2004). The oligopeptide elicitor Pep-13 induces salicylic acid-dependent and-independent defense reactions in potato. *Physiological and Molecular Plant Pathology*. 64 (6): 311-318.

Hansen, J., Colon, L., Cooke, D., Lassen, P., Nielsen, B., Cooke, L., Andrivon, D., and Lees, A. (2007). Eucablight - collating and analysing pathogenicity and resistance data on a European scale. *Bulletin OEPP*. 37: 383-390.

Hardham, A. R. (2001). The cell biology behind *Phytophthora* pathogenicity. *Australasian Plant Pathology*. 30 (2): 91-98.

Hardham, A. R. (2007). Cell biology of plant-oomycete interaction. *Cellular Microbiology*. 9 (1): 31–39.

Haverkort, A.J., Boonekamp, P.M., Hutten, R., Jacobsen, E., Lotz, L. A. P., Kessel, G. J. T., Visser, R. G. F., and van der Vossen, E. A. G. (2008). Societal costs of late blight in potato and prospects of durable resistance through cisgenic modification. *Potato Research*. 51: 47–57.

Haverkort, A. J., Struik, P. C., Visser, R. G. F., and Jacobsen, E. (2009). Applied biotechnology to combat late blight in potato caused by *Phytophthora infestans*. *Potato Research*. 52 (3): 249-264.

Heese, A., Hann, D. R., Gimenez-Ibanez, S., Jones, A. M., He, K., Li, J., Schroeder, J. I., Peck, S. C., and Rathjen, J. P. (2007). The receptor-like kinase SERK3/BAK1 is a central regulator of innate immunity in plants. *PNAS*. 104: 12217–12222.

Hein, I., Armstrong, M., Gilory, E. M., and Birch, P. R. J. (2009). The zig-zag-zig in oomycete- plant interactions. *Molecular Plant Pathology*. 10: 547–562.

Henfling, J. W. D. M., Bostock, R., and Kuc, J. (1980). Effect of abscisic acid on rishitin and lubimin accumulation and resistance to *Phytophthora infestans* and *Cladosporium cucumerinum* in potato tuber tissue slices. *Phytopathology*. 70 (11): 1074-1078.

Hohl, H. R., and Suter, E. (1976). Host-parasite interfaces in a resistant and susceptible cultivar of *Solanum tuberosum* inoculated with *Phytophthora infestans*: leaf tissue. *Canadian Journal of Botany*. 54: 1956–1970.

Hohl, H. R., and Iselin, K. (1984). Strains of *Phytophthora infestans* from Switzerland with A2 mating type behaviour. *Transactions of the British Mycological Society*. 83 (3): 529-530.

Hueck, C. J. (1998). Type III protein secretion systems in bacterial pathogens of animals and plants. *Microbiology and Molecular Biology Reviews*. 62 (2): 379-433.

Huitema, E., Vleeshouwers, V. G., Cakir, C., Kamoun, S., and Govers, F. (2005). Differences in intensity and specificity of hypersensitive response induction in *Nicotiana* spp. by INF1, INF2A, and INF2B of *Phytophthora infestans*. *Molecular Plant-Microbe Interactions*. 18 (3): 183-193.

Hulbert, S. H., Ilott, T. W., Legg, E. J., Lincoln, S. E., Lander, E. S., and Michelmore, R. W. (1988). Genetic analysis of the fungus, *Bremia lactucae*, using restriction fragment length polymorphisms. *Genetics*. 120 (4): 947-958.

Ingle, R. A., Carstens, M. and Denby, K. J. (2006). PAMP recognition and the plant-pathogen arms race. *BioEssays*. 28 (9): 880–889.

Jackson, S. L., and Hardham, A. R. (1998). Dynamic rearrangement of the filamentous actin network occurs during zoosporogenesis and encystment in the oomycete *Phytophthora cinnamomi*. *Fungal Genetics and Biology*. 24 (1): 24-33.

Jha, A. K., Bais, H. P., and Vivanco, J. M. (2005). *Enterococcus faecalis* mammalian virulence-related factors exhibit potent pathogenicity in the *Arabidopsis thaliana* plant model. *Infection and Immunity*. 73 (1): 464-475.

Jiang, R. H., de Bruijn, I., Haas, B. J., Belmonte, R., Löbach, L., Christie, J., van den Ackerveken, G., Bottin, A., Bulone, V., Díaz-Moreno, S. M., Dumas, B., Fan, L., Gaulin, E., Govers, F., Grenville-Briggs, L. J., Horner, N. R., Levin, J. Z., Mammella, M., Meijer, H. J., Morris, P., Nusbaum, C., Oome, S., Phillips, A. J., van Rooyen, D., Rzeszutek, E., Saraiva, M., Secombes, C. J., Seidl, M. F., Snel, B., Stassen, J. H., Sykes, S., Tripathy, S., van den Berg, H., Vega-Arreguin, J. C., Wawra, S., Young, S. K., Zeng, Q., Dieguez-Uribeondo, J., Russ, C., Tyler, B. M., van West, P. (2013). Distinctive expansion of potential virulence genes in the genome of the oomycete fish pathogen *Saprolegnia parasitica*. *PLoS Genetics*. 9 (6) :e1003272.

Jones, D. A., Thomas, C. M., Hammond-Kosack, K. E., Balint-Kurti, P. J., and Jones, J. D. (1994). Isolation of the tomato *Cf-9* gene for resistance to *Cladosporium fulvum* by transposon tagging. *Science*. 266 (5186): 789-793.

Jones, J. D. G., and Dangl, J. L. (2006). The plant immune system. *Nature*. 444 (16): 323–329.

Jones, R. W., and Ospina-Giraldo, M. (2011). Novel cellulose-binding-domain protein in *Phytophthora* is cell wall localized. *PLoS One*. 6 (8): e23555.

Joosten, M. H. (2012). Isolation of apoplastic fluid from leaf tissue by the vacuum infiltration-centrifugation technique. In *Plant Fungal Pathogens*. Humana Press. 603-610.

Judelson, H. S., and Roberts, S. (2002). Novel protein kinase induced during sporangial cleavage in the oomycete *Phytophthora infestans*. *Eukaryotic Cell*. 1: 687-695.

Judelson, H. S., Ah-Fong, A. M., Aux, G., Avrova, A. O., Bruce, C., Cakir, C., Cunha, L. D., Grenville-Briggs, G., Latijnhouwers, M., Meijer, H. J. G., Roberts, S., Thurber, C. S., Whisson, S. C., Birch, P. R. J., Govers, F., Kamoun, S., van West, P., and Windass, J. (2008). Gene expression profiling during asexual development of the late blight pathogen *Phytophthora infestans* reveals a highly dynamic transcriptome. *Molecular Plant-Microbe Interactions.* 21 (4): 433-447.

Judelson S. H. (2009). Sexual reproduction in oomycetes: Biology, Diversity, and Contributions to Fitness. Oomycete Genetics and Genomics. Wiley- Blackwell, 6: 121–138.

Jupe, F., Pritchard, L., Etherington, G. J., MacKenzie, K., Cock, P. J., Wright, F., Sharma, S. K., Bolser, D., Bryan, G. J., Jones, J. D. G., and Hein, I. (2012). Identification and localisation of the NB-LRR gene family within the potato genome. *BMC Genomics*. 13 (1): 75.

Jupe, J., Stam, R., Howden, A. J., Morris, J. A., Zhang, R., Hedley, P. E., and Huitema, E. (2013). *Phytophthora capsici*-tomato interaction features dramatic shifts in gene expression associated with a hemi-biotrophic lifestyle. *Genome Biology.* 14 (6): R63.

Kamoun, S., van West, P., de Jong, A. J., de Groot, K. E., Vleeshouwers, V. G. A. A., and Govers, F. (1997). A gene encoding a protein elicitor of *Phytophthora infestans* is down-regulated during infection of potato. *Molecular Plant-Microbe Interactions*. 10: 13–20.

Kamoun, S., van West, P., Vleeshouwers, V. G., de Groot, K. E., and Govers, F. (1998). Resistance of *Nicotiana benthamiana* to *Phytophthora infestans* is mediated by the recognition of the elicitor protein INF1. *The Plant Cell.* 10 (9): 1413-1425.

Kamoun, S., Hraber, P., Sobral, B., Nuss, D., and Govers, F. (1999). Initial assessment of gene diversity for the oomycete pathogen *Phytophthora infestans* based on expressed sequences. *Fungal Genetics and Biology.* 28: 94–106.

Kamoun, S. (2003). Molecular genetics of pathogenic oomycetes. *Eukaryotic Cell*. 2 (2): 191–199.

Kamoun, S. (2006). A catalogue of the effector secretome of plant pathogenic oomycetes. *Annual Review of Phytopathalogy*. 44: 41–60.

Kemen, E., Kemen, A. C., Rafiqi, M., Hempel, U., Mendgen, K., Hahn, M., and Voegele, R. T. (2005). Identification of a protein from rust fungi transferred from haustoria into infected plant cells. *Molecular Plant-Microbe Interactions*. 18 (11): 1130-1139.

Kemen, E., Gardiner, A., Schultz-Larsen, T., Kemen, A. C., Balmuth, A. L., Robert-Seilaniantz, A., Bailey, K., Holub, E., Studholme, D., MacLean, D., and Jones, J. D. (2011). Gene gain and loss during evolution of obligate parasitism in the white rust pathogen of *Arabidopsis thaliana*. *PLoS Biology*. 9 (7): e1001094.

Kim, D. S., and Hwang, B. K. (2012). The pepper MLO gene, *CaMLO2*, is involved in the susceptibility cell-death response and bacterial and oomycete proliferation. *The Plant Journal*. 72 (5): 843-855.

King, S. R., McLellan, H., Boevink, P. C., Armstrong, M. R., Bukharova, T., Sukarta, O., Win, J., Kamoun, S., Birch, P. R. J., and Banfield, M. J. (2014). *Phytophthora infestans* RXLR effector PexRD2 interacts with host MAPKKKε to suppress plant immune signaling. *The Plant Cell*. 26 (3): 1345-1359.

Krogh, A., Larsson, B., Von Heijne, G., and Sonnhammer, E. L. (2001). Predicting transmembrane protein topology with a hidden Markov model: application to complete genomes. *Journal of Molecular Biology*. 305 (3): 567-580.

Kunjeti, S. G., Evans, T. A., Marsh, A. G., Gregory, N. F., Kunjeti, S., Meyers, B. C., Kalavacharla, V. S., and Donofrio, N. M. (2012). RNA-Seq reveals infection-related global gene changes in *Phytophthora phaseoli*, the causal agent of lima bean downy mildew. *Molecular Plant Pathology*. 13 (5): 454–466.

Lamour, K. H., Mudge, J., Gobena, D., Hurtado-Gonzales, O. P., Schmutz, J., Kuo, A., Miller, N.A., Rice, B.J., Raffaele, S., Cano, L.M., Bharti, A.K., Donahoo, R.S., Finley, S., Huitema, E., Hulvey, J., Platt, D., Salamov, A., Savidor, A., Sharma, R., Stam, R., Story, D., Thines, M., Win, J., Haas, B., Dinwiddie, D.L, Jenkins, J., Knight, J.R., Affourtit, J.P., Han, C.S., Chertkov, P., Lindquist, E.A., Detter, C., Grigoriev, I.V., Kamoun, S., and Kingsmore, S. F. (2012). Genome sequencing and mapping reveal loss of heterozygosity as a mechanism for rapid adaptation in the vegetable pathogen *Phytophthora capsici*. *Molecular Plant-Microbe Interactions*. 25 (10): 1350-1360.

Larroque, M., Ramirez, D., Lafitte, C., Borderies, G., Dumas, B., and Gaulin, E. (2011). Expression and purification of a biologically active *Phytophthora parasitica* cellulose binding elicitor lectin in *Pichia pastoris*. *Protein Expression and Purification*. 80 (2): 217-223.

Livak, K. J., and Schmittgen, T. D. (2001). Analysis of relative gene expression data using real-time quantitative PCR and the $2^{\Delta\Delta CT}$ method. *Methods*. 25 (4): 402-408.

Lévesque, C. A., Brouwer, H., Cano, L., Hamilton, J. P., Holt, C., Huitema, E., Raffaele, S., Robideau, G. P., Thines, M., Win, J., Zerillo, M. M., Beakes, G. W., Boore, J. L., Busam, D., Dumas, B., Ferriera, S., Fuerstenberg, S., Gachon, C. M. M., Gaulin, E., Govers, F., Grenville-Briggs, L., Horner, N., Hostetler, J., Jiang, R. H. Y., Johnson, J., Krajaejun, T., Lin, H., Meijer, H. J. G., Moore, B., Morris, P., Phuntmart, V., Puiu, D., Shetty, J., Stajich, J. E., Tripathy, S., Wawra, S., van West, P., Whitty, B. R., Coutinho, P. M., Henrissat, B., Martin, F., Thomas, P. D., Tyler, B., De Vries, R. P., Kamoun, S., Yandell, M., Tisserat, N., and Buell, C. R. (2010). Genome sequence of the necrotrophic plant pathogen *Pythium ultimum* reveals original pathogenicity mechanisms and effector repertoire. *Genome Biology*. 11 (7): R73.

Lewis, J. D., Wan, J., Ford, R., Gong, Y., Fung, P., Nahal, H., Wang, P. W., Desveaux, D., and Guttman, D. S. (2012). Quantitative interactor screening with next-generation sequencing (QIS-Seq) identifies *Arabidopsis thaliana MLO2* as a target of the *Pseudomonas syringae* type III effector HopZ2. *BMC Genomics*. 13 (1): 8.

Links, M. G., Holub, E., Jiang, R. H., Sharpe, A. G., Hegedus, D., Beynon, E., Sillito, D., Clarke, W. E., Uzuhashi, S., and Borhan, M. H. (2011). *De novo* sequence assembly of *Albugo candida* reveals a small genome relative to other biotrophic oomycetes. *BMC Genomics*. 12 (1): 503.

Liu. Z., Bos, J. I., Armstrong, M., Whisson, S. C., da Cunha, L., Torto-Alalibo, T., Win, J., Avrova, A. O., Wright, F., Birch, P. R. J., and Kamoun, S. (2005). Patterns of diversifying selection in the phytotoxin-like *scr74* gene family of *Phytophthora infestans*. *Molecular Biology and Evolution*. 22 (3): 659–672.

Mackey, D., Holt, III B. F., Wiig, A., and Dangl, J. L. (2002). RIN4 interacts with *Pseudomonas syringae* type III effector molecules and is required for RPM1-mediated resistance in *Arabidopsis*. *Cell*. 108: 743–754.

Marín-Rodríguez, M. C., Orchard, J., and Seymour, G. B. (2002). Pectate lyases, cell wall degradation and fruit softening. *Journal of Experimental Botany*. 53 (377): 2115-2119.

Martin-Hernandez, A. M., Dufresne, M., Hugouvieux, V., Melton, R., and Osbourn, A. (2000). Effects of targeted replacement of the tomatinase gene on the interaction of *Septoria lycopersici* with tomato plants. *Molecular Plant-Microbe Interactions*. 13 (12): 1301-1311.

Martin, M. D., Cappellini, E., Samaniego, J. A., Zepeda, M. L., Campos, P. F., Seguin-Orlando, A.,Wales, N., Orlando, L., Ho, S. Y. W., Dietrich, F. S., Mieczkowski, P. A., Heitman, J., Willerslev, E., Krogh, A., Ristaino, J. B., and Gilbert, M. T. P. (2013). Reconstructing genome evolution in historic samples of the Irish potato famine pathogen. *Nature Communications*. 4: 2172.

Martin, M. D., Ho, S. Y., Wales, N., Ristaino, J. B., and Gilbert, M. T. P. (2014). Persistence of the mitochondrial lineage responsible for the Irish potato famine in extant New World *Phytophthora infestans*. *Molecular Biology and Evolution*. 31 (6): 1414-1420.

McLellan, H., Boevink, P. C., Armstrong, M. R., Pritchard, L., Gomez, S., Morales, J., Whisson, S. C., Beyon, J. L., and Birch, P. R. (2013). An RxLR effector from *Phytophthora infestans* prevents re-localisation of two plant NAC transcription factors from the endoplasmic reticulum to the nucleus. *PLoS Pathogens*. 9 (10): e1003670.

Millett, B. P., Mollov, D. S., Iorizzo, M., Carputo, D., and Bradeen, J. M. (2009). Changes in disease resistance phenotypes associated with plant physiological age are not caused by variation in *R* gene transcript abundance. *Molecular Plant-Microbe Interactions*. 22 (3): 362-368.

Miura, N., Yamamoto, M., Ueki, T., Kitani, T., Fukcuda, K., and Komatsu, Y. (1997). Inhibition of thymocyte apoptosis by berberine. *Biochemical Pharmacology*. 53 (9): 1315-1322.

Murashige, T., and Skoog, F. (1962). A revised medium for rapid growth and bioassays with tobacco tissue cultures. *Physiologia Plantarum*. 15 (3): 473-497.

Murphy, P. A., and McKay, R. (1925). Further experiments on the sources and development of blight infection in potato tubers. *J Dep Lds Agric, Dublin*. *25*: 10-21.

Nakashima, K., Takasaki, H., Mizoi, J., Shinozaki, K., and Yamaguchi-Shinozaki, K. (2012). NAC transcription factors in plant abiotic stress responses. *Biochimica et Biophysica Acta (BBA)-Gene Regulatory Mechanisms*. 1819 (2): 97-103.

Nattrass, R. M., and Ryan, M. (1951). New hosts of *Phytophthora infestans* in Kenya. *Nature*. 168: 85 - 86

Orsomando, G., Lorenzi, M., Raffaelli, N., la Rizza, M., Mezzetti, B., and Ruggieri, S. (2001). Phytotoxic protein PcF, purification, characterization, and cDNA sequencing of a novel hydroxyproline-containing factor secreted by the strawberry pathogen *Phytophthora cactorum. Journal of Biological Chemistry*. 276: 21578-21584.

Pandey, S. P., and Somssich, I. E. (2009). The role of WRKY transcription factors in plant immunity. *Plant Physiology*. 150 (4): 1648-1655.

Pathak, N., and Clarke, D. D. (1987). Studies on the resistance of the outer cortical tissues of the tubers of some potato cultivars to *Phytophthora infestans*. *Physiological and Molecular Plant Pathology*. 31 (1): 123-132.

Pel, A. M., Hutten, R. C. B., Jacobsen, E., Vander, Vossen, E. A. G., Govers, F., Visser, R. G. F., and Van Eck, H. J. (2010). Mapping, isolation and characterization of genes responsible for late blight resistance in potato. *PhD thesis*, Wageningen University, The Netherlands.

Petersen, T. N., Brunak, S., von Heijne, G., and Nielsen, H. (2011). SignalP 4.0: discriminating signal peptides from transmembrane regions. *Nature Methods*. 8 (10): 785-786.

Pieterse, C. M., and Dicke, M. (2007). Plant interactions with microbes and insects: from molecular mechanisms to ecology. *Trends in Plant Science*. 12 (12): 564-569.

Postel, S., and Kemmerling, B. (2009). Plant systems for recognition of pathogen-associated molecular patterns. In *Seminars in Cell & Developmental Biology*. 20 (9): 1025-1031. Academic Press.

Qi, J., Asano, T., Jinno, M., Matsui, K., Atsumi, K., Sakagami, Y., and Ojika, M. (2005). Characterization of a *Phytophthora* mating hormone. *Science*. 309: 1828.

Qutob, D., Hraber, P.T., Sobral, B.W.S., and Gijzen, M. (2000). Comparative analysis of expressed sequences in *Phytophthora sojae*. *Plant Physiology*. 123: 243-253.

Raffaele, S., Farrer, R. A., Cano, L. M., Studholme, D. J., MacLean, D., Thines, M., Jiang, R. H. Y., Zody, M. C., Kunjeti, S. G., Donofrio, N. M., Meyers, B. C., Nusbaum, C., and Kamoun, S. (2010). Genome evolution following host jumps in the Irish potato famine pathogen lineage. *Science*. 330 (6010): 1540–1543.

Randall, T. A., and Judelson, H. S. (1999). Construction of a bacterial artificial chromosome library of *Phytophthora infestans* and transformation of clones into *P. infestans*. *Fungal Genetics and Biology*. 28 (3): 160-170.

Randall, T. A., Dwyer, R. A., Huitema, E., Beyer, K., Cvitanich, C., Kelkar, H., Ah Fong, A. M. V., Gates, K., Roberts, S., Yatzkan, E., Gaffney, T., Law, M., Testa, A., Torto-Alalibo, T., Zhang, M., Zheng, L., Mueller, E., Windass, J., Binder, A., Birch, P. R. J., Gisi, U., Govers, F., Gow, N. A., Mauch, F., van West, P., Waugh, M. E., Jun Yu, J., Boller, T., Kamoun, S., Lam, S. T., and Judelson, H.S. (2005). Large-scale gene discovery in the oomycete *Phytophthora infestans* reveals likely components of phytopathogenicity shared with true fungi. *Molecular Plant-Microbe Interactions*. 18 (3): 229–243.

Rastogi, A., and Pospíšil, P. (2012). Production of hydrogen peroxide and hydroxyl radical in potato tuber during the necrotrophic phase of hemibiotrophic pathogen *Phytophthora infestans* infection. *Journal of Photochemistry and Photobiology B: Biology*. 117: 202-206.

Reddick, D. (1939). Whence came *Phytophthora infestans*. *Chron. Bot*. 5: 410-412.

Rehmany, A. P., Grenville, L. J., Gunn, N. D., Allen, R. L., Paniwnyk, Z., Byrne, J., Whisson, S. C., Birch, P. R. J., and Beynon, J. L. (2003). A genetic interval and physical contig spanning the *Peronospora parasitica* (At) avirulence gene locus *ATR1Nd*. *Fungal Genetics and Biology*. 38 (1): 33-42.

Reuber, T. L., Plotnikova, J. M., Dewdney, J., Rogers, E. E., Wood, W., and Ausubel, F. M. (1998). Correlation of defense gene induction defects with powdery mildew susceptibility in *Arabidopsis* enhanced disease susceptibility mutants. *The Plant Journal*. 16 (4): 473-485.

Richards, T. A., Dacks, J. B., Jenkinson, J. M., Thornton, C. R., and Talbot, N. J. (2006). Evolution of filamentous plant pathogens: gene exchange across eukaryotic kingdoms. *Current Biology*. 16 (18): 1857-1864.

Richards, T. A., Soanes, D. M., Jones, M. D., Vasieva, O., Leonard, G., Paszkiewicz, K., Foster P. G., Hall, Neil., and Talbot, N. J. (2011). Horizontal gene transfer facilitated the evolution of plant parasitic mechanisms in the oomycetes. *PNAS.* 108 (37): 15258-15263.

Rico, A., and Preston, G. M. (2008). *Pseudomonas syringae* pv. tomato DC3000 uses constitutive and apoplast-induced nutrient assimilation pathways to catabolize nutrients that are abundant in the tomato apoplast. *Molecular Plant-Microbe Interactions.* 2: 269-282.

Rose, J. K. C., Ham, K. S., Darvill, A. G., and Albersheim, P. (2002). Molecular cloning and characterization of glucanase inhibitor proteins: Coevolution of a counterdefense mechanism by plant pathogens. *Plant Cell*. 14: 1329–1345.

Sato, N. (1980). Sources of inoculum and sites of infection of potato tubers by *Phytophthora infestans* in soil. *Annals of the Phytopathological Society of Japan*. 46 (2): 231-240.

Saunders, D. G., Breen, S., Win, J., Schornack, S., Hein, I., Bozkurt, T. O., Champouret, N., Vleeshouwers, V. G., Birch, P. R., Gilroy, E. M., and Kamoun, S. (2012). Host protein BSL1 associates with *Phytophthora infestans* RXLR effector AVR2 and the *Solanum demissum* immune receptor R2 to mediate disease resistance. *The Plant Cell*. 24 (8): 3420-3434.

Savory, E. A., Adhikari, B. N., Hamilton, J. P., Vaillancourt, B., Buell, C. R., and Day, B. (2012). mRNA-Seq analysis of the *Pseudoperonospora cubensis* transcriptome during cucumber (*Cucumis sativus* L.) infection. *PLoS One*. 7 (4): e35796.

Schornack, S., Huitema, E., Cano, L. M., Bozkurt, T. O., Oliva, R., van Damme, M., Schwizer, S., Raffaele, S., Chaparro-Garcia, A., Farrer, R., Segretin, M. E., Bos, J. I. B., Haas, B. J., Zody, M. C., Nusbaum, C., Win, J., Thines, M. and Kamoun, S. (2010). Ten things to know about oomycete effectors. *Molecular Plant Pathology.* 10 (6): 795–803.

Schumann, G. L., and C. J. D'Arcy. (2000). *Late blight of potato and tomato*. The Plant Health Instructor. DOI: 10.1094/PHI-I-2000-0724-01.

Segonzac, C., and Zipfel, C. (2011). Activation of plant pattern-recognition receptors by bacteria. *Current Opinion in Microbiology*. 14 (1): 54-61.

Seidl, M.F., Wang, R.P., Van den Ackerveken, G., Govers, F., Snel, B. (2012). Bioinformatic inference of specific and general transcription factor binding sites in the plant pathogen *Phytophthora infestans*. *PLoS One*. 7 (12): e51295.

Shaat, M. M. N. (2002). Detection of mating types of potato late blight pathogen, *Phytophthora infestans* Mont. de Bary. *El-Minia Governorate, Egypt. Ass J Agricul Sci*. 33: 161-175.

Shaner, N. C., Campbell, R. E., Steinbach, P. A., Giepmans, B. N., Palmer, A. E., and Tsien, R. Y. (2004). Improved monomeric red, orange and yellow fluorescent proteins derived from *Discosoma* sp. red fluorescent protein. *Nature Biotechnology*. 22 (12): 1567-1572.

Shaner, N. C., Lin, M. Z., McKeown, M. R., Steinbach, P. A., Hazelwood, K. L., Davidson, M. W., and Tsien, R. Y. (2008). Improving the photostability of bright monomeric orange and red fluorescent proteins. *Nature Methods*. 5 (6): 545-551.

Soanes, D. M., Alam, I., Cornell, M., Wong, H. M., Hedeler, C., Paton, N. W., Rattray, M., Hubbard, S. J., Oliver, S. G., and Talbot, N. J. (2008). Comparative genome analysis of filamentous fungi reveals gene family expansions associated with fungal pathogenesis. *PLoS One*. 3 (6): e2300.

Song, J., Bradeen, J. M., Naess, S. K., Raasch, J. A., Wielgus, S. M., Haberlach, G. T., Liu, J., Kuang, H., Austin-Phillips, S., Buell, C. R., Helgeson, J. P., and Jiang, J. (2003). Gene *RB* cloned from *Solanum bulbocastanum* confers broad spectrum resistance to potato late blight. *PNAS*. 100 (16): 9128-9133.

Song, J., Win, J., Tian, M., Schornack, S., Kaschani, F., Ilyas, M., van der Hoorn, R. A. L., and Kamoun, S. (2009). Apoplastic effectors secreted by two unrelated eukaryotic plant pathogens target the tomato defense protease Rcr3. *PNAS*. 106 (5): 1654-1659.

Stassen, J. H., and Van den Ackerveken, G. (2011). How do oomycete effectors interfere with plant life? *Current Opinion in Plant Biology*. 14 (4): 407-414.

Stassen, J. H., Seidl, M. F., Vergeer, P. W., Nijman, I. J., Snel, B., Cuppen, E., and Van den Ackerveken, G. (2012). Effector identification in the lettuce downy mildew *Bremia lactucae* by massively parallel transcriptome sequencing. *Molecular Plant Pathology*. 13 (7): 719-731.

Sumit, R., Sahu, B. B., Xu, M., Sandhu, D., and Bhattacharyya, M. K. (2012). *Arabidopsis* nonhost resistance gene *PSS1* confers immunity against an oomycete and a fungal pathogen but not a bacterial pathogen that cause diseases in soybean. *BMC plant Biology*. 12 (1): 87.

Sunseri, M. A., Johnson, D. A., and Dasgupta, N. (2002). Survival of detached sporangia of *Phytophthora infestans* exposed to ambient, relatively dry atmospheric conditions. *American Journal of Potato Research*. 79 (6): 443-450.

Tanabe, S., Ishii-Minami, N., Saitoh, K. I., Otake, Y., Kaku, H., Shibuya, N., Nishizawa, Y., and Minami, E. (2011). The role of catalase-peroxidase secreted by *Magnaporthe oryzae* during early infection of rice cells. *Molecular Plant-Microbe Interactions*. 24 (2): 163-171.

Tian, M., Win, J., Song, J., van der Hoorn, R., van der Knaap, E., and Kamoun, S. (2007). A *Phytophthora infestans* cystatin-like protein targets a novel tomato papain-like apoplastic protease. *Plant Physiology*. 143: 364–377.

Tian, M. Y., Benedetti, B., and Kamoun, S. (2005). A second kazal-like protease inhibitor from *Phytophthora infestans* inhibits and interacts with the apoplastic pathogenesis-related protease P69B of tomato. *Plant Physiology*. 138: 1785–1793.

Tian, M. Y., Huitema, E., da Cunha, L., Torto-Alalibo, T., and Kamoun, S. (2004). A Kazal-like extracellular serine protease inhibitor from *Phytophthora infestans* targets the tomato pathogenesis-related protease P69B. *Journal of Biological Chemistry*. 279: 26370–26377.

Thines, M. and Kamoun, S. (2010). Oomycete- plant evolution: recent advances and future prospects. *Current Opinion in Plant Biology*. 13: 1–7.

Torto-Alalibo, T., Tian, M., Gajendran, K., Waugh, M. E., Van West, P., and Kamoun, S. (2005). Expressed sequence tags from the oomycete fish pathogen *Saprolegnia parasitica* reveal putative virulence factors. *BMC Microbiology*. 5 (1): 46.

Torto-Alalibo, T. A., Tripathy, S., Smith, B. M., Arredondo, F. D., Zhou, L., Li, H., Chibucos, M. C., Qutob, D., Gijen, M., Mao, C., Sobral, B. W. S., Waugh, M. E., Mitchell, T. K., Dean, R. A., and Tyler, B. M. (2007). Expressed sequence tags from *Phytophthora sojae* reveal genes specific to development and infection. *Molecular Plant-Microbe Interactions*. 20 (7): 781-793.

Toxopeus, H. J. (1961). On the inheritance of tuber resistance of *Solanum tuberosum* to *Phytophthora infestans* in the field. *Euphytica*. 10 (3): 307-314.

Tripathy, S., Deo, T., and Tyler, B. M. (2012). Oomycete transcriptomics database: A resource for oomycete transcriptomes. *BMC Genomics*. 13 (1): 303.

Tyler, B. M., Tripathy, S., Zhang, X., Dehal, P., Jiang, R. H., Aerts, A., Arredondo, F. D., Baxter, L., Bensasson , D., Beynon, J. L., Chapman, J., Damasceno, C. M. B., Dorrance, A. E., Dou, D., Dickerman, A. W., Dubchak, I. L., Garbelotto, M., Gijzen, M., Gordon, S. G., Govers, F., Grunwald, N. J., Huang, W., Ivors, K. L., Jones, R. W., Kamoun, S., Krampis, K., Lamour, K. H., Lee, Mi-Kyung., McDonald, W. H., Medina, M., Meijer, H. J. G., Nordberg, E. K., Maclean, D. J., Ospina-Giraldo, M. D., Morris, P. F., Phuntumart, V., Putnam, N. H., Rash, S., Rose, J. K. C., Sakihama, Y.o, Salamov, A. A., Savidor, A., Scheuring, C. F., Smith, B. M., Sobral, B. W. S., Terry, A.,Torto-Alalibo, T. A., Win, J., Xu, Z., Zhang, H., Grigoriev , I. V., Rokhsar, D. S., and Boore, J. L. (2006). *Phytophthora* genome sequences uncover evolutionary origins and mechanisms of pathogenesis. *Science*. 313 (5791): 1261-1266.

van Damme, M., Schornack, S., Cano, L. M., Huitema, E., and Kamoun, S. (2009). Interactions between *Phytophthora infestans* and *Solanum*. *Oomycete Genetics and Genomics*. Wiley-Blackwell. 14: 287–302.

Van Damme, M., Bozkurt, T. O., Cakir, C., Schornack, S., Sklenar, J., Jones, A. M., and Kamoun, S. (2012). The Irish potato famine pathogen *Phytophthora infestans* translocates the CRN8 kinase into host plant cells. *PLoS Pathogens*. 8 (8): e1002875.

van der Vossen, E., Sikkema, A., Hekkert, B. T. L., Gros, J., Stevens, P., Muskens, M., Wouters, D., Pereira, A., Stiekema, W., and Allefs, S. (2003). An ancient *R* gene from the wild potato species *Solanum bulbocastanum* confers broad-spectrum resistance to *Phytophthora infestans* in cultivated potato and tomato. *The Plant Journal*. 36 (6): 867-882.

van der Vossen, E. A. G., Gros, J., Sikkema, A., Muskens, M., Wouters, D., Wolters, P., Pereira, A., and Allefs, S. (2005). The *Rpi-blb2* gene from *Solanum bulbocastanum* is an *Mi-1* gene homolog conferring broad-spectrum late blight resistance in potato. *The Plant Journal*. 44: 208–222.

Vanittanakom, N., Supabandhu, J., Khamwan, C., Praparattanapan, J., Thirac, S., Prasertwitayakij, N., Louthrenoo, W., Chiewchanvit, S., and Tananuvat, N. (2004). Identification of emerging human-pathogenic *Pythium insidiosum* by serological and molecular assay-based methods. *Journal of Clinical Microbiology*. 42: 3970-3974.

van Kan, J. A. (2006). Licensed to kill: the lifestyle of a necrotrophic plant pathogen. *Trends in Plant Science*. 11 (5): 247-253.

van Poppel, P., Guo J., Vondervoort, P., Jung, M., Birch, P., Whisson, S., and Govers, F. (2008). The *Phytophthora infestans* avirulence gene *Avr4* encodes an RXLR-dEER effector. *Molecular Plant-Microbe Interactions*. 21: 1460–1470.

van Poppel, P. (2009). The *Phytophthora infestans* avirulence gene *PiAvr4* and its potato counterpart *R4*. *PhD Thesis*, Wageningen University, The Netherlands.

Van Poppel, P. M., Jiang, R. H., Śliwka, J., and Govers, F. (2009). Recognition of *Phytophthora infestans* Avr4 by potato R4 is triggered by C-terminal domains comprising W motifs. *Molecular Plant Pathology*. 10 (5): 611-620.

van West, P., de Jong, A. J., Judelson, H. S., Emons, A. M. C., and Govers, F. (1998). The *ipiO* gene of *Phytophthora infestans* is highly expressed in invading hyphae during infection. *Fungal Genetics and Biology*. 23 (2): 126-138.

Vetukuri, R. R., Tian, Z., Avrova, A. O., Savenkov, E. I., Dixelius, C., and Whisson, S. C. (2011). Silencing of the *PiAvr3*a effector-encoding gene from *Phytophthora infestans* by transcriptional fusion to short interspersed element. *Fungal Biology*. 1225-1233.

Vetukuri, R. R., Åsman, A. K., Tellgren-Roth, C., Jahan, S. N., Reimegård, J., Fogelqvist, J., and Dixelius, C. (2012). Evidence for small RNAs homologous to effector-encoding genes and transposable elements in the oomycete *Phytophthora infestans*. *PloS One*. 7 (12): e51399.

Vieira, P., Danchin, E. G., Neveu, C., Crozat, C., Jaubert, S., Hussey, R. S., Engler, G., Abad, P., de Almeida-Engler, J., Castagnone-Sereno, P., and Rosso, M. N. (2011). The plant apoplasm is an important recipient compartment for nematode secreted proteins. *Journal of Experimental Botany*. 62 (3): 1241-1253.

Vleeshouwers, V. G., Rietman, H., Krenek, P., Champouret, N., Young, C., Oh, S. K., Wang, M., Bouwmeester, K., Vosman, B., Visser, R. G., Jacobsen, E., Govers, F., Kamoun, S., and Van der Vossen, E. A. (2008). Effector genomics accelerates discovery and functional profiling of potato disease resistance and *Phytophthora infestans* avirulence genes. *Plos One*. 3: e2875.

Vleeshouwers, V. G., Raffaele, S., Vossen, J. H., Champouret, N., Oliva, R., Segretin, M. E., Rietman, H., Cano, L. M., Lokossou, A., Kessel, G., Pel, M. A., and Kamoun, S. (2011). Understanding and exploiting late blight resistance in the age of effectors. *Annual Review of Phytopathology*. 49: 507-531.

Walton, J. D. (1994). Deconstructing the cell wall. *Plant Physiology*. 104 (4): 1113.

Wang, Z., Mao, H., Dong, C., Ji, R., Cai, L., Fu, H., and Liu, S. (2009). Overexpression of *Brassica napus MPK4* enhances resistance to *Sclerotinia sclerotiorum* in oilseed rape. *Molecular Plant-Microbe Interactions*. 22 (3): 235-244.

Wang, Q., Han, C., Ferreira, A. O., Yu, X., Ye, W., Tripathy, S., Kale, S.D., Gu, B., Sheng, Y., Sui, Y., Wang, X., Zhang, Z., Cheng, B., Dong, S., Shan, W., Zheng, X., Dou, D., Tyler, B. M., and Wang Y. (2011). Transcriptional programming and functional interactions within the *Phytophthora sojae* RXLR effector repertoire. *The Plant Cell*. 23 (6): 2064-2086.

Whisson, S. C., van der Lee, T., Bryan, G. J., Waugh, R., Govers, F., and Birch P. R. J. (2001) Physical mapping across an avirulence locus of *Phytophthora infestans* using a highly representative, large-insert bacterial artificial chromosome library. *Molecular Genetics and Genomics*. 266: 289–295.

Whisson, S. C., Basnayake, S., Maclean, D. J., Irwin, J. A., and Drenth, A. (2004). *Phytophthora sojae* avirulence genes *Avr4* and *Avr6* are located in a 24kb, recombination-rich region of genomic DNA. *Fungal Genetics and Biology*. 41 (1): 62-74.

Whisson, S. C., Boevink, P. C., Moleleki, L., Avrova, A. O., Morales, J. G., Gilroy, E. M., Armstrong, M. R., Grouffaud, S., West, P. V., Chapman, S., Hein, I., Toth, L. K., Pritchard, L., and Birch, P. R. J. (2007). A translocation signal for delivery of oomycete effector proteins into host plant cells. *Nature*. 450 (1): 115–118.

Xiang, Q., and Judelson, H. S. (2014). Myb transcription factors and light regulate sporulation in the oomycete *Phytophthora infestans*. *PloS One*. 9 (4): e92086.

Yamakawa, H., Kamada, H., Satoh, M., and Ohashi, Y. (1998). Spermine is a salicylate-independent endogenous inducer for both tobacco acidic pathogenesis-related proteins and resistance against tobacco mosaic virus infection. *Plant Physiology*. 118 (4): 1213-1222.

Ye, X. S., Pan, S. Q., and Kuc, J (1989). Pathogenesis-related proteins and systemic resistance to blue mold and tobacco mosaic virus induced by tobacco mosaic virus, *Peronospara tabacina* and aspirin. *Physiological and Molecular Plant Pathology*. 35: 161- 175.

Ye, W., Wang, X., Tao, K., Lu, Y., Dai, T., Dong, S., Dou, D., Gijzen, M., and Wang, Y. (2011). Digital gene expression profiling of the *Phytophthora sojae* transcriptome. *Molecular Plant-Microbe Interactions*. 24 (12): 1530-1539.

Ye, W., Wang, Y., Dong, S., Tyler, B. M., and Wang, Y. (2013). Phylogenetic and transcriptional analysis of an expanded bZIP transcription factor family in *Phytophthora sojae*. *BMC Genomics*. 14 (1): 839.

Zhang, J., Luo, N., Luo, Y., Peng, Z., Zhang, T., and Li, S. (2012). microRNA-150 inhibits human CD133-positive liver cancer stem cells through negative regulation of the transcription factor c-Myb. *International Journal of Oncology*. 40 (3): 747-756.

Zheng, X., McLellan, H., Fraiture, M., Liu, X., Boevink, P. C., Gilroy, E. M., Chen, Y., Kandel, K., Sessa, G., Birch, P. R. J., and Brunner, F. (2014). Functionally redundant RXLR effectors from *Phytophthora infestans* act at different steps to suppress early flg22-triggered immunity. *PLoS Pathogens*. 10 (4): e1004057.

Zipfel, C., Robatzek, S., Navarro, L., Oakeley, E. J., Jones, J. D., Felix, G., and Boller, T. (2004). Bacterial disease resistance in *Arabidopsis* through flagellin perception. *Nature*. 428 (6984): 764-767.

Websites:

Bioinformatics (2014): jquery.venny; URL: http://bioinfo.genotoul.fr/index.php?id=116 [Date accessed: 28 May 2014]

Bio-Rad (2013) URL: http://arboretum.harvard.edu/wp-content/uploads/ptc200_manual.pdf [Date accessed: 01 May 2013]

Edwards High Vacuum Pump, Crawley, Sussex, England, URL: http://www.edwardsvacuum.com/Support/Reference.aspx [Date accessed: 28 May 2014]